Pea protein functionality

Tailor-made through fractionation

Remco Kornet

Propositions

1. Plant protein functionality carries its maximum potential in the seed.
   (this thesis)

2. Plant globulins and albumins should be considered functionally distinct proteins, just as casein and whey protein are in the field of dairy science.
   (this thesis)

3. The article of Rulli et al. (2017) can be extrapolated to the statement that the risk of future pandemics can be reduced by the protein transition.
   (Rulli, M. C., Santini, M., Hayman, D. T., & D'Odorico, P. (2017). The nexus between forest fragmentation in Africa and Ebola virus disease outbreaks. Scientific reports, 7(1), 1-8.)

4. The article of Nikolopoulou et al. (2007) proves the necessity to incorporate plant sciences in the study of plant protein functionality.
   (Nikolopoulou, D., Grigorakis, K., Stasini, M., Alexis, M. N., & Iliadis, K. (2007). Differences in chemical composition of field pea (Pisum sativum) cultivars: Effects of cultivation area and year. Food chemistry, 103(3), 847-852.)

5. Individualism is an expression of reductionism.

6. Globalization promotes inter-country solidarity and demotes intra-country solidarity.

Propositions belonging to the thesis, entitled
Pea protein functionality: tailor-made through fractionation

Remco Kornet
Wageningen, 26 November 2021

Pea protein functionality

Tailor-made through fractionation

Remco Kornet

Thesis committee

Promotors

Prof. Dr Erik van der Linden
Professor of Physics and Physical Chemistry of Foods
Wageningen University & Research

Prof. Dr Atze Jan van der Goot
Personal chair at Food Process Engineering
Wageningen University & Research

Co-promotors

Dr Paul Venema
Assistant professor, Physics and Physical Chemistry of Foods
Wageningen University & Research

Dr Marcel Meinders
Senior researcher
Wageningen Food & Biobased Research

Other members

Prof. Dr Vincenzo Fogliano, Wageningen University & Research
Dr Monique Axelos, INRAE, Paris, France
Prof. Dr Peter Fischer, ETH, Zurich, Switzerland
Prof. Dr Lilia Ahrné, University of Copenhagen, Denmark

This research was conducted under the auspices of the Graduate School VLAG
(Advanced Studies in Food Technology, Agrobiotechnology, Nutrition and Health Sciences).

Pea protein functionality

Tailor-made through fractionation

Remco Kornet

Thesis

submitted in fulfilment of the requirements for the degree of doctor
at Wageningen University & Research
by the authority of the Rector Magnificus,
Prof. Dr A.P.J. Mol,
in the presence of the
Thesis Committee appointed by the Academic Board
to be defended in public
on Friday 26 November 2021
at 4 p.m. in the Aula.

Remco Kornet

Pea protein functionality: tailor-made through fractionation
267 pages

PhD thesis, Wageningen University, Wageningen, the Netherlands (2021)
With references, with summaries in English and Dutch

ISBN: 978-94-6395-954-4
DOI: 10.18174/552551

Table of contents

Chapter 1

General Introduction

1

1.1 General introduction

The world population is growing and at the same time energy, water and other resources are becoming scarcer [1]. The food industry is thus challenged by making more food while using less resources. A route to make more food with less resources is argued to imply a shift from animal to plant-based food products, also referred to as the protein transition [2, 3]. Food science is one of the disciplines that may contribute to dealing with the technical and scientific challenges that the protein transition entails. In recent work, Lillford and Hermansson (2021) argued that a collaboration between food scientists, plant scientists and others is vital to study the agricultural production and subsequent processing of new plant protein sources [4].

Within the context of this protein transition, a research project was set-up by the Top Institute Food and Nutrition (TiFN) in 2017. The aim of this project is to safeguard product structure and mechanical properties while using new sustainable sources and processing routes. Two avenues were being pursued in the project: one focussing on intensively purified plant ingredients and the other focussing on mildly purified plant ingredients, both in the context of ingredient functionality and food structuring.

This thesis describes the outcomes of one of the subprojects regarding the latter. To obtain mildly purified plant ingredients, different fractionation routes were deployed that have fewer processing steps and / or require less water, compared with a commonly reported aqueous fractionation process that involves alkaline extraction and isoelectric precipitation. A Life Cycle Analysis (LCA) was out of scope, but it can be assumed that the extent of processing and process water usage are parameters that can strongly influence the sustainability of a fractionation process. This thesis focussed on how mild fractionation influences the functionality of the mildly processed plant protein fractions. Mild or limited fractionation and pea protein functionality are thus central concepts in this thesis. The knowledge and insights obtained from this thesis project may contribute to defining fractionation routes with tailored ingredient functionality.

1.2 Plant proteins

Plant-based ingredients that are commercially available originate from soybean, wheat and pea mostly. More recently, also protein concentrates or isolates from other plant sources appeared commercially, amongst others from rapeseed, mung bean, lupine, algae, rice and oats [5]. Research into the exploitation of new plant protein sources is ongoing. In addition to protein functionality, relevant factors in the selection of plant protein sources are availability, costs, and nutritional value [6, 7]. A schematic categorization of plant protein source categories is given in Fig. 1.1.

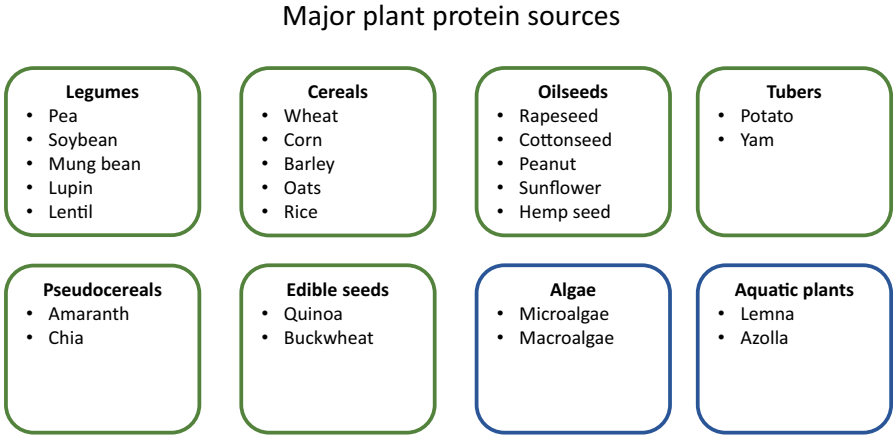

Figure 1.1 Overview of major plant protein sources, classified by origin [8-13]. Adapted from Loveday (2020) with permission.

The majority of the plant protein sources fall in the legume category [9]. Pea is one of the legumes that has been subject of a variety of studies. Available pea-based ingredients are pea starch and pea protein concentrate and isolate. An advantage of legumes, including pea, is that these plants can fixate nitrogen [14-16]. It has further been reported for pea that it has a low allergenicity and quite a complete essential amino acids profile [17, 18]. Like most legumes, pea lacks sulphur-rich amino acids and contains anti-nutritional components [17, 19].

1.3 Pea proteins and other constituents

The major constituents of pea are protein (17 – 30%) and starch (43 – 45%). The variation in composition can be explained by differences in climate and growth conditions, and also vary between pea cultivars [20-24]. Pea protein and starch are present in the pea cotyledon, where the proteins are situated in protein bodies and the starch in starch granules. Fig. 1.2 shows electron microscope images of the pea cotyledon and a storage cell within the cotyledon that contains protein bodies and starch granules. Pea also contains a variety of minor components, which includes the oligosaccharides raffinose, stachyose and verbascose (5%), minerals (4%), fat (2%), phytic acid (1%) and other antinutrients [25-27].

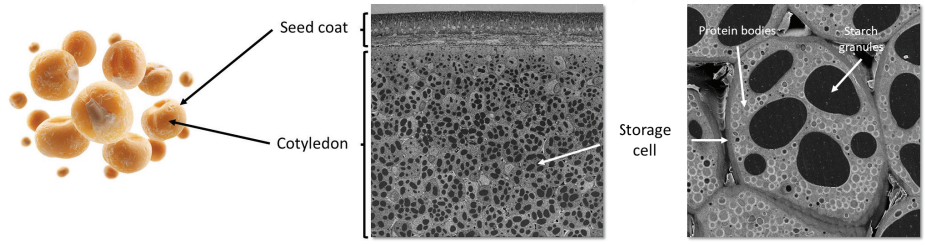

Figure 1.2 Electron microscopy images of the pea seed coat and cotyledon (middle) and of a storage cell within the cotyledon (right)

Pea protein is classified into globulins and albumins with a relative abundance of about 70% and 30%, respectively [28]. This classification originates from the Osborne classification that is based on the solubility properties, with albumins being soluble in water and globulins being soluble in dilute saline [29]. Globulin is the main pea storage protein [30] and is subclassified into 11S legumin, 7S vicilin and 8S convicilin, based on their sedimentation coefficients. Legumin is the largest pea globulin, which has a molecular weight of 320 – 380 kDa in its hexameric form [31, 32]. Depending on pH and ionic strength conditions however, legumin can dissociate into trimers and monomers [33]. A legumin monomer consists of an acidic (40 kDa) and basic subunit (20 kDa) that are linked by a disulphide bond [31, 34]. The second globulin subclass, vicilin, is typically present as trimer of 150 – 200 kDa. Vicilin trimers are built of monomers that show great molecular variety because of post-translational processing and glycosylation [35-37]. The different peptides remain associated to the vicilin trimer and have molecular weights ranging between 12.5 and 50 kDa [37,

[38]. The third globulin, convicilin, is a protein of around 70 kDa, which can form trimers of around 210 kDa. These trimers may also be heteromeric with both vicilin and convicilin polypeptides [39, 40]. In contrast to vicilin, convicilin is not known to undergo post-translation modification, nor is it glycosylated [38]. There is, however, no consensus as to whether convicilin is a separate storage protein. O'Kane et al. (2004) argued that convicilin should actually be denoted as an α-subunit of vicilin, based on a comparison with soy β-conglycinin and a comparison on vicilin and convicilin denaturation behaviour [40]. There is thus a dichotomy in literature regarding convicilin being a separate storage protein or belonging to the vicilin gene family. However, from a functionality point-of-view convicilin can be considered functionally distinct, as differences were seen between vicilin and convicilin in for instance heat-set gelation behaviour [41].

Pea albumin (PA) is a separate protein class The albumin family comprises different proteins, including PA1, PA2, lectin, lipoxygenase and protease inhibitors [42, 43]. The most abundant PA1 and PA2 are typically present as dimers with a molecular weight of around 10 and 50 kDa, respectively [44]. Albumin has received less attention in scientific research. This may be attributed to the fact that commonly applied aqueous fractionation recover only globulins, as albumins remain soluble upon precipitation and washing steps [32]. In fact, albumins are sometimes considered a by-product from the aqueous fractionation process [40]. One major disadvantage of the albumin protein class as a functional ingredient is that part of these proteins are antinutrients. This means that they can bind nutrients (e.g. phytic acid bind minerals) or inhibit enzymes (e.g. protease inhibitors) [45, 46]. Antinutrients generally need to be deactivated prior to application in food products [47, 48].

1.4 Pea protein fractionation

In industry, part of the pea seeds is fractionated so that the pea components can be used as functional ingredients in food applications. Such fractions are typically protein or starch concentrates and isolates, depending on the extent of fractionation and level of protein or starch purity (an isolate is purer than a concentrate). Industrially, pea protein could sometimes be considered a by-product from the main pea starch fractionation process. The first step in starch and protein fractionation is milling of the seed, either with hulls or de-hulled. If the subsequent fractionation process is designed to obtain protein-enriched fractions, insoluble components including starch granules are removed, for instance by centrifugation. Further fractionation often involves the removal of the soluble components, such as oligosaccharides and minerals, and can yield protein fractions with high purities. Aqueous fractionation is the mainstream protein fractionation process, which typically involves alkaline extraction followed by either isoelectric precipitation or membrane filtration [49, 50]. In an industrial process the pea protein is normally also pasteurized upon fractionation [51]. Fig. 1.3 shows a schematic overview of the steps involved in aqueous fractionation.

In recent years there has been an increased interest in sustainable fractionation, but aqueous or wet fractionation is still the most applied fractionation method in literature [49, 52-55]. The main alternative for aqueous fractionation processes is dry fractionation [56, 57]. In addition, a hybrid fractionation process was proposed that combines dry fractionation with part of the aqueous fractionation process [57, 58]. Despite of the advancements in plant protein fractionation, some argue that current fractionation processes are not optimized in terms of sustainability and protein functionality [49, 59]. While most studies focus on alternative more sustainable fractionation methods, there is limited research focussing on mild fractionation. Mild fractionation may not only be more sustainable, but could also lead to different functional properties for plant protein. In this thesis we take a commonly applied aqueous fractionation process as a starting point and modify it by applying fewer or alternative fractionation steps, so that less water and energy is required. We then use the obtained fractions and study their molecular and microstructural characteristics to establish a relation between fractionation and functionality.

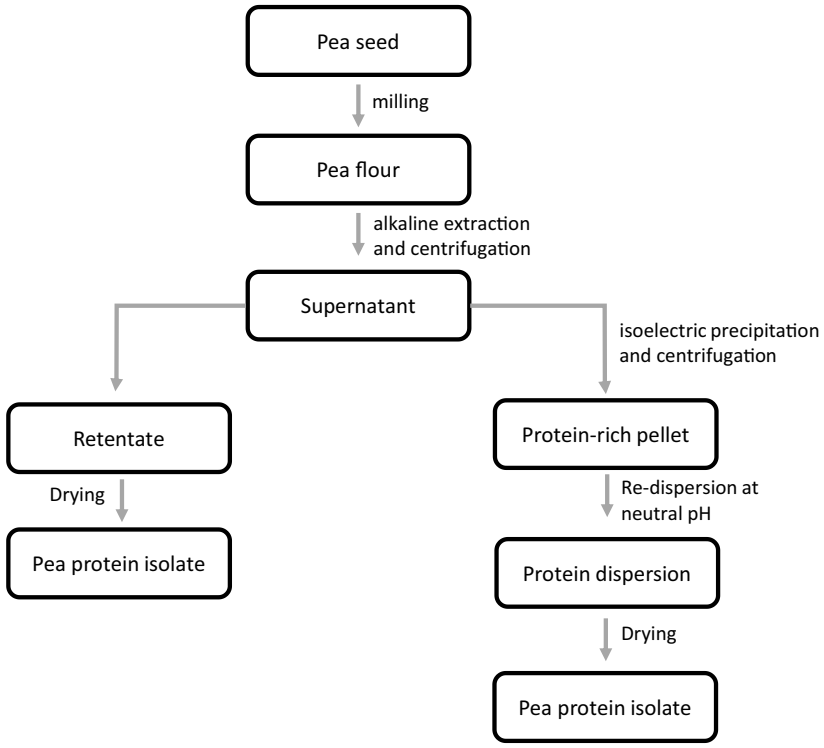

Figure 1.3 Simplified overview of the mainstream aqueous protein fractionation processes with alkaline extraction followed by either membrane filtration or isoelectric precipitation [49-51]

1.5 Pea protein functionality

Pea protein functionality is a central concept in this thesis. Functionality comprises properties such as solubility and the ability to form and / or stabilize foams, emulsions, and gels. This ability is generally related to plant protein properties, and solvent properties, like pH, ionic strength, and temperature. Fractionation processes can influence functionality, for instance by changing the composition of the fraction or by chancing the state of the proteins (e.g., denatured, partially denatured, aggregated).

When studying the functionality of pea protein in a dispersed or dissolved state (e.g., plant-based milks, high-protein beverages and infant or sports nutrition) solubility, viscosity and thermal stability are important factors to consider. Regarding the first, solubility, it is common practice to define it as the amount of protein that remains in the supernatant after applying a certain centrifugal force [21, 50, 55, 60-64]. It has been reported that globulins have a high solubility at an alkaline pH of 8-9 and a low solubility around pH 4.5 [20, 31, 55]. The solubility of legumin and vicilin depend on ionic strength. When establishing a link between fractionation and functionality it is thus relevant to consider that the solubility may be affected upon fractionation. The second, the viscosity of protein solutions or dispersions, depends on different factors. A simple approximation of a diluted pea protein dispersion is to consider it as suspension containing hard spheres. In such dispersion, viscosity only depends on the volume fraction of the spheres, as established by Einstein in 1905 [65]. However, at higher concentrations, factors such as excluded volume fraction (i.e. the excluded volume between particles caused by electrostatic or steric repulsion [66]) and interactions between proteins, become important. The third factor, thermal stability, is relevant for food products for that should gel upon heating (e.g., plant-based eggs) or for products that need to be pasteurized or sterilized without affecting the properties. The heat-set gelling behaviour of pea protein has been widely studied and is, amongst others, influenced by protein composition (e.g., legumin / vicilin ratio) and fractionation method [67-70].

Several food products can be described as an oil or air phase dispersed in protein solutions or soft solids. The emulsifying properties of pea protein have been extensively studied as well as the effect of fractionation method [21, 50, 71] and solubility [36, 62, 72]. Also, the foaming properties of pea proteins – mostly obtained through aqueous fractionation – has been reported in different studies [36, 61, 71, 73]. A common conclusion that can be drawn from those studies is that pea proteins can form gels

and stabilize foams and emulsions, and that their performance is highly dependent on the conditions (i.e. pH, temperature, ionic strength) and the fractionation method used. An emulsion-filled gel can be formed by gelling proteins in the continuous phase of an emulsion, using for instance heat or acidification. This results in a protein network in which oil droplets are incorporated [74]. Understanding the properties of emulsion-filled gels is relevant for designing novel food products such as plant-based cheeses. So far, most studies on emulsion-filled gels use dairy proteins as a gelling agent, and there are only a few studies where plant proteins were used [75-77]. To understand the formation of plant protein emulsion-filled gels it could be beneficial to understand the plant protein behaviour in gels and emulsions, as well as the interactions between the droplets and surrounding gelled matrix.

Part of this thesis also addresses gels from mixtures of plant and dairy proteins. The insights obtained from studies on such model mixtures is relevant for hybrid plant-dairy protein foods. An advantage of hybrid foods is that it can be easier to maintain the structural and sensorial properties of the original dairy product it is meant to replace. Moreover, it can be beneficial from a nutritional perspective to combine dairy and plant proteins, rather than completely replacing dairy proteins [78]. There is a variety of studies on the functionality of plant – dairy protein mixtures, and a few on the heat-set gelation and aggregation of pea and whey protein mixtures [79, 80] or pea proteins with casein micelles [81].

1.6 Rationale and thesis outline

In this thesis we use yellow pea to study how milder or limited fractionation influences protein functionality. Our starting point is a commonly applied aqueous fractionation process involving alkaline extraction and isoelectric precipitation. We initially focus on the question how mild or limited pea protein fractionation affect the resulting protein functionality. In later chapters our focus evolved towards fractionation that is tailored to obtain specific protein functionality. The **aim** of this thesis thus is to establish the effect of mild aqueous fractionation routes on the functionality of pea protein in terms of molecular and microstructural characteristics, in a variety of food model systems. The results of this thesis may guide scientists and ingredient manufacturers to modify their mainstream processes in such a way that fractionation becomes tailored to specific protein functionality needs. The thesis outline is given below, and schematically presented in Fig. 1.4.

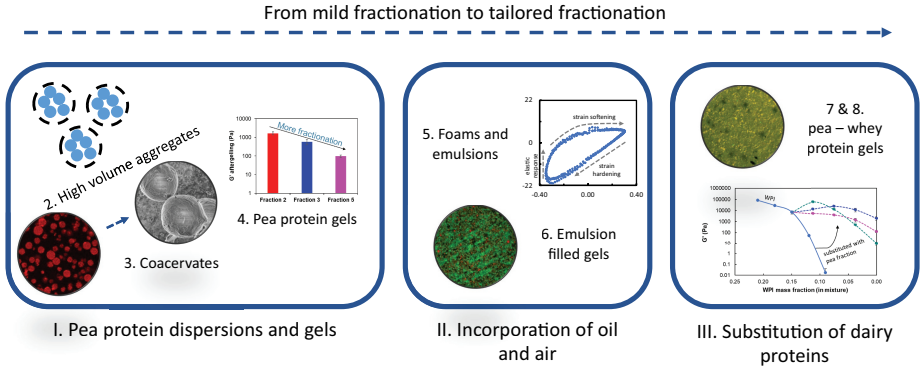

Figure 1.4 Overview of the thesis content in three parts. The numbers correspond with the chapters.

In **Chapter 2 - 4** the behaviour of pea protein in dispersed state is studied. In **Chapter 2** the effect of aqueous fractionation processing on pea protein fraction composition and viscosity is discussed. **Chapter 3** covers the behaviour of the same dispersed pea protein fractions at a range of pH and ionic strengths. In **Chapter 4** the pea protein fractions are heated to study their gelation behaviour.

In **Chapter 5 and 6**, oil and air are incorporated in pea protein fraction dispersions and gels. **Chapter 5** discusses the emulsion and foam properties of an albumin fraction, a globulin fraction and of a pea protein concentrate. In **Chapter 6** the effect

of different fractionation routes on emulsion-filled gelling capacity is discussed.

Chapters 7 and 8 discuss the behaviour of mixtures of pea and whey protein in dispersions and gels. In **Chapter 7** three pea protein isolates obtained via different fractionation routes are studied on their ability to replace whey protein isolate partially or completely, in dispersions and gels. **Chapter 8** discusses the use of less processed pea protein fractions in the context of whey protein isolate substitution in heat-set gels.

Chapter 9 summarizes the obtained results in a wider perspective by relating it to other research on plant protein dispersions, gels, emulsions, plant-dairy protein interactions and emulsion-filled gels. It also provides a literature overview on the relation between pea protein fractionation and functionality. Finally, the potential of pea protein as functional ingredients is discussed and a future outlook is provided.

Chapter 2

Yellow pea aqueous fractionation increases the specific volume fractions and viscosity of its dispersions

2

Abstract

Some studies have shown that mild fractionation may result in similar or even better functional properties, than those of highly purified ingredients. This study aimed to relate the level of aqueous purification to the composition, solubility and viscosity of yellow pea fractions. A seldomly used method of cryo-planing combined with Cryo-SEM revealed the presence of protein bodies and starch granules in the seeds and flour, with sizes of ~ 3 μm and ~20 μm, respectively. Fractions with protein purities ranging from 40 to 85 wt. % were obtained from the flour and characterized. These fractions were also compared to commerially available pea protein isolate. The fractions that were only exposed to a solubilisation step contained high quantities of carbohydrates (23.6 wt. %), which were mostly present as oligosaccharides. Subsequent fractionation steps increased the protein content and changed the ratio between the different pea proteins to some extent.We found that more fractionation steps reduced the solubility of the fractions. The most purified fraction contained 17 wt. % insoluble protein aggregates with radii ≥ 100 nm. This fraction showed a substantial thickening capacity, with a viscosity of up to 10^3 mPa.s at a concentration of 23 wt. %. The impurities (i.e. sugars, starch granules) present in the fractions only had a small effect on viscosity. Based on the protein specific volume fraction and particle size analysis, it was concluded that pea protein can form aggregates with a rarefied structure responsible for its thickening capacity.

This chapter is published as:

Kornet, C., Venema, P., Nijsse, J., van der Linden, E., van der Goot, A. J., & Meinders, M. (2020). Yellow pea aqueous fractionation increases the specific volume fraction and viscosity of its dispersions. Food Hydrocolloids, 99, 105332.

2.1. Introduction

The global protein demand is expected to grow rapidly in the coming years, due to an increasing world population and global welfare. To keep up with this demand, new initiatives are required to increase the production of high quality, functional and sustainable proteins [2, 49, 57]. One of these initiatives is the transition from animal proteins to more sustainable and cheaper plant derived proteins. In order to make plant proteins applicable in food products, it is needed to have a thorough understanding of their functionality, such as solubility, gelation, and emulsifying properties. Recent plant protein research is not limited to exploring the functional properties of proteins from different plant sources, but also focusses on synergistic effects with other ingredients and on novel extraction methods [49, 79, 81, 82].

Extensive research has been done on functional properties of proteins from plant sources such as soy, lupine, lentil, beans and peas [21, 22, 49, 83]. Soy is known for its unique functional characteristics and has already made a significant impact in the food industry, for instance as an ingredient for meat analogues or as a wheat flour replacer in bread making [84]. Specifically, in terms of gelling behaviour, soy protein isolate is considered superior compared to lupine and pea protein isolates [85, 86]. However, in contrast to pea, soy does not grow in moderate climates such as in Northern Europe. Hence soy has to be transported over longer distances, thereby possibly reducing its sustainability. In a life cycle assessment this could be a factor impairing the overall sustainability of this protein ingredient. Pea has the same advantage as soy with respect to nitrogen fixation ability, which reduces the need for fertilization [87]. To enhance the functional behaviour of pea proteins, different studies have focussed on synergistic effects with polysaccharides. Pea proteins were combined with polysaccharides, such as, gum arabic, alginate, chitosan, sodium alginate, and high methoxyl pectin, for encapsulation purposes or to enhance foam or emulsion stability [88]. For instance, it was reported that the stability of pea-protein based emulsions could be improved through steric repulsion and increased rigidity of the oil-water interfacial membrane after addition of pectin [89].

A new focus in the field of plant protein research is that development of plant ingredients should focus on functionality rather than purity. Some of the studies supporting this insight also show that functionality can be enhanced through synergistic interaction of pea protein with components naturally present in pea. Although mild processing results in lower protein purity and the presence of other components, such as carbohydrates, salts, phenols and oil, the overall functionality

may be equal or even better than a highly purified pea protein isolate. In previous work a mild aqueous fractionation method was used to obtain protein and starch enriched fractions. These fractions can be used to produce a more stable emulsion relative to emulsions made from commercial available pea ingredients. This enhanced stability was explained by a cooperative effect between the close packing of swollen starch granules and network formation of the protein-stabilized oil droplets [90]. Some studies use dry fractionation as a mild way for obtaining protein-enriched ingredients. Generally, in such a process, pea flour is divided into a protein-rich fine fraction and a starch-rich coarse fraction through grinding, air classification and less commonly, electrostatic separation [49, 56, 57]. Also a hybrid process of aqueous and dry fractionation has been used to fractionate pea flour [57].

To increase ingredient sustainability, mild fractionation methods like aqueous extraction are widely used to obtain functional protein fractions. However, a systematic study that relates the effect of purification steps on resulting composition and bulk behaviour, which allows industry to optimize product quality and sustainability, is missing. In this study we aim to narrow this gap by systematic exploring the effect of mild aqueous fractionation steps on the protein and non-protein composition, solubility and viscosity of the resulting fractions.

2.2 Materials and methods

2.2.1 Materials

Yellow pea seeds were purchased from Alimex Europe BV (Sint Kruis, The Netherlands). A commercial pea protein isolate was obtained from Roquette (Lestrem, France). All chemicals and reagents were obtained from Sigma Aldrich (Schnelldorf, Germany) and were of analytical grade, unless stated differently.

2.2.2 Pea protein fractionation and protein content determination

Five pea fractions varying in protein purity, were obtained by two aqueous extraction processes: a basic process (A) and a full fractionation process (B). Fig. 2.1 shows a schematic overview of both fractionation processes.

Pea flour (200 g, ground at 80 μm) was dispersed in deionized water in a ratio 1:10. In process A the pH was left unadjusted (~pH 6.7) and in process B the pH was adjusted to 8 by adding NaOH. The dispersion was stirred for two hours and centrifuged at 10000g for 30 min. Then the pellet was separated from the protein-enriched supernatant. The supernatant was labelled PPCn (neutral extracted pea protein concentrate) for the basic process A and PPCa (alkaline extracted pea protein concentrate) for the full process B. Part of PPCn was further purified by isoelectric precipitation at pH 4.5. The acid dispersion was then centrifuged, and the protein poor-supernatant was collected and labelled, which is referred to as ALB-F (albumin-fraction). Finally, the pellet was re-dispersed at pH 7 for two hours. This highly purified protein solution was labelled PPIp (precipitated pea protein isolate). The complete extraction process was performed at room temperature. Except for pea flour, all fractions were lyophilized at < 10 °C and < 1 mbar with an Alpha 2-4 LD plus freeze-dryer (Christ, Osterode am Harz, Germany) and then stored at -18 °C. To reduce the risk on chemical and microbiological deterioration, the freezing and lyophilisation time was kept as short as possible. This was achieved by separating the liquid into small volumes.

The ash content was determined by heating the samples to 550 °C in a furnace and weighing the remaining amount of solids afterwards. The protein content was determined from the nitrogen content (Flash EA 1112 series Dumas (Interscience, Breda, The Netherlands)). A nitrogen conversion factor of 5.7 was used. The average value of the conversion factors reported in literature has been used despite the fact that the nitrogen conversion factor may vary throughout the process due to

shifts in protein ratios. The latter could be one of the reasons why different nitrogen conversion factors for pea, ranging from 5.15 – 6.25, have been reported in literature [56, 91, 92]. All protein purities have been expressed as the weight percentage of protein in total dry matter.

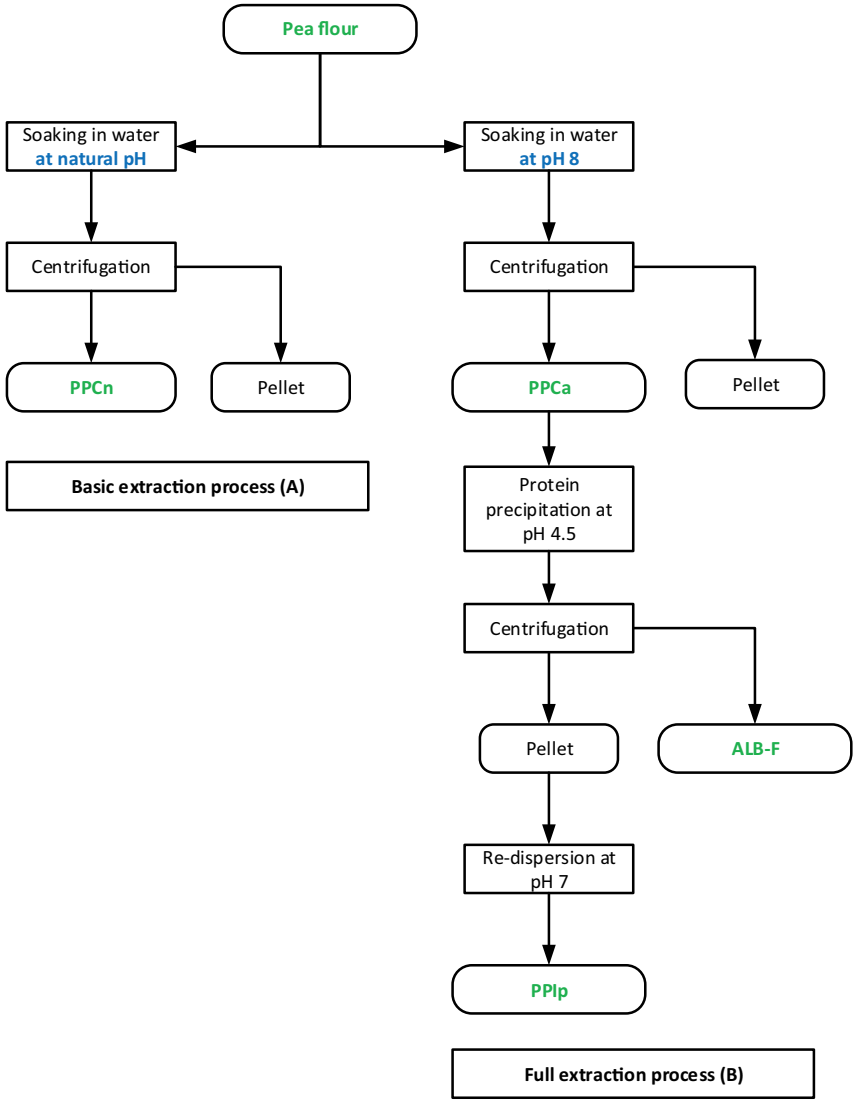

Figure 2.1 Schematic overview of the basic (A) and full extraction process (B) for pea.

2.2.3 Cryo Scanning Electron Microscopy (cryo-SEM) and Energy-dispersive X-ray Spectroscopy (EDS)

Cryo-SEM was used to visualize the yellow pea seed morphology. The peas were overnight imbibed between wet filter paper sheets in order to induce swelling and hence improve contrast of the cell components. A small piece of the imbibed pea was frozen in melting ethane and subsequently cryo-planed in a sealed cryo-chamber using a Leica EM FC7 microtome (Leica Microsystems, Amsterdam, The Netherlands) [93]. The samples were trimmed with a glass knife and further planed with a diamond knife. Subsequently, the block faces were subjected to slight sublimation to obtain depth contrast, and subsequently sputter coated with platinum in an Alto 2500 cryo transfer system (Gatan, Abingdon, UK). Finally, the samples were transferred into the SEM chamber (Auriga field emission SEM, Zeiss, Jena, Germany) and investigated at -125 ˚C. Elemental maps were obtained with the use of Energy-dispersive X-ray Spectroscopy (Aztec X-Max 80mm^2, Oxford Instruments, Abingdon, UK) [94].

2.2.4 Neutral sugar composition as alditol acetates

The monosaccharide composition was determined according to the method of Englyst & Cummings (1984). Pre-hydrolysis was done with 72 wt. % sulphuric acid at 30 ˚C for 1 h, followed by hydrolysis with 1 M sulphuric acid at 100 °C for 1 h. The resulting monosaccharides were derivatized to alditol acetates and analysed by gas chromatography, with inositol as an internal standard [95]. Additionally, the uronic acid content was determined using an automated colorimetric m-hydroxydiphenyl assay [96] on a Skalar autoanalyser (Skalar, Breda, The Netherlands) as described elsewhere [97].

2.2.5 Total starch content

Total starch content was analysed according to AOAC method 996.11 with an enzyme kit from Megazyme (Bray, Ireland). This method included extensive α-amylase and amyloglucosidase enzyme digestion and incubation with p-hydroxybenzoic (GOPOD) reagent combined with glucose oxidase and peroxidase. After incubation with the GOPOD reagent the absorbance was measured and used to calculate the D-glucose content, based on a D-glucose standard.

2.2.6 SDS-PAGE

Non-reducing and reducing SDS-PAGE were performed by using a 4 – 12% BisTris gel and a 20x diluted MES SDS running buffer. Sample was dissolved in deionized water at a concentration of 0.1 wt. %. A volume of 45 µl was added to 15 µl sample

running buffer for non-reducing conditions. For reducing conditions, 6 µl sample running buffer was replaced by 6 µl of 500 mM dithiothreitol (DTT). The sample mixtures were heated to 70 °C for 10 minutes. Then, 15 µl of the sample supernatants were loaded in each well. A marker of 2.5 – 200 kDa was loaded in a well at both sides of the gel. Electrophoresis was performed in a XCell Surelock Mini-Cell for 35 minutes at a constant voltage (200 V). The gels were subsequently stained with SimplyBlue SafeStain and washed with a 20% NaCl solution. These gels were scanned with a Biorad GS900 gel scanner the next day.

2.2.7 Size Exclusion Chromatography (SEC) and High Performance SEC

SEC was used to study the effect of the different processing steps on the type of proteins present in the fractions. Samples were eluted on a Superdex 200 increase 10 / 300 GL column (Merck, Schnelldorf, Germany) with a range of 10 – 600 kDa. The eluent used was a McIlvaine buffer (10 mM citric acid, 20 mM Na_2HPO_4, pH 7, 150 mM NaCl) filtered over 45 µm. Samples were dissolved in the same buffer at concentrations of 5 g/L and centrifuged at maximum speed for 10 minutes. The supernatants were transferred to HPLC vials and separated by an Akta Pure 25 chromatography system (GE Healthcare Europe, Diegem, Belgium). The system was coupled with an UV detection system and wavelengths of 214, 254 and 280 nm were used. To determine molecular masses of the proteins, a calibration curve was made using the following molecules: blue dextran, ferritin, aldolase, ovalbumin, β-lactoglobulin, and α-lactalbumin.

The molecular size of the carbohydrates was determined using HP-SEC coupled with a refractive index (RI) detector. Samples were dissolved in a 0.2 M $NaNO_3$ buffer and diluted to a concentration of 0.2 wt. %. Subsequently, they were centrifuged with a Hermle Z-306 (Hermle Labortechnik GmbH, Wehingen, Germany) eppendorf centrifuge at 3350 g for 10 minutes to ensure the removal of insoluble components. 150 µl of the supernatants were transferred to vials to be measured with an Ultimate 3000 HP-SEC system (Thermo Fisher Scientific, Waltham, United States), coupled with an RI detector. Molecular weights were determined with the use of a Pullulan calibration curve.

2.2.8 Solubility

2 wt. % pea fractions were allowed to dissolve in deionized water for 1 h under moderate stirring conditions. Subsequently, the samples were centrifuged at 17000 g for 30 minutes to remove insoluble components. The obtained supernatants were

freeze dried and weighed. The resulting dry mass was divided by the initial mass to express solubility.

2.2.9 Viscosity

Capillary viscometry

The kinematic viscosities at low concentrations (0 – 5%) were determined with an Ubbelohde viscometer No. 1046928 (SI Analytics, Weilheim, Germany). To calculate the dynamic viscosities from these kinematic viscosities, the densities of the pea fractions at each concentration were determined with a density meter DMA5000 (Anton Paar, Graz, Austria). The shear rate in the capillary was estimated 0.9 – 2.7 s^{-1}, depending on the protein concentration and assuming ideal viscous flow behaviour.

Shear viscosity

The shear viscosity of the pea fractions at different concentrations (5 – 25%) was measured over a shear rate of 1 – 1000 s^{-1}. Samples were analysed in a concentric cylinder (CC17) by an MCR 302 rheometer (Anton Paar, Graz, Austria). The viscosity at a shear rate of 55.8 s^{-1} was used to quantify the effect of concentration. This specific shear rate was the shear rate at which the torque fell within the minimum torque of the rheometer to measure accurately.

Calculations based on viscosity measurements

Krieger-Dougherty's empirical equation (Eq. 2.1) was used to estimate the specific volume fraction as function of concentration.

$$\frac{\eta}{\eta_0} = \left(1 - \frac{\Phi}{\Phi_m}\right)^{-\frac{5}{2}\Phi_m} \tag{2.1}$$

with η and η_0 the viscosities of the dispersion and continuous phase, respectively, Φ is the volume fraction of the dispersed phase and Φ_m the maximum volume fraction.

The viscosity contribution of sugars η_{sugar} was estimated using the empirical equation (Eq. 2.2) of Soesanto & Williams (1981) [98].

$$\eta_{sugar} = Ae^{kV(x)} \tag{2.2}$$

with $A = 6.3 \cdot 10^{-6}$ Pa.s and $k = 282 \cdot 10^3$ mol/kg are empirical coefficients and $V(x) = V_w + xV_s$ with x is the molar concentration of the sugar, and V_w and V_s are the molar volume of the solvent (water) and sugar respectively. The viscosity of the continuous phase in Eq. 2.2 is taken that of the sugar solution, thus $\eta_0 = \eta_{sugar}$.

An estimate of the radius *a* of the dispersed aggregates was obtained by the following equation (Eq. 2.3) for the Peclet number Pe.

$$Pe = \frac{8\pi G a^4 \Delta\rho}{3k_b T} \quad (2.3)$$

Here G is the centrifugal acceleration, k_b is Boltzmann's constant, and Δρ is the density difference between the solvent and aggregates. Evaluating Eq. 2.3 for Pe~1 gives an upper estimate for the radius of the aggregates that are still dispersed after the centrifugation step in the solubility experiment (2.2.8).

2.2.10 Particle size analysis

The particle size distribution of solutions from pea fractions in a concentration range of 10^{-5} to 10^{0} wt. % was measured using Multi-angle Dynamic Light Scattering (MADLS) with a Zetasizer Ultra (Malvern, Worcestershire, United Kingdom). The samples were dissolved in deionized water and the pH was adjusted to pH 7. The hydrodynamic radii were determined by the ZS Explorer software.

2.2.11 Statistical analysis

All measurements were performed at least in duplicate. The standard deviation of the mean value was calculated and used as a measure of the error. IBM SPSS Statistics 25 (IBM SPSS Inc., Chicago, USA) was used to apply one way ANOVA using post-hoc method Tukey. Significance was defined as $P < 0.05$.

2.3. Results and discussion

2.3.1 Yellow pea morphology and the effect of grinding

For a better understanding of the morphology of pea the seed was studied with Cryo-SEM (Fig. 2.2). To optimize the image quality, cryo-planing was used. Image 1 shows the outer seed coat and part of the cotyledon. Fig. 2.2B and C show that this cotyledon is filled with storage cells. The storage cells are by far the most abundant cell type in pea. The apparent sizes of storage cells range from 40 - 140 μm, containing starch granules (5 - 30 μm) and protein bodies (2 - 4 μm). These sizes are in line with those found in previous research, where sizes of 19 – 35 μm were reported for the starch granules (dry) and sizes of 1 – 3 μm for protein bodies [99-101]. The identification of starch granules and protein bodies were confirmed by EDS (Fig. 2.2D). The starch granules correspond with the regions of the carbon signal and the smaller spherical protein bodies correspond with the regions of the nitrogen signal. Fig. 2.2E and F show higher magnifications of the pea protein bodies. The appearance of the protein bodies varied between greyish and black, with a grey outer ring. This difference in electron emission between protein bodies could result from a different cryo-planing depth or a different orientation of the protein bodies. It could also be an artefact resulting from differences in ice crystal formation during the cryofixation step.

The first processing step in the fractionation process is grinding. This step is essential, because the cell should be fractured to liberate the starch granules and protein bodies. Fig. 2.3 shows pea flour ground to a mesh cut off size of 45 μm. The cells are broken up, but a large proportion of starch granules are still intact as can be concluded from the intact ellipsoid shapes. The smaller lumps associated with the starch granules are mainly protein bodies. The starch granules remain intact during dispersion at room temperature. Hence, they are insoluble and can be separated from the soluble components after the first centrifugation step.

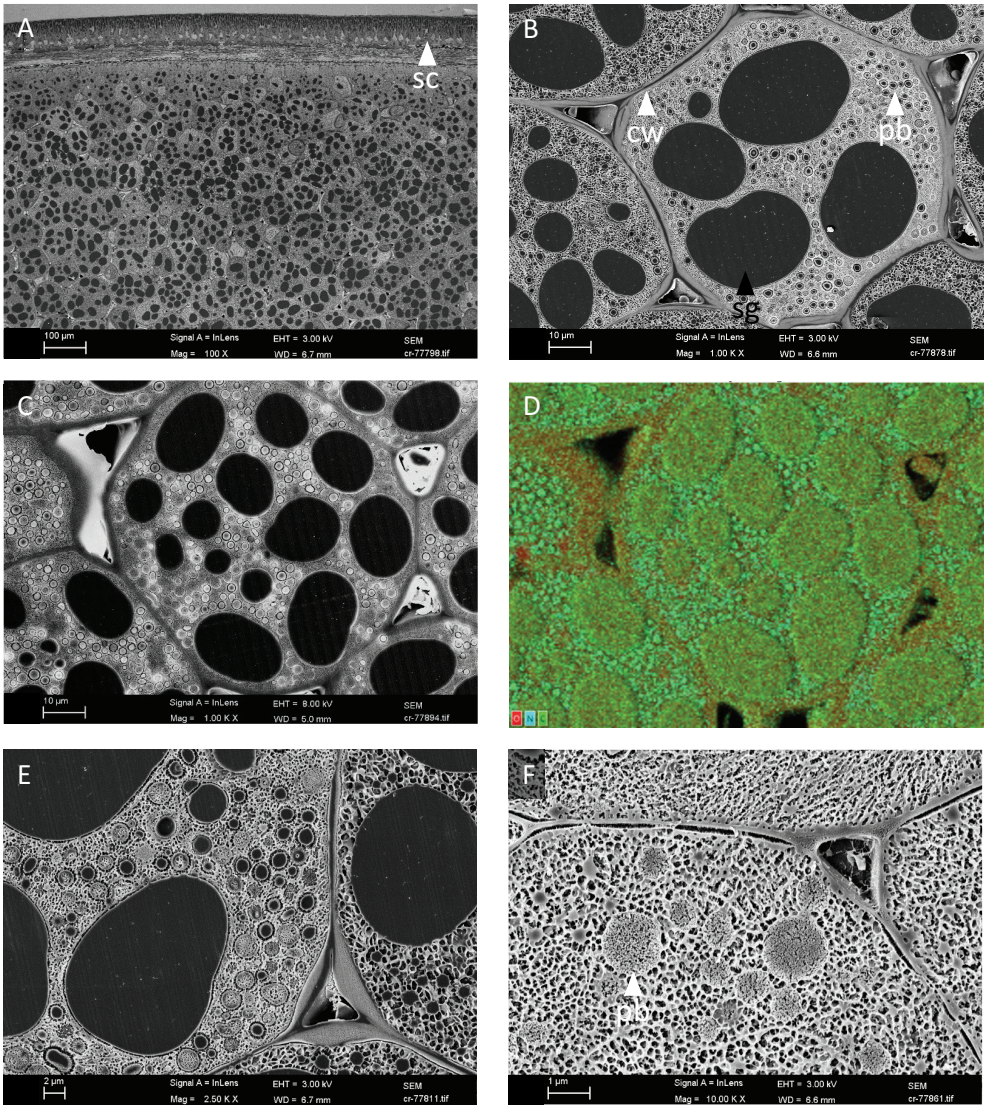

Figure 2.2 Morphology of imbibed yellow pea at different magnifications. A. Overview showing (sc) seed coat and cotyledon with storage cells. B. Storage cells containing (sg) starch granules, (pb) protein bodies, protected by a (cw) cell wall. C shows a storage cell and D an elemental map of the same area, where red = oxygen, blue = nitrogen and green = carbon. 5 and 6 shows the cell components at higher magnifications. Scale bars A : 100 µm, B-D : 10 µm, E : 2 µm and F : 1 µm.

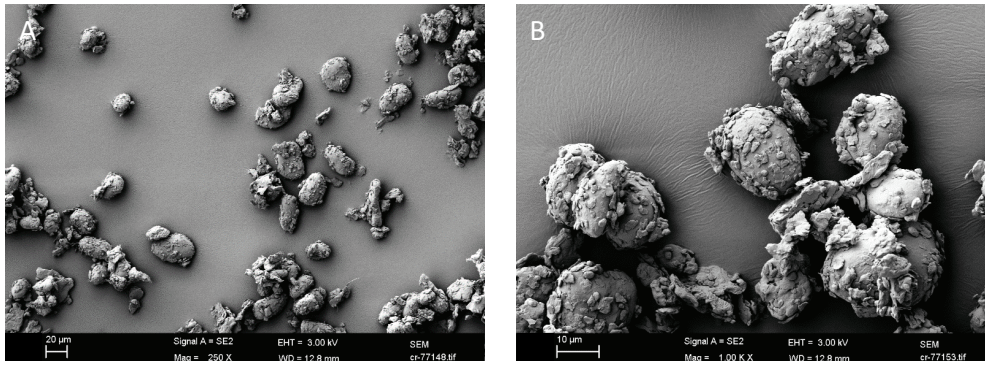

Figure 2.3 Yellow pea ground into flour, showing starch granules associated with protein bodies. Scale bars A. 20 µm, B. 10 µm

2.3.2 *Effect of processing on the composition of the fractions*

The effect of each purification step on the composition was studied in the pea aqueous extraction process (Table 2.1). The first step was grinding of pea seeds into pea flour. This flour was considered the first functional fraction, labelled as pea flour. PPCn (neutral extracted) and PPCa (alkaline exctracted) were obtained by a simple solubilisation step at unadjusted pH and pH 8, respectively, and resulted in fractions with a protein content of more than 46 and 51 wt. %, respectively.

Table 2.1 Dry matter composition (g / 100 g d.m.) of the pea flour fractions, insoluble part of pea (residue) and the commercial pea protein isolate (PPIc). The recovery (%) is defined as the recovered amount of protein divided over the initial protein content in the flour.

	Recovery (%)	**Protein content (wt. %)**	**Total carbohydrate content (wt. %)**	**Starch or starch derivative content (wt. %)**	**Ash content (wt. %)**
Pea flour	100	18.8	59.8	48.7	3.7
PPCn	53	46.3	30.9	4.1	13.2
PPCa	70	51.4	23.6	3.5	11.8
ALB-F	17	21.1	34.8	6.0	21.1
PPIp	44	87.3	3.4	0.3	6.0
Residue	NA	6.6	76.6	64.6	4.9
PPIc	NA	80.7	4.4	0.1	1.5

Additional purification (process B) by protein precipitation at pH 4.5 and subsequent centrifugation resulted in a protein-poor supernatant ALB-F (albumin-fraction) and a protein-rich pellet. This pellet was re-solubilized to obtain PPIp (precipitated pea protein isolate) containing 87% protein. It has been reported that pea contains around 2% fat, so it is assumed that the purified fractions contain only a negligible amount of oil [21, 102]. The protein purity of the pea protein isolate (PPI), labelled as PPIp, is consistent with that of the commercially obtained PPI (PPIc) and those found in other studies using similar aqueous extraction processes. Other studies reported protein purities of 90 – 95 wt. % (on dry matter basis) and yields of up to 80 wt. % [35, 50]. When correcting for the higher nitrogen conversion factor used in these studies, similar protein purities are found. Some studies reported higher proteins yields, which are often reached by solubilisation in extreme alkali environments (pH 9 – 10). However, in such conditions proteins are susceptible to a higher degree of protein denaturation, which might reduce the functionality of the protein isolate [68]. Moreover, differences in protein and starch purities and yields among literature sources can be caused by variations between pea cultivars and are dependent on climate conditions. A protein content of 18 – 30 wt. % and starch content of 43 and 45 wt. % has been reported for the whole seed [20, 21, 23, 24]. In conclusion, the extraction yield and purities found in this study are comparable with those reported in literature using other aqueous extraction processes.

Carbohydrate characterization

Pea is a seed rich in carbohydrates, which are mostly present in the form of starch granules. The presence of polysaccharides influences functional behaviour, dependent on their degree of polymerisation and degree of complexation. To determine which carbohydrates are present in the five fractions, the sugar composition was analysed. To evaluate their potential effect on the functional behaviour of these fractions the molecular weight of the carbohydrates was also determined.

Table 2.2 shows the monosaccharide composition of the five fractions, including the pellet or residue after the first solubilisation step at pH 8 (process B). Most of the saccharides are removed in the first processing step, but all fractions still contain a certain amount of saccharides. Glucose is the predominant monosaccharides present in all fractions, most likely originating from amylose, amylopectin and the pea oligosaccharides raffinose and stachyose. The starch molecules could emanate from remaining starch granules. The presence of uronic acid and rhamnose suggest original presence of pectin. Other saccharides could originate from polysaccharides such as galactose and arabinose, and soluble oligosaccharides such as raffinose and

stachyose [103]. From a functionality perspective it is important to determine whether the carbohydrates are present as mono-, oligo- or polysaccharides. Mono- and disaccharides are small and interact weakly, whereas polysaccharides may interact and contribute to the viscosity in a dispersion.

Table 2.2 Total saccharide composition (mole %) after hydrolysis of the pea flour fractions, insoluble part of pea and the commercial pea protein isolate. The samples were analysed on rhamnose, arabinose, xylose, mannose, galactose, glucose and uronic acid content. ND = not detected.

	Rha	Ara	Xyl	Man	Gal	Glc	Uronic acid
Pea flour	0.9	6.6	2.2	1.2	5.4	79	4.4
PPCn	1.2	2.5	0.2	6.9	34	52	3.1
PPCa	1.2	2.5	0.2	7.2	33	52	3.7
ALB-F	0.5	1.8	0.1	7.2	34	54	2.7
PPIp	NM	6.8	ND	17	20	36	20
Residue	0.6	6.9	2.1	0.2	1.5	84	4.7
PPIc	1.5	21	2.0	7.2	19	37	13

Fig. 2.4 shows an HP-SEC chromatogram of the five pea fractions analysed with a refractive index detector. Similar peaks were found for all fractions, varying in height. The four peaks at retention times 12.46, 13.92, 14.74 and 15.64 min correspond with molecular weights of 2743, 456, 165 and 55 Da, respectively. The 55 Da peak could not be the buffer salt, as the eluent and buffer were the same in this experiment. Most likely, this peak corresponds with sucrose, which is the most abundant sugar in pea. The peaks at 165 and 456 Da may correspond with the major pea oligosaccharides raffinose and stachyose. Raffinose is a trisaccharide composed of galactose, glucose and fructose and stachyose is a tetrasaccharide consisting of two galactose, one glucose and one fructose unit [104, 105].

A minor part of the carbohydrates are present as small polysaccharides. The relative area under the 2743 Da peaks ranges from 6.6% for PPCn to 2.1% for ALB-F. This means that there is more than ten times less polysaccharides than oligosaccharides. Hence, they would have a minor effect on the viscosity of these fractions. Although higher sugar content may influence the functional behaviour by increasing the thermal stability of proteins, it is not expected that sugars have a significant influence on the viscosity of non-heated mixtures [106, 107]. It is also noted that Fig.

2.4 only shows the soluble polysaccharide fraction and does not show the starch polymers that are present within the starch granules. Pea flour contains a high amount of starch granules since no centrifugation step was applied at this point, but smaller starch granules could be present in the other fractions given the high glucose quantities. These starch granules could influence functionality when exposed to a thermal treatment.

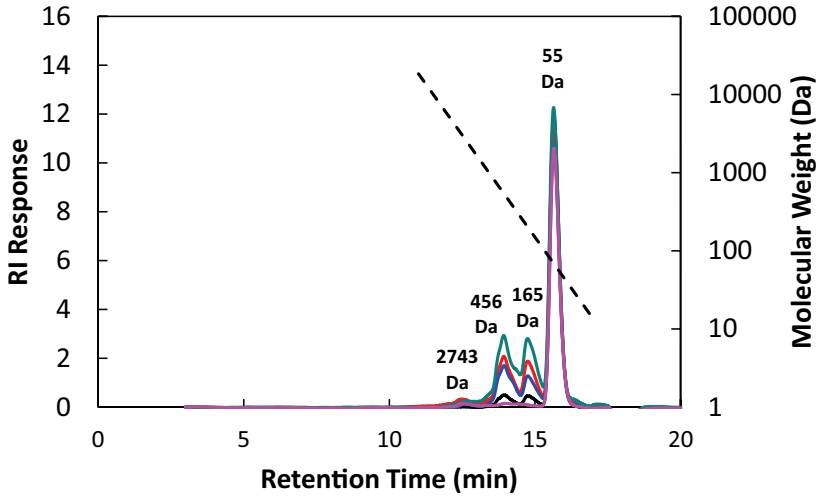

Figure 2.4 HP-SEC chromatogram of the five pea fractions, showing the RI response as function of retention time. Pea flour (—), PPCn (—), PPCa (—), ALB-F (—), PPIp (—). Molecular mass is indicated by a dashed black line.

Protein characterization

The SDS-Page profiles were analyzed to compare the protein composition after the aqueous extraction process to a commercial pea protein isolate and to what has been reported in literature. Furthermore, it gives an impression about the effect of purification on the protein composition.

Fig. 2.5A and Fig. 2.5B represents SDS-PAGE profiles under reducing and non-reducing conditions respectively. In both conditions SDS was added which means that all non-covalent bonds were broken and the proteins were present as monomers or dimers. Fig. 2.5A shows profiles in which, also the covalent bonds were broken using DTT. The main difference between the two is the presence of the 60 kDa legumin in Fig. 2.5B. Under reducing conditions, the disulphide bonds between the legumin subunits are cleaved by DTT. However, even under non-reducing

conditions part of the legumin is present as subunits, as indicated by the bands at 20 and 40 kDa in Fig. 2.5B.

In Fig. 2.5A band intensities differ because the samples vary in protein purity. There were no clear differences in band patterns observed between the fractions, except for the ALB-F. This fraction represents the supernatant after protein precipitation, and is expected to consist of proteins that are soluble at acidic pH. It indeed lacks most of the globulin subunits and shows a light band at 6 kDa, which represents low molecular weight albumins [54]. A similar observation is seen in Fig. 2.5B. It is also noted that the minor differences between fractions and the absence of smear indicate that the extraction process does not cause significant changes to the proteins (e.g. by seed proteolytic enzymes). Finally, it can be concluded that the PPIc contains the same type of proteins. The band intensities are lower compared to PPIp, due to poorer solubility of the PPIc.

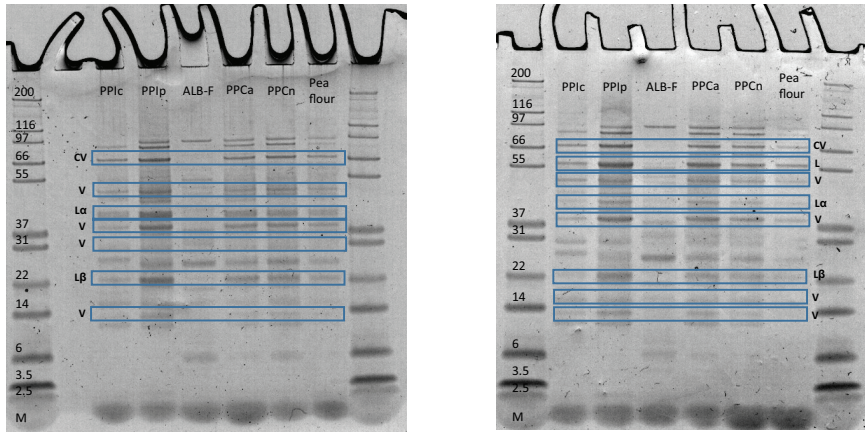

Figure 2.5 SDS-PAGE profiles of the yellow pea fractions under reducing (A) and non-reducing (B) conditions. Lane M indicates the standard protein marker (200 – 2.5 kDa). F1 – F5 correspond with yellow pea fractions 1 – 5 and C-PPI corresponds with the commercial pea protein isolate. The bands are probably corresponding with CV (Convicilin), L (Legumin subunit), V (Vicilin), Lα (Legumin alpha subunit) and Lβ (Legumin beta subunit), based on O'Kane (2004) [69].

To clarify the effect of the fractionation processes, and specifically the protein precipitation step on the protein composition of the resulting ALB-F and PPIp, the fractions were separated chromatographically. This complementary analysis made it possible to study a broader molecular range which also included the sizes of the native proteins. Fig. 2.6 shows the result of a SEC analysis coupled with UV detec-

tion where the five fractions are standardized on protein content.

The left part of Fig. 2.6 shows chromatograms of the five pea fractions. The peak surface corresponds to the protein content of the fractions. Because molecular weights of the proteins were quite close and peaks were overlapping, the protein content has not been quantified. However, the height differences provide a rough indication of the differences in protein content. The first peak corresponds with a molecular size of 487 kDa that indicates legumin hexamers. This molecular weight is close to the reported 320 – 380 kDa for legumin hexamers (S11) [36]. The native convicilin has a molecular weight of ~290 kDa, with a subunit of ~70 kDa [108]. This globulin probably corresponds with the smaller peak at 283 kDa. The third pea globulin vicilin (7S) has a molecular weight of 150 – 190 kDa in its trimeric state [109], which corresponds to the third peak from the left.

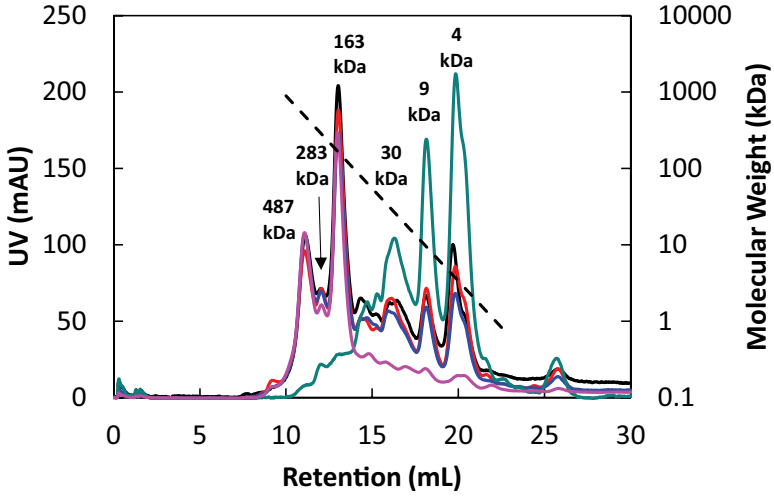

Figure 2.6 SEC chromatogram of the five yellow pea fractions (standardized on protein content) with UV detection at 214 nm as function of retention volume. Pea flour (—), PPCn (—), PPCa (—), ALB-F (—), PPIp (—). Molecular mass is indicated by the dashed black line.

Fig. 2.6 shows that the pea globulins are almost absent in the ALB-F. The ALB-F shows peaks at later retention times, whereas PPIp does not. These peaks correspond to smaller proteins, such as vicilin subunits and albumins. This is in line with what is shown in Fig. 2.5, and confirms that protein precipitation at pH 4.5 separates the larger globulins from the smaller subunits and albumins, with a cut off molecular

mass of ~ 80 kDa. The separation of albumins can be explained by their hydrophilicity and higher pI, which is at pH 8.03 when determined theoretically.

It is expected that these smaller pea proteins possess different functional behaviour. Albumins are small polypeptides (~50 and ~10 kDa in dimeric state) but contain 23% of all thiol groups that are present in pea seeds [110]. From a functionality perspective, the presence of these thiol groups could lead to disulphide bridge formation after heating. Furthermore, since albumins are small and hydrophilic they will contribute to the overall solubility and are expected to have minor effect on viscosity.

2.3.3 Bulk behaviour of pea fractions

Solubility

An important parameter associated with protein functionality is solubility. For instance, to enable surface adsorption of proteins to occur in emulsification processes, solubility is required. Protein solubility is thermodynamically defined as the concentration of protein in a saturated solution that is in equilibrium with a solid phase, under fixed conditions [111, 112]. Conditions that are relevant include temperature, pH, ionic strength and solvent additives [113]. Furthermore, solubility depends on hydrophilicity, electrostatic repulsion and hydrophobic and sulfhydryl disulphide interactions between proteins and peptides [114].

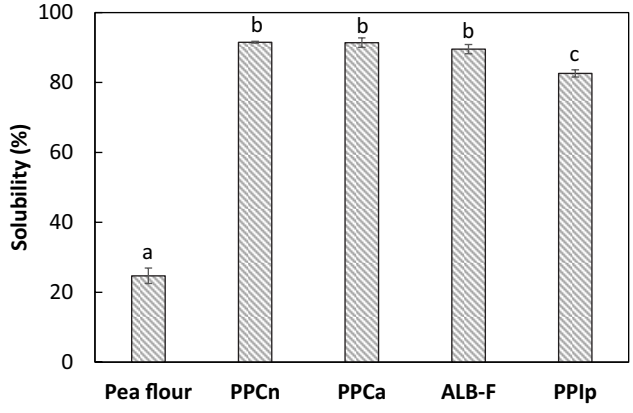

Figure 2.7 Dry matter solubility of the five yellow pea fractions at pH 7.

Although the common solubility measurement based on centrifugation does not measure the solubility according to thermodynamics, it reflects the time and centrifugal dependence of aggregates to remain in solution. Everything that remains

dispersed under these conditions, are not expected to sediment at 1 g within months. Fig. 2.7 shows the overall solubility of the five pea fractions at pH 7 and is expressed as the percentage dry matter left in the supernatant after centrifugation. The letters above the bars show statistical differences, indicating that PPCn, PPCa and the ALB-F are equally soluble. Pea flour is only 25% soluble, mainly due to the presence of starch granules and other cell wall material. The milder processed PPCn and PPCa show a solubility of 91%. Also the ALB-F shows a similar high solubility. This fraction is lower in protein but contains a higher amount of soluble oligosaccharides. PPIp is 83% soluble, which is less than the milder processed PPCn and PPCa. This observation also holds when compared on nitrogen solubility, which are 94% and 85% for PPCa and PPIp respectively (not shown in Fig. 2.7). The difference between PPCn, PPCa and the ALB-F and PPIp could be a result of the protein precipitation step that is required to obtain PPIp. It was found that protein precipitation may result in irreversible changes in the tertiary protein structure of soy protein and pea globulins [33, 115]. Such changes could induce hydrophobic interaction and aggregate formation, reducing the solubility.

Zero shear and shear dependent viscosity

The pea fractions resulting from a different number of fractionation steps were studied on their thickening properties by measuring their viscosities. Both zero shear (t = 1 – 3 min) and shear dependent viscosity were measured at a low concentration (0 – 5 wt. %) and high concentration (10 – 25 wt. %) regimes. The zero shear viscosities of PPCn, PPCa, ALB-F and PPIp were measured with a capillary viscometer. Pea flour could not be measured as the capillary of the viscometer would have been blocked with the larger flour fragments. The shear rate in the capillary was calculated to be close to 1 s^{-1}. Fig. 2.8 shows the viscosity over the full concentration range as function of the mass fraction solids (Fig. 2.8A) and mass fraction proteins (Fig. 2.8B). Fig. 2.8A shows that the viscosity of PPIp increases strongly with increasing concentration. This increase was larger than the other fractions that were milder processed. This fraction also possesses strong thickening capacity compared to e.g. whey proteins. The viscosity of PPIp at 25 wt. % is approximately 1000-fold higher compared to WPI at similar concentration [116].

The effect of saccharides, starch granules and protein on viscosity was estimated using the compositional data from Table 2.1, the protein molecular weights from Fig. 2.6, and Eq. 2.2. The contribution of saccharides in the saccharide-rich ALB-F and the contribution of starch in the starch-rich pea flour is shown in Fig. 2.8A as a black line and dashed black line respectively. These fractions were chosen because

of their high saccharide and starch content, which means that for the other fractions the contribution of these components is only lower. The contribution of the starch and saccharides to the viscosity is small compared to that of the protein, implying that the concentration of protein mainly determines the viscosity (Fig. 2.8B). With a similar protein concentration, the fractions behave comparably, despite the large variation in non-protein components of the fractions. This also confirms that the carbohydrates have minor impact on the viscosity of these mixtures.

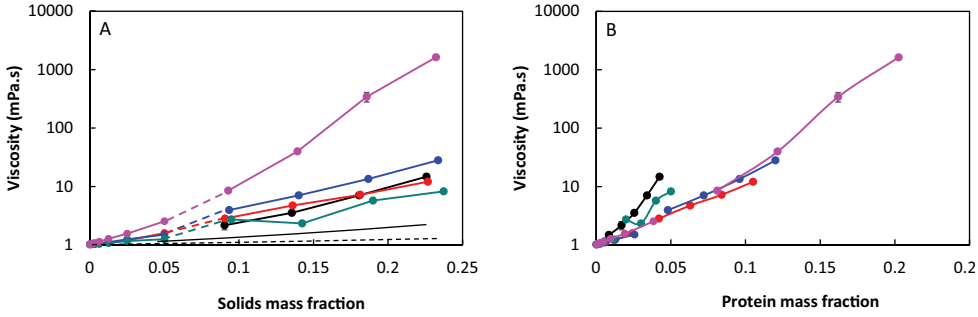

Figure 2.8 Viscosity as a function of the concentration solids (A) and protein (B) at a shear rate of 55.8 s^{-1}. Nearly all error bars are smaller than the points in the figures. Pea flour (—), PPCn (—), PPCa (—), ALB-F (—), PPIp (—). Additional lines left figure: estimated contribution of starch granules in pea flour (thin black line) and estimated contribution of saccharides in the ALB-F (dashed black line).

Thickening properties of pea protein through aggregation

Krieger-Dougherty's empirical model (Eq. 2.1) was used with $\Phi_{max} = 0.68$ to determine the specific volume fractions Φ as function of concentration of the five fractions. It is assumed that dispersed phase consists of starch granules and protein aggregates (Eq. 2.4) mainly so that

$$\phi = \phi_{starch} + \phi_{pa} \tag{2.4}$$

With Φ_{starch} and Φ_{pa}, the volume fraction of the starch and proteins aggregates. The volume fractions of starch granules Φ_{starch} was calculated by Eq. 2.5.

$$\phi_{starch} = \frac{\frac{m_{st}}{\rho_{st}}}{\frac{m_w}{\rho_w}+\frac{m_p}{\rho_p}+\frac{m_{st}}{\rho_{st}}+\frac{m_{su}}{\rho_{su}}} \quad (2.5)$$

With m_w, m_p, m_{st}, m_{su} the mass fractions of water, starch granules, protein and sugar and ρ_{st} = 1500 kg/m^3, ρ_p = 1400 kg/m^3, ρ_w = 1000 kg/m^3 and ρ_{su} = 1600 kg/m^3 the approximated densities [117]. Subtracting the volume fractions of starch granules yields the volume fractions of the protein particles or aggregates Φ_{pa}, which are shown in Fig. 2.9A. It shows that PPIp levels off and hence reaches close packing at lower concentrations than the other fractions.

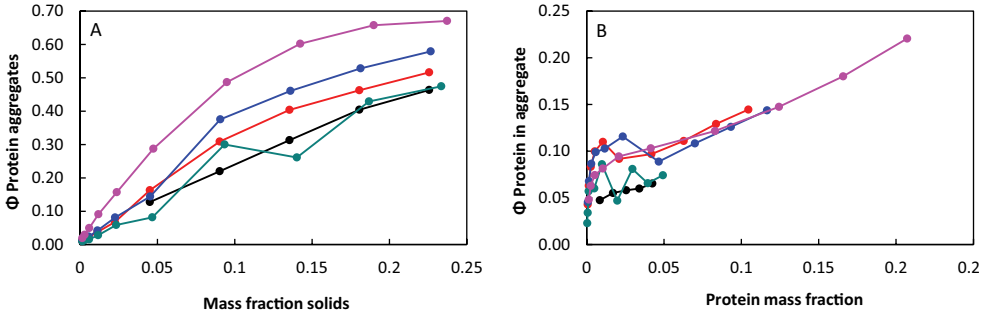

Figure 2.9 A. Estimation of the specific volume fractions of protein aggregates. B. The volume fraction of protein in these aggregates as function of concentration. Pea flour (—), PPCn (—), PPCa (—), ALB-F (—), PPIp (—).

Assuming that all proteins are in the aggregates, and that the aggregates consist only of proteins and the continuous phase (the sugar solution), the volume that the proteins occupy in these aggregates Φ_{pina} can be estimated using Eq. 2.6.

$$\phi_{pina} = \frac{\omega_p \rho_w}{\phi \rho_p} \quad (2.6)$$

with ω_p the protein dry matter fraction (Table 2.1) and ρ_w = 1000 kg/m^3 and ρ_p = 1400 kg/m^3 the approximated densities of the continuous phase and proteins [118]. Fig. 2.9B shows Φ_{pina} as a function of protein concentration for the different fractions. It is seen that the volume contribution of protein to these aggregates increases moderately with concentration and is only 10 – 20% (v/v). The high ratio of water to proteins in the aggregates indicates a rarefied structure.

Reaching close packing the aggregates could become smaller due to interpenetration of the particles in such dense systems. The estimated protein volume fractions of PPIp were similar to those found for aggregated WPI, which has been reported 0.25 and 0.38 for a 4 and 8% WPI solution respectively [119, 120]. Another study on WPI treated in a similar way, reported fractal dimensions of D = 2.1 – 2.2 at pH 5.4 [121]. The fractal dimension of the pea protein aggregates are expected to be in a similar range. Fig. 2.9 also shows that a lower degree of purification results in less volume per mass. This is consistent with previous conclusions regarding the minor contribution of other components to viscosity.

The presence of large aggregates has been verified by particle size analysis at multiple concentrations. It was found that the particle size remained constant in the studied concentration range of 10^{-5} to 10^{0} wt. %. Throughout this range, PPIp had an average particle size of 350 nm (± 3 nm) and PPCn, PPCa and ALB-F sizes of 94 (± 4), 242 (± 14) and 110 (± 8) nm respectively. Fig. 2.10 shows the particle size distributions of the pea protein fractions at a concentration of 0.1 g/L (Fig. 2.10A) and 1.0 g/L (Fig. 2.10B). It shows that the more extensively purified PPCa and PPIp are highly polydisperse with aggregate sizes of up to 10^{4} nm diameter. Although confirming the presence of large aggregates, the analysis does not provide information about the relative amounts of protein molecules, small aggregates and large aggregates. Since scattering increases with R^{6} it could well be that a significant amount of protein is present as single molecules, but did not scatter sufficient light to be shown as a peak here.

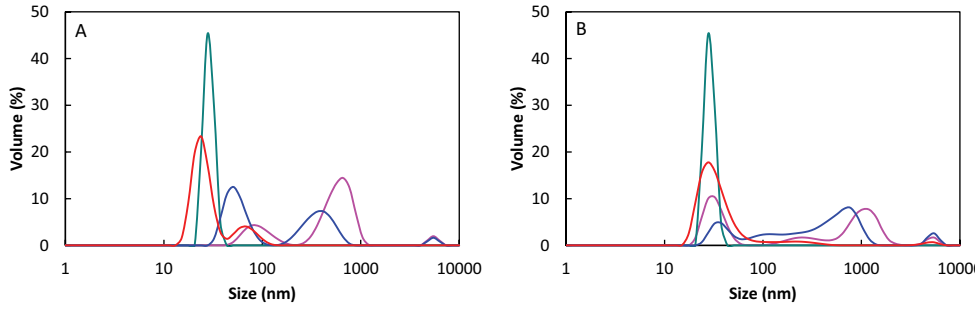

Figure 2.10 Particle size distributions of PPCn (—), PPCa (—), ALB-F (—) and PPIp (—) at a concentration of 0.1 g / L (A) and 1.0 g / L (B).

For further understanding of the solubility of these protein aggregates, the radius of the aggregates that remained soluble during the solubility experiment was estimated using Eq. 2.3. The radii of the aggregates that remained dispersed at the centrifugal force of 17000 g were smaller than 100 nm for PPIp. The sediment amounted to 17 wt. % of PPIp, confirming a substantial number of large protein aggregates (> 100 nm).

Purified pea protein showed high specific viscosity at the chosen experimental conditions. These conditions include sample preparation and analysis at pH 7, 20 °C and a conductivity of < 10^1 mS / cm, which is equivalent to an ionic strength of < 0.1 M NaCl at a concentration of 5 wt. % pea fraction. At the set conditions it has been found that the thickening capacity of pea protein is caused by the ability to form rarefied protein aggregates of different sizes. It is to be expected that changing these conditions may change the functional behaviour of the pea fractions and possibly also the formation of aggregates. In this study the formation of aggregates may be a result of globulin – globulin hydrophobic interactions. This interaction could be enhanced due to partial unfolding of the protein after the pH precipitation step. It has been reported that alkali extraction combined with isoelectric precipitation results in higher surface hydrophobicities at pH 7.0 for pea protein isolates, due to isolation of hydrophobic globulins from the hydrophilic albumins [50]. This is consistent with the results in our study, showing that the alkali extracted PPCa and PPIp formed aggregates (Fig. 2.9 and 2.10).

The pea protein aggregates were not broken up by shear, as hysteresis was not observed for PPIp (data not shown). The observed shear-thinning behaviour could be explained by flow alignment rather than shear-induced breakage of the aggregates. At rest, the protein polymers have a random orientation to maximize entropy. With increasing shear rate, the asymmetric dispersed molecules or aggregates tend to align themselves with the shear planes to reduce frictional resistance [122]. Other physical properties of the protein aggregates, the mechanism behind the formation of these rarefied aggregates and the dependency on pH and ionic strength remains to be investigated.

4. Summary and conclusion

We studied the effect of aqueous protein fractionation processes on the composition, solubility and viscosity of five pea fractions. Dispersing pea flour in water at neutral and alkaline (pH 8) pH values and subsequent centrifugation, produces protein concentrates with 40 – 50 wt. % protein, labelled as PPCn and PPCa, respectively. Further purification by pH precipitation resulted in purities up to 85% protein, but changes the protein composition. This fractionation step resulted in an albumin fraction (ALB-F) and a globulin-rich fraction PPIp. The latter showed compositions comparable to a commercially available pea protein isolate. Compositional changes resulted in different functional behaviour. PPIp was obtained after pH precipitation and showed reduced solubility. The same fraction showed higher specific viscosity than the less pure fractions. The viscosity was closely related to the protein purity of the fractions. Soluble carbohydrates were found to have a minor effect on viscosity due to their low molecular weight. The insoluble carbohydrates were mostly present as starch granules and had limited effect on the bulk behaviour in absence of a thermal treatment. PPIp showed the highest specific viscosity that could be explained by proteins present in the form of aggregates with a rarefied structure. The presence of large particles was confirmed by particle size analysis, showing that PPIp and PPCa had larger average particle sizes. This research showed that the specific viscosity of pea fractions can be altered by the degree of protein purification. Alkali extraction and isoelectric precipitation resulted in a higher number of globulin proteins and a higher protein purity, both increasing the specific viscosity through aggregate formation. Extended fractionation could also be beneficial as aqueous extracted pea protein isolate may function as an effective thickening agent.

Chapter 3

Coacervation in pea protein solutions: the effect of pH, salt, and fractionation processing steps

Abstract

We explored coacervate formation for pea protein solutions at varying pH and NaCl concentrations. The dispersed protein has also been varied by exposing them to different commonly applied fractionation processes. Confocal microscopy was used to confirm the presence of spherical shaped protein-rich domains; a signature of the concentrated coacervate phase. It was found that the mildest processed fraction – involving pea flour dispersions and subsequent removal of solids by centrifugation – formed coacervates as well as aggregates (i.e., non-spherical domains), between pH 6.0 and 6.5. At pH 6.25 only coacervates were observed. When 50 mM NaCl was added at pH 6.25, the coacervate average diameter increased from approximately 1 to 5 μm. When the salt concentration was increased to ≥200 mM NaCl, no coacervates were observed anymore. The coacervates formed at pH 6.25 with 0 and 50 mM added NaCl were examined further. It turned out that the coacervates contained pea globulins, with legumin being most abundant. Pea albumins were not found in the coacervates. The internal protein content of the coacervates formed at pH 6.25 was around 45 wt. %. When the mildest processed fraction was freeze dried, coacervates could still be formed at pH 6.25 and low salt concentrations (≤ 50 mM NaCl). After alkaline extraction, dispersions with both aggregates and coacervates were observed at pH 6.25. Isoelectric precipitated pea protein isolate did not show coacervates at any of the conditions tested. Our research shows that mildly fractionated pea protein was most suitable to form coacervates.

This chapter is submitted as:

Remco Kornet, Sarah Lamochi Roozalipour, Paul Venema, Atze Jan van der Goot, Marcel B.J. Meinders, Erik van der Linden. Coacervation in pea protein solutions: the effect of pH, salt, and fractionation processing steps

3.1 Introduction

Currently many studies focus on the functionality of plant proteins to support the ongoing transition from animal- to plant-derived proteins. Pea is one of the major plant protein sources that are being studied, because of its low allergenicity, non-transgenic status, high protein content, balanced amino acid ratio and property to be grown in moderate climates [18]. To benefit from these attributes, it is important that pea proteins can serve as a functional ingredient in food formulations. Such functional properties include solubility, gelling properties, emulsifying properties and more. The solubility of pea protein is highest at pH>6 and pH<4 [123] and when heat and pH changes are avoided upon processing [123, 124]. Harsh processing conditions can induce protein denaturation, which leads to aggregation and thus to a lower solubility. This is why protein solubility is sometimes considered a practical measure for the protein functionality [125]. A high protein solubility generally leads to better gelling properties, while a low solubility may be more beneficial for soft solid application, such as meat analogues, where the integrity index (i.e. the texturization degree of extruded protein) becomes higher with a lower protein solubility [126, 127]. Solubility and other functional properties can be controlled by the method of fractionation [50, 59, 128]. Differently fractionated pea proteins can thus display a range of functional attributes, including a high solubility, thickening and gelling capacity (Chapters 2 and 4).

A plant protein property that has gained increased interest recently is coacervation at slightly acidic pH [129, 130]. Such plant protein coacervation – sometimes referred to as self-coacervation, simple coacervation or liquid-liquid phase separation – can occur spontaneously upon changing the environmental conditions [131, 132]. These coacervates are spherical protein-rich domains embedded within a protein-poor continuous phase, typically identified using confocal microscopy [129, 130]. The functionality of protein coacervates can be seen as for example an aid in the production of low-viscosity dispersions with high protein content. It has also been reported that protein coacervates can be utilized to encapsulate bioactive compounds, for instance by cross-linked gelatine [133, 134]. In recent years, it was found that under certain conditions coacervates are formed in solutions of plant storage proteins spontaneously. This was already observed for corn, soy and pea proteins [129, 130, 135, 136] and typically occurred at a slightly acidic pH between pH 6.2 – 6.8 and ionic strengths of around 0.1 M NaCl. Also temperature and protein concentration were reported to play a role [129, 130].

Temperature and pH may have an opposite effect on the formation of coacervates. Coacervation or phase separation typically occurs somewhat above the isoelectric point. It was proposed that when a dispersion of coacervates is subsequently heated, coacervates can be either stabilized by the formation of permanent crosslinks or become redispersed. The redispersion occurs when the critical pH at which coacervates are formed decreases with increasing temperature, so that the proteins dissolve again, because the pH is not inducing coacervation anymore. A third possibility is the formation of hollow microcapsules, suggested to occur when the heat-induced aggregation rate equals the redispersion rate [130]. The role of temperature was also examined in a study on soy glycinin coacervation. Here it was concluded that coacervation was favoured below 40 °C and thermal aggregation was dominant above 40 °C and increased with increasing temperature. β-conglycinin was found to be only present in the coacervates – which became microcapsules after heating – when heating was applied to the dispersion. Below 40 °C the rate at which coacervates form decreased with an increasing protein concentration, as evidenced by turbidity measurements over time. This was attributed to β-conglycinin interacting with glycinin, thus hindering the formation of assumed glycinin coacervates [129]. The above literature shows that coacervation of plant sources can be controlled by pH, ionic strength, protein concentration and temperature.

No study has yet explored whether fractionation processes alter the ability of plant proteins to form coacervates. In this study we examine the influence of pH, salt concentration and various commonly applied pea protein fractionation steps on the property of pea proteins to form coacervates. We use the coacervates from the mildest processed fraction to further characterize and quantify the proteins involved in coacervate formation.

3.2 Material and methods

3.2.1 Materials

Yellow pea seeds (*Pisum sativum* L.) were obtained from Alimex Europe BV (Sint Kruis, The Netherlands). Chemicals and CLSM dyes were obtained from Merck (Darmstadt, Germany) and were of analytical grade. Stock solutions of 1 M HCl and NaOH were prepared and part was diluted to 0.1 M HCl and NaOH solutions.

3.2.2 Protein fractionation processes

Four processes that are commonly used in an aqueous protein fractionation process [49] were applied to obtain protein dispersion. The fractionation processes are visualized in Fig. 3.1, and included neutral extraction leading to a solution labelled PPCn (pea protein concentrate neutral extracted), freeze drying leading to a pea protein concentrate labelled PPCn-FD (freeze dried), alkaline extraction leading to a pea protein concentrate labelled fraction PPCa (alkaline extracted) and isoelectric precipitation leading to a pea protein isolate labelled PPIp (pea protein isolate precipitated). PPIp was obtained by a full aqueous fractionation process and is an extended version of the process used to obtain PPCa. PPCn was freeze dried (PPCn-FD) to study the effect of this drying procedure. One may note the absence of an ALB-F (albumin fraction). This fraction was used in previous studies, but was left out here based on preliminary experiments showing that this fraction could not form coacervates at any of the conditions studied. The methods of the fractionation processes were as follows.

In extraction process A, pea flour was dispersed in deionized water in a 1:10 ratio and the pH was left unadjusted. Proteins were allowed to solubilize under moderate stirring of the flour dispersion at room temperature for 2h. The dispersion was then centrifuged (10000g, 30 min, 20 °C) and the resulting supernatant was labelled PPCn. Further fractionation (i.e. removal of water) by means of freeze drying using an Alpha 2-4 LD plus freeze dryer (Christ, Osterode am Harz, Germany) resulted in PPCn-FD.

In the full extraction process B pea flour was also dispersed in deionized water (1:10 ratio), but now the pH was adjusted to pH 8 using 1 M NaOH, to aid protein solubilization. After pH adjustment, this dispersion was moderately stirred at room temperature for 2h. The supernatant after centrifugation was labelled PPCa. For extensive extraction PPCa was further fractionated by isoelectric precipitation. The

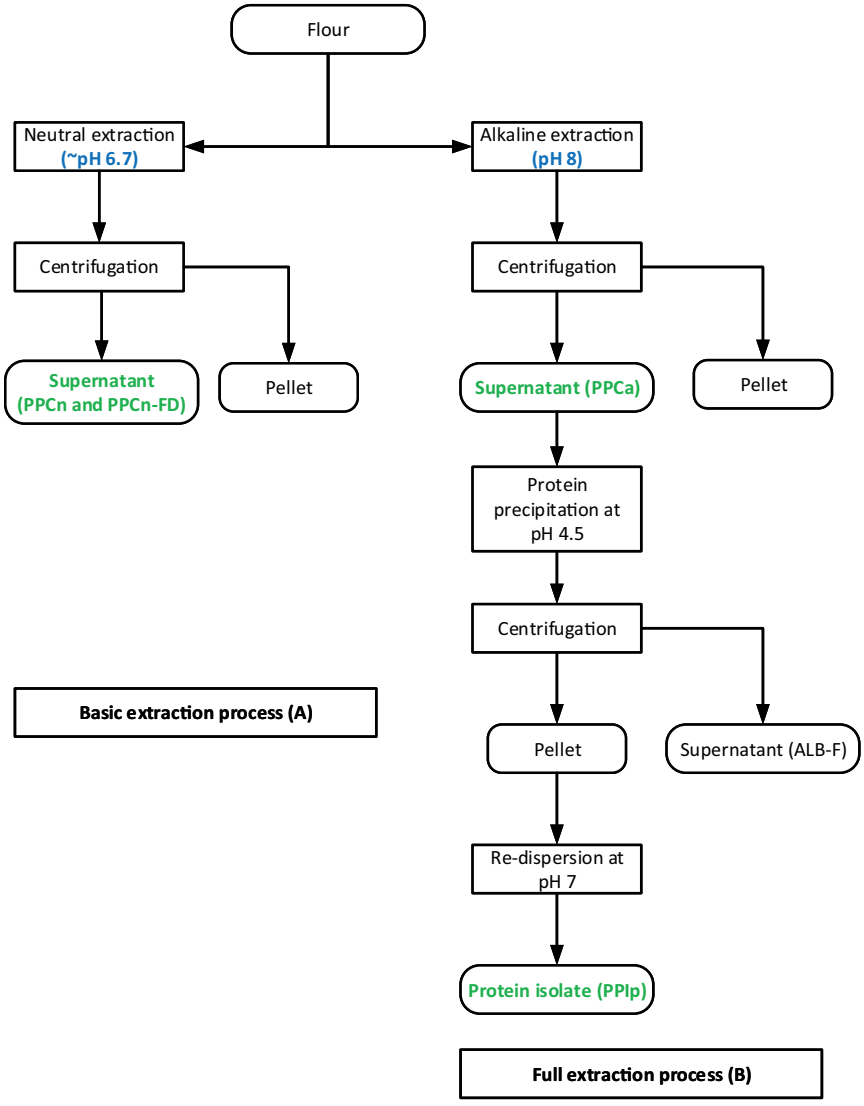

Figure 3.1. Schematic overview of the four fractionation processes used to yield PPCn, PPCn-FD, PPCa and PPIp.

pH of the supernatant was adjusted to pH 4.5 with 1 M HCl and the precipitated proteins were separated by centrifugation (10000 g, 30 min, 20°C). The precipitated

proteins, now present in the pellet, were re-dispersed at pH 7 for 2h. The resulting protein dispersion was labelled PPIp. A schematic overview is given in Fig. 3.1.

All fractionation processes were executed in duplicate. The protein content of the pea protein dispersions was determined with a Flash EA 1112 series Dumas (Interscience, Breda, The Netherlands) using a nitrogen conversion factor of 5.7. The protein concentrations are shown in Table 3.1.

Table 3.1 The measured protein content of the dispersions obtained after different fractionation steps. The concentration aimed for was 1.0 wt. %. All measurements were performed in triplicate and the average values and standard deviations are shown.

Extraction process	Protein content of dispersion (wt. %)
PPCn (neutral extraction)	1.27 $^{\pm 0.05}$
PPCn-FD (freeze drying)	1.00 $^{\pm 0.01}$
PPCa (alkaline extraction	1.36 $^{\pm 0.28}$
PPIp (isoelectric precipitation)	0.93 $^{\pm 0.01}$

3.2.3 Preparation of protein coacervate and aggregate dispersions

Except from PPCn-FD, the protein solutions were freshly prepared from pea flour. Based on protein recovery data from Chapter 2, the amount of flour required to yield a 1 wt. % protein solution was estimated. In the case of PPCn, dispersing flour in water in a 1:10 ratio yielded around 1 wt. % protein. For PPCa the protein yield was a bit higher, so the supernatant after centrifugation needed to be diluted by a factor 1.2. In the case of PPIp, the amount of precipitated protein in the pellet was redispersed in such a quantity that at 1 wt. % protein solution was obtained. The PPCn-FD dispersion was prepared by dissolving the freeze-dried powder in a concentration of 1 wt. % protein. Aliquots of the duplicate protein solutions were taken, and the salt concentration was increased with 0, 50, 200 and 500 mM NaCl followed by 30 min of moderate stirring at room temperature. Also, aliquots of the duplicate protein solutions were taken to prepare a pH series of 5.50, 5.75, 6.00, 6.25 and 6.50 (with a tolerance of ±0.05), using 1 M HCl and 1 M NaOH solutions. The conductivity of each sample was measured with an CO 3000 L conductivity meter (VWR International, Leuven, Belgium). All protein dispersions were heated in a water bath at 40 °C for 2 min, and cooled on ice to room temperature afterwards. This heating step was based on a previous study [130] and was found to yield coacervates that were more stable over time.

3.2.4 Confocal Laser Scanning Microscopy (CLSM)

Samples of the protein dispersions were taken and the protein was stained with 1 µl of a 0.2% Rhodamin B solution per mL of sample. The samples were shaken and allowed to incubate for 30 min. Aliquots of 65 µl were transferred to sealed glass chambers (Gene frame 65 µl adhesives, Thermo Fisher Scientific, Epsom, United Kingdom). The microscope slides were kept upside down for 10 – 15 min to allow the coacervates to sediment before imaging. The microstructures of the sedimented coacervates were visualized with a Leica SP8X-SMD confocal microscope (Leica, Amsterdam, The Netherlands), coupled to a white light laser. A water immersion objective (63x, 1.20) was used for magnification. The laser excitation wavelength was set to 540 nm and the emission detector wavelength between 560 – 630 nm.

3.2.5 Static Light Scattering (SLS)

The particle size distributions of the dispersed protein coacervates and aggregates were measured with a Mastersizer 2000 (Malvern Instruments, United Kingdom). The dispersant (water) and material (pea protein) refractive index was set to 1.33 and 1.45, respectively. Aliquots of the protein dispersion were added until the obscuration reached 15% with the motor rotation speed set to 1000 RPM. The particle size distributions and D50 values (median size) were automatically calculated from the static light scattering data with the Mastersizer2000 software. All measurements were performed in triplicate.

3.2.6 Estimation of the internal protein content and amount of protein that form coacervates

Coacervates were prepared at pH 6.25 with 0 and 50 mM NaCl, as described in section 3.2.3. The protein content of the dispersions was determined with a Flash EA 1112 series Dumas (Interscience, Breda, The Netherlands) using a nitrogen conversion factor of 5.7. Weighed amounts of coacervate dispersions were subsequently centrifuged (20000g, 30 min, 20 °C) to precipitate the coacervates. The supernatants were checked on the absence of coacervates with a light microscope, to confirm that the coacervates were successfully separated. The pellets and supernatants were weighed, and the protein content of the supernatant was also determined. The amount of dispersed protein that were involved in coacervate formation was determined using Eq. 3.1, where x is the mass fraction (-) and ϕ the mass (g), with subscripts for coacervate dispersion (cd), protein (p), supernatant (s) and pellet (pt).

$$Coacervated\ protein\ (\%) = \frac{\emptyset_{cd} \cdot x_{p,cd} - \emptyset_s \cdot x_{p,s}}{\emptyset_{cd} \cdot x_{p,cd}} \cdot 100\% \quad (3.1)$$

The internal protein concentration of the coacervates was subsequently determined using Eq. 3.2.

$$Internal\ protein\ concentration\ (\%) = \frac{\emptyset_{cd} \cdot x_{p,cd} - \emptyset_s \cdot x_{p,s}}{\emptyset_{pt}} \cdot 100\% \quad (3.2)$$

3.2.7 Size Exclusion Chromatography (SEC)

The protein composition of the coacervates was studied by size exclusion chromatography. Coacervates from the PPCn fraction pH 6.25 with 0 mM NaCl and 50 mM NaCl were first separated by centrifugation (20000g, 30 min, 20 °C). The coacervates were concentrated in the pellet. Both samples, as well as their pellet and filtered supernatant, were freeze dried. The protein content of freeze-dried samples was determined with a Flash EA 1112 series Dumas (Interscience, Breda, The Netherlands) using a nitrogen conversion factor of 5.7.

A McIlvaine buffer with 10 mM citric acid, 20 mM Na_2HPO_4, 150 mM NaCl was prepared, adjusted to pH 7 and filtered over 0.45 μm. The buffer solution was split into two equal fractions. To one of the fractions 2% Sodium Docedyl Sulfate (SDS) was added. The freeze-dried samples were redispersed in concentrations of 5 g protein / L in McIlvaine buffer with and without SDS. The samples were centrifuged in an Eppendorf centrifuge (3350g, 10 min, 20 °C) to remove insoluble material. The supernatants were transferred to HPLC vials. Both native-SEC and SDS-SEC were conducted on an Äkta Pure 25 System. The samples were eluted on a Superdex 200 increase 10/300 GL column (Merck, Schnelldorf, Germany) with a range of 10–600 kDa. The flow rate was set to 0.75 mL/min, the equilibration volume was 0.2 column volume (CV), the elution volume was 1.5 CV, and the injection volume was 50 μl. A detection UV-wavelength of 280 nm was used. A calibration curve, with and without SEC, was run with proteins of known molecular weights: Aprotinin (6.5 kDa), β-lactoglobulin (dimer, 18.4 kDa), Ovalbumin (43 kDa), Conalbumin (75 kDa), Aldolase (158 kDa), Ferritin (440 kDa) and Blue dextran (2000 kDa).

The legumin to vicilin ratio in PPCn as well as its coacervate-rich pellet and supernatant was estimated by fitting Gaussians on the legumin and vicilin peaks. The area of the Gaussians was divided over the total area of both legumin and vicilin,

to express the relative amounts. Peak fitting was done with the Multiple Peak Fitting function of the Origin Pro (OriginLab Corporation, Northampton, USA) software.

3.2.8 Cryo Scanning Electron Microscopy (CryoSEM)

The micro- and nanostructure of the coacervates were visualized with cryo scanning electron microscopy (CryoSEM). The PPCn fraction at pH 6.25 both with 0 mM and 50 mM NaCl were examined. A small droplet of the sample was placed between two aluminium (HPF) platelets (Wohlwend, Sennwald, Switserland) and this was plunge-frozen in liquid ethane. The samples were freeze-fractured and subjected to sublimation for 3 minutes to improve depth contrast (-94˚C, 1.3 x 10-6 mBar) in a cryo-preparation system (MED 020/VCT 100, Leica, Vienna, Austria). After 3 minutes the samples were sputter coated with a layer of 10 nm Tungsten. The samples were then cryo-shielded transferred into a field emission scanning microscope (Magellan 400, FEI, Eindhoven, the Netherlands) at -120°C at 4 x 10-7 mBar. The analysis was performed at a working distance of 4 mm, with SE detection at 2 kV, 13 pA.

3.2.9 Electrophoretic mobility

The electrophoretic mobility of particles in the dispersions was measured with a Zetasizer Ultra (Malvern Instruments, United Kingdom). ZS Explorer Software was used to calculate the zeta-potentials. Aliquots of the samples were diluted to 0.1 wt. % protein and the pH was readjusted to the initial values by 0.1 M NaOH and 0.1 M HCl. The diluted protein dispersions were transferred to a capillary zeta cell (DTS1070, path length 1 cm) and the electrophoretic mobility was determined using Phase Analysis Light Scattering (PALS). The measurement duration was optimized by the software. Each measurement was performed in triplicate and each sample was measured in duplicate. An average of all particle charges was obtained as function of pH and ionic strength.

3.2.10 Shear viscosity

The shear viscosity of the dispersions was measured with an MCR 302 rheometer (Anton Paar, Austria). The samples were transferred to a double-gap geometry (DG26.7) and the viscosity was measured at incrementing shear rates of 0.1, 0.5, 1.0, 5.0, 10, 50 and 100 s^{-1} and decrementing shear rates of 50, 10, 5.0, 1.0, 0.5 and 0.1 s^{-1} for 0.2 min per shear rate. The shear ramp was used to determine whether the dispersions showed shear-thinning behaviour. All samples were measured in duplicate and the standard deviations were calculated.

3.3 Results and discussion

3.3.1 Pea protein coacervates from a mildly processed pea fraction

PPCn (pea protein concentrate neutral extracted) was studied on the presence of coacervates at different conditions. This was the mildest processed fraction and has been confirmed to have a high protein solubility with proteins present in their native state (Chapters 2 and 4). The more extensively processed fractions PPCn-FD, PPCa and PPIp were also studied for the occurrence of coacervation and will be discussed in a later section. A more detailed characterization of the coacervates, for which only PPCn was used, is discussed in this section.

3.3.2 Effect of pH and ionic strength

The conditions required to form coacervates from pea protein were systematically examined. Fig. 3.2 shows the microstructure of dispersed pea protein (~1 wt. %) in a pH range of 5.5 – 6.5 (upper row) and in a NaCl range of 50 – 500 mM NaCl (lower row). Below pH 6 the proteins form irregularly shaped aggregates with sizes of around 10 μm. At pH 6.00 not only aggregates, but also protein coacervates are observed. These coacervates are recognized by their spherical shape [129], which were also observed in other studies on plant protein coacervates [129, 130, 137]. At pH 6.25 protein coacervates are abundantly present and some hollow microcapsules can also be observed. The latter could have been formed as a result of partial redispersion upon warming to 40 °C [130]. At pH 6.50 the slightly red-coloured continuous phase indicates that most of the proteins are soluble, and only few aggregates and microcapsules can be observed. At 50 mM NaCl, the coacervates initially increase in diameter and disappear when the salt concentration is increased further (Fig. 3.2, lower row). In the case of soy glycinin, an increased coacervate size with increasing concentration was ascribed to coalescence [135], which occurred between 100 and 200 mM NaCl. The pea protein coacervates in our study disappear at NaCl concentrations above 200 mM NaCl and the proteins dissolve into a stable single-phase solution. This might be due an enhanced solubility of pea globulins at higher salt concentrations, also known as a 'salting-in' effect [68, 138]. This observation is consistent with what has been seen for soy glycinin at higher salt concentrations of 250 mM NaCl [135]. After 5 days of storage at constant room temperature, pH and NaCl concentrations, coacervates were still observed. Coalescence was not seen upon confocal microscopy analyses in the timescale of one hour. The stability of the coacervates against coalescence into larger droplets is not well understood yet. It might be related to an increasing

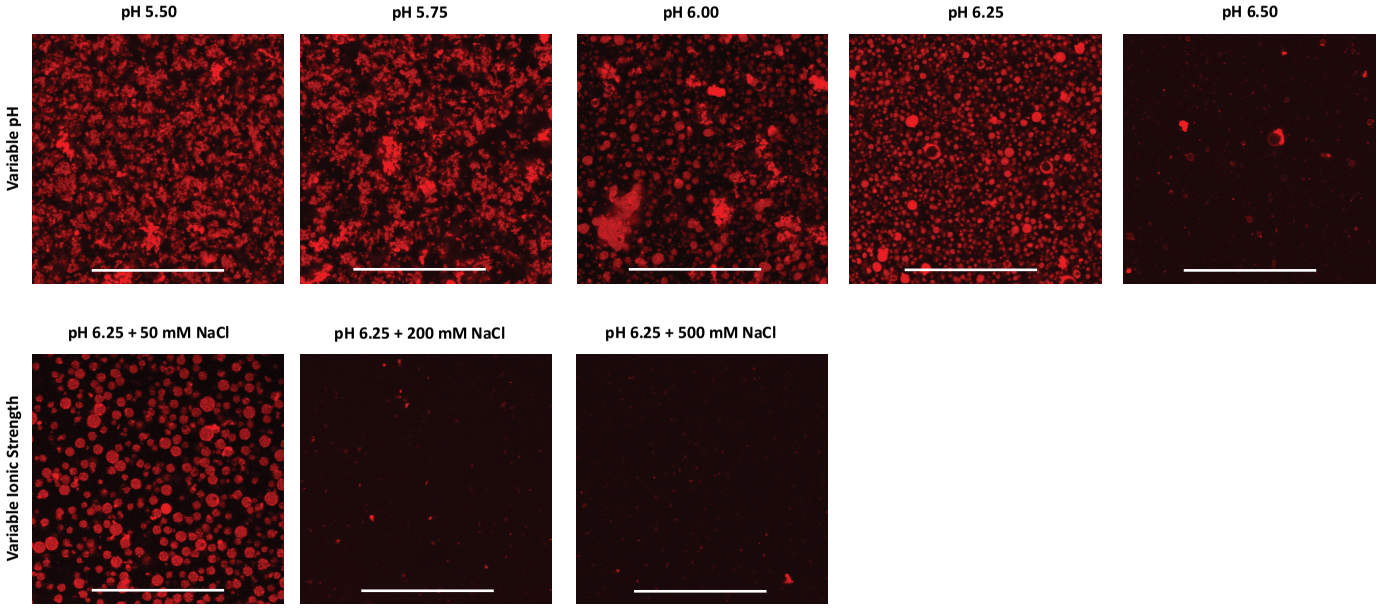

Figure 3.2 Confocal microscopy images of the PPCn protein dispersions (~ 1 wt. % protein) in a pH range of 5.5 - 6.5 and NaCl range of 50 - 500 mM. In the upper row no NaCl was added. In the lower row the pH was first standardized on 6.25. Coacervates are seen at pH 6.00, 6.25 and pH 6.25 with 50 mM NaCl. The proteins were stained with Rhodamin B and are shown in red. The images are not an accurate representation of the coacervate concentration, because the coacervate-rich sediment was imaged. The white scale bar represents 50 μm.

electrostatic repulsion with an increasing coacervate diameter. When the coacervates increase to a certain diameter the electrostatic force may become larger than the random Brownian force and prevent them from coalescence. Such a stabilization mechanisms was suggested for charged colloidal spheres [139].

Dispersions with coacervates and hardly any aggregates (non-spherical domains) were formed at pH 6.25 with 0 and 50 mM NaCl. The particle size distributions of these two dispersions are shown in Fig. 3.3A and correspond with the sizes from the confocal microscopy images. This implies that the coacervates were not affected by dilution, which was required to perform static light scattering. The coacervates with 50 mM NaCl have a larger average diameter of 4-5 μm, compared with the particles of 1-2 μm that are formed at 0 mM NaCl. The particle size distributions for the coacervates with 50 mM NaCl also show a shoulder at 20-30 μm, which indicates either flocs of coacervates or protein aggregates. Fig. 3.3B shows the median diameter of all peaks in the particle size distributions of the protein dispersions at pH 5.5 – 6.5. Between pH 5.75 and 6.00, there is a clear drop in median particle size, reflecting a transition from the regime where pea proteins aggregate to the regime where they form coacervates. A similarly abrupt transition from coacervates to aggregates was seen for 2 wt. % pea protein solutions when the pH was adjusted from 6.3 to 6.0 [130]. At a pH above 6.25 the median particle size starts to increase again, which could be attributed to the formation of protein aggregates with a rarefied structure (Chapter 2). These aggregates do not easily sediment and have a thickening effect in pea protein dispersions. The strong pH dependency of coacervation hints in the direction of a charge-controlled mechanism.

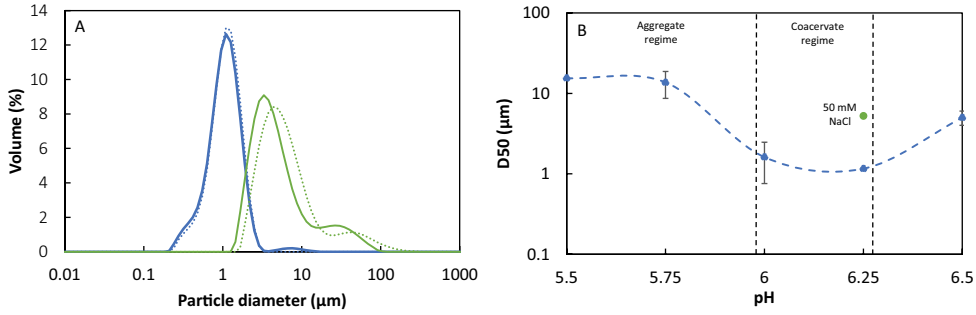

Figure 3.3 A. Particle size distributions of PPCn protein dispersions at pH 6.25 (—) and at pH 6.25 + 50 mM NaCl (—). The dashed lines represent the duplicate measurements. B. median particle diameter as function of pH. The green datapoint represents the dispersion at pH 6.25 + 50 mM NaCl. Samples with higher NaCl concentrations could not be measured because of low laser obscuration. The error bars represent the standard deviations.

3.3.3 Quantification of proteins participating in coacervate formation

The amount of protein in the coacervates was estimated using centrifugation to separate the coacervates. By determining the protein content of the coacervate-rich pellet, also the internal protein content of the coacervates could be estimated. It was assumed that the droplets completely coalesced after centrifugation, which has also been reported to be the case for soy coacervates [137]. Table 3.2 shows the average coacervate diameter, the amount of coacervated protein and the coacervate internal protein content at pH 6.25 with 0 and 50 mM NaCl. From the total amount of extracted protein from the pea flour, roughly 25% is in the coacervates. When 50 mM NaCl is added, the coacervate yield increases from 22.7 to 29.5 wt. % and larger coacervates are formed.

Table 3.2 The measured protein content of the dispersions obtained after different fractionation steps. The concentration aimed for was 1.0 wt. %. All measurements were performed in triplicate and the average values and standard deviations are shown.

Solvent conditions	Coacervate diameter (μm)	Amount of protein that form coacervates (wt. %)	Internal protein content (wt. %)
pH 6.25 + 0 mM NaCl	1.2 $^{\pm 0.0}$	22.7 $^{\pm 1.5}$	44 $^{\pm 10}$
pH 6.25 + 50 mM NaCl	5.3 $^{\pm 1.0}$	29.5 $^{\pm 1.9}$	47 $^{\pm 4.0}$

The internal protein content is another relevant parameter for coacervates. A higher internal protein content implies that more protein could be incorporated in a coacervate dispersion at the same volume fraction. It was found that the internal protein content of the small coacervates without added NaCl is around 44 wt. %, and the larger coacervates with 50 mM NaCl around 47 wt. %. These numbers are based on the assumption that the pellet only contains protein and water. The internal protein contents are higher than what has been observed for soy glycinin coacervates [137] and for whey protein particles that were obtained by emulsification followed by heat-induced gelation [140]. In the case of soy glycinin coacervates the internal protein content ranged between 20 and 35 wt. %, and in the case of whey protein particles between 18.5 and 39.2% (w/v), depending on the pH and ionic strength. The internal protein content of the coacervates is comparable to what was found for whey protein particles. In view of plant the protein transition, the observation that such protein-dense coacervates can be formed from plant proteins is particularly relevant.

3.3.4 Coacervate protein composition and morphology

The coacervates seen at pH 6.25 without and with 50 mM NaCl were further studied regarding their protein composition and morphology. Fig. 3.4 shows the SEC chromatograms of the native proteins (A) and of the proteins dissociated by SDS (B). The black line represents an uncentrifuged sample, the dashed blue line represents the coacervates concentrated in the pellet after centrifugation, and the solid blue line represents the supernatant depleted of coacervates. The absence of coacervates in the supernatant was verified with light microscopy. From the native-SEC (Fig. 3.4A) it can be concluded that the pellet only contains globulins. This means that only pea globulins are incorporated in coacervates, and the albumins are not. The same result was observed for the pH 6.25 sample with 50 mM NaCl (therefore not included in the graphs).

With size exclusion chromatography the soluble proteins can be measured only. Addition of SDS led to complete resolubilization of the pellet (evidenced by the absence of pellet after centrifugation of the dispersion with SDS at 3350 g), which made it possible to measure the complete coacervate composition. When looking at the results in Fig. 3.4B, it is confirmed that only globulins participate in the coacervation of pea protein. The major peak around an elution volume of 10.5 mL represents proteins with a molecular weight of 60 kDa, which corresponds to the 11S legumin subunit. In the native state legumin is present as hexamer (360 kDa). With SDS this hexamer dissociates into subunits, which are composed of a covalently bound acidic and basic part [141]. Also the 7S vicilin dissociates in the presence of SDS, but here polypeptides of different sizes are being formed, ranging in molecular weight range from 12.5 – 50 kDa [40]. From the SDS-SEC chromatogram it can also be observed that most of the legumin ends up in the coacervates, while most of the vicilin remains in the continuous phase. A similar observation was reported by Lui et al. (2007), where over 80% of the coacervate phase consisted of the 11S glycinin, and less than 20% of the 7S β-conglycinin [137]. A rough estimation in which the overlapping peaks of Fig. 3.4B are fitted with Gaussians, indicates that the coacervate fraction has a legumin to vicilin ratio of at least 60:40 (L:V). The initial ratio of the protein solution was 30:70 (L:V), which indicates that particularly legumin takes part in coacervation. These results imply that coacervation could be a very simple and mild method to separate 11S and 7S globulins from pea and soy.

The morphology of the coacervates was further characterized using cryo scanning electron microscopy (CryoSEM) to visualize the surface of the coacervates on a micro- to nanoscale level. Fig. 3.5 shows coacervates prepared at pH 6.25 with 0 mM

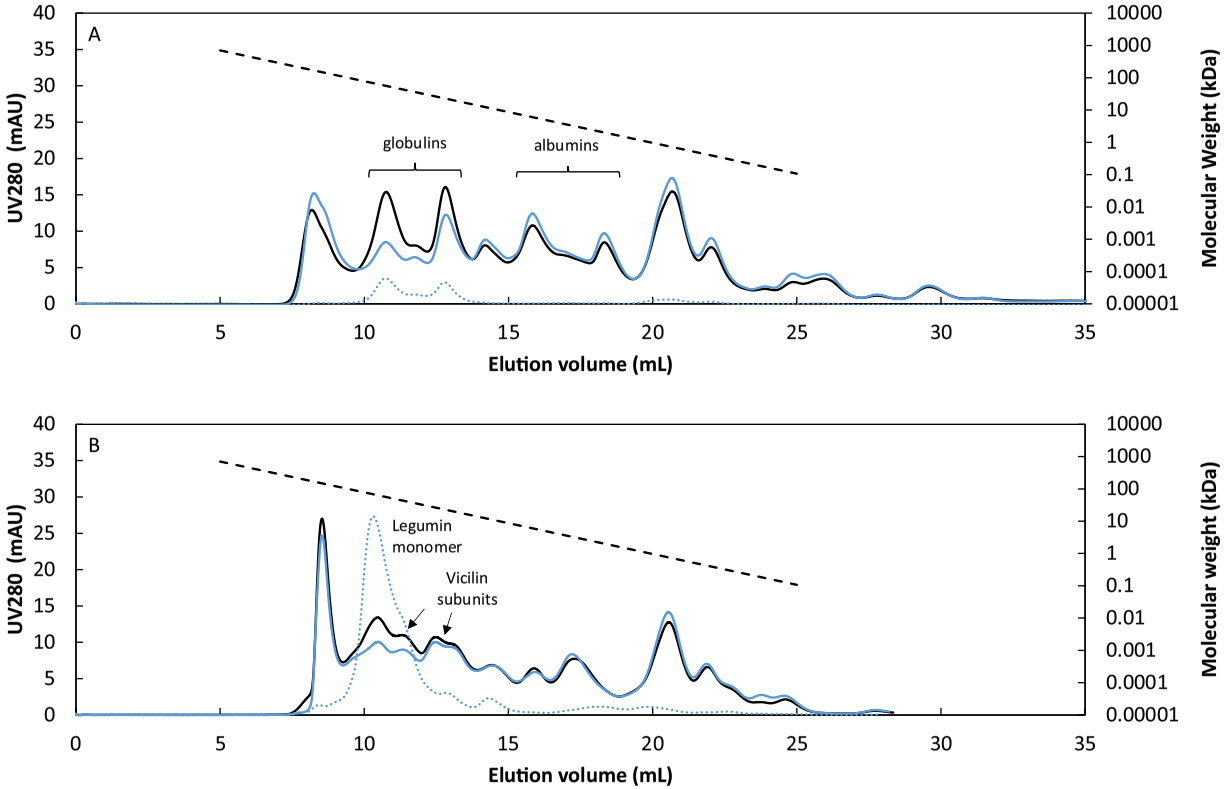

Figure 3.4 A. Native protein composition of PPCn (—), the coacervates in this fraction (— dashed) and the continuous phase depleted of coacervates (— solid). The dashed black line represents the molecular weight as a function of elution volume. B. The composition of the same samples after protein dissociation by SDS. The coacervates were prepared at pH 6.25 without NaCl. In the case pH 6.25 with 50 mM NaCl the SEC chromatograms were similar.

NaCl (Fig. 3.5A) and 50 mM NaCl (Fig. 3.5B). The coacervates with 0 mM NaCl show a rougher surface with more details, compared with the coacervates with salt. In the right image, less details are seen on the coacervate surface, which suggests that addition of NaCl made the surface smoother.

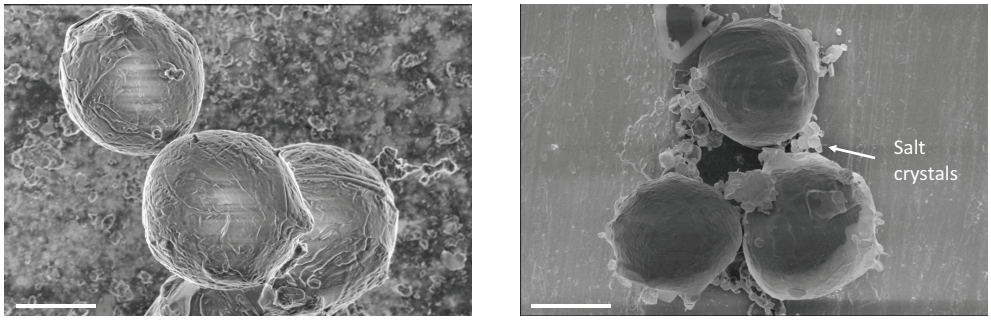

Figure 3.5 A. CryoSEM images of pea coacervate droplets obtained from F2 at pH 6.25 with 0 mM NaCl. B. the pea coacervate droplets obtained from F2 at pH 6.25 with 50 mM NaCl. The white scale bar represents 5 μm.

3.3.5 Coacervates in dispersion

Fig. 3.6A shows the average zeta potential of protein solutions as function of pH. At the conditions tested the net charge was negative and the zeta potential ranged between -15 and -25 mV. Coacervates were observed at pH 6.00 and 6.25 with and without 50 mM NaCl. These conditions corresponded with a narrow negative zeta potential range of -18 to -23 mV. This indicates that coacervation only occurs at a specific charge range. However, having a pea protein dispersion in this range does not guarantee coacervation, as we will see in section 3.3.6. When the protein zeta potential becomes less negative than -18 mV, protein aggregation will be favoured because of reduced electrostatic repulsion (as shown in Fig. 3.2 at pH < 6.00). In current isoelectric precipitation fractionation processes pea protein is typically brought to its isoelectric point of around pH 4.5 [64, 68].

Fig. 3.6B shows the shear viscosity over a shear rate of 5 – 100 s^{-1}. At each shear rate the viscosity was measured three times within 20 seconds, and no decrease in viscosity was observed. In other words, no thixotropy was observed within the timescale measured. There was an effect of shear on the viscosity of the coacervate dispersions; the viscosity decreased with increasing shear rate. This shear-thinning behaviour was seen for both samples (0 mM and 50 mM NaCl). Shear-thinning behaviour may

indicate that the particles align with flow and / or are (partially) broken down by shear. It is likely that particles break down upon shear since also hysteresis was observed (that is, the shear viscosity ends lower at the end of the backward shear rate loop, compared with the initial shear viscosity). The observation that the shear viscosity does not recover after reversing the shear implies that coacervates, or clusters of coacervates, do not recover within the timescale of this measurement.

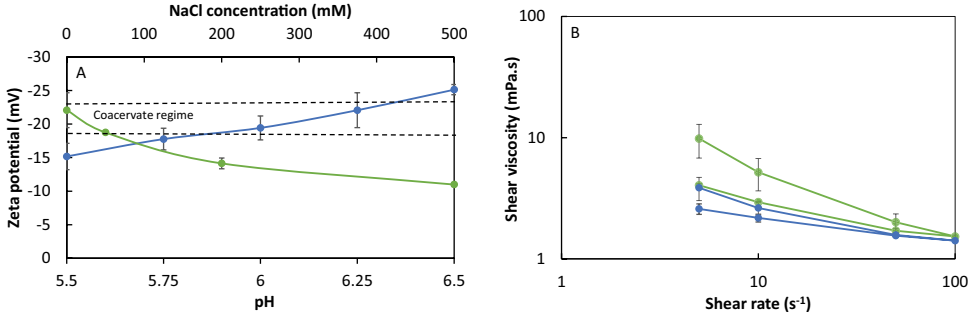

Figure 3.6 A. Average zeta-potential of PPCn dispersions as function of pH (—) and NaCl concentration (—). B. Shear viscosity of PPCn coacervate dispersions at pH 6.25 with 0 mM NaCl (—) and with 50 mM NaCl (—) as function of shear rate. Higher viscosities are seen in the forward loop and lower viscosities in the backward loop. The error bars represent the standard deviations.

A practical convenience of using coacervate droplets would be the re-dispersibility of the coacervates after drying. Coacervates are likely to disappear upon drying, as changes in solvent conditions (i.e., protein concentration, salt concentration, temperature) may undo the phase separation that initially caused the formation of coacervates. To qualitatively establish a possible effect of freeze-drying on the coacervate dispersion, an additional experiment was performed. The coacervates at pH 6.25 with and without 50 mM NaCl were freeze-dried and re-dispersed in deionized water. Fig. 3.7 shows both dispersions with 0 mM NaCl (bottom left) and with 50 mM NaCl (bottom right). In both cases aggregates are seen, which means that the freeze-drying step induced protein aggregation. The formation of aggregates after freeze drying has also been observed for lupin protein isolate [142]. In the case of 0 mM NaCl, with freeze drying and re-dispersing the coacervates mostly disappeared or did not form again. When 50 mM NaCl was added part of the coacervates remained visible after freeze drying and rehydration, but also more aggregation was observed. It has been reported that salts can stabilize protein structures. The suggested mechanism is that salts provide protein hydrogen bonds

that substitute those with the surrounding water molecules and stabilize protein structures [143]. Further stabilization of proteins – and possibly protein coacervates – could be achieved by the addition of sugars, such as trehalose or trehalose esters [144, 145].

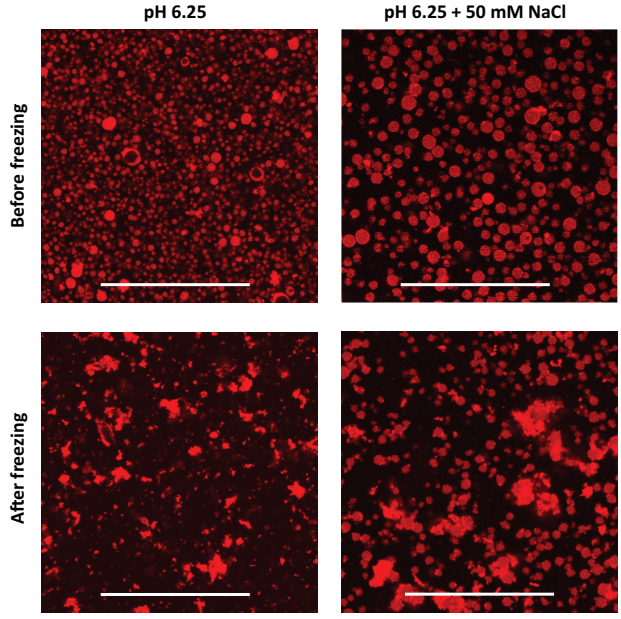

Figure 3.7 Top left panel: Confocal microscopy images of coacervates from PPCn prepared at pH 6.25 with 0 mM NaCl. Top right panel: Images of coacervates formed at the same conditions but now 50 mM NaCl was added. Bottom panels: The corresponding freeze-dried coacervates after re-dispersion. The proteins were stained with Rhodamin B and are shown in red. The white scale bar represents 50 μm.

3.3.6 The effect of fractionation processes on pea protein coacervation

In Fig. 3.8 the microstructures of protein dispersions are seen with different treatments prior to coacervation: neutral extraction (PPCn), neutral extraction and freeze drying (PPCn-FD), alkaline extraction (PPCa) or isoelectric precipitation (PPIp). The dispersions at conditions that did not yield protein coacervates are not shown (i.e., pH 5.50, 5.75, 6.25 with 200 and 500 mM NaCl and 6.50). PPCn formed coacervates at all three conditions, but at pH 6.00 also non-spherical domains (i.e., protein aggregates) were observed. After freeze drying (PPCn-FD) only aggregates

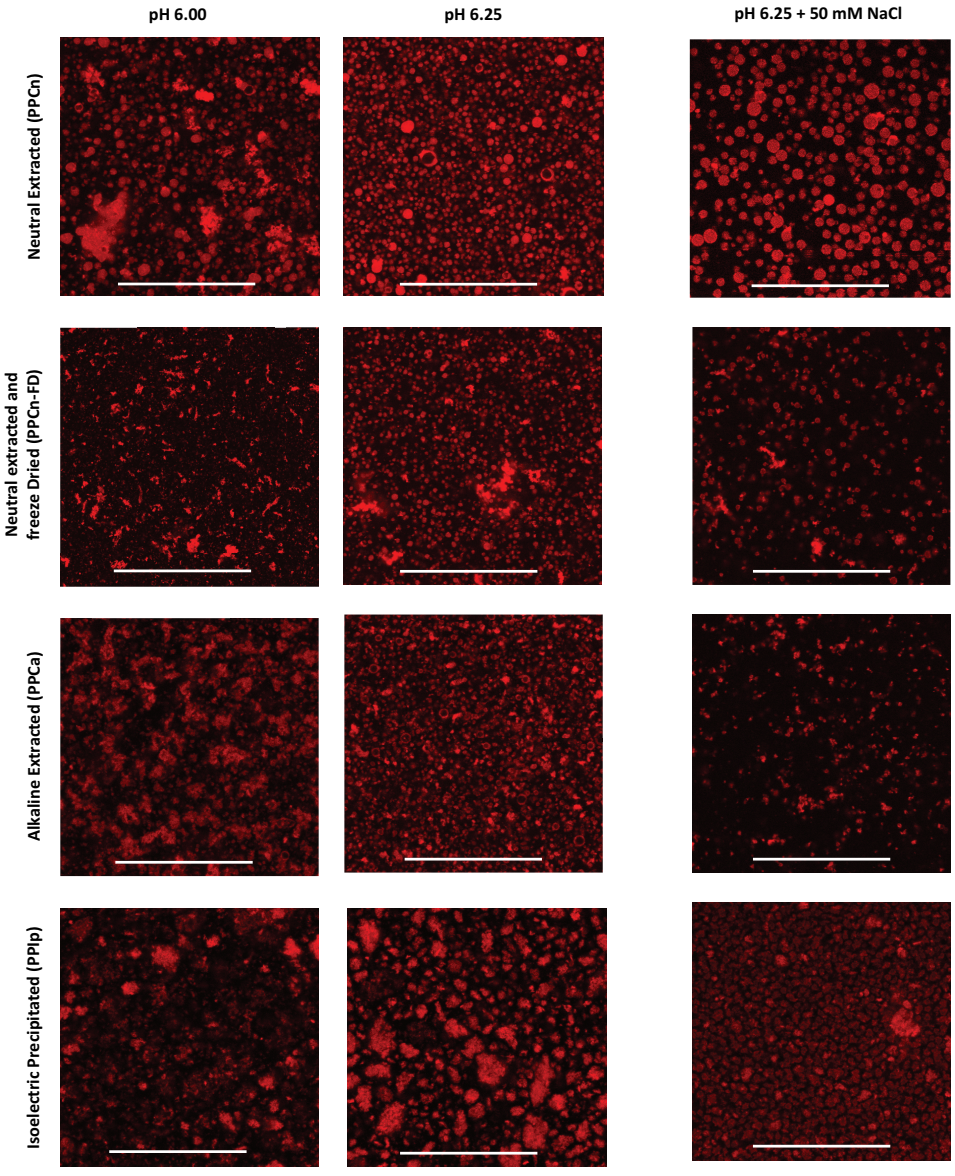

Figure 3.8 Confocal microscopy images of differently processed pea fractions at pH 6.00, 6.25 and 6.25 with 50 mM NaCl. The proteins were stained with Rhodamin B and are shown in red. The white scale bar represents 50 μm.

were seen at pH 6.00 (note that in section 3.3.5 the coacervates were freeze-dried, and here the protein was freeze-dried as part of a pea protein fractionation process). However, aggregates and coacervates were observed at pH 6.25, also in the case of 50 mM NaCl. When alkaline extraction (at pH 8) was applied, also only aggregates were seen at pH 6.00. At pH 6.25 coacervates and aggregates were seen, with a seemingly higher proportion of hollow microparticles. When 50 mM NaCl was added, the coacervates disappeared and only few irregular particles were left. Alkaline extraction has the advantage that proteins are better soluble and thus a higher extraction yield (Chapter 2). However, with this type of functionality in mind, one might consider applying neutral extraction instead of alkaline extraction. To yield pea protein fractions with a high purity, isoelectric precipitation is typically applied. However, Fig. 3.8 shows that after extensive fractionation no coacervates were formed. The right image (pH 6.25 with 50 mM NaCl) shows small non-spherical particles that could be (parts of) aggregates formed upon isoelectric precipitation. At all conditions, including the ones not shown in Fig. 3.8 (pH 5.5 – 6.5 and 0 – 500 mM NaCl), coacervates were absent. This is in contrast with another study, where coacervates could be formed from pea protein isolate (PPI) that was obtained by alkaline extraction and isoelectric precipitation. However, only the soluble fraction of the PPI was used as well as higher protein concentrations [130]. The lack of coacervate formation in PPIp is most likely a result of process-induced changes in the protein conformation and surface hydrophobicity [50] and resulting irreversible aggregation (Chapter 4), which lowers the amount of protein available to form coacervates.

Also, the conductivity (Table 3.3) at different pH and NaCl concentrations and the zeta potential (Fig.3.9) as function of pH and NaCl concentration were determined

Table 3.3 Conductivity (mS/cm) of the protein dispersions at all pH and salt conditions tested.

Solvent conditions	F2	F2-FD	F3	F5
pH 5.50	2.41 ±0.01	2.10 ±0.01	2.40 ±0.02	0.71 ±0.08
pH 5.75	2.30 ±0.01	2.14 ±0.02	2.36 ±0.01	0.66 ±0.03
pH 6.00	2.24 ±0.00	2.09 ±0.01	2.29 ±0.01	0.67 ±0.01
pH 6.25	2.18 ±0.02	2.10 ±0.08	2.26 ±0.02	0.66 ±0.05
pH 6.50	2.10 ±0.01	1.93 ±0.02	2.26 ±0.08	0.55 ±0.06
pH 6.25 + 50 mM NaCl	6.45 ±0.01	6.54 ±0.09	6.59 ±0.09	5.35 ±0.02
pH 6.25 + 200 mM NaCl	17.87 ±0.1	18.42 ±0.2	18.22 ±0.3	17.90 ±0.1
pH 6.25 + 500 mM NaCl	38.52 ±0.2	37.95 ±0.2	37.45 ±0.6	38.30 ±0.3

for each fraction. The conductivities of PPCn, PPCn-FD and PPCa were quite similar at the same pH or NaCl concentration. Only PPIp showed a somewhat lower conductivity in the case where no NaCl was added. This is probably caused by the isoelectric precipitation step, where proteins are separated from the soluble components, including salt. The lower conductivity of PPIp can also explain the somewhat higher zeta potential as function of pH. This is shown in Fig. 3.9A, where the zeta potential as function of pH is plotted for each fraction. This figure also shows that for the dispersions with coacervates, the charge was always around -20 mV, regardless of which fraction was used. However, it was not the case that an average charge of -20 mV always led to the formation of coacervates, as shown by PPIp with 50 mM NaCl. This means that the ability of pea protein to form coacervates also depends on the way they are fractionated.

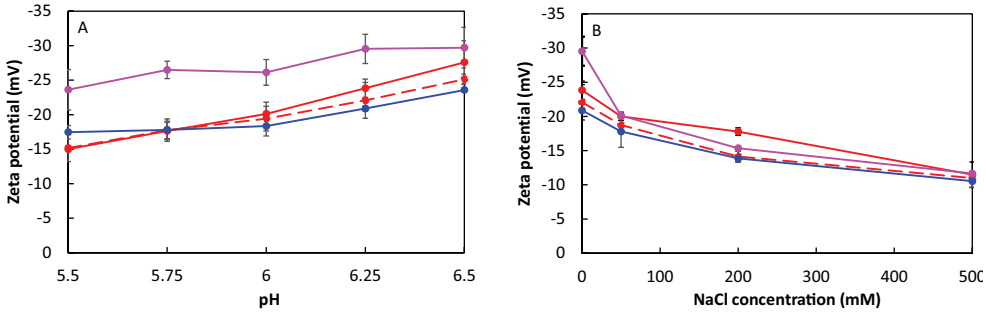

Figure 3.9 A. Zeta-potential as function of pH. B. Zeta-potential as function of NaCl concentration. The four pea fractions are shown: PPCn (—), PPCn-FD (— dashed), PPCa (—) and PPIp (—). The error bars represent the standard deviations.

3.4 Conclusion

In this study we examined the solvent conditions at which different pea protein fractions form coacervates. Confocal microscopy revealed how the microstructure of a mildly fractionated pea protein dispersion changes with pH and ionic strength. The coacervate dispersions were homogeneous (i.e., no protein aggregates present) at pH 6.25 and NaCl concentrations of 0 and 50 mM. At the conditions where coacervates were observed, the measured average zeta potential of the dispersion was consistently around -20 mV. At a pH below 6.00 – where the net charge was reduced further – the protein aggregated. It turned out that around a quarter of the dispersed proteins were able to form coacervates, and that the proteins composing these coacervates were globulins and not albumins.

Another insight obtained in this study is that the fractionation history influenced the ability of pea protein to form coacervates. Freeze drying induced protein aggregation, but the non-aggregated protein could still form coacervates. After alkaline extraction – commonly applied to increase protein solubility upon extraction – part of the protein-rich domains was not spherical anymore, probably indicating the presence of protein aggregates. After isoelectric precipitation only protein aggregates were observed on a microscale. We showed that pea protein can form coacervates at certain pH and salt concentration, but also that commonly applied fractionation routes affect this property. Our research provides new insights on the effect of fractionation processes on the ability of pea protein to form coacervates. These insights could initiate and support further research in this fascinating field of plant protein coacervates.

Chapter 4

Less is more: Limited fractionation yields stronger gels for pea proteins

Abstract

Limited fractionation of yellow pea yielded functional protein fractions with higher gelling capacity. Pea protein concentrates were obtained by dispersing flour at unadjusted pH (~ 6.7) and at pH 8. An additional isoelectric precipitation step resulted in a protein-rich isolate and a protein-poor supernatant. Aqueous solutions of these pea fractions (up to 15 wt. %) were heated from 20 to 95 and subsequently cooled to 20 °C, and their viscoelastic response was characterized by small and large amplitude oscillatory shear measurements (SAOS and LAOS, respectively). SAOS rheology showed that the limited processed pea fractions formed significantly firmer gels per mass of protein after cooling, than the more extensively fractionated pea ones, with elastic moduli of G'~10^3 Pa and G'~10^2 Pa, respectively. LAOS rheology showed an overall strain softening behaviour for all pea fractions and a transition from elastic to viscous behaviour at higher strain for the limited fractionated pea protein isolate. Confocal and electron microscopic images were consistent with those observations, and revealed a more homogeneous network for the limited fractionated samples, and a more heterogenous network for the protein isolate. A number of experiments showed that there are different processing and compositional factors affecting gelling capacity. These are isoelectric precipitation, amount of sugars upon lyophilization and differences in ash content. Furthermore, differences in pre-aggregated state, as found in earlier research, may be partially responsible for the different gelling behaviour. In conclusion, we explain how fractionation affects pea proteins and found that limited fractionation yields pea proteins that form firmer and more ductile gels.

This chapter is published as:

Kornet, R., Veenemans, J., Venema, P., van der Goot, A. J., Meinders, M., Sagis, L., & van der Linden, E. (2021). Less is more: Limited fractionation yields stronger gels for pea proteins. Food Hydrocolloids, 112, 106285.

4.1 Introduction

In recent years, quite a few studies appeared with a focus on functional behaviour of mildly or limited processed plant proteins [62, 146-148]. The main reason that mild processing receive considerable interest is that it could contribute to a more sustainable production of foods [149]. Although extensive purification may be beneficial in reducing off-flavours and increasing the general applicability of ingredients, mildly processed fractions often exhibit richer behaviour due to the higher number of components in those fractions, which may lead to a more detailed control of microstructural features. Furthermore, mild or limited processing of plant material may better preserve native properties of biopolymers; less mild processing steps such as heating, pH adjustments and drying can alter the physical state of proteins and (poly)saccharides irreversibly and thus change their functional behaviour. Hence, the functional behaviour of yellow pea fractions will not only depend on the extent of fractionation and its direct consequences for molecular composition, but also on the extent of processing as a determinant of the state of the biopolymers present. The above explains within the field of plant protein food research the interest on functionality as a function of composition and processing history, rather than molecular composition only. Indeed, preventing protein denaturation during fractionation processes can result in better heat-induced gelling properties [50, 150].

Protein purification can be achieved in different ways, including dry and aqueous fractionation. The latter can be considered as a conventional route [57] and has been widely applied. This method has the advantage of achieving high protein purities. It typically involves a solubilization step at elevated pH (8 – 10), separation of the soluble and insoluble part and subsequent isoelectric precipitation (pH 4 – 5) of the formerly soluble proteins and spray or freeze drying [142, 151, 152]. At the same time, different studies have reported the pH sensitivity of pea and soy proteins on their functionality. Shifting the pH-value to acidic pH (< 3.5) or alkaline pH (> 9) were found to induce irreversible modification of the proteins, leading to e.g. reduced solubility [33, 115]. Furthermore, it was found that precipitation of pea proteins at pH 4.5 resulted in a 20% reduction of solubility and the formation of both soluble and insoluble aggregates (Chapter 2). The solubility of commercial pea protein isolates (PPI) is substantially lower, with reported solubility values ranging from 20 - 60% at pH 7 [55, 61, 68]. The proteins in those isolates are often completely denatured, probably as a result of pH changes combined with elevated temperatures upon extraction or drying.

Thermal stability of proteins is an important functional property in food applications (e.g. high protein drinks and food gels) and there have been several studies on the gelation behaviour of pea proteins. It was found that native pea globulins mostly aggregate through hydrophobic interaction upon heating, and hydrogen bonding upon cooling, and that disulphide bonding does not play a major role [69, 141, 153]. Other studies found that the protein extraction process influences the gel firmness of PPI and that commercial PPI generally perform poorer compared to lab-extracted PPI [70]. Despite these studies, a gap exists on the effects of the different steps in a conventional aqueous extraction on the gelling properties of yellow pea protein, allowing to optimize the intensity of fractionation and according gel properties. Here we will address this gap for yellow pea, building further on our findings in Chapter 2, on the compositional and physicochemical changes upon aqueous fractionation of yellow pea.

In this study we examine the effect of aqueous fractionation on the thermal stability and gelling behaviour of the resulting yellow pea. The viscoelastic behaviour during and after heating is studied and related to the microstructure of the obtained gels. These measurements were complemented with rheological measurements and chemical analyses to find explanations for differences in gelling capacity upon more extensive fractionation.

4.2 Materials and methods

4.2.1 Materials

Yellow pea (*Pisum sativum* L.) seeds were obtained from Alimex Europe BV (Sint Kruis, The Netherlands). All chemicals and reagents were obtained from Merck (Darmstadt, Germany) and were of analytical grade.

4.2.2 Yellow pea extraction process

Yellow pea protein fractions varying from limited to extensively fractionated, were obtained according to the method described in Chapter 2. Two aqueous purification processes were used (Fig. 4.1). In both processes flour was dispersed in deionized water and pH was adjusted by adding 1 M NaOH or HCl solutions.

A limited fractionation process (A) included yellow pea flour dispersion at unadjusted pH under mild agitation for two hours, and subsequent centrifugation at 10000g for 30 min. The supernatant was labelled PPCn (pea protein concentrate neutral extracted). The second, more extensive fractionation process (B) also started with flour dispersion under mild agitation for 2 hours, but the pH was adjusted to pH 8 beforehand. The dispersion was centrifuged (10000g, 30 min) and the supernatant was labelled PPCa (pea protein concentrate alkaline extracted). This fraction was further purified by isoelectric precipitation at pH 4.5 and subsequently centrifuged (10000g, 30 min). The obtained supernatant was labelled ALB-F (albumin-fraction) and the pellet was re-dispersed at pH 7 and labelled PPIp (pea protein isolate precipitated). All steps in the fractionation processes, including centrifugation, were conducted at room temperature and the obtained fractions were frozen and lyophilized with an Alpha 2-4 LD plus freeze-dryer (Christ, Osterode am Harz, Germany) and then stored at -18 °C.

Protein content was determined by a Flash EA 1112 series Dumas (Interscience, Breda, The Netherlands) using a nitrogen conversion factor of 5.7. In Chapter 2 the effect of the fractionation processes on composition and protein recovery was studied. The results from this study are shown in Table 4.1, where the composition of pea flour is identical to that of the yellow pea seed. The pea flour can be considered a starch-rich fraction, PPCn and PPCa protein concentrates, the ALB-F a protein-poor side stream and PPIp a protein isolate.

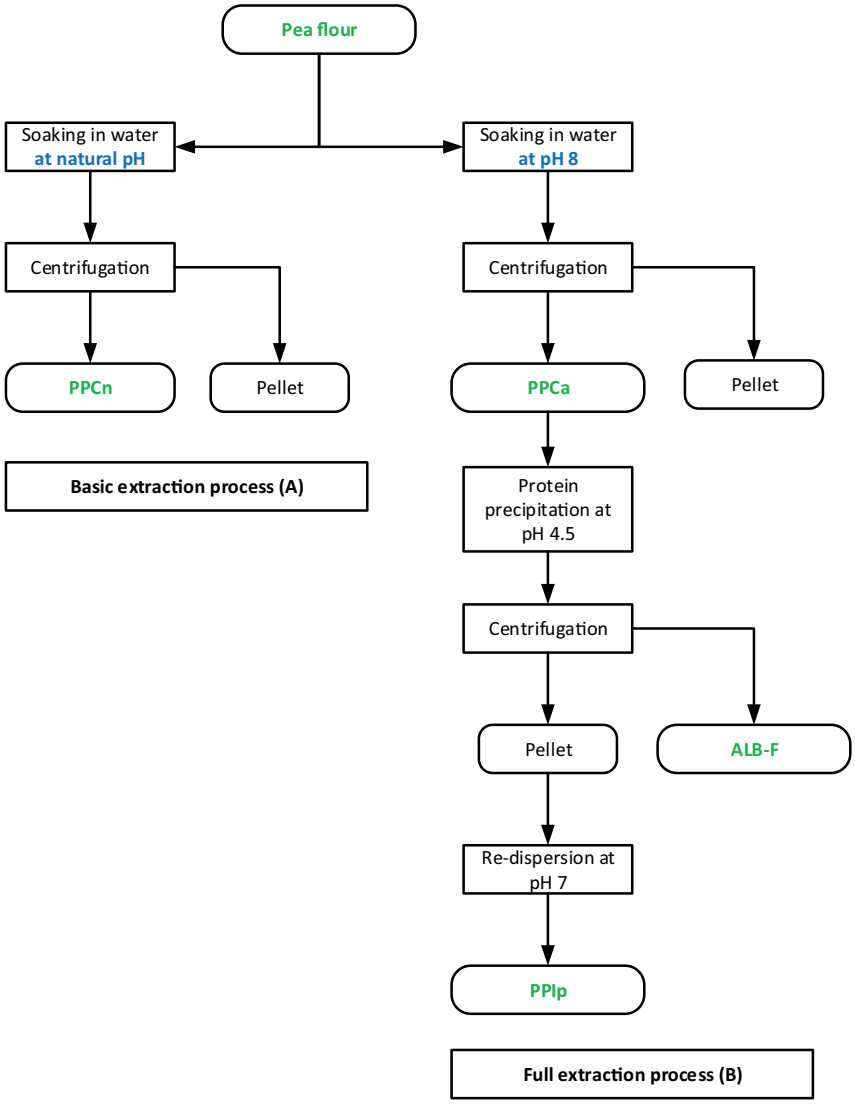

Figure 4.1 Schematic overview of the basic (A) and full extraction process (B) for pea.

Table 4.1 Dry matter composition of the yellow pea fractions. The recovery is defined as the recovered amount of protein divided over the initial protein mass from the flour. Standard deviations are shown in superscript.

	Recovery (%)	Protein content (wt. %)	Total carbohydrate content (wt. %)	Starch or starch derivative content (wt. %)	Ash content (wt. %)
Pea flour	100	18.8 $^{\pm 0.2}$	59.8 $^{\pm 2.1}$	48.7 $^{\pm 1.7}$	3.7 $^{\pm 0.3}$
PPCn	53	46.3 $^{\pm 0.9}$	30.9 $^{\pm 0.3}$	4.1 $^{\pm 0.3}$	13.2 $^{\pm 0.8}$
PPCa	70	51.4 $^{\pm 0.8}$	23.6 $^{\pm 0.1}$	3.5 $^{\pm 0.2}$	11.8 $^{\pm 0.3}$
ALB-F	17	21.1 $^{\pm 0.2}$	34.8 $^{\pm 2.2}$	6.0 $^{\pm 0.0}$	21.1 $^{\pm 0.5}$
PPIp	44	87.3 $^{\pm 1.0}$	3.4 $^{\pm 0.6}$	0.3 $^{\pm 0.1}$	6.0 $^{\pm 0.0}$

4.2.3 Preparation of gels for microscopy

The dried fractions were dissolved in deionized water at a concentration of 15 wt. % at room temperature, under mild agitation with a magnetic stirrer for two hours. Within the first hour the pH was adjusted to 7, using 1 M NaOH or HCl solutions. The solutions were transferred to 15 mL syringes, with paraffin applied on the inside, and closed with a syringe cap. The samples were heated by bringing the syringes to a water bath set to 95 °C and keeping them at this temperature for 15 min. After heat treatment, the samples were cooled to room temperature. The samples were taken out of the syringes gently and cut into small slices with a height of 2 mm.

4.2.4 Hydrophobicity

Hydrophobicity was determined using 8-anilino-1-naphthalenesulfonic acid (ANSA) as a fluorescent probe, according to the method of Kato and Nakai (1980) [154]. The yellow pea fractions were dissolved and pH was adjusted to 7. The stock solution was diluted five times to protein concentrations within a range of 0.03 – 0.16 wt. %. ANSA reagent (8 mM) was added to the sample in concentrations of 10 µl / 3 mL sample. The samples were stored in the dark for one hour to allow ANSA to bind to the hydrophobic sites on the surface of the proteins. Subsequently, fluorescence intensity was measured with a luminescence spectrometer LS50B (Perkin Elmer, Waltham, United States) at wavelengths of 390 nm (excitation) and 470 nm (emission). The measured values were corrected for the intrinsic fluorescence of all dilutions before addition of ANSA. All samples were measured in duplicate. The initial slope of fluorescence intensity versus protein concentration was used as an index for hydrophobicity.

4.2.5 Sulfhydryl content

The number of exposed sulfhydryl groups was determined using the Ellman protocol [155-157]. The Ellman's reagent or 2-nitro-5-mercaptobenzoic acid (DTNB) reacts with free thiol groups of the protein and is used as a reagent for spectrophotometric analysis. A 0.2% DNTB solution was prepared by dissolving DNTB in a 0.1 M sodium phosphate buffer pH 8. A protein stock solution was prepared with 5 mg protein in 1 mL 0.1 M sodium phosphate pH 8.0 buffer. From this stock solution 250 µl was taken and 10 times diluted by 0.1 M sodium phosphate pH 8.0 buffer. To this dilution 50 µl of the Ellman's reagent solution was added. Also, a blank sample without protein was prepared. The solutions were subsequently incubated for 15 min. After incubation, the absorbance was measured with a Shimadzu UV1800 spectrophotometer (Shimadzu, Kyoto, Japan) at a wavelength of 412 nm. All samples were measured in duplicate.

Since literature values for the extinction coefficient of the NTB anion vary within a wide range, a calibration curve with cysteine as calibration standard was made. For this calibration curve, a dilution series was prepared from a 0.5 mM L-cysteine HCl monohydrate (Sigma, C-4820) in 0.001 N HCl stock solution. The calibration curve provided an extinction coefficient for the reduced conjugate of 13,691 M^{-1} cm^{-1} (R^2 = 0.998). The absorbance value for the blank was subtracted from all absorbance values to calculate the net absorbance value.

4.2.6 Electrophoretic mobility

The electrophoretic mobility, a measure for the ζ-potential, of the yellow pea fractions was determined with a ZS Nanosizer (Malvern, Worcestershire, United Kingdom). The sample was dissolved in 0.1 M phosphate buffer pH 7 to obtain a 0.1 wt. % solution. This solution was transferred to a capillary zeta cell and the electrophoretic mobility was determined using Phase Analysis Light Scattering (PALS). The phase is shifted in proportion to the particles velocity. This phase shift is determined by comparing the phase of the light scattered by the particles with the phase of a reference beam. The electrophoretic mobility, and the according ζ-potential, is generated by summing the phase shifts during the Fast Field Reversal (FFR) part of the measurement.

4.2.7 Differential Scanning Calorimetry (DSC)

The protein denaturation and starch gelatinisation temperatures in the pea fractions were determined using DSC. The samples were prepared by dissolving 10 (w/v)

protein in deionized water for 2 hours at pH 7. This solution was transferred to TA high volume pans in quantities of 20 – 30 mL. The pans were closed and measured with a TA Q200 Differential Scanning Calorimeter (TA Instruments, Etten-Leur, The Netherlands), in a range of 20 °C to 120 °C with incrementing temperature of 5 °C/ min. All samples were measured in triplicate.

4.2.8 Small Amplitude Oscillatory Shear (SAOS)

The dried fractions were dissolved in deionized water at a concentration of 15 wt. % drat room temperature, under mild agitation with a magnetic stirrer for two hours. Within the first hour the pH was adjusted to 7, using NaOH or HCl. For certain experiments the samples were standardized on 10 wt. % protein with varying dry matter. The amount of dry matter was calculated based on the protein content of the pea fractions.

The linear viscoelastic properties of the samples were evaluated with SAOS. The samples were measured with an MCR302 rheometer (Anton Paar, Graz, Austria) combined with a sand-blasted CC-17 concentric cylinder geometry. Gelling occurred within the cylinder and to prevent solvent evaporation during heating, a solvent trap was placed on top of the cylinder. The samples were sequentially exposed to a temperature, frequency and strain sweep. Upon thermal treatment the temperature increased from 20 – 95 ˚C at a rate of 3 ˚C/min. The samples were kept at 95 ˚C for 10 minutes before cooling back to 20 °C at a rate of 3 °C/min. Subsequently, the gels were subjected to a frequency sweep from 0.01 to 10 Hz (at a strain of 1%). The storage (G') and loss modulus (G'') dependency on temperature and frequency was recorded.

The pea fractions are compared on different parameters, including gelling capacity and gel strength. The gelling capacity is defined as the capacity per mass of protein to increase the G' upon thermal treatment. Gel strength is defined as the elastic modulus after heat treatment. The end of the linear viscoelastic regime is defined as the strain at which the elastic modulus has decreased to 90% of its plateau value.

4.2.9 Large Amplitude Oscillatory Shear (LAOS)

After the SAOS measurements, a strain sweep was applied to determine the elastic and viscous behaviour of the 15 wt. % yellow pea fraction gels in the nonlinear regime. LAOS was a continuation of SAOS so the same geometry and gels were used. The gels were studied at a logarithmically increasing strain range of 0.1 – 1000% in 10 min to collect 80 data points. The temperature and frequency were kept

constant at 20 °C and 1 Hz. The oscillating strain, stress, and shear rate signals were recorded for an imposed sinusoidal strain and used to construct Lissajous plots. The intra-cycle stiffening behaviour (S factor) and intra-cycle thickening behaviour (T factor) were determined as described by Ewoldt et al. (2008):

where, and are the shear elastic modulus at maximum strain (i.e. the secant modulus) and the tangential modulus at zero strain, respectively. The viscosities and are the viscosity at maximum shear rate and tangential viscosity at zero shear rate respectively. The S- and T-factors were automatically calculated using the Anton Paar Rheocompass Software.

Stress decomposition was done manually to visualise the elastic and viscous contribution to the measured stress response. This method originates from orthogonal stress decomposition [158], using symmetry arguments to decompose the generic nonlinear stress response into a superposition of an elastic and viscous stress, and . The decomposition is based on the idea that the elastic stress should exhibit odd symmetry with respect to and even symmetry with respect to the and for the viscous stress vice versa. [159]. The stress and viscous contribution was determined from:

4.2.10 Confocal Laser Scanning Microscopy (CLSM)

The proteins in the gel were stained in a 0.002% fluorescent dye Rhodamine B solution for two hours and washed with water twice for two hours. The microstructures were visualised using a Leica SP8X-SMD confocal laser scanning microscope (Leica, Amsterdam, The Netherlands), coupled with a white light laser. A dry objective (10x, 0.40) and water immersion objectives (20x, 0.70 and 63x, 1.20) were used for magnification. The laser excitation wavelength and the filter emission wavelength were 543 and 580 nm respectively.

4.2.11 Cryo-Scanning Electron Microscopy (CryoSEM)

CryoSEM was used to visualise the microstructure of gelled pea flour and 5. A small piece of the gel was frozen with liquid ethane and transferred to a sealed cryo-chamber for planing with a Leica EM FC7 microtome (Leica, Eindhoven, the Netherlands). The sample was pre-planed with a glass knife and planing was finalized with a diamond knife to ensure a smooth surface. Subsequently, the sample was sublimated under vacuum and sputter coated with platinum. It was then transferred to the SEM chamber (Jeol, Nieuw-Vennep, The Netherlands) and cooled to -110 °C. The surface of the samples was scanned with a focussed beam of electrons to produce images

of different regions in the sample. Energy-dispersive X-ray Spectroscopy (EDS) was used to obtain elemental maps of some of these regions.

4.2.12 Additional rheological experiments to test specific hypotheses

Additional rheological tests were performed to test different hypothesis regarding observed differences between pea fractions. The results of these tests are described in section 4.3.6 and here the methods are briefly discussed. In all cases, dispersion of 15 wt. % dry matter in deionized water were made and the pH was adjusted to 7 with NaOH or HCl. All rheological measurements were performed as described in section 4.2.8.

To test the effects of ionic strength an estimation of the initial ionic strength was made based on the ash content and verified with conductivity measurements. For the calculation it was assumed that all salts was present as sodium chloride, as this is the most abundant salt as a consequence of pH adjustments with NaOH and HCl in the fractionation process. Sodium chloride was added to dispersions in concentrations of 20 and 200 mM NaCl.

The impact of composition was tested by reversing the fractionation process ALB-F and PPIp were mixed in a ratio of 54 : 46 to obtain a similar composition and the same protein content as PPCa. The mixture was dispersed and measured the same way as all other samples.

The effects of isoelectric precipitation and pH changes were also determined by rheology measurements. The isoelectric precipitated PPIp was compared to PPCn that was further purified by dialysis with a 12 – 14 kDa cut-off size. The dialysis tubes were placed in a bucket of demineralized water at 4 °C and dialysis was finished when the conductivity of the surrounding water remained constant. The dialysed PPCn was freeze dried and measured the same way as the other samples. For the experiments showing the effect of pH shifts, a separate batch of PPCn was made of which half was taken and exposed to 2 hours stirring at pH 4.5 and 2 subsequent hours at pH 7. To compensate for the added salt after the pH adjustments, the conductivity between the two halves was made constant by adding sodium chloride to the part that was not exposed to pH changes. Both fractions were freeze dried afterwards.

The contribution of thiol groups to the gel formation was studied by adding a thiol blocking agent. For this experiment, 15 wt. % pea fractions were dissolved in a 20 mM N-Ethylmaleimide (NEM) solution, the pH was adjusted to 7, and the dispersions

were measured as described in section 4.2.8.

4.2.13 Statistical Analysis

All measurements were performed at least in duplicate. The mean values and standard deviations were calculated and used as a measure of error. Claims regarding significant effects were supported by ANOVA analysis, followed by Tukey's post hoc test. Significance was defined as $P < 0.05$.

4.3 Results and discussion

This results and discussion section starts with the thermal properties and gelation behaviour of the pea fractions. Then their according microstructures are discussed, and finally different experiments are described to explain the differences between limited fractionated and extensively fractionated pea fractions.

4.3.1 Differential scanning calorimetry

To determine the effect of fractionation processes on protein denaturation, the pea fractions were exposed to a thermal treatment and the heat flow was recorded. The peak denaturation temperatures and heat enthalpies are shown in Table 4.2. It was found that the proteins remained at least partially native in all pea fractions. Pea flour shows starch gelatinization and protein denaturation in the different fractions with their standard deviations. Starch gelatinization occurred at 67.1 °C (± 0.24 °C). The globulins in the protein-enriched fractions PPCn, PPCa and PPIp denatured at 83.8 °C (± 0.41 °C). The albumin-enriched ALB-F showed a denaturation peak at 88.1 °C (± 0.19 °C). The temperatures for pea starch gelatinization and globulin denaturation are in line with what has been reported in literature [160, 161]. In contrast to the denaturation temperatures reported in literature, there is quite some variation in the reported heat enthalpies of pea protein. Shand et al. (2007) reported ΔH values for native pea protein isolate (81% protein) ranging from 0.725 to 0.922 J/g, depending on the salt concentration and at a pH of ~6.5 [55]. Another study reported values of 15.81 and 17.84 J/g protein at 0 M and 0.3 M NaCl respectively and at a pH of around 5.7 [150]. The ΔH reported in Table 4.2 do not vary to a great extent and range between 5.5 and 8.9 J/g. Factors that influence the denaturation temperate and heat enthalpy include moisture content, heating rate and presence of salts and sugars. In this study there is significant variation in dry matter and sugar content, which could be an important factor that explains the differences in heat enthalpy between the protein-enriched PPCn, PPCa and PPIp.

4.3.2 Small amplitude oscillatory shear (SAOS)

The gelation behaviour of the yellow pea fractions upon and after thermal treatment was studied by SAOS, shown in Fig. 4.2 and Fig. 4.3. The pea fractions were standardized on 15 wt. % dry matter to study the gelling behaviour of the overall pea fractions. To better compare the protein-enriched PPCn, PPCa and PPIp additional experiments were conducted in which those fractions were standardized on 10 wt. % protein.

Table 4.2 Onset and peak denaturation temperatures (°C) and denaturation enthalpies (J / g) of the pea fractions at pH 7. All standard deviations are smaller than 1 °C or 1 J/g.

Pea fraction	Denaturation onset (°C)	Peak denaturation (°C)	Heat Enthalpy (J/g)
Pea flour	59.3	67.1	-
PPCn	73.6	83.7	5.5
PPCa	77.4	84.3	3.6
ALB-F	81.8	88.1	3.3
PPIp	73.8	83.6	8.9

Gelation behaviour of dry matter standardized dispersions

The gelation behaviour of the yellow pea fractions upon and after thermal treatment was studied by SAOS, shown in Fig. 4.2. The maximum temperature during the thermal treatment was higher than the denaturation temperature of the globular pea proteins. Also the onset of gelation is consistent with Table 4.2. Fig. 4.2 shows an abrupt increase of the elastic moduli for the starch-rich pea flour at around 70 °C and the protein-rich PPCn, PPCa and PPIp upon heating from ~75 to 95 °C. The steep increase in G' observed in pea flour is expected to mainly originate from water absorption and swelling of the starch granules, since starch is the major constituent. The subsequent decrease in G' could be due to loss of crystallinity, subsequent uncoiling, dissociation of double helices and leaching of amylose in the continuous phase [24]. The gelling of the limited processed PPCn and PPCa (46 and 51 wt. % protein resp.) is caused by protein denaturation, as earlier research showed that the carbohydrate impurities are only present in the form of small sugar molecules (Chapter 2). Protein denaturation results in a gradual increase in G' at around 75 °C. Gelling of pea globulins was reported to be mainly based on hydrophobic and electrostatic interactions [153]. Upon heating, the hydrophobic interior of the proteins become exposed, resulting in hydrophobic interactions and subsequent network formation. During the holding time at 95 °C, G' increases more for these limited processed PPCn and PPCa than for pea flour. The decrease afterwards as observed in pea flour, is virtually absent for PPCn and PPCa. Upon cooling the gel firmness increases further. The protein-poor ALB-F (21.1 wt. % protein), which is the supernatant after a protein precipitation step, shows limited gel formation. The $G'(T(t))$ and G'' $(T(t))$ of the extensively processed PPIp (87 wt. % protein) shows a similar behaviour as that of PPCn and 3, but with a reduced gelling capacity, as indicated by the less pronounced G' increase upon heating and cooling. Moreover,

the limited processed PPCn and PPCa (~ 50 wt. % protein) form firmer gels on protein weight basis than the further fractionated PPIp. Explanations for this reduced gelling capacity of the protein in PPIp are discussed in section 4.3.6. Table 4.3 shows the G' and tan δ of all pea fractions after heat treatment. It was found that the G'-values of PPCn, PPCa and PPIp are of the same order of magnitude (10^3 Pa), despite of the substantial differences in protein content between PPCn or PPCa and PPIp. The tan δ values of the studied yellow pea fractions were all below 0.25, indicating solid-like behaviour after heat treatment. Furthermore, it is noted that PPCn has the lowest tan d of 0.04, indicating a more solid-like response. Overall, the pea fractions showed tan d values that correspond with weak elastic gels. Hence the non-linear regime of the gelled fractions was studied by applying oscillatory deformation with a rheometer. Using the same concentrations as used for SAOS measurements, the gels were not firm enough to cut uniform pieces that are required for compressional deformation with a texture analyser.

The G' and G'' dependencies on frequency were determined through a frequency sweep in a range of 0.1 – 10 Hz. For all fractions, G' and G'' remained fairly constant over this frequency range, indicating that G' and G'' are only slightly dependent on frequency in this range. Although generally a stronger dependency on frequency is observed for weak gels, a similar observation was seen by Sun et al. (2010). For commercial and salt-extracted pea protein isolate only a small increase of G′ was observed over a range of 0 – 10 Hz, despite of tan δ values of 0.8 and 0.2 respectively, indicating a weak gel. The almost flat line with increasing frequency could indicate the presence of a broad relaxation spectrum that is typical for a disordered system. Generally colloidal gels in a low viscosity solvents show little to no frequency dependency [162]. The elastic moduli at f < 0.1 Hz could not be studied due to the low signal to noise ratio of the rheometer in these regions. After heat-induced gelation, the length of the linear viscoelastic (LVE) regime was studied by a strain sweep at constant frequency (Fig. 4.2). The end the LVE regime was expressed as the critical strain (γ_c), shown in Table 4.3. The starch-rich pea flour appeared slightly more tensile, whereas the length of the LVE regimes of PPCn, PPCa and PPIp were rather similar. A more detailed analysis on the transition from elastic to viscous behaviour is discussed in section 4.3.3.

The similar elastic moduli of the gels from PPCn, PPCa and PPIp, despite their differences in protein purity, indicate a higher gelling capacity. This higher gelling capacity is discussed further in the next section, where PPCn, PPCa and PPIp are standardized on protein content.

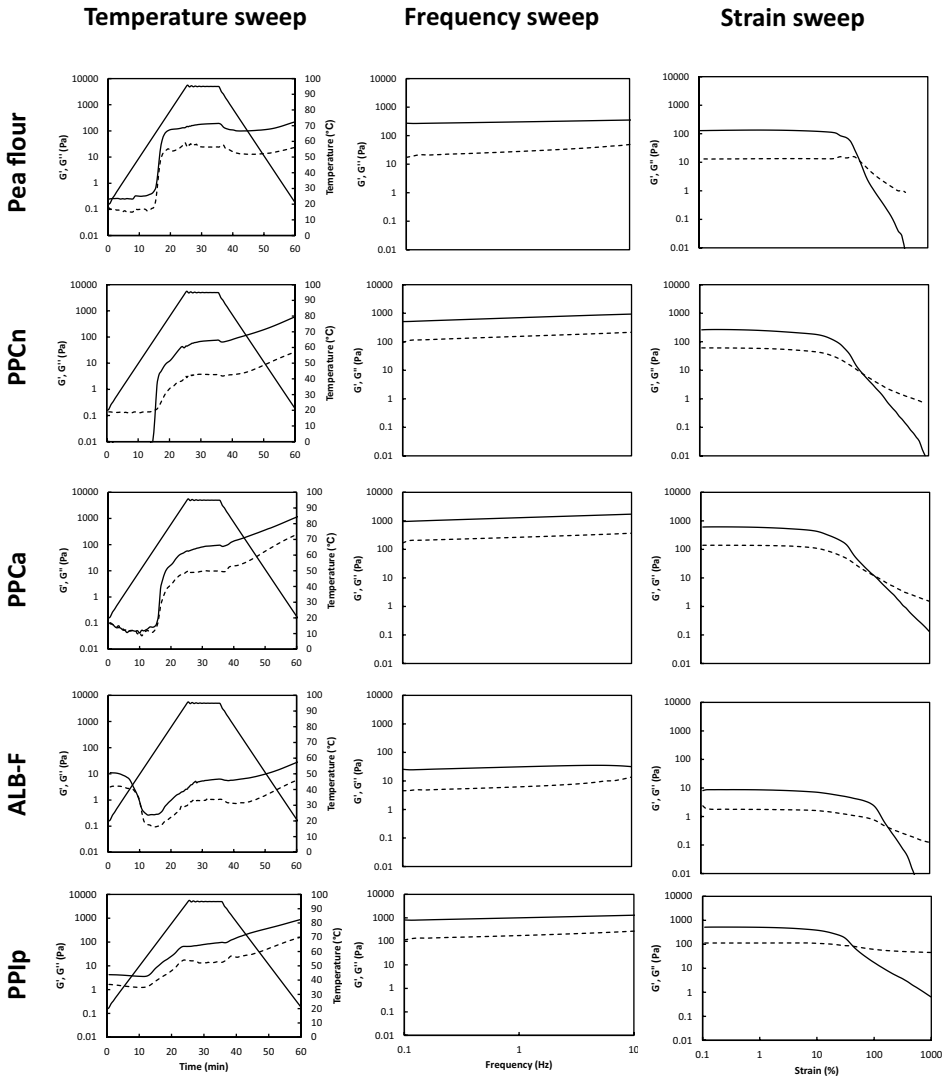

Figure 4.2 Temperature (20 – 95 °C, f = 1 Hz, γ = 1%), frequency (0.1 – 10 Hz) and strain sweeps (0.1 – 1000%) sequentially applied on yellow pea fractions standardized on dry matter (15 wt. % in water adjusted to pH 7) at 20 °C. G' : closed symbols, G'' : open symbols, Temperature: solid line.

Gelation behaviour of protein standardized dispersions

As the main impurities of PPCn, PPCa, ALB-F and PPIp are sugars, the contribution of protein on the gelling capacity was studied further by standardizing PPCn, PPCa

and PPIp on protein content. For pea flour and the ALB-F it was not possible to standardize on 10 wt. % protein, as this would require dispersion of 50 wt. % dry matter because of lower protein purities. Results are depicted in Fig. 4.3 showing the G', G'' dependency on temperature, frequency and strain of PPCn, PPCa and PPIp that are standardized on 10 wt. % protein. The corresponding dry matter concentrations were 21.6, 19.5 and 11.5 wt. % respectively.

The left panels of Fig. 4.3 show the results of the temperature sweeps. The initial elastic modulus G' was higher for the fractions that were more extensively fractionated, while the eventual G' values after gelation were higher for the fractions that were limited fractionated. PPIp has the highest initial elastic modulus and PPCn has the highest final elastic modulus. The first phenomenon has been described earlier in Chapter 2, where pea protein was found to possess high intrinsic viscosity. The higher gelling capacity of the limited processed fractions at equal protein content of 10 wt. % indicates that gel strength is not only related to protein quantity.

Table 4.3 Average elastic moduli (G'), loss factors (tan δ) and critical strains (%) of the gelled pea fractions. The elastic moduli and loss factor correspond with the values of the last data point from the temperature sweeps and the critical strains are determined from the temperature sweeps. All results presented here originate from one batch of pea fractions that was used for this study. Standard deviations are shown in superscript.

	Pea flour	**PPCn**	**PPCa**	**ALB-F**	**PPIp**
Rheological properties of dry matter standardized gels					
G' (Pa)	229 $^{\pm 103}$	623 $^{\pm 127}$	1174 $^{\pm 185}$	28 $^{\pm 11}$	921$^{\pm 4.9}$
Tan δ	0.11$^{\pm 0.02}$	0.04 $^{\pm 0.00}$	0.21$^{\pm 0.00}$	0.21$^{\pm 0.02}$	0.18 $^{\pm 0.01}$
γ_c (%)	11.2 $^{\pm 6.3}$	3.32 $^{\pm 1.8}$	4.95 $^{\pm 3.4}$	2.43 $^{\pm 0.2}$	7.02 $^{\pm 4.8}$
Rheological properties of protein standardized gels					
G' (Pa)	-	1658 $^{\pm 315}$	573 $^{\pm 175}$	-	97 $^{\pm 15.2}$
Tan δ	-	0.24 $^{\pm 0.00}$	0.21$^{\pm 0.00}$	-	0.23 $^{\pm 0.01}$
γ_c (%)	-	1.12 $^{\pm 0.45}$	4.95 $^{\pm 1.22}$	-	14.5 $^{\pm 5.80}$

Fig. 4.3 shows that the protein-standardized fractions showed G' to be independent of frequency in this range. From the strain sweeps (Fig. 4.3), it was found that the length of the LVE regime correlated inversely with the gel strength. Table 4.3 shows that PPCn had the shortest linear viscoelastic (LVE) regime (γ_c = 1.12%), whereas PPIp had the largest maximum linear strain (γ_c = 14.5%). The decline of G' at lower strain is explained by disruption of the gel network structure, resulting in more fluid-like behaviour. PPIp visually appeared to be of paste-like character, which

is presumably due to non-connected protein aggregates, as further discussed in section 4.3.6. For paste-like materials such as PPIp, increasing strain may result in deformation and displacement of protein aggregates or other components, rather than disruption of a network. Another study that compared two types of waxy rice starch gels also showed that a waxy rice starch, which appears more paste-like (G' ~ 30 Pa), was significantly more stretchable than the firmer debranched waxy rice starch gel [163]. At small deformations and equal protein concentrations, the limited processed fractions resulted in firmer gels, but the extensively processed PPIp was able to withstand larger deformation.

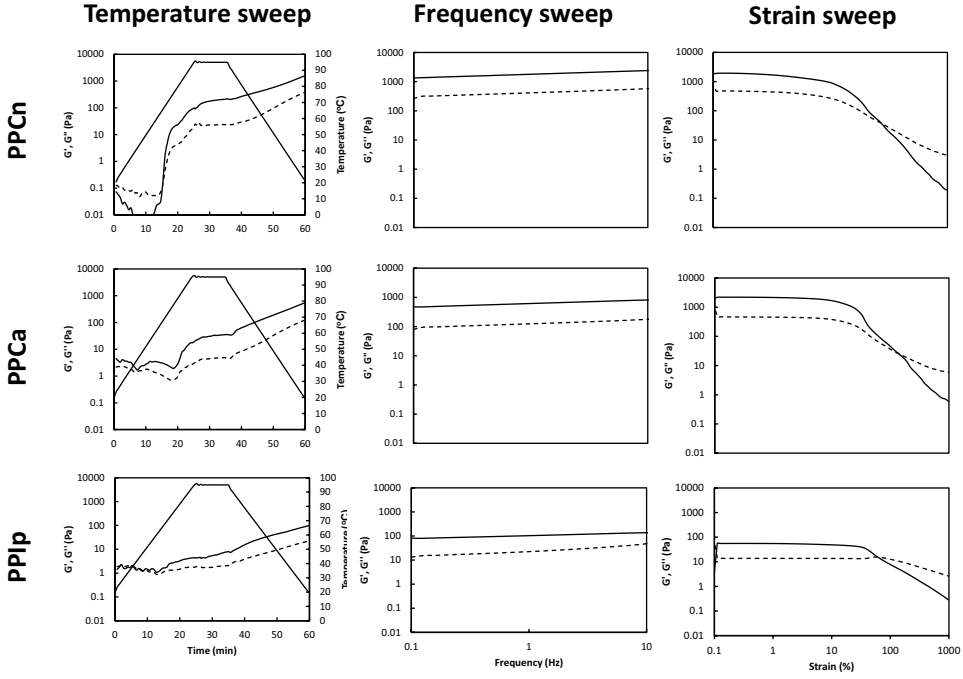

Figure 4.3 Temperature, frequency and strain sweeps sequentially applied on PPCn, PPCa and PPIp standardized on protein content (10 wt. % in water adjusted to pH 7). G' : closed symbols, G'' : open symbols. Temperature: solid line.

4.3.3 Large amplitude oscillatory shear (LAOS)

LAOS measurements were performed to further characterize gel properties of the 15 wt. % (dry matter based) gels by understanding their rheological behaviour beyond the LVE regime. From the LAOS data Lissajous plots were constructed with stress

versus strain and stress versus strain rate (Fig. 4.4A and 4.4B, respectively). Also, the elastic and viscous stress contributions were plotted (black solid lines). At a strain of 1%, Fig. 4.4A shows elliptical shapes indicating predominantly elastic or linear viscoelastic behaviour, particularly for the starch-based pea flour. The Lissajous plot of ALB-F show some irregularities due to its low G' and resulting machine inertia effects. At 26% strain, deflections of the elliptical shape at maximum deformation indicate a mild intracycle strain stiffening behaviour. This intracycle stiffening behaviour is most pronounced in PPCn and PPCa, and to lesser extent in pea flour. However, the apparent stiffening effect is small, and as we will see later in Fig. 4.5, the behaviour of these samples in the overall strain sweep, shown earlier in Fig. 4.2, is mildly strain softening. At a deformation of 170%, PPCa gave a Lissajous plot with an almost rhomboidal shape. This implies that, the initial response is highly elastic at

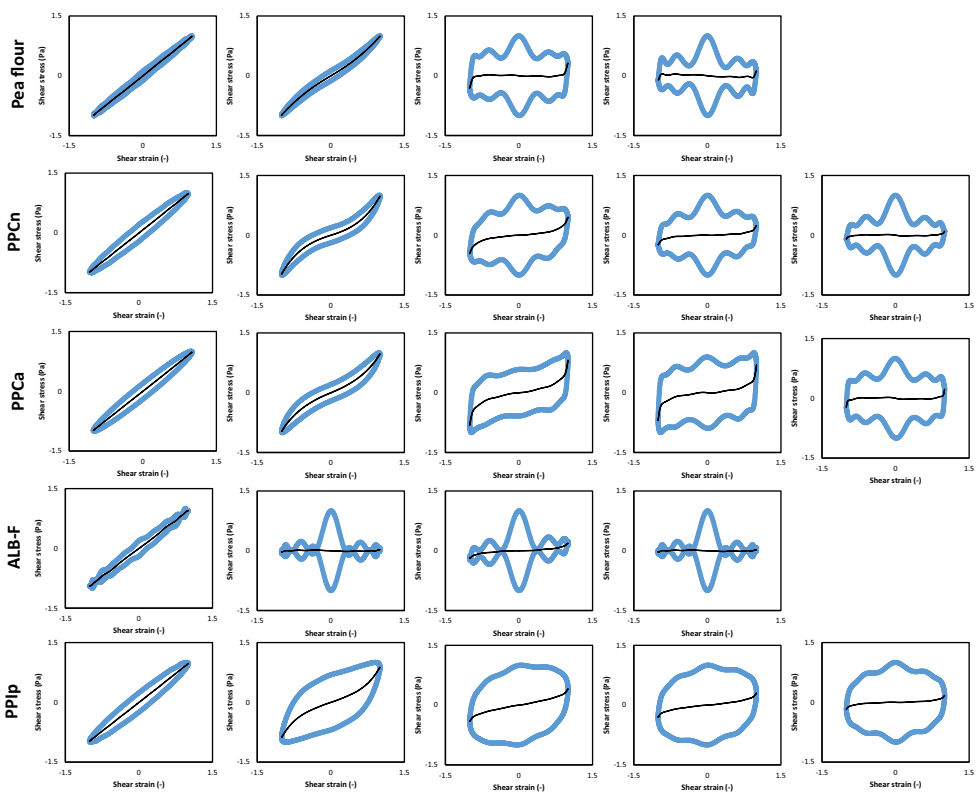

Figure 4.4 A. Elastic lissajous plots of stress versus strain, at strain amplitudes of 1, 26, 170, 305 and 846% applied on the gelled pea fractions (15 wt.% d.m., pH 7). The black line represents the elastic stress contribution.

the start of a cycle, at γ = -1.7. When γ increases, abrupt yielding of the gel structure occurs (as indicated by the sudden change in slope of the plot). In the subsequent part of the cycle, the elastic contribution to the stress is nearly zero, and the response is predominantly viscous. At the end of this part of the cycle, the structure recovers, which results in an increase of the elastic contribution and an *apparent* stiffening behaviour. At even higher strain (≥ 170%) PPCn and PPCa again show cyclic yielding and recovery, but now clear oscillations are visible in the rhomboidal shape. It could be argued that such behaviour is caused by inertia effects of the measuring device, as seen by Birbaum et al. (2016) for interfacial rheology. Oscillations were observed at higher strains and they appeared to be highly reproducible, also when particles on the interface were absent [164]. The oscillations in Fig 4.4A are more regular however, and also correspond with intersections in the viscous Lissajous curves shown in Fig

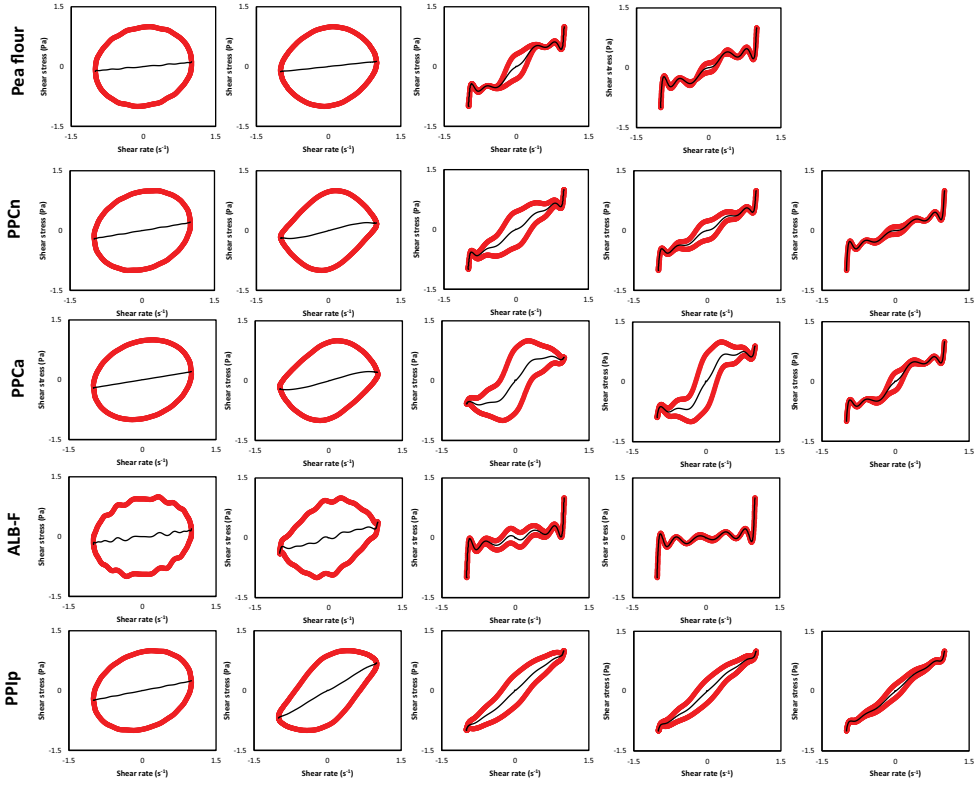

Figure 4.4 B. Viscous lissajous plots of stress versus strain rate, at strain amplitudes of 1, 26, 170, 305 and 846% applied on the gelled pea fractions (15 wt. % d.m., pH 7). The black line represents the viscous stress contribution.

4.4B. Such self-intersections were also seen for tomato paste and wheat flour dough [165, 166] and can emerge from a timescale for restructuring that is shorter than the oscillatory deformation time scale. Hence the Lissajous curves for PPCn and PPCa at higher strain probably reflect material properties. The type of plots are typical when the higher harmonics in the response have a phase close to $\pi/2$, so after yielding the response is almost completely viscous. This is also clear from the elastic contribution to the stress, which is nearly zero except when close to γ_0. PPIp did not show yielding at larger deformations and the transition to flow occurred at smaller strain, which is also indicated by the lack of elastic contribution at a strain of ≥ 170%. [159, 163, 167]. For pea flour and the ALB-F the LAOS data at largest strain (846%) could not be measured. Overall, it is noted that the transitions from elastic to viscous occur at smaller strain for the extensively processed PPIp than the limited processed PPCn and PPCa. For PPIp the Lissajous plot is already circularly shaped at a deformation of 170% (Fig. 4.4A), indicating predominantly viscous behaviour.

The viscous behaviour of the yellow pea fractions is shown in Fig. 4.4B. The shapes of the plots corresponding to PPCn, PPCa and PPIp changed from a circular-shape to a rhomboidal-shape at low strain (26%), reflecting a transition from elastic to viscous dominated behaviour. At higher deformation the signal again showed strong oscillations, due to extreme nonlinearity and the presence of higher harmonics.

Fig. 4.5A shows that $S < 0$ within a large strain region, indicating an overall mild strain softening behaviour for all fractions. Fig. 4.5B shows stronger shear thinning behaviour ($T < 0$) for PPCn and PPCa, mild shear thinning behaviour for pea flour and no shear thinning behaviour for PPIp. The absolute value of the T-factor is much higher than that of the S-factor, indicating an overall response of shear thinning for pea flour, PPCn and PPCa. PPIp is denser in protein than PPCn and PPCa and it shows an earlier transition from elastic to viscous behaviour at large deformation. It seems that PPIp leads to a dense but weakly interacted network, whereas the limited processed PPCn and PPCa leads to a firmer, cohesive and more stretchable system at large deformation.

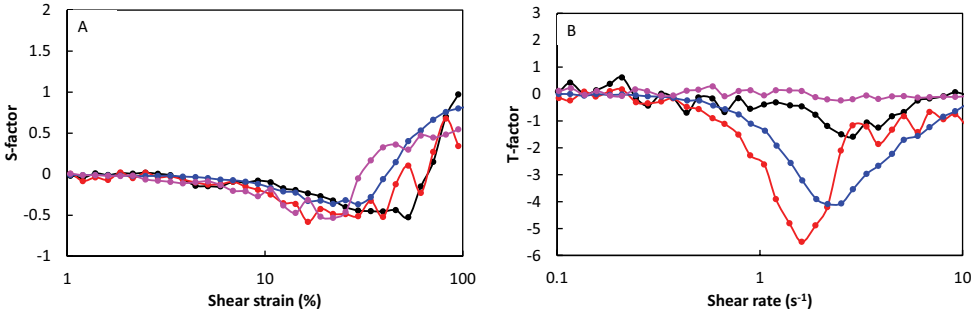

Figure 4.5 A. Ratio of shear stiffening (S-factor) and B. ratio of shear thickening (T-factor) for pea flour (—), PPCn (—), PPCa (—), ALB-F (—), PPIp (—) standardized on 15 wt. % dry matter ad measured at pH 7.

4.3.4 Reproducibility of the fractionation processes and resulting observations

For consistency reasons nearly all experiments were done with pea fractions originating from the same batch. Those results are representative of results that were observed for other batches. In order to strengthen our main statement that limited pea fractionation yields firmer gels per mass of protein at pH 7, we show the average and standard deviations of different batches regarding protein recovery and gel firmness. The results from different fractionation processes (n = 3) are compared for the protein-rich PPCn, PPCa and PPIp. Table 4.4 shows the protein recovery based on the separate fractionation processes. It also shows the average elastic moduli of the gelled fractions that originated from the different batches with a total number of at least seven measurements. The protein recovery and G' observed for the batch used in this study, as shown in Table 4.1 and 4.3, are consistent with the average numbers shown in Table 4.4.

Table 4.4 The protein-rich fractions from batches of different fractionation processes (n = 3) were averaged on their protein recovery and elastic moduli after heating. All gels were measured with 15 wt. % pea fraction solubilized in deionized water at pH 7. The numbers in superscript represent the standard deviations and the different letters represent significant differences.

	PPCn	**PPCa**	**PPIp**
Recovery (%)	59 $^{\pm 9.8}$	74 $^{\pm 3.2}$	52.4 $^{\pm 7.3}$
G' (Pa)	756 $^{\pm 424\ \mathbf{a}}$	1565 $^{\pm 751\ \mathbf{b}}$	518 $^{\pm 144\ \mathbf{a}}$

4.3.5 Microstructure

Fig. 4.6 shows CLSM images of the gels with the stained proteins shown in red. Pea flour seems to form a dense network at mesoscale, with large flour particles incorporated. The image indicates a continuous starch phase with protein distributed throughout. PPCn and PPCa show a somewhat discontinuous, but more homogeneous protein network at mesoscale. This is consistent with the rheological observations that indicated higher gel strength and strain softening behaviour. ALB-F shows a dispersion of protein aggregates combined with some non-protein material. The extensively processed PPIp shows a more heterogenous network with protein dense regions, indicated by a higher colour intensity in the CLSM images. Those regions are also seen in the electron microscopy images and could be caused by a higher protein content or by the presence of protein aggregates, as found in Chapter 2.

CryoSEM was performed to further understand the microstructural properties and interactions of the starch-rich and protein-rich systems of pea flour and PPIp (Fig. 4.6). Energy-dispersive X-ray Spectroscopy (EDS) was used to obtain an elemental map of the imaged area, which is used to identify components based on their element density. The gelled matrix was found to be heterogeneous with swollen starch granules, protein aggregates and a few oil droplets. Based on the elemental maps it was concluded that the continuous phase consisted of starch, substantiated by low nitrogen and denser oxygen and carbon. It is seen that the starch granules swell irregularly, fill the volume, leading to a dense starch system. Protein-dense regions are observed in between the starch granules and other cell components. The CryoSEM images are consistent with the assumption that starch is predominantly responsible for gelation in pea flour.

The protein-rich PPIp was also visualized by CryoSEM, providing additional insight in the protein distribution in this heated paste-like system. The image shows protein-dense areas and EDS was used to confirm the presence of protein, showing indeed higher intensities of carbon and nitrogen. Pea protein in PPCn, PPCa and PPIp were hypothesized in Chapter 2 to be already in a partially aggregated state before heat treatment, as the protein was found to have a high volume to mass ratio. The presence of more protein aggregates in PPIp than in PPCn and PPCa, could cause a lack of connectivity in the gelled matrix of PPIp and concomitant reduced gelling capacity due to the lower number of connections per unit volume that bare energy. We note however that this is not the only factor that is relevant to explain all observations as we will address from section 4.3.6 onwards.

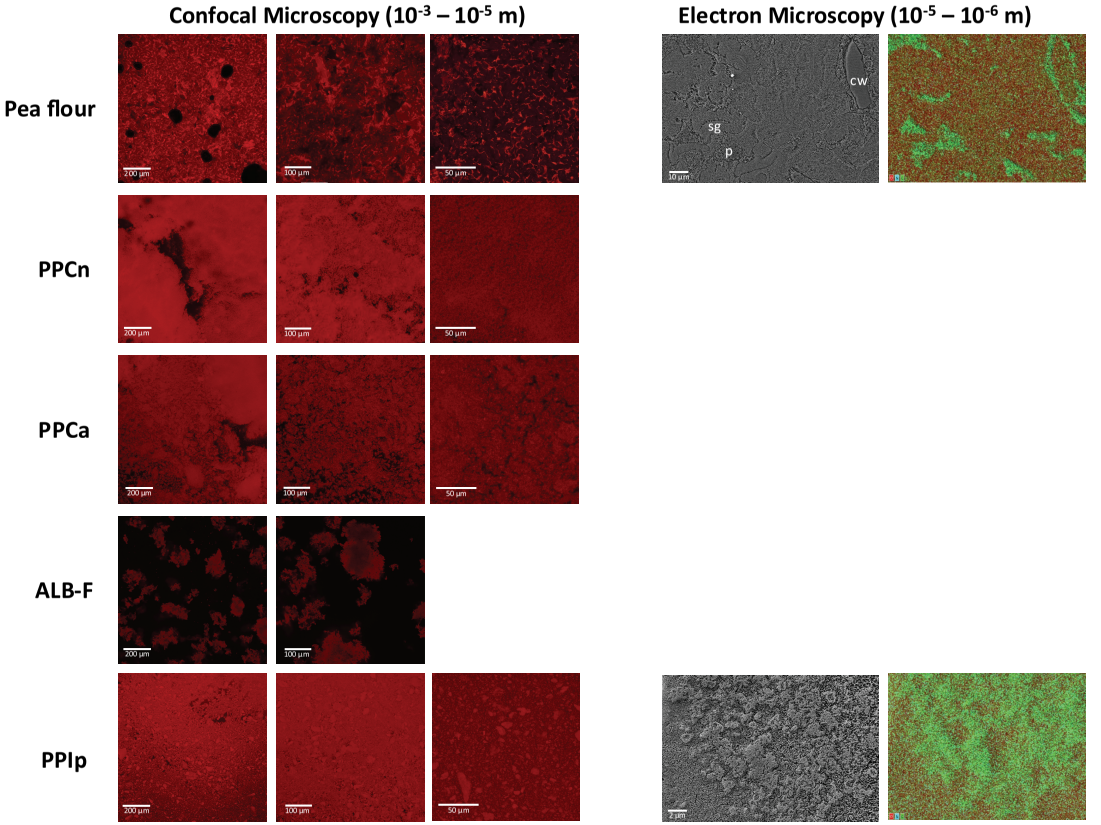

Figure 4.6 CLSM images of gelled fraction 1 - 5 and CryoSEM images of gelled fractions 1 and 5 coupled with EDS, where red = oxygen, blue = nitrogen and green = carbon. sg = starch granule, p = protein, cw = cell wall material. All gels were made with 15 wt. % pea fractions at pH 7.

4.3.6 Reduced gelling capacity upon fractionation

To understand why more extensive fractionation resulted in reduced gelling capacity per mass of protein at pH 7, different hypotheses were proposed and tested. The first set of tests were done to see whether impurities (i.e. sugars, salt, albumins) promoted the gelling capacity of PPCn and PPCa. The second set of tests were based on the suggestion that pH shifts in the fractionation process could result in irreversible changes in the protein structure, reducing their gelling capacity.

Ionic strength

One hypothesis was that differences in ionic strength, as indicated by differences in ash content (Table 4.1), could explain the reduced gelling capacity of PPIp compared to PPCn and PPCa. The elastic modulus G' after thermal treatment was measured at initial ionic strength, 20 mM NaCl and 200 mM NaCl addition. The G' of PPIp increased from $3.1 \cdot 10^2$ to $1.4 \cdot 10^3$ Pa and PPCn and PPCa increased even less. Also at higher ionic strength PPIp did not significantly exceed the gel firmness of PPCn and PPCa, confirming the higher gelling capacity per mass of protein for PPCn and PPCa. To illustrate this, Fig. 4.7A shows the elastic moduli of fractions PPCn, PPCa and PPIp after standardization on an ionic strength of ~0.3 M. The finding of a higher gelling capacity per amount of protein for fractions PPCn and PPCa at standardized ionic strength, shows that the salt concentration has a relatively small influence.

Composition

In general, the composition itself had minor impact on the gelling capacity of the fractions. This is shown by reversing the fractionation by combining ALB-F and PPIp to yield a combined fraction with a composition of impurities and proteins equal to that of PPCa. So, this combined fraction had the same composition as PPCa, but its components experienced more severe processing due to the processing history of PPIp. Fig. 4.7B shows that PPCa was significantly firmer than the combined fraction. This indicates that the fractionation processing altered the functionality of pea proteins. Interestingly, in this case the less severely processed fraction with a given composition exhibited a firmer gel than the fraction with the same composition but more severely processed, or, in other words, limited fractionation in this case implies a gel that is firmer. Following up on the importance of processing we look into the effect of lyophilization and isoelectric precipitation.

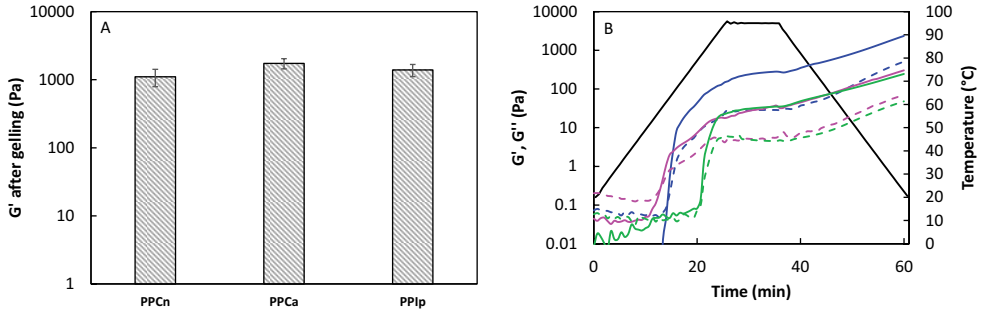

Figure 4.7 A. The G′ of PPCn, PPCa and PPIp at a standardized ionic strength of ~0.3 M with the error bars indicating the standard deviation. B. Comparison of PPCa and PPIp with a mixture of ALB-F and PPIp to mimic PPCa, with PPCa (—), PPIp (—) and ALB-F/ PPIp mixed (—). All gels were made with 15 wt. % pea fractions at pH 7. G′ : closed symbol and G″ : open symbol.

Lyophilization

It was hypothesized that the reduced gelling capacity of PPIp could be explained by a reduced thermal stabilization of sugars upon lyophilization. Table 4.1 shows that PPCn and PPCa contain more carbohydrates than PPIp and from Chapter 2 it is known that the vast majority of these carbohydrates are sugars. Sugars can stabilize proteins upon lyophilization [145]. To verify the effect of freeze drying, PPCn was further purified with a 12.5 kDa membrane, to remove all sugars and salts, and its gelling capacity was compared to PPIp after lyophilization. Fig. 4.8A shows that, despite of the similar low sugar content, PPIp still had a significant lower elastic modulus ($9.2 \cdot 10^2$ Pa) than the dialysed PPCn ($6.2 \cdot 10^3$ Pa). This does not result in rejection of the hypothesis, but it is clear that the potential thermal stabilization cannot fully explain the differences between PPCn, PPCa and PPIp. Lyophilization probably has some effect on the protein state and functionality, but this again cannot fully explain the differences between PPCn, PPCa and PPIp.

pH changes and isoelectric precipitation

Another hypothesis was that pH changes or the isoelectric precipitation step is responsible for the reduced gelling capacity of PPIp. Previous studies showed that pH changes can induce irreversible changes in soy and pea protein structure [33, 115]. Although the pH changes applied in those studies were more extreme (i.e. <3.5 and >9) than during the fractionation process (≥4.5 and ≤8), it was considered a plausible hypothesis, as even minor pH changes (i.e. pH 7 - 6) can have significant impact on the state of pea proteins (i.e. plant protein microcapsules) in dispersion [130]. This

hypothesis was tested in two different ways, of which the results are shown in Fig. 4.8A and 4.8B. Fig. 4.8A shows a comparison between the precipitated PPIp and the non-precipitated (i.e. dialysed) PPCn. It shows that replacement of a protein precipitation step by dialysis, yields a pea protein isolate (84 wt. % protein) that has significantly ($P < 0.05$) higher G' after thermal treatment than the precipitated PPIp (87 wt. % protein). This implies that isoelectric precipitation affects the gelling capacity of pea protein. Fig. 4.8B shows the sole effect of a pH change (7 to 4.5 and back to 7) on the gelling capacity of pea protein. PPCn with and without pH shift are compared and a reduction of the eventual G' is observed ($1.4 \cdot 10^3$ to $6.0 \cdot 10^2$ Pa). This difference turned out to be insignificant ($P > 0.05$) when taking into account the average G′ (756 Pa) observed for PPCn, as shown in Table 4.4. In the pellet after centrifugation proteins are highly concentrated and around their is··oelectric point, which may induce (irreversible) formation of protein aggregates. Based on the results from Fig. 4.8 we conclude that isoelectric precipitation can reduce the gelling capacity of pea protein.

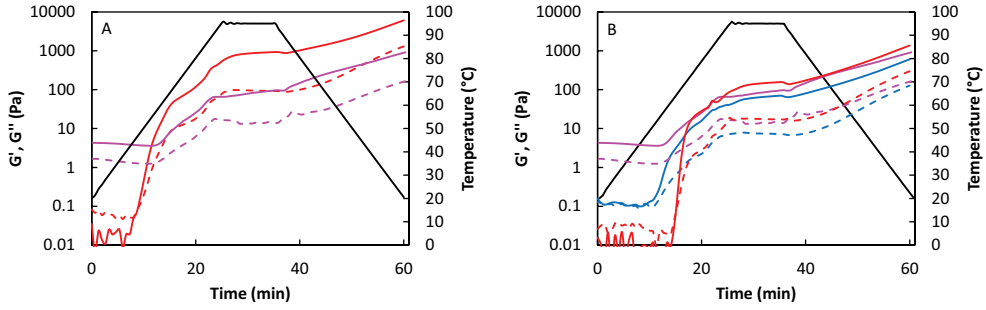

Figure 4.8 A. The gelling behaviour of PPCn after dialysis (—) and PPIp (—). B. Comparison between PPCn (—) and PPCn exposed to a pH shift (—), with PPIp (—) shown as a reference. All gels were prepared with 15 wt. % pea fractions at pH 7. G′ : closed symbol and G″ : open symbol.

Pre-aggregation and interactions upon heating

In Chapter 2 it was found that pea proteins form aggregates with a low-density structure, which was also reflected in their average particle size (Table 4.5). The average particle size (350 nm) of PPIp is larger than that of PPCn and PPCa (94 and 242 nm respectively). Those numbers originate from dynamic light scattering measurements and the corresponding particle size distributions indicated polydispersity . These size distributions are obtained as a plot of the relative intensity of the light scattered by the particles in the various size classes.

Although there is a reduction in exposed thiol groups after heating the fractions (Table 4.5), S-S bonding does not play an active role in the heat-induced gelation process [153]. This was also confirmed by an additional experiment with the thiol-blocking agent NEM on PPCa and PPIp. The incubated samples showed similar gelling behaviour upon heating as the non-incubated ones (not shown here). The observed reduction in exposed thiol groups could mean that upon heating there is S-S bonding to some extent, but it does not greatly affect the eventual network structure. Another possibility is that fever thiol groups were detected, not because they formed S-S bonds, but simply because they were buried in the protein aggregates after heating. Furthermore, it has been reported for pea proteins that hydrophobic interactions and hydrogen bonding are mainly responsible for heat-induced gelation [153]. However, differences in relative hydrophobicity, as shown in Table 4.5, could not explain differences in gelling behaviour. To exclude the effect of electrostatic interactions, the electrophoretic mobility was measured and is shown in Table 4.5. The values indicate that the average charges of all dispersed fractions are at pH 7. This means that in the measured systems there is electrostatic repulsion that prevents the proteins from interacting at room temperature and influences the rate and extent of gelation upon heating. As the ζ-potentials are of a similar order of magnitude, it cannot explain the differences in gelling capacity observed for the different fractions.

Table 4.5 An overview of the physical properties of the pea fractions at pH 7 and I < 0.1 M NaCl equivalent. The type of proteins and average particle size originate from Chapter 2. The number of sulfhydryl groups per gram of protein was determined before and after heating, measured at pH 8. Standard deviations (and R^2 for hydrophobicity) are displayed in superscript.

Pea fraction	Type of proteins	Average particle size (nm)	Relative hydrophobicity (Arb. Unit)*	Thiol groups (μmol SH-groups / g protein)	ζ-potential (mV)
Pea flour	Both	ND	6.6 $^{0.99}$	32.2 $^{\pm0.4}$ | 46.3 $^{\pm0.1}$	-23.4 $^{\pm1.1}$
PPCn	Both	94 $^{\pm3}$	6.7 $^{0.95}$	55.6 $^{\pm0.2}$ | 33.7 $^{\pm0.0}$	-20.7 $^{\pm1.8}$
PPCa	Both	242 $^{\pm4}$	9.5 $^{0.98}$	52.3 $^{\pm0.7}$ | 39.5 $^{\pm0.1}$	-23.3 $^{\pm1.0}$
ALB-F	Albumins	110 $^{\pm14}$	<< 1	168 $^{\pm3.3}$ | 138 $^{\pm0.7}$	-15.1 $^{\pm1.2}$
PPIp	Globulins	350 $^{\pm8}$	9.5 $^{0.97}$	49.6 $^{\pm1.9}$ | 43.9 $^{\pm0.8w}$	-24.7 $^{\pm1.2}$

4.4 Conclusion

In this study we linked the extent of aqueous fractionation on the gelling capacity, defined as the capacity per mass of protein to increase the *G'* after thermal treatment, and linear and non-linear gel properties of the resulting fractions. SAOS rheology showed that limited fractionation yields higher protein gelling capacity. Gelation of pea flour was mainly caused by starch gelatinization, whereas the gelation of protein-enriched fractions was caused by interacting proteins. Limited processed fractions were found to form firmer gels with strain softening behaviour. The more extensively fractionated sample was less firm and showed an earlier transition to viscous behaviour at large deformation, indicating a weakly interacting network. Microstructure images were consistent with these observations. A number of experiments, involving changes in the extraction process and rheological measurements, indicated that the reducing gelling capacity upon fractionation is caused by a combination of factors, which are isoelectric precipitation, amount of sugars upon lyophilization and differences in ash content. All three factors would unequivocally decrease the gelling capacity upon fractionation. In conclusion, limited fractionation in the case of pea protein leads to a higher gelling capacity and firmer gels per mass of protein.

From a scientific perspective, the outcome of this study could be taken further by systematically exploring the effect of concentration, pH and ionic strength on the gelling capacity of the pea fractions. Furthermore, future research could focus on characterizing the gels by varying the frequency in LAOS experiments and studying the gel recovery behaviour by applying multiple strain sweeps. From an industrial perspective, our research and future research could help optimizing their fractionation processes in view of sustainability and ingredient functionality.

Chapter 5

Pea fractionation can be optimized to yield protein-enriched fractions with a high foaming and emulsifying capacity

Abstract

Specific pea protein fractionation steps can be used to control ingredient functionality, which was demonstrated by studying foaming and emulsifying properties of three pea protein fractions at pH 7.0. Mild fractionation, involving alkaline extraction from the flour at pH 8.0 and subsequent centrifugation, yielded a pea protein concentrate (PPC). Further fractionation was done by isoelectric precipitation and centrifugation. The pellet was re-dispersed and resulted in the globulin-rich fraction (GLB-RF), and the supernatant – which could be considered a by-product – was diafiltrated to obtain the albumin-rich fraction (ALB-RF). Size exclusion chromatography showed that PPC contained mostly globulins and some albumins, whereas GLB-RF and ALB-RF indeed contained mainly either globulins or albumins. The smaller and less charged albumins displayed strong in-plane interactions at the air-water interface, thereby forming a stiff and cohesive interfacial layer which led to high foam overrun (258%) and stability (272 min). PPC- and GLB-RF contained larger and highly charged globulins, showing substantially lower foam overruns (<81%) and stability (<70 min), which can be attributed to the formation of weaker and more mobile interfacial layers than ALB-RF. For the emulsifying properties, it was found that the larger size and higher net charge of globulins resulted in the formation of oil droplets that were stable against coalescence and flocculation, while albumin-stabilised oil droplets flocculated due to lower surface charges. The functionality of the fraction is largely determined by the protein composition. We have demonstrated how targeted fractionation can be used to control this composition, and hence the functionality of pea protein fractions.

This chapter is to be submitted as:

Remco Kornet, Jack Yang*, Paul Venema, Erik van der Linden, Leonard Sagis. Pea fractionation can be optimized to yield protein-enriched fractions with a high foaming and emulsifying capacity. (*the authors have contributed equally to this work)*

5.1 Introduction

In recent years, there has been an increased interest in plant-based proteins. One of the commonly studied protein sources is pea, as it possesses good nutritional and functional properties [168]. To utilise the proteins that pea has to offer, it is required to process pea seeds into pure protein-fractions. Aqueous fractionation is the mainstream process that is applied to obtain protein-enriched fractions and can yield high protein purities [49]. Such a process is based on solubilisation and subsequent isoelectric precipitation, with intermediate centrifugation steps to obtain the final protein fraction. The drawback of such a process is the requirement of copious amounts of energy and water. Therefore, milder fractionation methods have been developed, such as dry fractionation and mild wet fractionation [169, 170]. Generally, these processes have a lower environmental impact, but also yield fractions with lower protein purities [171].

An alternative way of looking at milder fractionation is to limit the number of fractionation steps in a commonly reported aqueous fractionation process. An advantage of fewer processing steps is a less radical change with respect to the current plant protein manufacturing process. Limited fractionation yields fractions with lower protein purities and a more heterogenous composition, caused by components such as sugars, salts, phenols and oil. On the other hand, mildly fractionated protein concentrates were found to possess better overall functionality compared to extensively fractionated ones [90, 147], as milder processed fractions are more likely to preserve the native properties of the proteins. Additionally, the protein composition, influenced by the fractionation steps used, can be optimised for specific functional behaviour.

Chapter 4 demonstrated better gelling capacity for limited fractionated samples and Chapter 2 showed how the protein composition and viscosity of the fractions can be altered by the extent of fractionation. In the latter study, three different protein fractions could be obtained from a commonly reported aqueous fractionation process: an albumin-enriched fraction, a globulin-enriched fraction and a fraction with both globulins and albumins. The separation of these proteins is based on the characteristic of globulins to precipitate around pH 4.5 [22, 68], while albumins remain soluble [172]. Related to those differences in protein composition, these fractions appeared to display different solubilities, specific volumes and viscosities. The pea fractions with different protein compositions are expected to also behave differently with respect to other types of functional behaviour.

In addition to gelling capacity, many foods require ingredients with good foaming or emulsifying properties, which could also be provided by an optimised protein fractionation. In this work, the foaming and emulsifying properties of different protein fractions were studied. Mildly fractionated pea proteins (containing albumins and globulins) have received some attention with respect to emulsion stabilising properties [147, 173], but a comprehensive study on the interface- and foam-stabilising properties does not exist. Extensively fractionated pea proteins have been studied, but the majority of these studies focus on the globulin fraction [36, 61, 71, 73], whereas the functionality studies on pea albumin were found to be limited to one study [174]. Here, we aim to directly compare pea albumins and globulins for their foaming and emulsifying properties, and to better understand their contribution in the mildly processed fraction containing both albumins and globulins. The protein fractions were studied by a multi-length scale approach, where the molecular properties (protein size, charge and structure) were linked to the macroscopic properties (foam and emulsion) by studying interfacial properties. By using such an approach, we demonstrate how pea can be fractionated to yield protein-enriched fractions with optimal foaming and emulsifying properties. The implementation of such fractionation techniques could increase the potential of plant proteins as functional ingredients, and simultaneously increase the sustainability aspect of fractionation processes.

5.2 Materials and methods

5.2.1 Materials

Yellow pea (Pisum Sativum L.) seeds were obtained from Alimex Europe BV (Sint Kruis, The Netherlands). Rapeseed oil was obtained from Danone Nutricia Research (Utrecht, the Netherlands). Materials for the SDS-PAGE (Invitrogen Novex, ThermoFischer Scientific, USA) were used as received. All chemicals and reagents were obtained from Merck (Darmstadt, Germany) and were of analytical grade. All samples were prepared in ultrapure water (MilliQ Purelab Ultra, Germany), unless stated otherwise.

5.2.2 Protein fractionation process

Three protein-enriched fractions were produced from an aqueous fractionation process based on Chapter 2, and is visualised in Fig. 5.1. Pea was milled into flour with an average particle size of 100 μm. The flour was dispersed in deionised water in a ratio of 1:10 and the pH was adjusted to 8.0 using 1 M NaOH. Proteins and other flour constituents were solubilized for 2 hrs under moderate stirring. Subsequently, the soluble components were separated from the insoluble components by centrifugation (10.000g, 30 min, 20 °C). Part of the resulting supernatant was lyophilised and labelled as pea protein concentrate (PPC), which is the same as PPCa in other chapters. The remainder was adjusted to pH 4.5 using 1 M HCl to precipitate the globulins, and kept there for 2 hrs under moderate stirring. The precipitated globulins were separated from the soluble albumins by centrifugation (10.000g, 30 min, 20 °C). The resulting supernatant and pellet were separated, and the supernatant was diafiltrated using a 2 kDa membrane. The retentate was lyophilised and labelled as the albumin-rich fraction (ALB-RF). The pellet, containing the precipitated globulins, was re-dispersed at pH 7.0 for 2 hrs and lyophilised afterwards. This fraction was labelled as the globulin-rich fraction (GLB-RF) and is the same as PPIp in other chapters. The labels ALB-RF and GLB-RF are based on protein composition analysis, which is discussed later in this work. All steps in this fractionation process were conducted at room temperature. Lyophilisation was done in an Alpha 2-4 LD plus freeze-dryer (Christ, Osterode am Harz, Germany) and the powders were stored at -18 °C.

The ash content was determined by heating the samples overnight in a furnace 550 °C and expressed as the mass after heating divided by the initial mass minus the moisture content. The protein content was calculated from the nitrogen content,

measured by a FLASH EA 1112 series Dumas (Interscience, Breda, The Netherlands) using a nitrogen conversion factor of 5.7. All protein purities have been expressed as the weight percentage of protein in total dry matter.

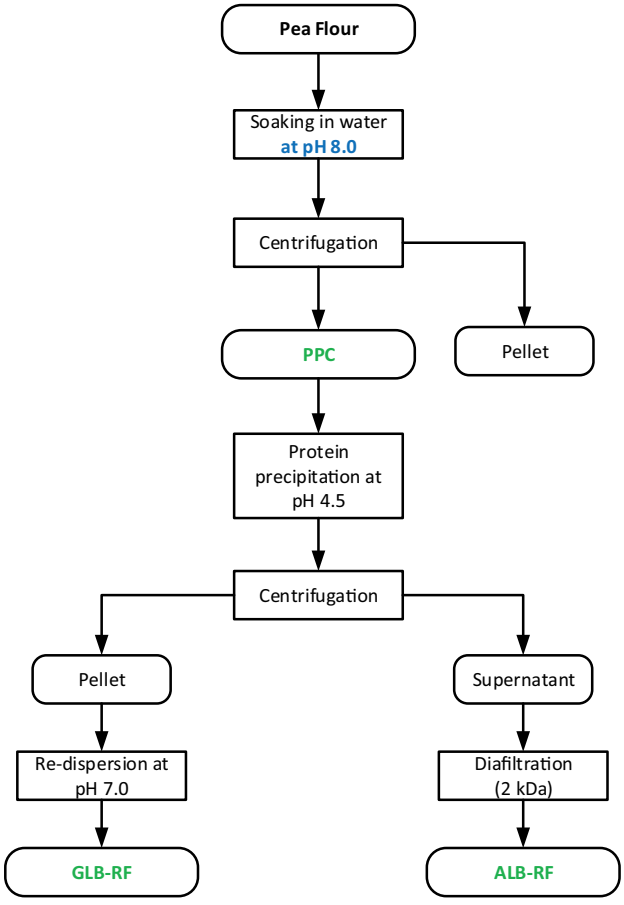

Figure 5.1 Schematic representation of the pea protein fractionation process.

5.2.3 Sample preparation

All samples were dissolved in phosphate-buffer (20 mM, pH 7.0, mixture of Na_2HPO_4 and NaH_2PO_4), unless stated otherwise. Samples were stirred for at least 4 hrs at room temperature.

5.2.4 Size Exclusion Chromatography (SEC)

The protein composition of the pea fractions was determined by separation on an Akta Pure 25 chromatography system (GE Healthcare, Diegem, Belgium), and subsequently detected using an UV detector. Samples were prepared by dissolving 5 g protein / L in a McIlvaine buffer (10 mM citric acid, 20 mM Na2HPO4, pH 7.0, 150 mM NaCl, filtered over 45 μm). The solutions were centrifuged at 3350g for 10 min and the supernatants were transferred to HPLC vials. The samples were run on a Superdex 200 increase 10/300 GL column (Merck, Schnelldorf, Germany) with a molecular weight range of 10 – 600 kDa, with the McIlvaine buffer used as an eluent. Proteins were detected at an UV wavelength of 280 nm. To determine the molecular masses, a calibration curve was used, obtained from molecules of known molecular weights: Aldolase, Blue Dextran, Carbonic Anhydrase, Conalbumin, Ferritin, Ovalbumin and Ribonuclease.

5.2.5 Differential Scanning Calorimetry (DSC)

The thermal properties of the pea fractions were measured with DSC, to gain understanding on the effect of fractionation on protein denaturation. Samples were prepared by dissolving 10 wt. % protein in deionised water for 2 hrs and adjusted to pH 7.0. The protein solutions were transferred to high volume pans in weights of 30 – 40 mg. The pans were closed with a lid and measured with a TA Q200 Differential Scanning Calorimeter (TA Instruments, Etten-Leur, The Netherlands). The heat flow was recorded over a temperature range of 20 – 120 °C, with a heating rate of 5 °C / min. All samples were measured in triplicate.

5.2.6 Determination of zeta-potential

The zeta-potential of the proteins in phosphate buffer were determined using dynamic light scattering in a Zetasizer Nano ZS (Malvern Instruments, UK). The refractive indices were set on 1.45 for the proteins and 1.33 for the buffer phase. The measurements were performed in triplicates at 20 °C.

5.2.7 Capillary viscometry

The kinematic viscosities were measured with an Ubbelohde viscometer No. 1046928 (SI Analytics, Weilheim, Germany) at 0.1, 0.7 and 2.0 wt. % protein. These concentrations are identical to the concentrations at which the foams and emulsions were prepared. The density was measured with a density meter DMA5000 (Anton Paar, Graz, Austria). The results were used to determine the dynamic viscosities.

5.2.8 Determination of surface tension and surface dilatational properties

The interfacial properties were studied by surface dilatational rheology using a drop tensiometer PAT-1M (Sinterface Technologies, Germany). Solutions containing 0.1 wt. % protein were pumped through a needle to create a hanging droplet with a surface area of 20 mm^2. The droplet contour was captured by a camera and analysed by fitting the contour of the droplet with the Young-Laplace equation to obtain the surface tension. The interfaces were equilibrated for 3 hrs before starting the dilatational deformations. The amplitude dependence was studied in amplitude sweeps, where the amplitude of deformation was increased from 3 to 30% with 9 increments, while the frequency remained constant at 0.02 Hz. The frequency dependence was studied in frequency sweeps, where the frequency of an oscillation cycle was increased from 0.002 to 0.1 Hz with 7 increments, and the amplitude of deformation was constant at 3%. Each amplitude or frequency in the sweeps was performed with five oscillatory cycles, followed by a rest period with the same frequency. The relaxation response of the interfaces was studied by performing step-dilatations by a sudden compression or extension of 10% area change with a step time of 2 sec. After the step, the area was kept constant for 1000 s. All experiments were performed at least in triplicate at 20 °C.

5.2.9 Interfacial rheological data analysis

From the amplitude sweeps, the raw data was analysed using Lissajous plots by plotting the surface pressure ($\Pi = \gamma - \gamma_0$) versus the relative surface deformation ($(A-A_0)/A_0$). Here, γ and A are the surface tension and area of the deformed interface, γ_0 and A_0 are the surface tension and area of the non-deformed interface. The middle three oscillations, of a total of five oscillations, were used to produce the plots.

5.2.10 Preparation of Langmuir-Blodgett films

A Langmuir trough (Langmuir-Blodgett Trough KN 2002, KSV NIMA/Biolin Scientific Oy, Finland) with an area of 243 mm^2 was used to produce Langmuir-Blodgett films of the protein interfaces. The trough was filled with phosphate buffer (20 mM PO4, pH 7.0), and the surface pressure was measured with a Wilhelmy plate (platinum, perimeter 20 mm, height 10 mm). A total of 200 µL of 0.04 wt. % protein solution was spread on top of the surface using a gas-tight syringe, followed by an equilibration step of 30 min. Afterwards, the interface was compressed by barriers at a moving speed of 5 mm/min. First, surface pressure isotherms were constructed, and based on these isotherms, two surface pressures (15 and 25 mN/m) were chosen to extract Langmuir-Blodgett films. The protein layer was transferred onto a freshly

cleaved mica sheet (Highest Grade V1 Mica, Ted Pella, USA) at a speed of 1 mm/min. The films were produced in duplicate at 20°C, and dried in a desiccator for further analysis.

5.2.11 Determination of the interfacial structure by AFM

The interfacial microstructure of the Langmuir-Blodgett films was analysed using atomic force microscopy (AFM) on a Multimode 8-HR (Bruker, USA). The topographical measurement was performed with a Scanasyst-air model non-conductive pyramidal silicon nitride probe (Bruker, USA) with a normal spring constant of 0.40 mN/m, and images were recorded in tapping mode with a lateral frequency of 0.977 Hz. At least two areas of 2x2 μm^2 with a resolution of 512x512 $pixels^2$ on each replicate were analysed to ensure good representativeness. The images were analysed and processed using Nanoscope Analysis software v1.5 (Bruker, USA).

5.2.12 Determination of foaming properties

Foam ability

A whipping method was used to study the foam ability of a solution with a protein content of 0.1 wt. %. Aliquots of 15 mL sample were whipped in a plastic tube (3.4 cm diameter) for 2 min at 2000 rpm by an aerolatte froth (Aerolatte Ltd., UK) connected to an overhead stirrer. The top of the foam was marked on the tube, and the height of the foam was measured with a ruler. The foam height and tube diameter were used to calculate the foam volume. The overrun was calculated by Eq. 5.1.

$$Overrun\ (\%) = \frac{Foam\ volume\ (mL)}{Liquid\ volume\ (15\ mL)}\ x\ 100\% \qquad (5.1)$$

All experiments were performed in triplicate at room temperature.

Foam stability

A sparging method was used to study the foam stability, as the initial foam height can be regulated in this method. Foams were sparged using nitrogen gas in a Foamscan foaming device (Teclis IT-concept, France). A glass cylinder with 60 mm diameter was filled with 60 mL of a 0.1 wt. % protein solution. The gas was sparged through a metal frit (27 μm pore size, 100 μm distance between centres of pores, square lattice) at a gas flow rate of 400 mL/min to create a foam with a volume of 500 mL. The

foam volume was analysed by a camera until half of the initial foam volume had collapsed, which is also known as the foam volume half-life time. Images of the air bubbles were also recorded and analysed using a custom made Matlab script with the DIPlip and DIPimage analysis software (TU Delft, Delft, the Netherlands), which calculated the average air bubble size. All experiments were at least performed in triplicate at 20 °C.

5.2.13 Determination of emulsifying properties

Removal of impurities in rapeseed oil

Impurities in rapeseed oil were removed using magnesium silicate (100-200 mesh Florisil, Sigma-Aldrich, USA). Florisil and rapeseed oil were mixed in a ratio of 1:2 (v/v) (Florisil:oil) in air-tight tubes. To prevent light oxidation, the tubes were covered with aluminium foil. Afterwards, the tubes were rotated overnight at room temperature. The following day, the sample was centrifuged twice at 2000g for 20 min to remove the pellet containing Florisil. The final supernatant, containing purified rapeseed oil, was recovered, and stored at -20 °C for further use.

Preparation of oil-in water emulsions

Oil-in-water emulsions were prepared with solutions containing 0.7 and 2 wt. % protein. Purified rapeseed oil was added to a total oil content of 10 wt. %. The mixture was pre-homogenised with an Ultra-Turrax (IKA, USA) at 12000g for 1 min. The pre-emulsion was further homogenised in a high-pressure homogeniser (LAB, Delta Instruments, The Netherlands) at 200 bars for 10 passes, while the emulsion was cooled in ice water.

Determination of emulsion droplet size

Static light scattering in a Mastersizer 2000 (Malvern Instruments Ltd, UK) was used to determine the emulsion droplet size distribution. The droplet size distribution was measured directly after homogenisation (day 0), on day 1, and on day 7, while stored at 4 °C. Potential flocculation was studied by measuring the droplet size distribution of a mixture containing 0.5 mL of emulsion with 0.5 mL of 1 wt. % sodium dodecyl sulphate (SDS) solution. The refractive indices used for the dispersed phase (rapeseed oil) and dispersant (demineralised water) were 1.469 and 1.330, respectively. Measurements were performed in triplicate at room temperature.

Visualisation of emulsion droplets

Emulsions were studied in an Axios 2 Plus light microscope (Carl Zeiss AG,

Germany) using a 40x magnification lens. Images were recorded using the Axiocam (Carl Zeiss AG, Germany), which was connected to the microscope.

Determination of emulsion creaming

Creaming was studied by filling a 15 mL tube (1.2 cm diameter) with 10 mL emulsion on day 0. Images were taken on day 0, 1, and 7. The emulsions were also studied visually using a light source to evaluate the volume of the creamed layer. A creaming percentage (%) was determined by Eq. 5.2.

$$Creaming\ percentage\ (\%) = \frac{Volume\ of\ (bottom)\ serum\ layer\ (mL)}{Volume\ of\ emulsion\ (10\ mL)}\ x\ 100\ \% \qquad (5.2)$$

5.3 Results and discussion

5.3.1 Compositional and physical properties of the pea fractions

Fractionation process and fraction composition

The aqueous fractionation process yielded three pea fractions that varied in protein content. Table 5.1 shows that pea protein concentrate (PPC) and the albumin-rich fraction (ALB-RF) contained over 50 wt. % protein, whereas the globulin-rich fraction (GLB-RF) contained 86 wt. % protein. The lower protein purity of PPC is a consequence of fewer fractionation steps, which was also reflected in a higher protein recovery of 74.6%, compared with 54.4% of GLB-RF. Generally, more extensive fractionation results in higher purities and lower yields [12], due to protein losses throughout the process. This is also reflected in the lower combined protein recovery of ALB-RF and GLB-RF (66.7%), relative to the recovery of PPC (74.6%), from which ALB-RF and GLB-RF originate. In other words, there is 7.9% loss of protein upon isoelectric precipitation. The low recovery of ALB-RF could be explained by the low albumin content in pea seeds, which comprised only 13 – 30% of the total protein content [175]. The major impurities of PPC and ALB-RF were soluble sugars, based on Chapter 2. The ash contents in Table 5.1 indicate the amounts of the second largest impurity, which were salts. PPC contained around 10% salt, whereas ALB-RF and GLB-RF contained about 5%. The lower salt contents of ALB-RF and GLB-RF can be attributed to a diafiltration and a precipitation step, respectively.

Table 5.1 Protein recovery and dry matter composition of the pea protein concentrate (PPC), albumin-rich fraction (ALB-RF) and globulin-rich fraction (GLB-RF). The protein recovery is defined as the recovered amount of protein divided over the amount of protein before fractionation. All values are averages from two fractionation processes and the standard deviations are shown in superscript.

Pea fraction	Protein recovery (%)	Protein content (wt. %)	Ash content (wt. %)
PPC	74.6 $^{\pm 0.8}$	54.8 $^{\pm 4.8}$	10.3 $^{\pm 2.1}$
ALB-RF	12.3 $^{\pm 0.7}$	52.0 $^{\pm 1.7}$	5.5 $^{\pm 1.2}$
GLB-RF	54.4 $^{\pm 2.8}$	86.3 $^{\pm 1.4}$	5.6 $^{\pm 0.5}$

Protein composition

The SEC chromatogram (Fig. 5.2) shows the presence of larger proteins in PPC and GLB-RF, corresponding to the globulins. Globulins can be classified into legumin

(11S) and vicilin (7S), and debatably to a third group called convicilin [36]. The latter can also be considered as α-subunit of vicilin [40]. At pH 7.0, legumin is mostly present as a hexamer with a molecular weight ranging from 320 – 380 kDa. This hexamer comprises of six subunits that are non-covalently bound. Each of these subunits consist of an acidic and basic subunit of 40 kDa and 20 kDa. Vicilin is commonly present as a trimer with a molecular weight of 170 kDa. Convicilin has a subunit of ~70 kDa and it has a molecular weight of ~290 kDa in its native form [36, 108]. The first peak in the chromatogram (Fig. 5.2) is denoted as legumin in its hexameric form (L), the second peak as convicilin (CV) and the third peak as vicilin (V). These proteins are absent in ALB-RF.

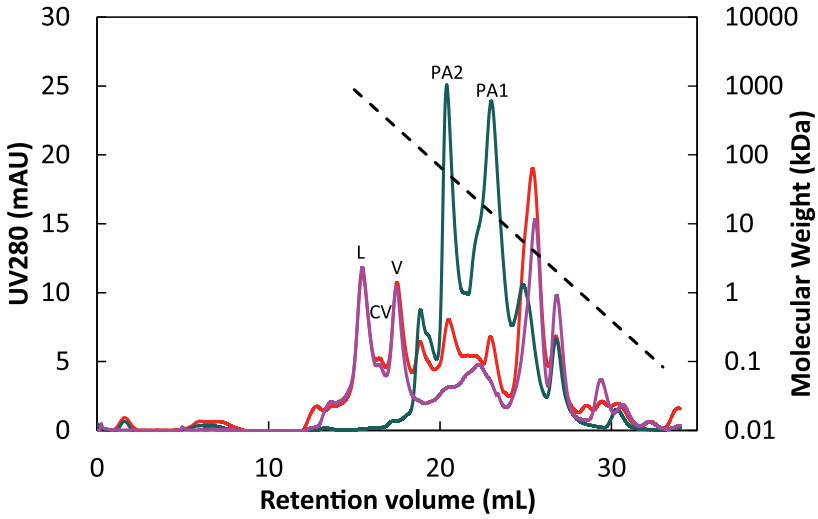

Figure 5.2 SEC chromatogram showing the protein composition of PPC (—), ALB-RF (—) and GLB-RF (—), measured from 5 g/L protein solutions at pH 7.0. L = legumin, CV = convicilin, V = vicilin, PA1 and PA2 = albumins PA1 and PA2. The black dashed line represents the molecular weight as function of retention volume.

Albumin is used as a collective name for a group of proteins, including albumin PA1, albumin PA2, lectin, and protease inhibitors [42]. Albumin PA1 can be subdivided into PA1a (6 kDa) and PA1b (4 kDa), and these polypeptides were previously suggested to be able to form dimers. Albumin PA2 comprises PA2a and PA2b that can form homodimers of 53 and 48 kDa, respectively [44]. Albumins PA1 and PA2 probably correspond to the major peaks of ALB-RF, as depicted in Fig. 5.2. Albumins are absent in GLB-RF, as they do not precipitate upon isoelectric precipitation [172]. This

means that in the aqueous fractionation process the albumin proteins are generally discarded, despite of their potential as functional ingredient. Lower amounts of albumins are still present in PPC, but globulins remain the major protein, as globulins are more abundantly present in pea seeds.

Thermal properties

DSC was primarily conducted to confirm that the proteins were not denatured upon fractionation, but also the denaturation temperature and heat enthalpy of the protein mixtures were determined. It is noted that the measured heat enthalpy slightly deviates from the actual value, as the change of enthalpy only equals the heat exchange when the pressure in the pans remains constant as function of temperature. This is not the case when the pans are hermetically sealed. As pea proteins do not have a random coil conformation and denaturation peaks were visible, it was concluded that the proteins in all fractions were (at least partially) native. Table 5.2 shows a denaturation temperature of 82.3 °C for the proteins in the GLB-RF. This is consistent with other values reported for pea globulins in literature, where T_d ranges between 75 – 85 °C [68, 160]. Variation in denaturation temperatures in literature can be explained by different heating rates, presence of salts and sugars and different ratios of legumin versus vicilin. Globulins are abundant in PPC, which is reflected in a similar heat enthalpy as GLB-RF and a slightly higher denaturation temperature. The latter could also be the result of a higher salt content (Table 5.1). The ALB-RF displays the highest denaturation temperature and the lowest heat enthalpy. The denaturation profiles of pea albumins have not been studied previously, but the values reported here correspond with Chapter 4 on a less purified albumin fraction. It appeared that, despite of higher number of cysteine residues in albumins [44] and a compact structure that involves disulphide bonds [42], thermal unfolding required less energy compared to larger pea globulins.

Table 5.2 Thermal denaturation properties of the pea protein concentrate (PPC), albumin-rich fraction (ALB-RF) and globulin-rich fraction (GLB-RF) in 10 % (w/w) protein solutions at pH 7.0. Averages of the denaturation onset (T_{onset}), denaturation peak temperature (T_d) and heat enthalpy (ΔH_d) are given. All samples were measured in triplicate and standard deviations are shown in superscript.

Pea fraction	T_{onset} (°C)	T_d (°C)	ΔH_d (J/g)
PPC	75.7 $^{\pm 0.2}$	85.0 $^{\pm 0.1}$	9.0 $^{\pm 0.2}$
ALB-RF	81.8 $^{\pm 0.0}$	87.7 $^{\pm 0.2}$	1.8 $^{\pm 0.1}$
GLB-RF	72.5 $^{\pm 0.2}$	82.3 $^{\pm 0.1}$	8.6 $^{\pm 0.4}$

Viscosity

There are numerous factors influencing foam and emulsion stability, including air bubble or oil droplet size, protein adsorption behaviour, interfacial layer formation, and solvent viscosity. The latter appeared to be a relevant characteristic for pea protein. Globulin-enriched pea fractions have the ability to form aggregates that occupy large volumes in the system and hence display a significant thickening capacity (Chapter 2). The zero-shear viscosities of the pea fractions at 0.1, 0.7 and 2.0 wt. % protein were measured and displayed, relative to the solvent viscosity, in Fig. 5.3. At a concentration of 0.1 wt. %, differences between the pea fractions are smaller than 0.1 mPa·s. At higher concentrations PPC and GLB-RF show a similar increase, which can be attributed to the globulins. The ALB-RF displays a lower increase in viscosity, which indicates a lower tendency to form protein aggregates.

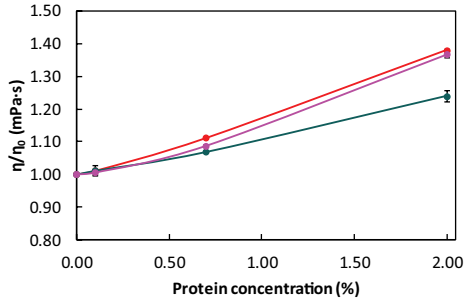

Figure 5.3 Viscosities of the PPC (—), ALB-RF (—) and GLB-RF (—) relative to the solvent viscosity, measured by capillary viscometry at three concentrations (0.1, 0.7 and 2.0 wt. %) at pH 7.0. Samples were measured in duplicate and standard deviations are shown as error bars.

5.3.2 Interfacial properties of the pea protein fractions

Adsorption behaviour

The interfacial properties were evaluated using a drop tensiometer, and the protein adsorption behaviour is presented in Fig. 5.4A. All samples had an immediate increase of surface pressure at the start of the experiment. PPC started at 8 mN/m, followed by a continuous increase up to 25 mN/m. The ALB-RF started at the same surface pressure of 8 mN/m, but showed a slower increase compared to PPC with a final surface pressure of 17 mN/m after 3 hrs. The GLB-RF had the lowest initial surface pressure of 4 mN/m, but increased rapidly, and followed the curve of the PPC from 80 sec onwards to 24 mN/m. Albumins showed a faster adsorption on

the air-water interface compared to globulins in the initial 10 sec, but afterwards the globulins are able to reach higher values. These differences in initial adsorption rate are most likely related to the differences in molecular weights of the proteins, as the main albumins PA1 and PA2 are between 48 to 53 kDa and the globulins vary from 170 to 380 kDa. The lower charge of albumins also tends to promote faster adsorption, as albumins and globulins had a zeta-potential of -2.0 and -10.3 mV, respectively. Therefore, albumins are expected to adsorb faster at the interface in the initial phase [176], and the same proteins are likely to be responsible for the fast initial adsorption phase of the PPC. Afterwards, the globulins are responsible for the further increase of surface pressure for PPC. The nature of these interfaces was further evaluated by applying dilatational deformations.

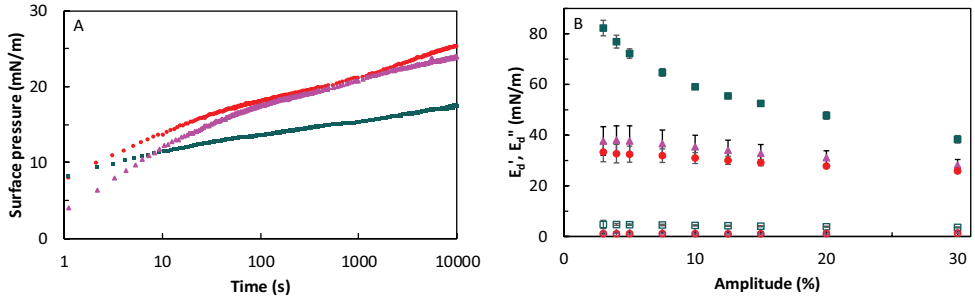

Figure 5.4 A. Surface pressure isotherms of the PPC (■), ALB-RF (■) and GLB-RF (■). B. Surface dilatational moduli as a function of deformation amplitude applied on air-water interfaces stabilised by PPC, ALB-RF and GLB-RF at pH 7.0, measured at an oscillatory frequency of 0.02 Hz. The E_d' are shown by the closed symbols, and the E_d'' are shown as open symbols. For figure A, the samples were measured at least in triplicate, and one representative curve is shown. For figure B, the samples were measured at least in triplicate and the standard deviations are given in the figure.

Dilatational rheology

First, frequency sweeps were performed on the pea protein-stabilised interfacial films, where the frequency of deformation was varied at a constant deformation amplitude. The E_d' versus frequency (data not shown) revealed a power-law behaviour and a weak frequency-dependency, which was quantified using Eq. 5.3.

$$E_d' \sim \omega^n \tag{5.3}$$

Here, ω is the frequency (s^{-1}), and the n-value describes the frequency-dependency.

An n-value of 0.5 was previously correlated to an interfacial film, where the elasticity was predominantly determined by mass exchange of surface stabiliser between the bulk and the interface, as expected to occur for small molecular surfactants with the absence of in-plane interactions [177]. The n-value of PPC, ALB-RF and GLB-RF was found to be 0.20, 0.13, and 0.13, respectively. These values are much lower than 0.5, and suggest that other phenomena are dictating the elasticity of the interface, such as momentum transfer between the interface and bulk, and in-plane interactions between the proteins at the interface [178].

To further assess the mechanical properties of the interfacial films, amplitude sweeps were performed by subjecting the protein-stabilised interfaces to amplitude deformations increasing from 3 – 30%, at a fixed frequency of 0.02 Hz, and the resulting surface dilatational moduli are presented in Fig. 5.4B. All interfaces had a higher E_d' (storage modulus) compared to E_d' (loss modulus), resulting in a tanδ'= E_d''/E_d' of below 1, revealing elastic-dominated and solid-like behaviour. The E_d' of PPC-stabilised interface declined slightly from 33 to 26 mN/m, when increasing the amplitude from 3 to 30%. A comparable behaviour was found for the GLB-RF-stabilised interface with moduli decreasing from 38 to 28 mN/m. The moduli for both PPC- and GLB-RF-stabilised interfaces were found to be (nearly) independent of the applied deformations, especially compared to the ALB-RF-stabilised interfaces. The ALB-RF-stabilised interface had remarkably high moduli at low deformations, decreasing from 82 to 38 mN/m upon increasing the deformation amplitude.

Deformations in the nonlinear viscoelastic (NLVE) regime result in the presence of higher-order harmonics in the Fourier spectrum of the stress response. These higher harmonics are neglected, when the surface dilatational moduli are obtained from only the first harmonic of the Fourier spectrum, as is the case for moduli shown in Fig. 5.4B. Therefore, analysing only the first harmonic moduli in the NVLE regime is of limited value. Higher harmonics can be included in the analysis by plotting the surface pressure over the deformation $(A\text{-}A_0)/A_0$ in so-called Lissajous plots [179].

Lissajous plots

The PPC- and GLB-RF-stabilised interfaces showed nearly identical Lissajous plots (Fig. 5.5). At 5% deformation, the Lissajous plots were narrow and nearly symmetric, and suggest near linear viscoelastic behaviour. The plots became asymmetric at higher deformations, for instance at 30% deformation, showing different behaviour in extension and compression of the interfacial area. At the start of the extension (bottom left corner, deformation of -0.35), the surface pressure increased steeply,

which indicated a predominantly elastic response. After this point, the curve started to flatten, suggesting gradual softening and disruption of the interfacial microstructure. Consequently, the elastic contribution of the response diminishes, whereas the viscous contribution increases, and, finally, results in intra-cycle strain softening in extension. In the compression part of the cycle, the surface pressure showed a steep increase with a higher absolute maximum surface pressure compared to extension, which is known as intra-cycle strain hardening in compression. In previous work, this behaviour was related to the formation of densely clustered regions on the surface that started jamming at such large deformations [180].

The asymmetries were even more obviously present in the Lissajous plot of ALB-RF-stabilised interfaces at 30% deformation. Here, we can observe a nearly vertical

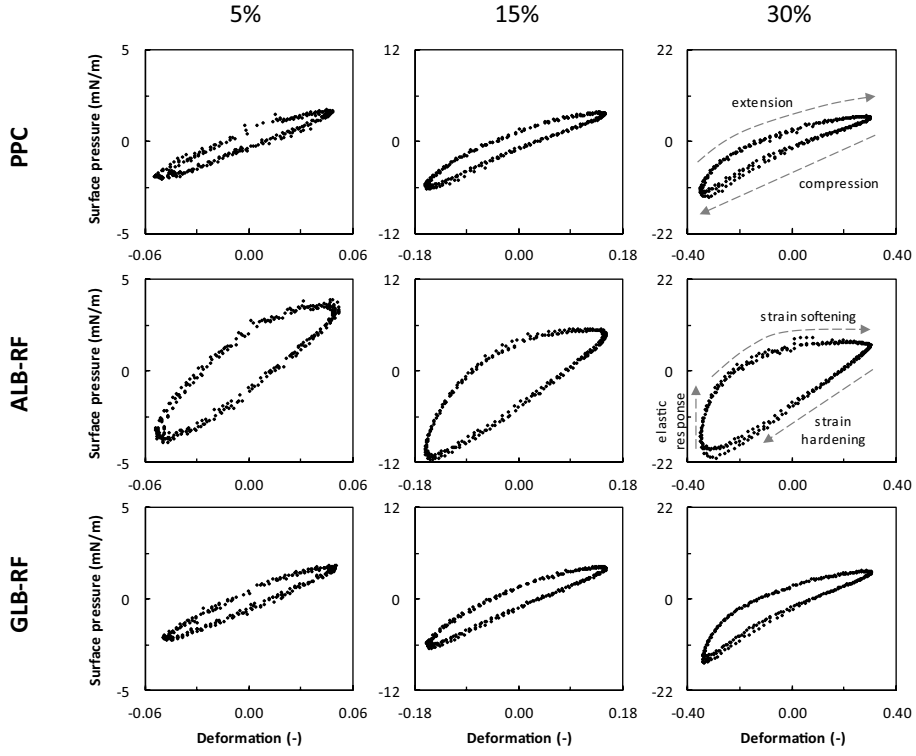

Figure 5.5 Lissajous plots of surface pressure as a function of applied deformation, obtained from amplitude sweeps of air-water interfaces stabilised by the pea protein concentrate (PPC), albumin-rich fraction (ALB-RF) and globulin-rich fraction (GLB-RF) at pH 7.0. The samples were measured at least in triplicate and one representative plot is shown.

increase of surface pressure at the start of the extension phase, a zero-slope part at the end of the extension, and a much higher maximum surface pressure of 22 mN/m in compression compared to PPC- and GLB-RF-stabilised interfaces. As a result, the Lissajous plot of ALB-RF were wider compared to the other two interfaces, suggesting more dissipation of energy upon deformation. The extreme strain softening in extension can also be attributed to a density effect, as the interfacial layer is stretched upon extension. This leads to the dilution of adsorbed proteins, as new proteins are probably not introduced upon extension. Additionally, the increased strain hardening in compression could also be the result of a density effect, where adsorbed proteins are concentrated upon compression, leading to interaction and jamming of the proteins. Asymmetries in the extension and compression cycle of Lissajous plots demonstrate strong in-plane interactions between stabilisers at the interface, which allows the albumins to form a stiff and viscoelastic solid-like interfacial layer, which is disrupted and yields at large deformation. Both the PPC and GLB-RF formed similar interfaces, which were weaker and more easily stretchable interfaces compared to ALB-RF. The globulins dominated the interfacial properties of the PPC, which was also indicated by the adsorption behaviour (Fig. 5.4A).

The protein properties of albumins and globulins can explain the differences in interfacial layer formation. The albumins are smaller compared to globulins, and also possesses a lower net protein charge (Chapter 4). As a result, the electrostatic repulsion between albumins at the interface is lower, and more albumins can fit on the interface, as the proteins can closely approach each other. This could strengthen the interactions between the proteins on the surface. Additionally, their smaller size could result in a more efficient coverage of the interface by the albumins. Another explanation can be found in the protein surface hydrophobicity. For albumins from rapeseed, it was shown that two distinct regions exist on the protein surface: a hydrophobic and a hydrophilic one [181], thus resembling an amphiphilic Janus-particle. Unfortunately, such information on the pea protein pea structure is unavailable, but it was demonstrated that albumins from various plant sources showed great similarities in their protein tertiary structure [182]. Therefore, it is likely that the pea albumins also have this distinct amphiphilic structure. Such amphiphilicity could allow these proteins to have stronger in-plane interactions on the surface compared to globulins, which have more evenly distributed hydrophobic regions on the protein's surface [181].

Interfacial microstructure

The pea protein-stabilised interfacial films were further evaluated by producing Langmuir-Blodgett films, and were analysed using atomic force microscopy to study the topography of the films (Fig. 5.6). Surface pressure isotherms obtained from the Langmuir trough can be observed in the Fig. A5.1 in the Appendix. The PPC and GLB-RF-stabilised films at a surface pressure of 15 mN/m showed similarities, as both films had larger structures, which were not observed for ALB-RF. These larger structures could be clusters of proteins, to be more specific, of the globulins. The formation of such clusters was also observed for rapeseed proteins [183]. The similarities between the films of PPC and GLB-RF again reveal the dominance of globulins at the air-water interface.

The changes in the microstructure of the interface upon deformation were evaluated by further compressing the Langmuir films to a surface pressure of 25 mN/m, before film deposition. For PPC and GLOB-RF-stabilised interfacial films, the interfaces remained similar to the films at a lower compression (15 mN/m). This can be linked

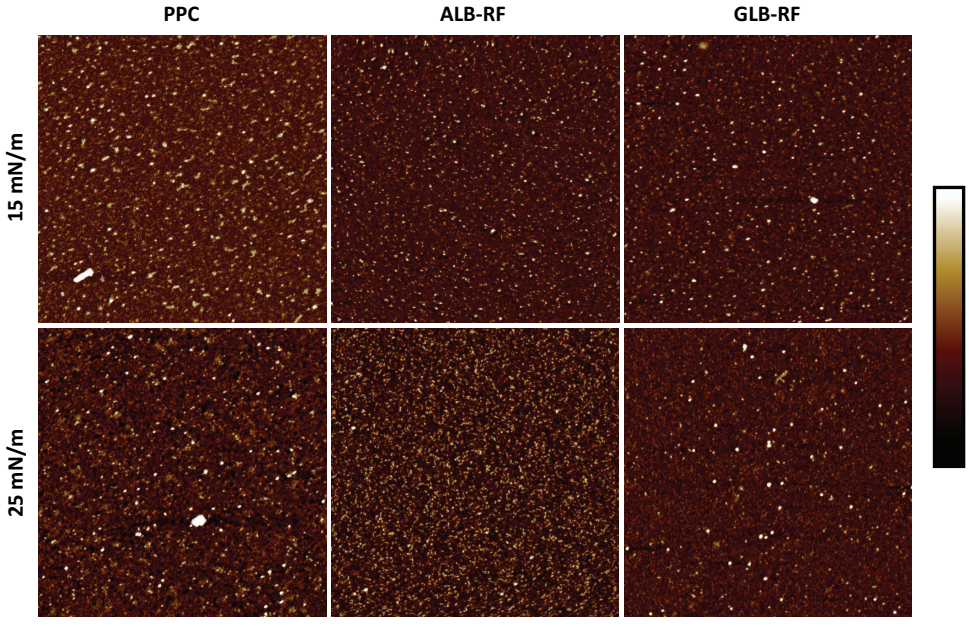

Figure 5.6 AFM images of Langmuir-Blodgett films made from pea protein concentrate (PPC), albumin-rich fraction (ALB-RF) and globulin-rich fraction (GLB-RF) stabilised air-water interfaces. The surface pressure indicates the conditions during film sampling.

to formation of a weak and highly stretchable interfacial layer, as shown in the dilatational surface rheology. Due to low in-plane forces between the globulins, these proteins could be pushed out of the interface. We should keep in mind that the AFM only studies the topography of the interface, the larger structures could also be pushed to the other side of the film or become covered at higher compressions. At 25 mN/m, the ALB-RF-stabilised interfacial film was found to be denser and finer compared to the other two interfacial films. This interface closely resembles one shown by whey protein isolate in our previous work [180]. Here, we suggested that whey proteins were able to form stiff layers with a heterogeneous microstructure, and the pea albumins are able to form such highly interlinked layers as well, as exhibited in the rheology. The strong in-plane interactions between albumins allows the proteins to remain on the surface upon compression, forming such dense microstructures. The heterogeneity in the interfacial microstructure is observed for the films of all three protein fractions, and has been demonstrated for other protein sources, such as whey [184] [185], pea [186] and rapeseed [183]. Such structural arrangement of the proteins can be further analysed using step-dilatations.

Step-dilatational behaviour

The air-water interfacial layers stabilised by the pea protein fractions were subjected to step-dilatations, where the surface area is suddenly compressed or extended. Afterwards, the new surface area was maintained to obtain a relaxation response, which was fitted to a Kohlraus-William-Watts (KWW) stretch exponential coupled with a regular exponential term (Eq. 5.4) [187] [178].

$$\gamma(t) = ae^{-(t/\tau_1)^{\beta}} + be^{-t/\tau_2} + c \tag{5.4}$$

Here, γ is the surface stress (mN/m), t is the time (s), τ_1 is the relaxation time, and β is the stretch exponent. The second term is required to decouple the continuous decrease of surface stress, due to aging of the interface. Here, the characteristic time τ_2 describes this process. The a, b and c are used as fitting parameters. An overview of all parameters can be found in Table A5.1 in the Appendix.

The stretch exponent β in the KWW equation indicates dynamic heterogeneity when the β-value is <1. This implies there are local variations in the relaxation response, which result in a wide spectrum of relaxation times [188]. The β-values of the pea protein-stabilised interfaces were found to be between 0.55 and 0.74, revealing dynamic heterogeneity (Table 5.3). The heterogeneous microstructure (Fig. 5.6)

could cause this type of response, which was previously confirmed for disordered (or heterogeneous) solids [178, 189]. From the results of the interfacial properties, we conclude that all that these three pea protein fractions form comparable heterogeneous structures at the air-water interface, which was also reflected in comparable relaxation times (τ_1). The ALB-RF-stabilised interface also had a slightly higher β-value upon compression compared to one stabilised by GLB-RF. This difference could be related to the stiffer interfacial films formed by albumins. The AFM images, especially at 25 mN/m, showed the formation of a denser and probably more homogeneous structure by albumins, which could cause the β-value upon compression to increase compared to globulin-stabilised interfaces.

Table 5.3 β and τ1 obtained from step-dilatation experiments of air-water interfaces stabilised by pea protein concentrate (PPC), albumin-rich fraction (ALB-RF) and globulin-rich fraction (GLB-RF) at pH 7.0. The samples were measured at least in triplicate and standard deviations are given in superscript.

	Compression		**Extension**	
	β	**τ_1**	**β**	**τ_1**
PPC	0.67 $^{\pm 0.07}$	4.6 $^{\pm 1.5}$	0.58 $^{\pm 0.04}$	8.3 $^{\pm 2.6}$
ALB-RF	0.74 $^{\pm 0.05}$	6.4 $^{\pm 0.9}$	0.55 $^{\pm 0.02}$	6.2 $^{\pm 0.8}$
GLB-RF	0.63 $^{\pm 0.08}$	4.1 $^{\pm 0.9}$	0.56 $^{\pm 0.04}$	8.4 $^{\pm 2.5}$

5.3.3 Foaming properties of the pea protein fractions.

Foams stabilised by the pea proteins were analysed for their foaming ability (overrun and air bubble size) and stability (half-life time). The ALB-RF were far more superior in foaming ability compared to PPC and GLB-RF, as the overrun (% foam volume generated, Eq. 5.1) was 258% for ALB-RF, while PPC and GLB-RF only had an overrun of 81 and 61%, respectively (Fig. 5.7A). Albumins were also able to form smaller air bubbles compared to the other two samples (Fig. 5.7B). This difference could be attributed to the surface activity (Fig. 5.4), as the albumins adsorb faster to the air-water interface in the initial 10 seconds compared to the globulins, which is also reflected in the four times smaller air bubble size of albumins. Additionally, the albumins form stiffer interfacial layers, and could allow the formation and retention of a higher foam volume. Weaker interfacial layers formed by globulins could result in the immediate collapse of the air bubble, thus resulting in a lower overrun. The albumins in the PPC mixture seemed to have increased the overrun and decreased the air bubble size slightly, which suggests the contribution of albumins on the air

bubble formation. This is also reflected in the adsorption behaviour, as the PPC exhibited a faster increase in the initial adsorption phase compared to globulins, suggesting a contribution of albumins to the initial adsorption phase and the air bubble formation. As the absolute number of albumin molecules is lower in the PPC, the foam ability is less compared to the ALB-RF-stabilised foams.

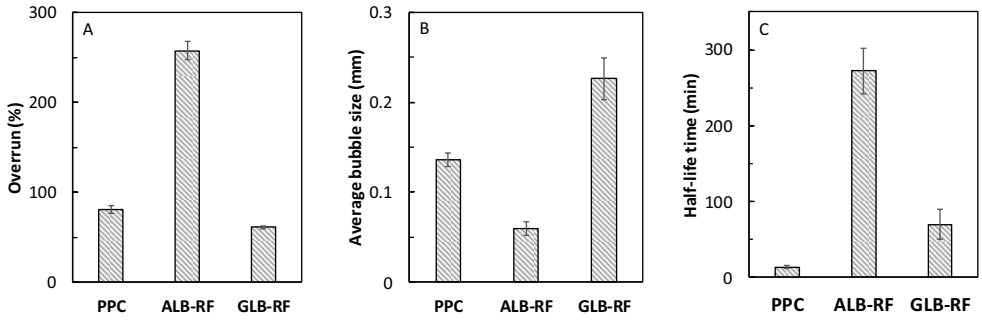

Figure 5.7 The overrun (A), average air bubble size (B), and foam volume half-life time (C) of foams stabilised using the pea protein concentrate (PPC), albumin-rich fraction (ALB-RF) and globulin-rich fraction (GLB-RF) at pH 7.0. The samples were measured in triplicate and the standard deviations are given in the figure.

The foam stability was assessed by comparing the foam volume half-life time (time where foam volume decays by half) (Fig. 5.7C). The ALB-RF stabilised foams showed a half-life time of 272 min, while the PPC and GLOB-RF showed substantially lower half-life times of 14 and 70 min, respectively. The remarkably stable albumin-stabilised foams are the result of the small air bubble size and the stiff interfacial layer around this air bubble. Generally, small air bubbles increase the total interfacial area in the foam, thereby increasing the liquid captured around the bubbles and in the foam, thus slowing down drainage. Also, small air bubbles (with a narrow size distribution) decrease the disproportionation of gas between air bubbles. The stiff solid-like interfacial layers formed by albumins could further slowdown the disproportionation and increase the resistance of air bubbles against coalescence. A combination of these factors probably explain the exceptionally high foam stability of albumin-stabilised foams.

5.3.4 Emulsifying properties of the pea protein fractions.

The emulsifying properties of the pea protein fractions were studied at protein concentrations of 0.7% and 2 wt. %. A protein-poor and -rich regime was previously

established for protein-stabilised emulsions, where the oil droplet size (determined as droplet diameter) decreased with higher protein concentration, as more protein was available to stabilise the generated interface during droplet break-up in the homogeniser. Above a certain protein content, the droplet size is independent of the protein concentration, also known as the protein-rich regime. For this study, the emulsifying properties were evaluated at the boundary of the protein-poor and -rich regime, also known as the critical protein concentration. Based on previous work on pea protein emulsions, we chose a protein content of 0.7 wt. % [190]. A protein content in the protein-rich regime was also studied, which was 2 wt. %.

Emulsions with 10 wt. % oil were studied for the average droplet size ($d_{3,2}$) directly after emulsion preparation, and after 7 days of storage (Table 5.4). In the protein-rich regime at 2 wt. % protein, all three pea protein fractions formed emulsions with droplet sizes between 0.50 and 0.55 μm. Potential flocculates were broken down by addition of sodium dodecyl sulphate (SDS), as the SDS replaces the proteins at the surface, introducing a high surface charge, thereby breaking up flocculated droplets. The emulsions formed with 2 wt. % protein had a similar droplet size after addition of SDS, which suggested that the oil droplets are stable against flocculation. After 7 days, the droplet sizes remained constant, demonstrating stability against coalescence and flocculation for at least 7 days.

At a lower concentration of 0.7 wt. %, more distinct differences between the pea protein stabilised emulsions are present. As the droplet sizes of ALB-RF-stabilised emulsions were about three times larger compared to PPC and GLB-RF-stabilised emulsions. The emulsions at these concentrations can be analysed more precisely with the droplet size distribution graphs (Fig. 5.8). Both PPC- and GLB-RF-stabilised emulsions had a similar size distribution with a peak at 1 μm. Addition of SDS resulted in an overlapping graph, indicating the absence of flocculation. The ALB-RF-stabilised emulsions showed a different size distribution with two peaks, the first peak between 0.3 – 3 μm, and a second peak between 3 – 30 μm. The second peak disappeared upon addition of SDS, which indicates flocculation of oil droplets stabilised by ALB-RF. The single droplet size of ALB-RF-stabilised oil droplets was still larger compared to those of PPC and GLB-RF. Albumins were found to be less effective in oil droplet stabilisation upon emulsion formation, and protected the droplets less against flocculation. The flocculation could occur due to a lower net protein charge of the albumins compared to the globulins (as measured in Chapter 4). This will result in a lower surface charge around the oil droplets, as the proteins

Table 5.4 Average droplet size ($d_{3,2}$) of 10% (w/w) oil-in-water emulsions stabilised by 0.7 or 2% (w/w) protein concentration at pH 7.0. The overall droplet size was studied directly after emulsion preparation, and after 7 days of storage at 4 °C. The single droplet size was also studied by breaking up potential flocculates using SDS. The samples were prepared in duplicate and each replicate is measured in triplicate. Standard deviations are shown in superscript.

	Pea fraction	**0.7 wt. % protein**		**2 wt. % protein**	
		Overall droplet size (µm)	Single droplet size (µm)	Overall droplet size (µm)	Single droplet size (µm)
Day 0	PPC	0.72 $^{\pm 0.03}$	0.69 $^{\pm 0.02}$	0.50 $^{\pm 0.04}$	0.49 $^{\pm 0.01}$
	ALB-RF	2.04 $^{\pm 0.10}$	0.83 $^{\pm 0.04}$	0.51 $^{\pm 0.04}$	0.49 $^{\pm 0.03}$
	GLB-RF	0.71 $^{\pm 0.04}$	0.67 $^{\pm 0.03}$	0.55 $^{\pm 0.02}$	0.55 $^{\pm 0.02}$
Day 7	PPC	0.69 $^{\pm 0.04}$	0.64 $^{\pm 0.03}$	0.57 $^{\pm 0.02}$	0.55 $^{\pm 0.02}$
	ALB-RF	3.78 $^{\pm 0.14}$	1.99 $^{\pm 0.33}$	0.58 $^{\pm 0.02}$	0.59 $^{\pm 0.02}$
	GLB-RF	0.75 $^{\pm 0.03}$	0.70 $^{\pm 0.05}$	0.50 $^{\pm 0.02}$	0.51 $^{\pm 0.02}$

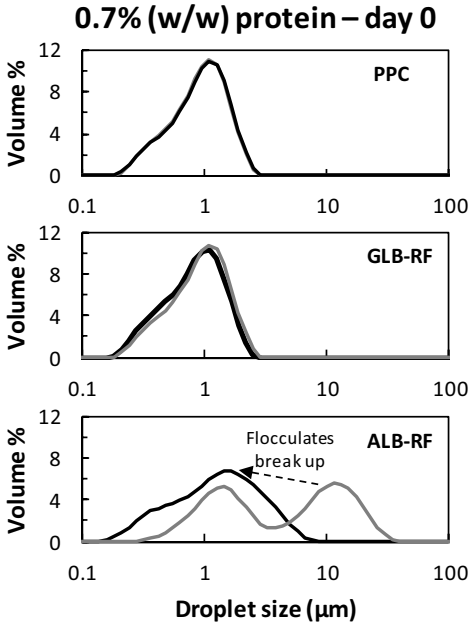

Figure 5.8 Droplet size distribution of 10 wt. % oil-in-water emulsions prepared from PPC, ALB-RF and GLB-RF with 0.7 wt. % protein at pH 7.0, directly after emulsion preparation (grey line). The size distribution of single droplets after breaking up flocculates with SDS were also shown (black line). The samples were prepared in duplicate and each replicate is meas-ured in triplicate. A representative size distribution was shown.

are on the outer layer of the droplets. Consequently, less electrostatic repulsion is present between the oil droplets, leading to droplet flocculation. Also, the lower protein net charge could allow more albumins to fit on the interface, due to less electrostatic repulsion between the proteins. As more proteins can fit on the interface, more proteins would be required to stabilise the interface. This point is proven by increasing the protein content to 2 wt. % into the protein-rich regime, where the albumins give stable emulsion droplets, similar to globulin-stabilised emulsions. A higher number of proteins on the surface could have increased the overall surface charge of the droplet, as the ALB-RF-stabilised emulsions at 2 wt. % did not show flocculation.

At 0.7 wt. %, the pea globulins are more effective in stabilising emulsions, and are responsible for the comparable stability of PPC-stabilised emulsions, thus suggesting that the globulins dominated the emulsifying properties. The pea protein globulins

(legumin and vicilin) were previously described as surface active molecules, which were able to stabilise the oil-water interface effectively [36, 190]. The pea globulins are larger in molecular weight (170 - 380 kDa) compared to pea albumins (10 - 53 kDa), and the globulins also form aggregates in the bulk, as demonstrated for our samples in Chapter 2. The large globulins could contribute to a thicker layer around the oil droplet, which has a sufficiently high surface charge to avoid the droplets from aggregating into flocculates.

The emulsions with a protein content of 0.7 wt. % were also studied for their stability after 7 days of storage. The PPC- and GLB-RF stabilised emulsions had coinciding $d_{3,2}$-values and droplet size distribution graphs (data not shown) after 7 days. Slight differences can be observed in the droplet size distribution graph of the ALB-RF-stabilised emulsions (Fig. 5.9). After 7 days of storage, the left peak diminished, while the right peak shifted further to the right, revealing a continuous flocculation of the emulsion droplets during the storage period. After addition of SDS, we also observe a slight shift of the single droplet size towards the right, which is also reflected in a $d_{3,2}$ increase from 0.83 to 1.99 μm after 7 days of storage. An increase of the single droplet size indicates two instability phenomena, coalescence of emulsion droplets or irreversible aggregation of the droplets that could not be broken up after addition of SDS. The irreversible flocculation was confirmed using microscopy (Fig. 5.9), as several larger flocculates were observed among many single droplets.

Another studied emulsion stability property was creaming, which was not visible after 7 days of storage at 4 °C for emulsions stabilised with 2 wt. % protein. At 0.7 wt. %, only the ALB-RF stabilised emulsions showed creaming, which was measured and converted into a creaming factor (see Eq. 5.2). Directly after preparation, the ALB-RF showed no creaming (creaming factor of 0%), but after 4-5 hrs a transparent layer was observed at the bottom of the tubes. After 24 hrs, the creaming factor was 65%, and further increased to 74% after 7 days of storage. According to Stokes law, two major parameters play a role in this case, which are the droplet size and viscosity. The ALB-RF protein solution only had a slightly lower viscosity (1.7 – 3.9%) compared to PPC and GLB-RF. Therefore, large flocculated droplets seem to play a major role in the creaming of the droplets. At higher concentrations, the albumins could form small droplets that were stable against flocculation, and thus against creaming.

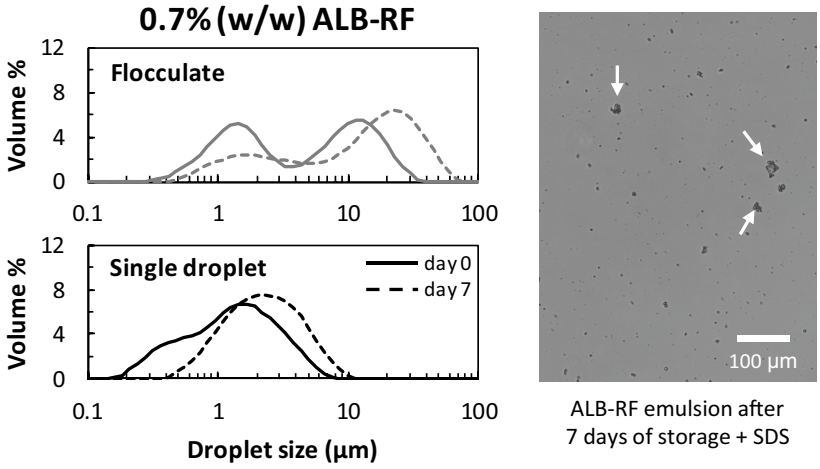

Figure 5.9 Droplet size distribution of 10 wt. % oil-in-water emulsions prepared from albumin-rich fraction (ALB-RF) with 0.7 wt. % protein at pH 7.0, directly after emulsion preparation (solid line), and after 7 days of storage at 4 °C (dotted line). Single droplets were also studied after breaking up flocculates. The samples were prepared in duplicate and each replicate is measured in triplicate. A representative size distribution was shown. A microscopy image of an ALB-RF-stabilised emulsion after 7 days storage with addition of SDS was also shown. The arrows indicate irreversibly aggregated flocculates.

We proved that pea globulins are more effective in stabilising emulsions at 0.7 wt. % protein than albumins. Another important finding is that an extensively purified pea protein isolate (GLB-RF) showed similar emulsion properties as a mildly purified pea protein concentrate (PPC). For the preparation of stable emulsions, a PPC could already be sufficient.

5.4 Conclusion

Aqueous fractionation of pea yielded three different fractions with significantly different functionalities. The small size and lower net protein charge of albumins led to high in-plane interactions at the air-water interface, thus resulting in a stiff and cohesive interfacial layer. Such a strong interfacial layer around the air bubble could explain a four times higher foam ability, and almost twenty times higher foam stability compared to the globulin-dominated fractions. The poor foaming properties of globulins could be related to the formation of a weak and stretchable interface, caused by a more aggregated state and higher net protein charge. It is worth mentioning that the foaming properties of albumin-stabilised foams are remarkably similar to whey protein isolate. On the other hand, the pea protein concentrate (PPC) and globulin-rich fraction (GLB-RF) contained mainly globulins, which led to smaller emulsion droplets with higher stability against flocculation compared to the albumin-rich fraction (ALB-RF). This difference in functionality can be attributed to the molecular properties, as the globulins are larger and more highly charged, leading to a droplet with a thicker interfacial layer and a higher surface charge.

In this work, we showed that the plant protein fractionation method can be tuned to obtain protein ingredients with either promising foaming or emulsifying properties. Albumins can be used as a foam stabiliser, while globulins can be used as an emulsion stabiliser. In a mild fractionation process, where albumins and globulins were co-extracted, the globulins seemed to dominate the functional properties, thus resulting in good oil droplet stabilisation. Our mild fractionation method consists of fewer processing steps compared to commonly reported aqueous protein fractionation methods, which lowers the ecological footprint and may optimize pea resource efficiency by also using by-products in a fractionation process. The combination of mild and targeted plant protein fractionation is a powerful tool in the utilisation of plant proteins as functional ingredients in our foods.

Appendix

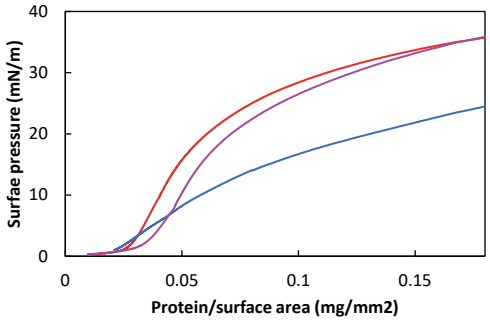

Figure A5.1 The surface pressure isotherm of PPC (—), ALB-RF (—) and GLB-RF (—), obtained in the Langmuir trough. The samples were measured at least in duplicate, and one representative curve is shown.

Table A5.1 Fitting parameters of the KWW equation on step-dilatation experiments. The samples were measured at least in triplicate and standard deviations are given.

	Compression			**Expansion**		
	PPC	ALB-RF	GLB-RF	PPC	ALB-RF	GLB-RF
a	-6.8 $^{\pm 1.3}$	-8.2 $^{\pm 2.3}$	-6.4 $^{\pm 2.4}$	2.5 $^{\pm 0.8}$	2.7 $^{\pm 0.1}$	2.9 $^{\pm 0.8}$
b	-0.5 $^{\pm 0.1}$	-1.0 $^{\pm 0.1}$	-0.8 $^{\pm 0.1}$	0.7 $^{\pm 0.1}$	0.6 $^{\pm 0.1}$	1.0 $^{\pm 0.1}$
c	50.9 $^{\pm 1.1}$	51.9 $^{\pm 0.8}$	50.3 $^{\pm 1.5}$	47.8 $^{\pm 2.4}$	51.9 $^{\pm 1.0}$	47.6 $^{\pm 1.4}$
β	0.67 $^{\pm 0.07}$	0.74 $^{\pm 0.05}$	0.63 $^{\pm 0.08}$	0.58 $^{\pm 0.04}$	0.55 $^{\pm 0.02}$	0.56 $^{\pm 0.04}$
τ_1	4.6 $^{\pm 1.5}$	6.4 $^{\pm 0.9}$	4.1 $^{\pm 0.9}$	8.3 $^{\pm 2.6}$	6.2 $^{\pm 0.8}$	8.4 $^{\pm 2.5}$
τ_2	203 $^{\pm 30}$	138 $^{\pm 30}$	183 $^{\pm 23}$	319 $^{\pm 61}$	320 $^{\pm 61}$	405 $^{\pm 108}$

Chapter 6

Fractionation methods affect the gelling properties of pea proteins in emulsion-filled gels

Abstract

Plant proteins from sources such as pea can be used as functional ingredients in emulsions and gels, after fractionation from the seed matrix. However, the protein fractionation route used affects the protein functionality. We investigated the differences in rheological properties of emulsion-filled gel (EFGs) structured by pea protein isolate obtained using either isoelectric precipitation (PPIp) or diafiltration (PPId), at varying pH and oil content. PPIp and PPId had a protein content of 75.3 and 77.7 wt. %, respectively. We first studied the oil-water interfacial rheology and composition in emulsions, as these interfacial and emulsion properties can influence EFG properties. Both PPIp and PPId formed a viscoelastic, soft-solid protein layer around the oil droplets and both PPIs were able to stabilize emulsions with monomodal droplet size between 1-10 μm. Gelation was induced by heating, and at pH 5, PPIp and PPId formed EFGs with comparable firmness (i.e. similar G') and with a heterogeneous microstructure. At pH 7, PPIp formed less firm and cohesive gels compared to PPId. This difference was attributed to differences in protein solubility and aggregation, caused by different fractionation methods. In the EFGs, oil did not reinforce the gel structure, which could be explained by weak interactions between the droplet interface and protein matrix. Our results show that pea protein fractionation routes affect the properties of PPI gels and EFGs. These insights may contribute to pea protein fractionation that is tailored to specific structural requirements for gel-based foods.

This chapter is submitted as:

Remco Kornet, Simha Sridharan*, Paul Venema, Leonard Sagis, Constantinos V. Nikiforidis, Atze Jan van der Goot, Marcel Meinders, Erik van der Linden. Fractionation methods affect the gelling properties of pea proteins in emulsion-filled gels (*the authors have contributed equally to this work)*

6.1 Introduction

Proteins are used as structuring agents in foods. They can stabilize oil droplets in oil-water mixtures to form an emulsion. Proteins can also be used as gelling agents; in which case they form a space spanning network that incorporates other constituents such as water and oil. Further, proteins can be used to simultaneously stabilize oil droplets and form gels, often referred to as an emulsion-filled gel. There are a variety of foods that can be classified as emulsion-filled gels, such as yoghurt, cheese, ice cream and processed meat products [191]. Most of these products are structured using animal-based proteins. However, the consumption of plant-based foods is rapidly increasing, due to environmental and health concerns. There is thus interest in replacing dairy proteins with plant proteins as structuring agents. Plant proteins, however, have different physicochemical properties than dairy proteins, and often behave differently than their dairy counterparts, for instance, in terms of gelation [192] and emulsifying properties [190]. Different technical solutions have been proposed to solve the challenges related to replacing dairy proteins. These include enzymatic treatment of plant proteins [193, 194], partial replacement of dairy by plant proteins [195, 196], recombinant dairy proteins [197] and alternative fractionation routes to influence plant protein functional behaviour [147, 198-201].

A commonly reported way of fractionating plant protein is aqueous fractionation, which involves a solubilization step at alkaline pH followed by a precipitation step at acidic pH [18]. Alternative methods of fractionation include dry fractionation [56], salt-extraction [70] and membrane filtration [202]. Different fractionation routes yield pea protein isolates with different protein composition. Upon isoelectric precipitation only pea globulins are recovered, while membrane filtration and salt extraction recover both pea globulins and albumins [50, 152]. Furthermore, the physicochemical properties are affected by the fractionation method. For instance, membrane filtration leads to pea protein with a higher solubility than the mainstream isoelectric precipitation process [62, 203]

An important type of protein functionality is the emulsifying capacity and emulsion stability. A few studies have focussed on the effect of different fractionation routes (i.e. isoelectric precipitation, salt-extraction and membrane filtration) on the emulsion properties of pea proteins. It was found that isoelectric precipitation yielded pea protein that could form smaller droplet sizes in oil-water emulsions, than those obtained by salt extraction and membrane filtration [71, 152, 168]. In the light of emulsion-filled gels, a relevant functionality type to consider is the gelling behaviour. For

different plant protein sources, it has been reported that the gelling behaviour was affected by the fractionation method and that this had a larger impact on the gelling behaviour than the protein isolate composition [146, 204]. In previous research it was found that using membrane filtration (more specifically, diafiltration) – as opposed to isoelectric precipitation – resulted in a pea protein isolate that could form firm gels, comparable in firmness to whey protein isolate gels [203]. A similar conclusion was reported for lentil protein isolate [202] and chickpea protein isolate [146], where diafiltration yielded protein isolates with better gelling properties than isoelectric precipitated pea protein. The differences in gel firmness between isoelectric precipitated and membrane filtrated pea protein are probably related to fractionation process-induced aggregation. Isoelectric precipitation induces protein aggregation, which is also reflected in a lower solubility. These aggregates formed more heterogeneous and less cohesive heat-set gels, as opposed to the proteins obtained by membrane filtration. Membrane filtrated protein was not aggregated and thus showed a higher solubility [203]. Also in other studies, the solubility of a globular protein such as pea globulin, has been related to its ability to participate in heat-induced protein gel formation [55, 205].

The gelling and emulsion properties of pea protein – whether or not in the context of different fractionation routes – have been subject of numerous studies. However, only few studies combine the emulsion and gelling properties of plant protein, by focussing on emulsion-filled gels [77, 192, 206, 207]. In this study we aim to understand how fractionation methods affect the emulsion-filled gelling behaviour of pea protein. We investigate the ability of two differently fractionated pea protein isolates to form emulsion-filled gels at different pH and oil content. While building on previous research, we aim to get a mechanistic understanding of the relation between fractionation processes and emulsion-filled gelling capacity of pea protein. The new insights obtained may facilitate the development of plant-based food products such as cheese and meat analogues, by tailoring the fractionation method to specific product requirements.

6.2 Material and methods

6.2.1 Materials

Yellow pea (Pisum sativum L.) seeds were acquired from Alimex Europe BV (Sint Kruis, the Netherlands). Rapeseed oil was provided by Danone Nutricia Research (Utrecht, the Netherlands). Chemicals and CLSM dyes were obtained from Merck (Darmstadt, Germany). All samples were prepared with deionized water.

6.2.2 Pea protein fractionation

Two pea protein isolates (PPI) were prepared, one using isoelectric precipitation (PPIp) and the other one using diafiltration (PPId). The fractionation methods are from previous work [203] and are briefly described below and a schematic overview is given in Fig. 6.1.

PPIp was obtained using isoelectric precipitation. First pea flour was dispersed in deionized water (1:10 ratio) for 2h at room temperature, with a pH adjusted to 8 using 1 M NaOH. The flour dispersion was subsequently centrifuged (10000g, 30 min, 20 °C) to remove solids. The supernatant was brought to pH 4.5 with 1 M HCl to precipitate the pea globulins. After 2h of stirring at room temperature, the precipitated proteins were separated by centrifugation (10000g, 30 min, 20 °C). The protein-rich pellet was re-dispersed at pH 7 and freeze-dried afterwards.

PPId was obtained without any pH adjustments and fractionation was achieved by diafiltration instead. Pea flour was dispersed in deionized water for 2 h, with the pH left unadjusted (~pH 6.7). Then the dispersion was centrifuged at 10000 g for 30 min and the supernatant was collected and further fractionated by ultrafiltration and diafiltration at room temperature with a Sartocon Slice crossflow set, consisting of a SartoJet pump, Sartocon Slice filter holder, pressure gauges and valves, all connected via sanitary Tri Clamp adapters (Sartorius AG, Goettingen, Germany). Two Sartocon Slice cassettes with a 5 kDa Hydrosart membrane (Sartorius AG, Goettingen, Germany) were applied at a transmembrane pressure of 2 bar. The cellulose-based membranes were non-protein binding and had a filter area of 2 × 0.1 m^2. At the start of the filtration process the supernatant was diluted with an equivalent amount of water. The supernatant was then concentrated using ultrafiltration up to a concentration factor of 2. During diafiltration the filtrate, with mostly sugars and peptides, was discarded and the retentate was recirculated. To maintain diafiltration efficiency, water was added when the retentate became too concentrated, eventually

leading to a total diafiltration factor of about 8. After diafiltration the concentrated retentate was collected and freeze-dried.

The freeze-dried pea protein isolates were stored at -18 °C. The nitrogen content was measured with a Flash EA 1112 series Dumas (Interscience, Breda, the Netherlands) and used to calculate the protein content (with a nitrogen-conversion factor of 5.7). The protein content of the freeze dried PPIp was found to be 75.3 (± 0.7) wt. % and PPId 77.7 (± 0.4) wt. %. The protein recovery of the precipitation and diafiltration process has previously been reported to be 52 (± 7.3) and 63 (± 63) %, respectively [203].

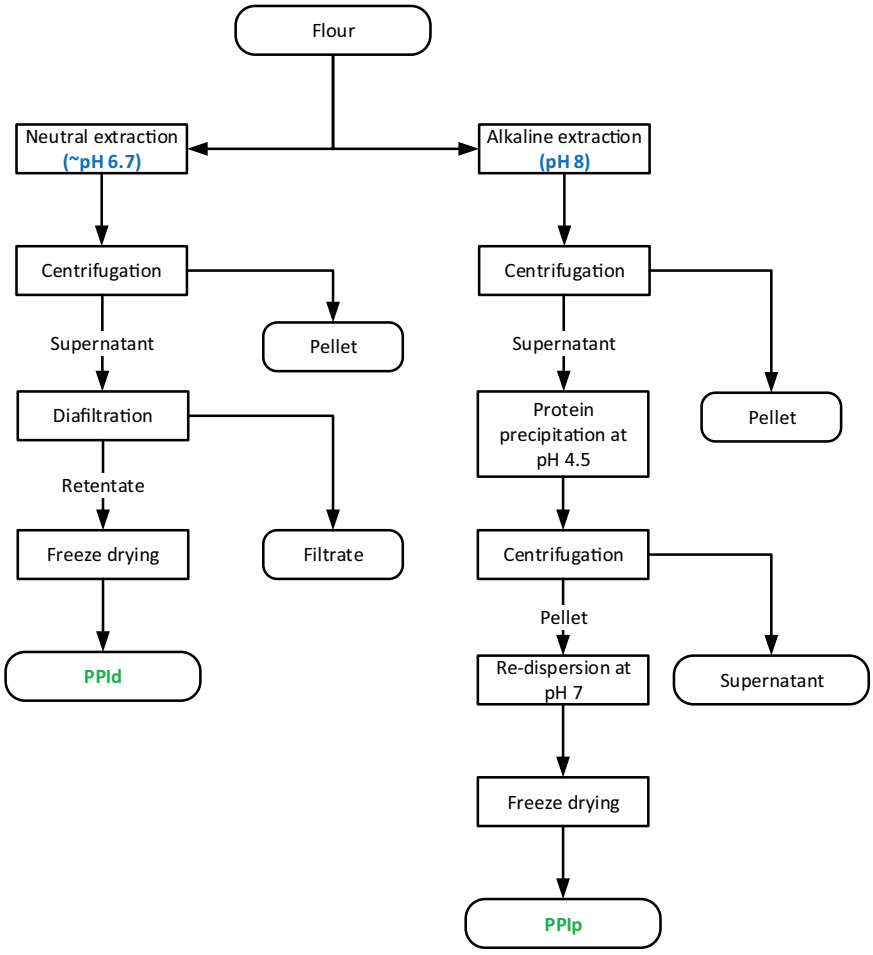

Figure 6.1 Schematic overview of the two fractionation processes. The left process used neutral extraction and diafiltration to yield PPId and the right process uses alkaline extraction and isoelectric precipitation to yield PPIp.

6.2.3 Interfacial tension and dilatational rheology

The interfacial tension reduction and dilatational rheology of the oil–water interface stabilized by pea protein was measured with an automated drop tensiometer (Tracker, Teclis Instruments, Tassin, France). Dispersions of PPIp and PPId containing 0.01 wt. % were prepared in deionized water and the pH was adjusted to pH 7. The dispersion could solubilize under magnetic stirring for 3 h.

Rapeseed oil was treated with Florisil overnight to remove impurities and was used as the oil phase in the emulsions. In brief, a 1:3 (w/w) ratio of Florisil to oil was mixed overnight and centrifuged the next day to obtain contaminant-free oil, which was used in the interfacial study.

In the drop tensiometer, a droplet of the stripped rapeseed oil with 20 mm^2 area was created at the tip of a J-shaped needle, in a clean 7 mL optical glass cuvette filled with the aqueous protein solution. The needle was fitted to a 500 µL syringe. The shape of the oil droplet was monitored continuously with a camera. From this shape the interfacial tension was calculated by the Wdrop® software from Teclis® Instruments (Tassin, France). The dynamic interfacial tension reduction profile was monitored continuously for 2 h and plotted against time.

After 2 h of interfacial tension measurement, dilatational viscoelasticity was measured by changing the surface area of the droplet in a sinusoidal manner. The droplet was subjected to changes in surface area with amplitudes of 5%, 10% and 15% deformation with respect to the initial surface area (20 mm^2). Each amplitude was applied for 50 s with five subsequent cycles. This was followed by 250 s of rest period before the next higher amplitude was applied. The interfacial tension change and change in area were recorded during the oscillation, and the dilatational elastic (Ed′) and viscous moduli (Ed″) were obtained from the intensity and phase of the first harmonic of the frequency spectrum (obtained by FFT of the interfacial tension signal).

6.2.4 Emulsion preparation for emulsion-filled gels

The aim was to produce emulsion-filled gels (EFGs) with final oil concentration of 10 wt.%, 20wt% and 30wt%, using PPIp or PPId dispersions. To obtain this final concentration in EFGs, emulsions with 11.56 wt.%, 22.7 wt.%, and 33.5 wt.% oil concentrations were prepared, respectively. The protein to oil ratio was kept constant at 1g protein/50g oil by adjusting the concentration of proteins in the aqueous phase. This protein to oil ratio was used based on previous work, where a 1:50 wt ratio

protein to oil was found to be sufficient to cover the oil droplet interface [147].

Firstly, the required amount of proteins was dispersed in deionized water. Then the pH was adjusted to pH 7, using 0.5 M NaOH, and allowed to stir for 3 h under magnetic stirring. The dispersions were then sheared for 15 s at 6000rpm in an IKA (Ultra-Turrax, IKA, Staufen, Germany) Ultra-Turrax to ensure homogeneous dispersion of proteins. Subsequently, rapeseed oil was added slowly, while the mixtures were sheared for another 60 s at 10000 rpm to produce a coarse emulsion. The formed coarse emulsions were further homogenized by passing through a GEA (Niro Soavi NS 1001 L, Parma, Italy) high pressure homogenizer for five passes with a homogenization pressure between 250-350 bars to obtain similar droplet sizes, depending on the oil concentrations. Detailed compositions are given in Table 6.1.

Table 6.1 Final emulsion composition and emulsification pressure for emulsions stabilized by PPIp (precipitated) and PPId (diafiltrated).

Oil content (wt. %)	Protein content (wt. %)	Homogenization pressure (bar)
11.6	0.2	250
22.7	0.4	300
33.5	0.6	350

6.2.5 Static light scattering

The individual droplet size of the emulsions was measured with laser diffraction in a Malvern Mastersizer® 3000 (Malvern® Instruments Ltd., Malvern, U.K.). The samples were dispensed with a hydrodispenser®, and the droplet size was represented by the volume mean diameter ($D_{4,3}$).

To measure individual droplet sizes, the emulsions were treated with 1 wt. % SDS solution. Addition of SDS breaks droplet aggregation driven by non-covalent protein interaction, so the size of individual oil droplets could be measured in this manner [208]. Equal volumes (1 mL) of emulsion and 1 wt. % SDS solution were mixed, and the size was immediately calculated by the Malvern Mastersizer software, with the refractive index set to 1.47.

6.2.6 Sodium dodecyl sulphate polyacrylamide gel electrophoresis (SDS-PAGE)

SDS-PAGE was conducted to qualitatively analyse the protein classes that are present in the pea protein isolates and at the interface of the emulsion oil droplets. The protein isolates were prepared by weighing dry protein powder directly and dissolving in the appropriate SDS buffer as explained below. In order to separate

the oil droplets in the emulsion samples, first the emulsions were centrifuged. About 12 mL of emulsions were centrifuged at 10,000g for 30 minutes at 4°C. The cream layer was removed and re-suspended in water at 1:10 weight ratio. Then, another centrifugation at 3000g for 15 minutes at 4°C was conducted. The cream layer after centrifugation was collected, labelled as the 'em' phase and the oil droplet free aqueous phase was collected, labelled as 'aq' phase.

The samples (i.e. em phase and aq phase) were dispersed in 250 μL NuPAGE® LDS sample buffer and about 750 μL deionized water was added so that the final protein concentration was about 2 mg/mL. The samples were subsequently heated at 90°C for 15 min followed by centrifugation at 425 g for 1 min. Next, 20 μL of the supernatants were loaded into the wells of a NuPAGE® 4–12 wt% Bis-Tris precast gel. A protein standard (10 μL) (10 kDa–200 kDa) was also loaded and the gel was fixed in the electrophoresis chamber. After filling the chamber with MES Buffer, the electrophoresis was run at 200 V for 40 minutes. Further, the gel was separated and washed with deionized water and was gently shaken for 4 h in Comaisse® blue stain. The gel was then destained with a solution containing 20% ethanol, 50% acetone, 30% water for 4 h. Finally, the gel was washed with deionized water.

6.2.7 Emulsion-filled gels preparation

After the emulsions were formed, additional proteins were added to form the protein enriched emulsions. To the formed PPIp and PPId emulsions, PPIp and PPId were added respectively. The amount of protein added was standardized to a final concentration of 15 wt% of the emulsion aqueous phase for all the emulsions. The pH of the protein enriched emulsions was adjusted to pH 7 or pH 5 and magnetically stirred at 300 rpm for 3 h. Subsequently the samples were stored at 4°C overnight, prior to rheological analysis.

6.2.8 Small amplitude oscillatory shear (SAOS) rheology of gels

The gelling behaviour of the dispersed PPI isolates and the protein-enriched emulsions was examined by temperature sweeps using an MCR302 rheometer (Anton Paar, Graz, Austria) with a sand-blasted concentric cylinder geometry (CC-17). A sand-blasted geometry was used to reduce the chance of wall slip and a solvent-trap was placed on top of the concentric cylinder to reduce solvent evaporation upon heating. The sample was heated from 20 °C to 95 °C with 3 °C/min, kept at 95 °C for 10 min, and cooled to 20 °C with 3 °C/min. To verify whether no further gel maturation occurred after the temperature sweep, the sample was kept for another 5 min at 20

°C. Throughout the temperature sweep, an oscillatory deformation was imposed at a constant frequency of 1 Hz and a strain amplitude of 1%, which fell within the linear viscoelastic (LVE) regime of the gel. The recorded response was processed by the Rheocompass software (Anton Paar, Graz, Austria) to calculate the elastic modulus (G') and viscous modulus (G''). All samples were prepared in duplicate.

6.2.9 Medium and large amplitude oscillatory shear (MAOS & LAOS) rheology of gels

The gels formed during the temperature sweep were further characterized by applying non-linear deformation, using the same rheometer and geometry as for the SAOS measurements. The gel was deformed by applying a strain sweep from 0.1 – 1000% in a logarithmic manner, at a constant frequency of 1 Hz and temperature of 20 °C. For each imposed strain amplitude, the oscillating strain, stress and shear rate were recorded. The strain, stress and shear rate values were normalized and elastic and viscous Lissajous plots (i.e. shear stress vs shear strain and shear stress vs shear rate, respectively) were constructed. Also, the elastic and viscous contributions at each strain amplitude were extracted from the Rheocompass software, normalized, and plotted within the Lissajous figures. Lissajous plots were only constructed for the MAOS regime (10 – 100% strain amplitude), which is the regime where the transition from a predominantly elastic to a predominantly viscous response takes place.

The area that is enclosed within the Lissajous curves represents the dissipated energy per unit volume during an oscillatory cycle. This area thus represents important information from the Lissajous plots, as it reflects the loss of stored energy at a given strain amplitude. When dividing this dissipated energy by the energy dissipated by a perfectly plastic material, the energy dissipation ratio (Φ) is obtained. The energy dissipation ratio can be calculated from the loss modulus (G'') and the maximum stress (σ_{max}) at an applied strain amplitude (γ_0) and is determined by Eq. 6.1 [209].

$$\Phi = \frac{E_d}{(E_d)_{pp}} = \frac{\pi G'' \gamma_0}{4\sigma_{max}} \quad (6.1)$$

6.2.10 Multi photon microscopy (MPM)

The microstructure of emulsion-filled gels (EFGs) was visualized by using multiphoton microscopy. Multiphoton microscopy differs from a confocal set up in that it uses a low energy near infrared femtosecond laser. The fluorescent molecules are excited by multiple photons of low energy, which enables deeper penetration

and reduces photobleaching in the samples [210]. Therefore, MPM was used to image deeper into the dense gel samples in our study.

The protein-enriched emulsions (before heating) were stained with 7 μl Nile red (1mg/ml stock) for oil and 7 μl of Fast green FCF (1mg/ml stock) for protein. About 60 μL of the stained samples were transferred to a microscope glass slide fitted with a gene frame (Gene frame 65 μL adhesives, Thermo Fisher Scientific, United Kingdom). The gene frames were sealed with a 1.5H cover slip glass and they were placed in a water bath (100°C,15 min). The samples were then cooled and visualized using a multiphoton microscope.

The multiphoton microscope is a Leica confocal setup fitted with a Ti: Sapphire laser tuneable from 700-1080 nm. The samples were imaged at a wavelength of 920 nm using a 40X water immersion objective. The emissions were captured between 480-600 nm for Nile red and between 700-800 nm for Fast green. Both 2D images and 3D constructs were obtained using a 4 times line averaging sequence. The images were processed using the accompanying Leica® confocal software.

6.3 Results and discussion

6.3.1 Emulsion properties

Interfacial properties of PPI dispersions

The gelling and gel properties of emulsion-filled gels (EFGs) are affected by the interaction of the oil droplet interface with the gelled protein matrix [211] and the droplet stiffness [212]. Before studying the emulsion-filled gels, the interfacial tension and rheology and interfacial composition of pea proteins in PPIp and PPId were investigated and compared. Also, the emulsion oil droplet size may impact oil reinforcement in EFG matrices, as droplet stiffness scales inversely with droplet size. Therefore, emulsions were prepared and their size distributions were measured.

Fig. 6.2A shows the interfacial tension as a function of time for PPIp and PPId dispersions at the oil-water interface. The interfacial tension for both PPIp and PPId decreases over time (6000 s). The tension decreases from about 25 mN/m to about 10 mN/m after 6000 s. In the case of PPId, the tension value decreases from about 25 mN/m to about 6 mN/m after 6000 s. Overall, PPId decreases interfacial tension more than PPIp. For PPIp, within the first 400 s, the interfacial tension drops from about 25 mN/m to about 15 mN/m. After this point, the decrease is slow and gradually goes from 15 mN/m around 400 s to about 10 mN/m at 6000 s. For PPId, within the first 400 s, the tension goes from 25 mN/m to about 10 mN/m. Further in time, the decrease is also slow and gradual to about 6 mN/m after 6000 s. Therefore, within the first 400 s, PPId decreases tension faster than PPIp.

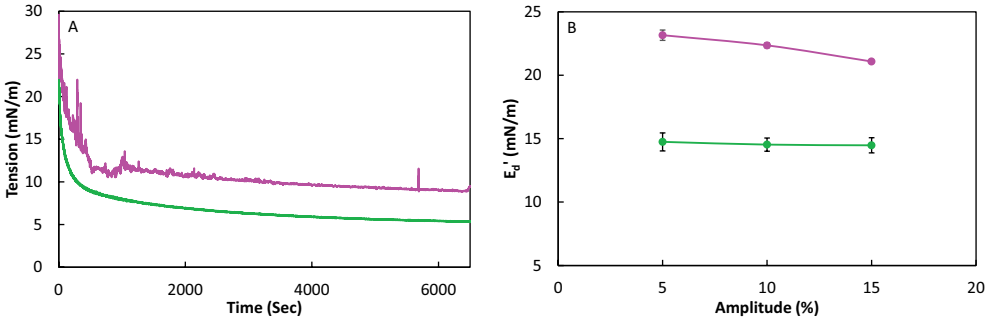

Figure 6.2 A. Interfacial tension measured at the oil-water interface for 0.01 wt% PPIp (—) and PPId (—) measured at 20°C, pH 7. B. Dilatational elastic modulus (E_d') as a function of dilatational amplitude for PPIp and PPId measured after 2 hours of interfacial tension measurement.

The faster decrease in the interfacial tension at the beginning indicates that, proteins in PPId adsorb at the oil-water interface and reduce the tension faster compared to proteins in PPIp [213]. The faster adsorption of PPId could be attributed to its higher solubility compared to PPIp. A higher protein solubility indicates that most proteins are present in soluble, individual form [203], so they can diffuse to the interface. Upon adsorption, these proteins can more easily reconfigure and form an interfacial layer, compared to more aggregated proteins. Previous work has shown that PPId is about 85% soluble at pH 7, while PPIp was only 70% soluble. The lower solubility of PPIp is caused by partially irreversible aggregation of proteins after isoelectric precipitation. In addition to insoluble aggregates, part of the PPIp protein is present in the form of soluble aggregates [203]. The fact that more proteins in PPIp exist in an aggregated state, could lead to longer adsorption and rearrangement times before noticeable change in interfacial tension occurs [213]. Also due to aggregates being present, the PPIp interfacial tension curve appears noisy, as droplet tensiometry is a visual technique and the presence of aggregates can disturb the measurement resulting in a noisy signal.

The interfacial dilatational rheology of PPIp and PPId were also measured as a function of different amplitudes of dilatation immediately following the interfacial tension measurement. Fig. 6.2B shows the dilatational elastic moduli (E_d') of PPIp (blue) and PPId (black). PPIp shows an E_d' between 25-20 mN/m with a small decrease in E_d' with increasing amplitude. PPId has an E_d' of about 15 mN/m without any amplitude dependency. For both PPIp and PPId, the elasticity is much lower than what was reported for WPI; the latter showed a much higher modulus for the oil-water interface (Perez, Carrara, Sánchez, Santiago, & Patino, 2009). Therefore, the interfaces formed with both pea protein fractions reported here, are relatively weak soft solid-like with limited in-plane protein-protein interactions.

The E_d' of the PPIp stabilized interface is higher than that of a PPId stabilized interface. In other words, PPIp formed a stiffer interface compared to PPId, implying more protein-protein interactions at the interface. PPIp also showed a decrease in E_d' with increasing dilatational amplitude. The amplitude dependency of PPIp could mean that even though the interface of PPIp is firmer at rest, the additional interaction is weak and is disrupted upon increasing amplitude [181]. The E_d' of the PPIp stabilized interface showed amplitude dependency, while for PPId it did not. To further investigate the interfacial properties, Lissajous figures of the interfacial modulus were plotted and analysed [214]. The interfacial Lissajous plots are given in Fig. 6.3.

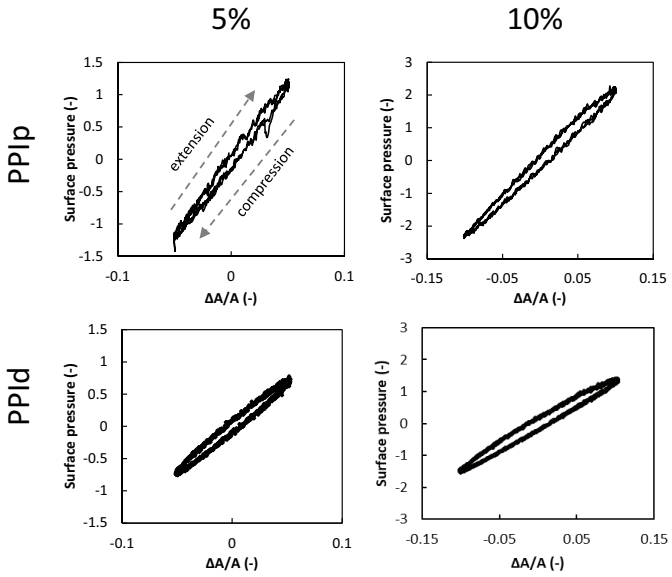

Figure 6.3 Interfacial Lissajous plots for 0.01 wt% PPIp (precipitated) and PPId (diafiltrated) dispersion at oil-water interface obtained from dilatational modulus at 5% and 10% dilatation amplitudes.

Fig. 6.3 shows the Lissajous plots of surface pressure as a function of relative change in surface area for 5% and 10% amplitudes, and for both PPIp and PPId. The plots from -0.05 to +0.05 along the upward arrow represents the expansion phase and the plot from +0.05 to -0.05 represents compression phase. All four plots show narrow elliptical loops, characteristic of visco-elastic interfaces with a dominant elastic nature [181, 214]. The PPIp curves at both strain amplitude show a narrowing effect upon compression (bottom left), which indicates that the response of the interface becomes relatively more elastic upon compression. This shape implies that the proteins at the interface were jammed upon compression, which is consistent with the weak protein-protein interactions (i.e., low E_d'). In PPId curves, the response of the interface was linear with a dominant elastic nature. No narrowing of the loop was visible upon compression, and the resulting interfacial microstructure was significantly stretchable and not affected by the amplitude of deformation. The loops of PPIp showed slightly higher surface pressure than PPId, both upon compression and expansion. This higher surface pressure change in PPIp could be due to stronger interactions occurring compared to PPId. In addition, the dilatational rheology shows decreasing interfacial elasticity in PPIp interfaces and was not observed in

PPId. This suggests that the slightly higher stiffness in PPIp interfaces could be due to weak secondary interactions, for example between adsorbed proteins and protein aggregates in the sub-phase which was disrupted due to dilatation of the interface, as seen for rapeseed proteins [181]. Overall, the interfacial rheology suggests that both PPIp and PPId formed interfaces with relatively soft solid-like behaviour through weakly interacting protein networks.

Emulsion properties

The droplet sizes of the freshly prepared emulsions were measured to evaluate the emulsifying properties of PPIp and PPId. The size distribution curves of a representative PPIp and PPId emulsion measured with SDS are shown in Fig. 6.4. The curves for both PPIs show a monomodal size distribution starting around 800 nm up to about 10 μm. Despite the differences in interfacial tension (IFT), the droplet sizes are similar for both emulsions, most likely due to a dynamic emulsification process used compared with the static IFT measurement condition. The similarities in size distributions of oil droplets indicate that the ability to stabilize oil droplets is similar for both pea protein isolates.

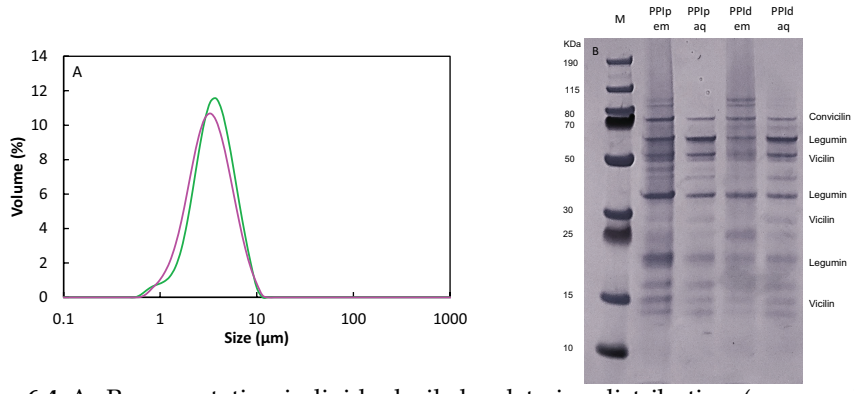

Figure 6.4 A. Representative individual oil droplet size distribution (measured with SDS) of 11.56 wt% oil-in-water emulsion stabilized by 0.02 wt% protein in PPIp (—)and PPId (—). B. SDS-PAGE of PPIp and PPId stabilized 11.6 wt.% oil emulsions at pH 7, with lanes named as follows, M: molecular weight marker, PPIp em.: Interfacial protein profile in PPIp; PPIp Aq.: Aqueous phase protein profile in PPIp; PPId em.: Interfacial protein profile in PPId; PPId Aq.: Aqueous phase protein profile of PPId. Identification of the bands is based on earlier research [30, 40].

Interfacial protein composition may influence droplet interaction with the matrix. The composition of proteins at the droplet interface and the unabsorbed proteins in PPIp and PPId were analysed using SDS-PAGE. Fig. 6.4B shows the electropherogram

of protein composition at the droplet interface and in the aqueous phase of PPIp and PPId under non-reducing conditions. The figure shows that for both PPId and PPIp, the interfacial composition of proteins (PPIp em and PPId em) were similar. In both emulsion, major storage proteins are present at the interface: Legumin at 60, 36 and 20 kDa, and Vicilin at 50, 25 and 16 kDa. Other minor constituents such as convicilin at 70 kDa and enzymes such as lipoxygenase ~90 kDa are also associated with the emulsion droplets [30, 40].

From these results we can conclude that the PPIp and PPId emulsion properties are quite similar, both in term of oil droplet size and protein composition. A similar interfacial composition for both PPIp and PPId emulsions makes it likely that the interactions between proteins in the matrix and interface will be similar in EFGs from both PPIs. The fact that the interfacial composition is similar, implies that differences in interfacial rheology cannot be explained by the composition. This supports our hypothesis that the higher dilatational moduli in PPIp is related to the secondary interaction between protein (aggregates) in the sub-phase and proteins at the interface. Knowing the droplet sizes is also important, as it influences the droplet stiffness and thus the potential of reinforcing the protein network in EFGs. These considerations will be further discussed in the next section.

6.3.2 Emulsion-filled gels

Small amplitude oscillatory shear (SAOS) rheology

The PPIp and PPId dispersions and protein-enriched emulsions were heated to study their gelling behaviour. Fig. 6.5 shows the development of G′ (elastic modulus) upon heating and cooling as a function of time at pH 7 and at pH 5. Upon heating at pH 7 (Fig. 6.5A) PPIp dispersions and protein-enriched emulsions show a gradual G′ increase, starting around 50 °C. When 95 °C is reached the G′ continues increasing while the temperature remains constant for 10 min. Upon cooling the G′ increases further until 20 °C is reached. The PPIp samples with and without 10 wt. % oil, follow similar gelling dynamics at pH 7. At pH 5 (Fig. 6.5B) the G′ increase of PPIp starts around 80 °C and is more abrupt. Upon cooling the G′ increase is more gradual compared with the increase at pH 7. Another difference between pH 5 and 7, is that at pH 5 the presence of oil causes a reduction of the eventual G′, compared with the PPIp gel without oil. PPId on the other hand, shows an abrupt G′ increase upon heating at pH 7 (Fig. 6.5A) around a temperature of 60 °C. Then the G′ remains quite constant, until the moment cooling starts. The G′ gradually increases further till a temperature of 20 °C is reached. At pH 5 (Fig. 6.5B) the G′ increase upon heating is

more gradual and more subtle. Also, upon cooling a subtle G' increase is observed. A both pH 7 and 5 oil has little effect on the gelling behaviour of PPId.

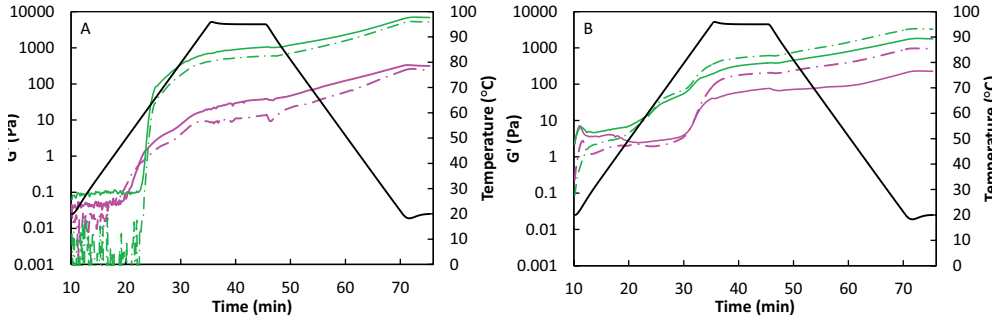

Figure 6.5 Temperature sweeps applied at pH 7 (A) and pH 5 (B) on PPIp (—) and PPId (—) dispersions without oil (15 wt. % dry matter) and on PPIp and PPId dispersions with 10 wt. % oil, represented by the dashed lines. All samples were measured in duplicate.

The difference between the PPIp and PPId gelling behaviour at pH 7, is that the G' increase is much more abrupt and pronounced for PPId. The abrupt transition from viscous to gel-like behaviour starts around 60 °C, which is at higher temperature than were the G' of PPIp starts to increase. This implies that network formation occurs at higher temperatures for PPId than PPIp. The gelation onset temperatures are below their denaturation onset temperature of around 70 °C [203], which may be related to the lower heating rate (3 °C/min versus 5 °C/min) and higher protein concentration (15 wt. % versus 10 wt. % dry matter) in the gelation experiment, compared with the experiment to determine the denaturation temperature [215, 216]. The abrupt G' increase observed for PPId is probably related to the previous observation that it is much less aggregated and more soluble [203], which allows homogeneous distribution of the protein and more freedom to interact with other proteins, as opposed to the more aggregated PPIp. Both PPIp and PPId show a subtle increase in G' upon cooling, which can be attributed to hydrogen bonding [153]. The G' of PPId after heat-set gelation is around 7 kPa, and is higher than the G' of PPIp, which is around 0.3 kPa. Based on earlier findings [203], it is known that the small difference in dispersed protein content (11.7 versus 11.3 wt. %) cannot account for this difference in gel firmness. Furthermore, it can be observed from the temperature sweeps that the addition of 10 wt. % oil has limited effect on the gelling behaviour of both PPIp

and PPId.

At pH 5 (Fig. 6.5B) PPIp and PPId behave more similar in terms of gelling behaviour. The G′ values before heating are higher compared to those at pH 7, and higher than G″, which is indicative of a network already present before heat-set gelation. This network present before heating is probably a result of aggregation, facilitated by a reduced electrostatic repulsion, as the isoelectric point of pea globulins is between pH 4 and 5 [217]. In other words, both PPIp and PPId are aggregated before heating and even though aggregation of the pea proteins proceeds further – as demonstrated by the G′ increase upon heating – the effect is more subtle. It is also observed that the final G′ of PPIp becomes slightly higher compared to the final value at pH 7, while the G′ of PPId becomes lower than its value at pH 7.

Fig. 6.6 shows the G′ of the gels as function of the incorporated oil mass fraction at pH 7 (Fig. 6.6A) and pH 5 (Fig. 6.6B). At both pH 5 and 7, the G′ does not increase with an increased oil content. This implies that oil does reinforces the gel structures, of neither PPIp nor PPId. At pH 5, there is even an initial decrease until 10 wt. % oil, after which G′ increases to roughly the same value as compared to the gel without oil. The absence of oil reinforcement either means that oil droplets are less stiff than the matrix, or that the oil droplet interface does not, or weakly, interacts with the gel matrix [191, 212, 218]. To estimate the stiffness of the oil droplets Eq. 6.2 is used with the dilatational elastic modulus (E_d') and the droplet radius (r).

$$G'_{filler} = \frac{2E'_d}{r} \tag{6.2}$$

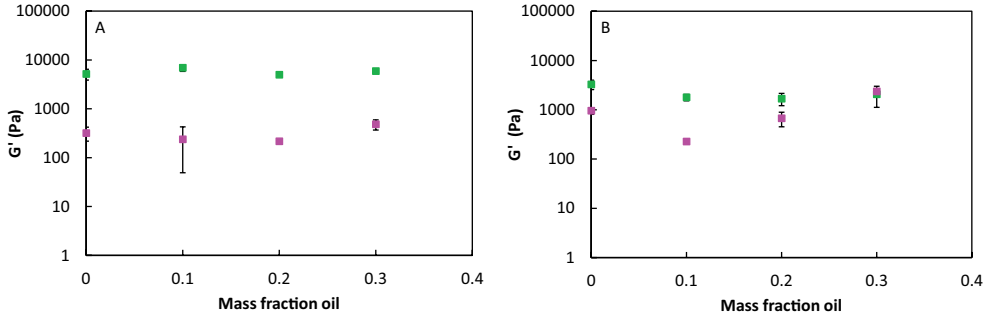

Figure 6.6 Gel firmness (G') as function of mass fraction oil of PPIp (■) and PPId (■) at pH 7 (A) and pH 5 (B). All samples were measured in duplicate and standard deviations are shown.

Eq. 6.2 is based on an expression given by van Vliet (1998) with the modification that the surface tension is replaced by the dilatational elastic modulus, after considering the viscoelastic nature of the protein-stabilized interface. Based on the E_d' and r from section 6.3.1, the droplet stiffness was estimated to be around 23 and 15 kPa for PPIp and PPId, respectively. This is higher than the stiffness of the matrix, meaning that in theory these droplets could reinforce the gel structure, if the droplets interact with the matrix and become an integral part of the gel network. Several models have been reported to predict the complex modulus (G^*) of soft solids with a continuous matrix and dispersed particles [219]. Two of these models, those of Mooney (1951) and Pal (2002), were tested on their ability to predict the G^* of the pea EFGs [220, 221]. It turned out that the models were not suitable to predict the complex moduli of the samples in this study, partially because the overall G' differences at different oil contents were small. This suggests that oil does not reinforce the pea protein gels, probably due to weak interactions between droplet interface and matrix.

Medium and large amplitude oscillatory shear rheology

The heat-set gels and emulsion-filled gels were further characterized by medium and large amplitude oscillatory shear (MAOS & LAOS) rheology. From the sinusoidal waveform data at each strain amplitude the energy dissipation ratio was calculated. The energy dissipation ratio is the dissipated energy within one cycle divided by the dissipation of an ideally plastic material. This ratio reflects the dissipated energy at a certain deformation – with a purely elastic response when $\Phi = 0$ and a perfectly plastic response when $\Phi = 1$ [222] – and hence provides a compact overview of its breakdown behaviour.

Fig. 6.7 shows the energy dissipation ratios (EDR) of PPIp and PPId without oil and with 10 wt. % oil, as function of strain amplitude Fig. 6.7A shows an increase of the EDR at around 10% strain for PPIp gels without oil. When oil was present the EDR already increased at lower strain. After reaching 10% strain, the viscous dissipation of the PPIp gel with 10 wt. % oil increased much faster with increasing strain. This implies that addition of oil made the PPIp gels at pH 7 more brittle. The lack of oil reinforcement could be due to weak oil droplet – protein matrix interactions, which also aligns with the interfacial rheology, where in-plane protein interactions were found to be weak. This weak interaction would disrupt the bulk protein-protein interactions and cause break down at lower strain, reflected in an increased brittleness.

The difference at pH 5 (Fig. 6.7B) between PPIp gels with and without oil was much

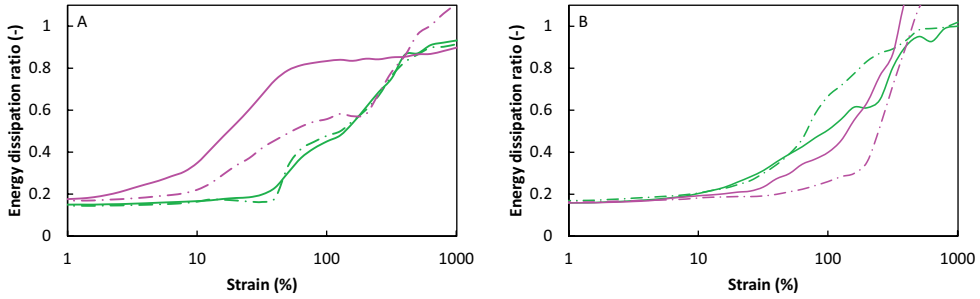

Figure 6.7 Average energy dissipation ratios at pH 7 (A) and pH 5 (B) of PPIp (—) and PPId (—) dispersions without oil (15 wt. % dry matter) and on PPIp and PPId dispersions with oil (10 wt. % oil, 15 wt. % dry matter in aqueous phase), represented by the dashed lines.

smaller, as the EDRs showed a similar trend. Also, viscous dissipation became significant at much larger strain, compared with the PPIp gels at pH 7. This means that at pH 5 the PPIp gels were more ductile, compared with the PPIp gels at pH 7. The PPId gels at pH 7 showed a significant EDR increase at around 30% strain (Fig. 6.7A). This was also the case for the PPId gel with 10 wt. % oil, which implies that oil had little effect on the response to large deformation of PPId gels at pH 7. The same is true at pH 5 (Fig. 6.7B), where little difference was observed between the PPId gels with and without oil. Compared with pH 7, the EDR at pH 5 started to increase at lower strain but evolved more gradually. PPIp gels showed an earlier increase in dissipation ratio than PPId, at pH 7. This indicates that PPIp (emulsion-filled) gels were more brittle, probably because of the weakly-connected network of pre-formed protein aggregates. Also, a major difference was seen between the PPIp gel and the emulsion-filled gel (10 wt. % oil), as the latter showed significantly more viscous dissipation at a lower strain. This indicates that oil weakens the PPIp gel structure at pH 7, which may be related to oil occupying the interstitial space between protein aggregates and consequently a decreased interaction between these aggregates. Another difference between PPIp and PPId is that the breakdown behaviour is more gradual for PPIp and more abrupt for PPId. The more gradual breakdown of PPIp is probably related to a more heterogeneous network, leading to a spectrum of interactions, that are broken at different extents of deformation. This heterogeneity was already observed for heat-set gels at pH 7 in a previous study [203] and will further be discussed in section 6.3.2 for the EFGs. At pH 5 (Fig. 6.7B) the breakdown behaviour of PPId became more gradual and more comparable with PPIp. This can be explained by the fact that close to the isoelectric point of pea protein, PPId now also forms a heterogeneous gel network just like PPIp.

A more detailed overview of the gel responses to large deformation is given in Fig. 6.8, where Lissajous plots at three strain amplitudes within the MAOS (medium amplitude oscillatory shear) regime are shown. Fig. 6.8A (top panel) shows the elastic Lissajous plots of stress versus strain for PPIp (left) and PPId (right) gel matrix and emulsion-filled gels with 10 wt. % oil at pH 7 (black) and pH 5 (green).

The left panel shows a clear difference between PPIp at pH 7 and pH 5. Already at 50% strain the gels at pH 7 display a somewhat rhomboidal shape, indicating a predominantly viscous response, whereas at pH 5 they show a more elastic strain stiffening response (indicated by the increased slope of the stress at higher strain). This strain stiffening persists in the MAOS regime until 100% strain deformation. In line with Fig. 6.7, it shows that PPIp has a higher stretchability at pH 5, compared with pH 7, and here we also see a strain stiffening response at medium amplitude. A similar observation is seen in the viscous Lissajous plots (bottom row for PPIp), where the Lissajous plots representing the gels at pH 5, remain wider over the MAOS strain amplitude range. In the right panels of Fig. 6.8 the elastic and viscous Lissajous plots for PPId gels and emulsion-filled gels (10 wt. % oil) are shown. It can be observed that the non-linear response in the MAOS regime is much more similar at pH 5 and 7, compared with PPIp gels. Even though the gel stiffness of PPId gels decreased at pH 5, the nonlinear response remained quite similar. At 100% strain the Lissajous plots representing the gels at pH 5 become wider, indicating a more viscous response. This is consistent with Fig. 6.7, where the energy dissipation ratio increased at a somewhat lower strain. At a strain of 50% the gels at pH 5 and 7 still behaved nearly identical with a strain stiffening response, indicated by the increase in stress near maximum strain. Also, the response in the viscous Lissajous plots were similar between pH 5 and 7, with a transition to a rhomboidal shape at 50% strain amplitude and a narrower more sigmoidal-shaped curve at 100% strain amplitude. The overall narrowing indicates a transition towards a more viscous response, and the sigmoidal shape seen at larger strain is indicative of strain-thinning behaviour. A similar transition from predominantly elastic to viscous behaviour was seen for gels from high concentrations of debranched starch [163].

In conclusion, it appeared that PPId gels are more ductile and less influenced by pH, in their response to large deformation compared with PPIp gels. Gels and emulsion-filled gels from PPIp showed a higher deformability at pH 5 compared with pH 7. These results again show that plant protein isolates from the same protein source can display different functional behaviour, depending on the method of fractionation.

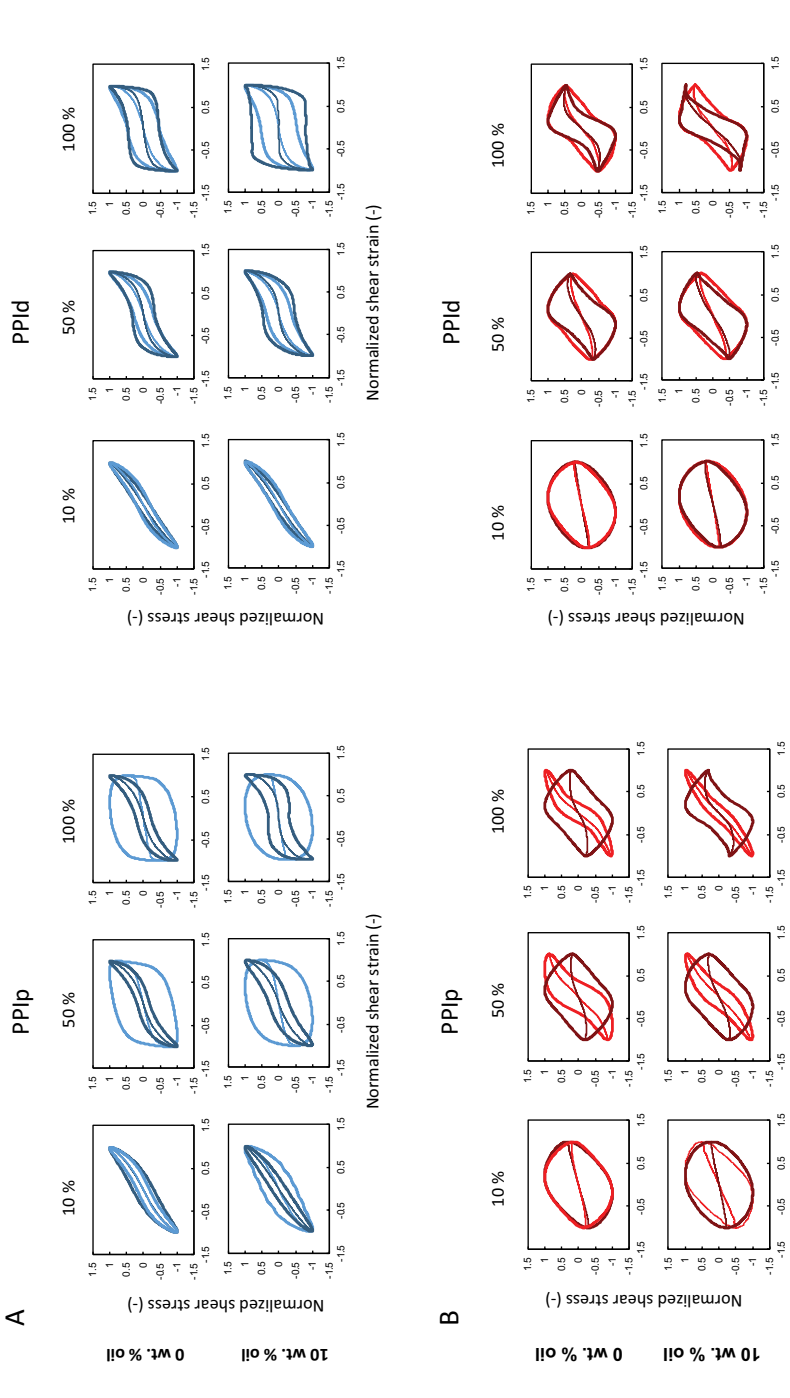

Figure 6.8 A. Elastic Lissajous plots of stress versus strain for PPIp (precipitated) and PPId (diafiltrated) gels without oil (15 wt. % PPI) and with oil (15 wt. % PPI, 10 wt. % oil) at pH 5 (—) and 7 (—) and B. viscous Lissajous plots of stress versus strain rate at pH 5 (—) and 7 (—). The response at 10, 50 and 100% strain deformation are shown. The strain, stress and strain rate axis values are normalized (min-max normalization).

Microstructure of emulsion-filled gels

Microscopic analysis of the gels can provide further visual information on the microstructure to support and explain rheological behaviour. Therefore, multi photon microscopy was employed to visualize the microstructure of gels and the EFGs. Fig. 6.9 shows confocal images of PPIp and PPId matrices and EFG with 10 wt% oil after heating at both pH 7 and pH 5. The figure also shows 3D construct of the matrix of all four samples. The green fluorescence represents proteins, and the red fluorescence represents oil droplets.

The images of PPIp at pH 7 (1st row) shows a patchy distribution of protein aggregates (green). The 3D image of the matrix also indicates that the protein network is highly heterogeneous and constituted of protein aggregates with a wide range of sizes. In PPId at pH 7 (2nd row), the protein network is more homogenous on a microscale and is void of large protein aggregates. The 3D image of the matrix also indicates that PPId forms a more cohesive homogeneous network, in stark contrast to PPIp at pH 7. This is also reflected in the rheology of the matrix, which shows that PPId (G': ~5000 Pa) forms a firmer gel compared to PPIp (G': ~500 Pa). Addition of oil droplets in both PPIp and PPId matrix (EFGs) does not change the microstructure compared to the matrix. The oil droplets also do not seem to be incorporated within the protein network, as the protein concentration at the oil droplet interface does not appear higher than in the matrix. The microstructural analysis in combination with the negligible effect on G' upon addition of oil (Fig 6.5) indicates that the oil droplets, simply act as inert fillers. The image of the PPIp matrix at pH 5 (3rd row) indicates that the protein network is still constituted of a heterogeneous protein network. This microstructure is more evident in the 3D image of the matrix. The microstructure protein aggregates seem smaller and more homogeneous than at pH 7. This is also related to the higher G' values of PPIp at pH 5, compared with PPIp at pH 7. Moreover, the gel at pH 5 remains predominantly elastic for much larger strains (~100%) compared to pH 7 (~10%). On the other hand, in PPId at pH 5 (4th row), the microstructure was much different from PPId at pH 7. The PPId matrix formed a more aggregated protein network as opposed to a homogenous, cohesive network, which may explain the lower G' values at pH 5. The EFG images of PPIp at pH 5 indicate that the oil droplets were distributed evenly throughout the protein network. This means that the oil droplets evenly occupied the interstitial space between the protein network on microscale, which could be related to the slight G' increase at higher oil concentrations seen for PPIp EFGs at pH 5 (Fig. 6.6). In PPId at pH 5, addition of oil (EFGs), did not contribute to an increase in EFG firmness. The

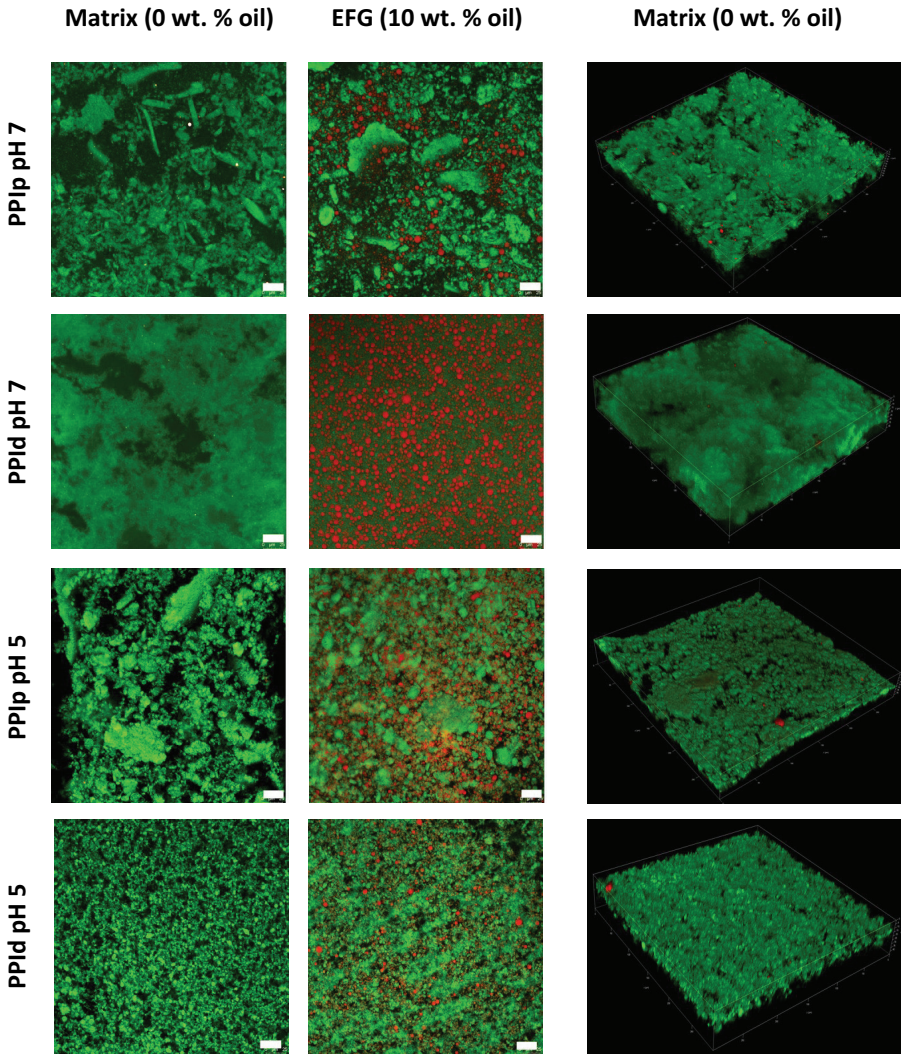

Figure 6.9 Multi photon microscope images of PPIp (precipitated) and PPId (diafiltrated) gels without oil (15 wt. % PPI) and gels with oil (15 wt. % PPI, 10 wt. % oil) at pH 7 and pH 5 with Nile Red for the oil (red) and Fast Green for proteins (green).

oil droplets do not seem to be incorporated into the protein network, so they could also be considered inert fillers.

Overall, pea protein EFGs show different microstructural and rheological characteristics. At pH 7, PPId clearly formed more ductile and cohesive protein gels and EFGs compared with PPIp. In both cases, the incorporation of oil droplets (EFGs), did not reinforce the protein matrix. At pH 5, both PPIp and PPId formed gels and EFGs with similar firmness. So, for PPIp, the gels became firmer at pH 5 compared with pH 7 and for PPId, the gels became slightly softer at pH 5 compared with pH 7. The difference in microstructure and rheological behaviour between the two PPIs stems from the different fractionation routes used to obtain them. PPIp is fractionated using isoelectric precipitation, which caused some proteins to undergo irreversible aggregation. At pH 7, these process-induced aggregates further grow upon heating to form patchy, softer PPIp EFGs. In PPId, the proteins are not subjected to aggregation during fractionation, leading to more soluble proteins. The more soluble proteins in PPId forms a cohesive network upon heating. Such a cohesive network leads to a more homogeneous distribution of oil droplets and to the formation of firmer gels and EFGs.

6.4 Conclusion

In this study we compared two pea protein isolates that were obtained using different fractionation routes: one fractionated by isoelectric precipitation (PPIp) and the other by diafiltration (PPId). Despite of a different gelling behaviour, it appeared that both pea protein isolates behaved rather similar in terms of emulsifying behaviour and interfacial properties. When these emulsions were used to form emulsion-filled gels (EFGs), differences in gelling behaviour were seen, that could be largely attributed to the different fractionation routes. Although both pea protein isolates could form emulsion-filled gels at pH 5 and 7, it appeared that diafiltrated pea protein isolate formed firmer gels and emulsion-filled gels than isoelectric precipitated pea protein isolate. Lowering the pH to 5 however, was beneficial for PPIp in terms of emulsion-filled gel firmness, whereas this was not the case for PPId. Moreover, oil did not play an active role in terms of gel reinforcement for any of the EFGs. This indicates a weak protein-protein interaction between the oil droplets and the pea protein matrix, as we also observed weak in-plane interactions at the interface.

The observation that pea protein isolates can form emulsion-filled gels could be relevant for food applications, such as plant-based cheeses and meat analogues. Our observations also reiterate the importance of processing routes when using plant proteins for such applications. For instance, from our observations, it was found that PPId form firmer gels at pH 7, also in the presence of oil droplets (EFGs) compared to PPIp. However, if the application desires to produce EFGs at pH 5, PPIp or PPId form almost equally firm gels, especially in the presence of oil droplets. Therefore, we show that the fractionation process plays a significant role in the microstructure and gel formed when using pea proteins, and that such effect is also pH dependent. The insights from this study may contribute to the design of pea protein fractionation routes that are tailored to the food product conditions and the type of gel envisioned.

Chapter 7

Substitution of whey protein by pea protein is facilitated by specific fractionation routes

Abstract

In this study we investigated the effect of different aqueous fractionation processes on the suitability of pea protein isolates (PPI) to substitute whey protein isolate (WPI) in heat-set gels. We found that a milder fractionation process based on diafiltration was successful in substituting WPI, yielding similar gel strength (i.e. elastic modulus) at a range of concentrations. Three different pea protein isolates were analysed, one obtained using diafiltration (PPId), another obtained using isoelectric precipitation (PPIp), and a commercial one (PPIc) as a reference. The isolates PPIp and PPId contained mainly native proteins, whereas the proteins in PPIc were denatured. PPId had a protein solubility almost similar to that of WPI at pH 7, while PPIp and PPIc were less soluble. PPIp and PPIc had better thickening capacities, larger aggregate/particle sizes and higher viscosities compared to PPId. After heat-induced gelation all PPI's showed similar or higher gel strength than WPI between a 7 - 13 wt. % protein concentration. Between 13 - 15 wt. % PPId showed a similar gel strength compared to WPI. Above 15 wt. % WPI formed the firmest gels. It was concluded that PPId can fully replace WPI up to protein concentrations of 15 wt. %. For mixtures of WPI with the other PPI's, it turned out that up to half of the WPI could be replaced by any of the PPI's without compromising on gel strength. This makes us conclude that PPI is a suitable substitute for WPI in heat-set gels.

This chapter is published as:

Kornet, R., Shek, C., Venema, P., van der Goot, A. J., Meinders, M., & van der Linden, E. (2021). Substitution of whey protein by pea protein is facilitated by specific fractionation routes. Food Hydrocolloids, 117, 106691.

7.1 Introduction

Regarding the ongoing transition from dairy to plant proteins, different scientific fields and technological routes are currently explored. One route is to completely exchange dairy proteins by plant proteins. Another route is a partial replacement of dairy proteins by plant proteins, resulting in hybrid food products. The latter approach might put less constraints on the plant protein functionality, amongst others, due to the fact that synergistic functional effects can occur in such systems [190, 195, 223, 224].

The potential of exchanging dairy by plant proteins depends on the functionality of the proteins. Different studies showed that mild or limited fractionation can not only yield proteins with at least similar properties than those extensively fractionated [58, 90], but also require less resources [149]. Another study found that varying the processing pH in soy protein fractionation processes can alter functional properties such as protein solubility, water holding capacity, and viscosity [201]. For pea protein it was found that protein purification was unnecessary to achieve stable oil-in-water emulsions, as pea flour was able to stabilize oil-in-water emulsions equally well as pea protein concentrate [147]. In addition, it was found that the extent of aqueous fractionation determines the viscosity, solubility and gelling behaviour of the resulting protein-enriched ingredients. We found in Chapter 2 that pea proteins obtained through isoelectric precipitation can lead to substantially thickening of the dispersion, compared to for instance whey protein. By estimating the volume to mass ratio, it was concluded that pea proteins are, at least partially, present as aggregates with a rarefied structure. Limited fractionation of pea was also found to yield pea protein concentrates with better gelling ability, compared to extensively fractionated pea protein isolate (Chapter 4). It is therefore suggested that pea can be used to derive plant protein isolates with similar functionalities as dairy proteins, making pea protein isolates suitable for replacement of dairy proteins, provided that the fractionation process is optimised for that purpose.

Generally, whey proteins form firmer gels than plant proteins, including pea protein [79]. In case a firm gel is required, partial replacement of whey protein could be an approach. As such, understanding the synergistic or antagonistic effects in these plant dairy protein mixtures is relevant. Hence, there have been a number of studies that focusses on substituting an animal-derived protein, such as whey protein or casein, by a plant-derived protein. It has been reported that blending whey protein isolate (WPI) with soy protein isolate (SPI) and wheat gluten increased

the viscosity of WPI [225], which could be beneficial when aiming for a thickening effect in beverages. For mixtures of micellar casein with soy protein in a 1:1 ratio, it was found that rheological behaviour (i.e. viscosity as function of temperature), was closer to soy than to casein [226]. A contrasting result was observed for heat-set gels from WPI – SPI blends, where WPI seemed to dictate the gel strength. Even so, the gel strengths generally reduced with an increased portion of soy protein [195, 196] and also phase inversion has been reported [227]. Rheological gelling behaviour could also be influenced by homogenizing certain components, prior to gelation [228], or by varying the gelling technique, such as sequential gelling of mixed systems [229] or acid-induced gelation [230, 231].

Only a limited number of studies reported the heat-induced gelling behaviour or co-aggregation of mixtures from pea protein with whey protein. Previous research on salt-extracted pea and whey protein mixtures showed an increase in the elastic modulus, hardness, and minimum gelling concentration at a pea / whey ratio of 2:8 in heat-set gels, relative to pure whey protein systems. Limited enhancement was seen at pH 4 and 8, but significant synergistic enhancement was seen at pH 6 [79]. Another study on heat-induced aggregation of whey and soy protein mixtures concluded that these proteins could interact, and that the ratio of soy to WPI had major impact on the type of network that was formed [232]. Co-aggregation was also seen for β-lactoglobulin and pea globulins mixtures, where β-lactoglobulin seemed to dominate the sizes and molecular weights of the aggregates [233].

In this study we use yellow pea as a model system to investigate how fractionation can facilitate the substitution of whey protein by plant protein. Three pea protein isolates are compared: one fractionated using diafiltration, another fractionated using isoelectric precipitation and a commercial pea protein isolate as a reference. The functionalities of these pea protein isolates are examined and compared to whey protein isolate. In addition, mixtures of the pea protein isolates with whey protein are studied.

7.2 Materials and methods

7.2.1 Materials

Yellow pea seeds were obtained from Alimex Europe BV (Sint Kruis, The Netherlands). WPI (BiPro, Davisco, Switzerland) and PPIc (NUTRALYS, s85 F, Roquette, France) were used as received. All chemicals and reagents were obtained from Merck (Darmstadt, Germany) and were of analytical grade.

7.2.2 Yellow pea fractionation processes

Three different pea protein isolates were used in this research and two of them were produced in the laboratory. One protein isolate is obtained using protein precipitation (PPIp), another is purified using diafiltration (PPId) and a commercial pea protein isolate (PPIc) was used as a reference.

PPIp was obtained by a process earlier described in Chapter 2, and here denoted as process 1. In short, 10% (w/v) pea flour was dispersed in deionized water and the pH was adjusted to 8 by adding NaOH. The dispersion was stirred for 2 h and centrifuged at 10000g for 30 min to remove solids (i.e. starch granules, cell wall material). The resulting supernatant was exposed to a protein isoelectric precipitation step, where the solution was brought to pH 4.5 and centrifuged again (10000g, 30 min). The protein-rich pellet was re-dispersed at pH 7 for 2 h and freeze-dried afterwards.

PPId was produced using an alternative fractionation process, denoted as process 2, and earlier described in Chapter 6. In short, pea flour was dispersed in deionized water for 2 h, with the pH left unadjusted (~pH 6.7). Then the dispersion was centrifuged at 10000g for 30 min and the supernatant was collected and further fractionated by ultrafiltration and diafiltration (5 kDa membrane). After diafiltration the concentrated retentate was collected and freeze-dried.

All fractionation steps were conducted at room temperature and the obtained protein-enriched solutions were frozen and freeze-dried. Dried protein isolates were stored at -18 °C. The ash content was determined by heating weighted samples to 550 °C in a furnace and weighing the ash afterwards. The protein content was calculated from the nitrogen content, measured with a Flash EA 1112 series Dumas (Interscience, Breda, The Netherlands). Nitrogen conversion factors of 5.7 for PPI and 6.38 for WPI were used. The protein recovery was defined as the recovered amount of protein in the protein isolate divided over the initial amount of protein in the flour. All subsequent measurements with the pea protein isolates were performed

after re-dispersing the samples in deionized water and adjusting the pH to 7 by addition of NaOH or HCl, unless stated otherwise.

7.2.3 Solubility

The solubility of the different protein isolates in deionized water at pH 7 was determined by centrifugation. Dispersions of 2 wt. % protein isolate were prepared and stirred for 2 h, after which they were centrifuged at 15000g for 30 min. The obtained supernatants and pellets were freeze-dried. The dry matter solubility is expressed as the mass of solids in the supernatant divided by the initial mass of solids. The protein solubility was determined by dividing the mass of proteins in the supernatant over the initial mass of the solids in solution.

7.2.4 Size exclusion chromatography (SEC)

The protein composition of the pea protein isolates was determined with an Akta Pure 25 chromatography system (GE Healthcare, Diegem, Belgium) coupled to an UV detector. First a McIlvaine buffer was prepared with 10 mM citric acid, 20 mM Na2HPO4 and 150 mM NaCl, adjusted to pH 7 and filtered over 0.45 µm. Samples were prepared by dissolving 10 g protein / L in the McIlvaine buffer and centrifuged at maximum speed for 10 min. The supernatants were transferred to HPLC vials. The samples were eluted on a Superdex 200 increase 10/300 GL column (Merck, Schnelldorf, Germany) with a range of 10 – 600 kDa and the McIlvaine buffer as eluent. Proteins were detected at an UV wavelength of 280 nm. For identification of the proteins based on their molecular weight, a calibration curve was prepared with molecules of known molecular weights: Aldolase, Blue Dextran, Carbonic Anhydrase, Conalbumin, Ferritin, Ovalbumin and Ribonuclease.

7.2.5 SDS-PAGE

The protein composition of the different protein isolates was determined by SDS-PAGE. Gel electrophoresis was performed using a 4 – 12% Bis Tris gel with a MES SDS running buffer. First, the samples were prepared by dissolving 0.1 wt. % protein isolate in deionized water. For non-reducing conditions, 45 µl running buffer was added to 15 µl sample solution. For reducing conditions, 6 µl running buffer was replaced by 6 µl of a 500 mM dithiothreitol (DTT) solution. The Eppendorf tubes with solutions were vortexed and centrifuged afterwards for 5 min (Hermle Z306, 4500 rpm). The solutions, either with or without DTT, were heated to 70 °C for 10 min and allowed to cool down to room temperature afterwards. Then, 15 µl of the supernatants were loaded in each well. A marker of 2.5 – 200 kDa was loaded in a

well at both sides of the gel. Electrophoresis was performed in a Xcell Surelock Mini-Cell for 35 min at a constant voltage of 200 V. Subsequently, the gels were stained with SimplyBlue SafeStain and washed with a 20% NaCl solution afterwards. The stained gels were scanned with a Bio-Rad GS900 gel scanner the next day.

7.2.6 Mineral composition

The mineral composition of the different protein isolates were analysed by the Chemical Biological Soil Laboratory (CBLB) of Wageningen University in The Netherlands. The freeze-dried protein isolates were first heated in a microwave in the presence of HNO_3 and concentrated HCl to destruct organic compounds. Then H_2O_2 was added and the samples were heated again to remove nitrous fumes. Subsequently, the elements in the samples could be detected and quantified by Inductively Coupled Plasa Atomic Emission Spectroscopy (ICP-AES) with a Thermo iCAP-6500 DV (Thermo Fischer Scientific, Cambridgeshire, United Kingdom).

7.2.7 Differential scanning calorimetry (DSC)

The denaturation temperatures of the different protein isolates were determined using DSC. Around 30 – 40 mg of 10 wt. % protein solutions in deionized water, adjusted to pH 7, were transferred to high volume pans. The samples were measured with a TA Q200 Differential Scanning Calorimeter (TA Instruments, Etten-Leur, The Netherlands) upon heating from 20 to 120 °C with incrementing temperature of 5 °C/min. All samples were measured in triplicate and subsequent data processing was done with TA Universal Analysis software.

7.2.8 Viscosity

After dispersing the protein isolates in deionized water and adjusted the pH to 7 with 1M NaOH and HCl, the viscosity of the protein solutions was measured with an MCR302 Rheometer (Anton Paar, Graz, Austria) combined with a sand-blasted CC-17 concentric cylinder geometry. The shear viscosity was measured as a function of shear rate varying from 0.1 to 1000 s^{-1} at 20 °C. A shear rate of 54.2 s^{-1} was selected for comparison of viscosities, as this was the minimum shear rate where all viscosities could be measured reliably. All samples were measured in duplicate.

7.2.9 Particle size analysis

Samples were prepared by dispersing 0.1 wt. % of the protein isolates in deionized water and the pH was adjusted to 7 using 0.1 M NaOH or HCL. The samples were measured with a Zetasizer Ultra (Malvern, Worcestershire, United Kingdom)

at 25 °C, using dynamic light scattering (DLS). The volume-based particle size distributions were obtained from the ZS Explorer software. All samples were measured in duplicate.

7.2.10 Small amplitude oscillatory shear (SAOS)

Gelation of the protein isolates, dispersed in deionized water and adjusted to pH 7, was induced by applying a temperature sweep with an MCR302 rheometer (Anton Paar, Graz, Austria). The sample was transferred to a CC-17 concentric cylinder that was sand-blasted, to prevent wall slip. With this measure taken, no sign of wall slip was observed. Solvent evaporation upon heating was prevented by placing a solvent trap on top of the outer cylinder. During the temperature sweep the samples were heated from 20 to 95 °C at a rate of 3 °C/min. The samples were kept at 95 °C for 10 min and cooled back to 20 °C with a same rate. Finally, the sample was kept at 20 °C for 5 min to verify that there was no further gel maturation. The viscoelastic response to an oscillatory imposed stress at a frequency of 1 Hz and a strain of 1% was recorded. In addition, strain sweeps were applied to confirm that the linear viscoelastic regime was not exceeded by the 1% strain applied during the temperature sweep. To study the effect of disulphide bonding by the use of a thiol-blocking agent, deionized water was replaced by a 20 mM N-Ethylmaleimide (NEM) solution, and the pH was also adjusted to 7. All samples were measured in duplicate.

The rheological parameters used in this study to describe the gels are the storage modulus (G'), loss modulus (G") and the loss factor tan δ (G"/G'). G' and G" represent the elastic and viscous portion of the viscoelastic behaviour and tan δ described the ratio of these two portions. A material can be considered a solid when tan $\delta < 1$ and a strong solid when tan $\delta \ll 1$.

7.2.11 Covalent labelling of WPI

WPI was covalently labelled with fluorescein isothiocyanate (FITC) based on a method described earlier [140]. First a WPI solution of 1 wt. % in 0.1 M carbonate buffer (pH 9) was prepared. Then another solution of 0.4% (w/v) FITC solution in DMSO was made. Subsequently, 50 µl of the FITC solution per mL of WPI solution was slowly added upon gentle stirring. The sample was incubated in the dark for 6h and after incubation the WPI solution was dialysed using dialyses membranes with 12 – 14 kDa pore size. Dialysis was performed in the dark at 4 °C for ~72h and water was refreshed once a day. The solution was then freeze-dried and the powder was stored in the dark at -18 °C. The labelled WPI is further referred to as WPI-FITC.

7.2.12 Confocal laser scanning microscopy (CLSM)

Protein solutions were prepared by dissolving 15 wt. % protein isolate and the pH was adjusted to 7 with 1 M HCl or NaOH. The proteins in the single PPI and WPI solutions were labelled non-covalently to Rhodamin B using a final concentration of 0.0003% of the fluorescent dye. PPI was labelled in the same way for the combined systems with WPI. Subsequently, WPI was added to these solutions in final ratios of 1:3, 2:2 and 3:1, where 1 wt. % of the WPI was replaced by WPI-FITC. After 2h of solubilization the protein solutions were transferred to sealed glass chambers (Gene frame 65 µl adhesives, Thermo Fisher Scientific, United Kingdom) and heated in a water bath at 95 °C for 15 min and cooled back to room temperature afterwards. The microstructures were visualised using a Leica SP8X-SMD confocal microscope (Leica, Amsterdam, The Netherlands), coupled to a white light laser. A dry objective (10x, 0.40) and water immersion objectives (20x, 0.70 and 63x, 1.20) were used for magnification. For the PPI samples labelled to Rhodamin B, the laser excitation wavelength and the filter emission wavelength were 540 nm and 580 nm, respectively. For the combined samples imaging was performed in sequential mode. Rhodamin B was now excited at 561 nm and the emitted signal was detected between 570 and 790 nm. FITC was excited at 488 nm and the signal was acquired between 500 and 570 nm.

7.2.13 Statistical analysis

All measurements were conducted at least in duplicate. The mean values are shown and the standard deviations are given as a measure of error. Claims regarding significant effects were supported by a Welch's unequal variances t-test performed in R, applied on independent samples (i.e. at least two different PPI batches). Significance was concluded when $P < 0.05$.

7.3 Results and discussion

7.3.1 General characterization

Table 7.1 shows the protein content, protein recovery and solubility of the different protein isolates. The protein contents are from the protein isolate batches used in this study, whereas the recovery and solubility are averages of multiple extraction processes (n ≥ 2). In Chapter 2 it was found that the carbohydrate content of the protein isolates was typically below 4 wt. %, and were mainly present as small sugars. In most cases there is a trade-off between purity and recovery in plant protein extraction [9], but here PPId displays both a higher purity and a higher protein yield. The reason for a higher purity and yield of PPId is that both the globulins and albumins are retained. The protein composition of the PPI's will be discussed in more detail in the next section.

Table 7.1 Protein content, protein recovery, overall solubility and protein solubility of the protein isolates. Protein recovery is defined as the percentage of protein that was recovered in the PPI after fractionation. Dry matter and protein solubility are defined as the percentage of dry matter or protein that remained in the supernatant after centrifugation at pH 7. The recovery and solubility of PPIp and PPId are the averages of ≥2 fractionation processes. The numbers in superscript represent the standard deviations.

Sample	Protein content (wt. %)	Protein recovery (%)	Dry matter solubility (%)	Protein solubility (%)
PPIc	78.7 $^{\pm 1.0}$	-	32.2 $^{\pm 1.9}$	28.1 $^{\pm 1.3}$
PPIp	83.0 $^{\pm 0.7}$	52 $^{\pm 7.3}$	77.2 $^{\pm 8.8}$	79.4 $^{\pm 8.0}$
PPId	88.3 $^{\pm 3.3}$	63 $^{\pm 2.1}$	91.4 $^{\pm 4.0}$	94.0 $^{\pm 8.0}$
WPI	100 $^{\pm 1.0}$	-	100 $^{\pm 0.8}$	100 $^{\pm 0.8}$

Pea protein isolate compositions

The protein composition of the different pea protein isolates was studied by size exclusion chromatography (SEC). Pea contains two major groups of proteins, which are globulins and albumins. Globulins comprise legumin (11S), vicilin (7S) and convicilin (7-8S). The latter is highly homologous with vicilin, but contains an extended N terminus [36, 40, 69]. At pH 7 legumin is mainly present as a hexamer with a molecular weight of 320 – 380 kDa. These hexamers consist of six subunits that are non-covalently bound, with each subunit consisting of an acidic and basic subunit. At pH 7 Vicilin is mainly present as trimer of ~170 kDa and convicilin in its native form has a molecular weight of 280 - 290 kDa. The latter can be present as homo- or

heterotrimers with convicilins and vicilins [36, 108, 234]. Pea albumin (PA) comprises a group of proteins, including PA1, PA2, lectin, lipoxygenases and protease inhibitors [42]. PA1 and PA2 are most abundant and are commonly present as dimers. PA1 dimers are comprised of PA1a and PA1b and have a combined molecular weight of 10 kDa. PA2 can be subdivided in PA2a and PA2b and form homodimers with molecular weights of 53 kDa and 48 kDa respectively [44].

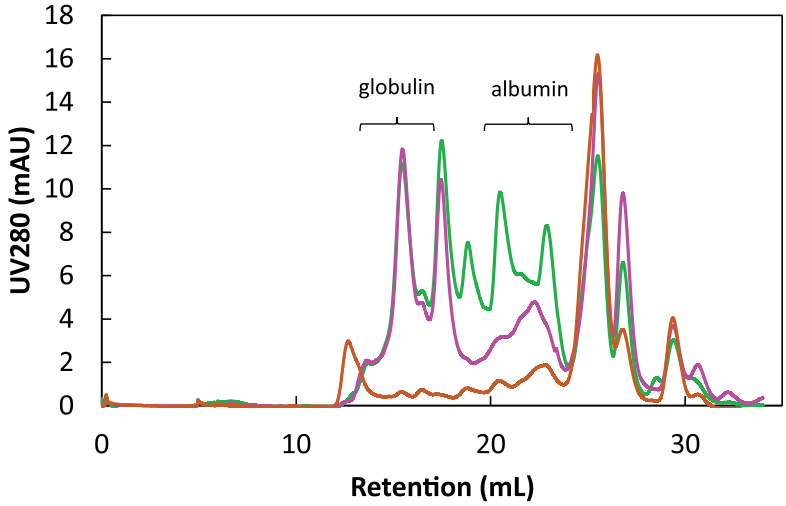

Figure 7.1 SEC chromatogram of PPIp (—), PPIc (—) and PPId (—) with UV detection at 280 nm as function of retention volume.

The two peaks in Fig. 7.1 that are denoted as albumins are only present in PPId and correspond to PA2 (left) and PA1 (right), with retention volumes of 20.5 and 22.9 mL respectively. These albumins are hydrophilic [174] and remain soluble upon isoelectric precipitation [172], which is why they are absent in PPIp and PPIc. The three globulin peaks correspond to legumin, convicilin and vicilin with retention volumes of 15.5, 16.5 and 17.6 mL respectively. They appear for PPId and PPIp, but not for PPIc. The latter only shows a peak at a lower retention volume of 12.7 mL, which corresponds to a molecular weight of ~2700 kDa. This single peak indicates that nearly all globulins in PPIc are aggregated. This is likely to be an underestimation, as larger aggregates were filtered out before bringing the samples on the column. This is in line with the SDS-PAGE profiles. Fig. 7.2A shows the gel where all non-covalent bonds are broken by the addition of SDS. Fig. 7.2B shows the gel where also

the disulphide bonds are broken by the addition of DTT. The presence of globulin bands in Fig. 7.2A indicate that aggregates observed in Fig. 7.1 are formed from non-covalently bound pea globulins. It has been reported that the legumin acidic subunit (40 kDa) and basic subunit (20 kDa) are covalently linked by one or more disulphide bonds [235]. This is also confirmed by the band at 60 kDa visible in Fig. 7.2A but not visible in Fig 7.2B, where disulphide bonds were broken by DTT. Fig. 7.2 also confirms the previous statement that PPId contains pea albumins, whereas PPIp and PPIc only contain globulins.

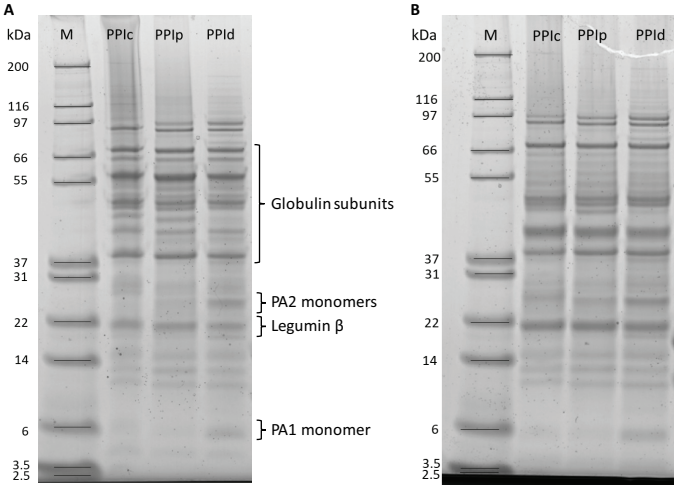

Figure 7.2 SDS-PAGE profiles of the pea protein isolates under non-reducing conditions (a) and reducing conditions (b). Lane M indicates the protein marker from 2.5 - 200 kDa. Identification of the bands is based on multiple studies [44, 54, 69, 235].

7

Mineral composition

The mineral composition of the protein isolates is shown in Table 7.2. It can be observed that PPId is particularly rich in the multivalent ions such as Ca^{2+}, Mg^{2+}, Mn^{2+} and Zn^{2+}. PPId is also high in the monovalent ion K^{+}, but substantially lower in Na^{+} compared to PPIc and PPIp. The high potassium content present in the pea seed is retained in process 2 and probably bound to phytate. K-phytate is readily water soluble and may be discarded in process 1 during the precipitation step [236, 237]. The higher phosphorus content origins from phytic acid, which serves as a phosphorus storage during seed dormancy [238]. Its ability to chelate divalent ions such as Ca^{2+}

and Mg^{2+} [237] can also explain the higher contents of these minerals in PPId, as phytic acid remains in process 2 and is discarded in process 1. The high sodium contents of PPIc and PPIp can be explained by the use of NaOH for pH adjustments in the precipitated isolates. The mineral composition of WPI is similar to what has been reported elsewhere [239].

Table 7.2 The total ash content and mineral composition (g / kg) of the pea seed and dried protein isolates.

Sample	Ash	Ca^{2+}	Cu^{+}	$Fe^{+2/+3}$	K^{+}	Mg^{+2}	Mn^{+2}	Na^{+}	P^{+3}	Zn^{+2}
Pea	33	0.62	0.01	0.06	10.4	1.07	0.01	0.01	4.53	0.04
PPIc	36	0.69	0.02	0.12	4.1	0.78	0.02	10.3	9.83	0.08
PPIp	46	0.44	0.01	0.22	2.2	0.41	0.02	16.4	14.9	0.04
PPId	59	2.09	0.04	0.24	14.4	4.25	0.06	1.37	18.6	0.11
WPI	12	0.88	0.00	0.00	0.4	0.06	0.00	6.31	0.61	0.00

Protein nativity

Differential scanning calorimetry (DSC) was conducted to determine whether the proteins were still native after processing. The resulting temperatures of denaturation onset and denaturation peak as well as the heat enthalpies are shown in Table 7.3. Protein denaturation of WPI starts at 63.6 °C (± 0.37) and the peak denaturation temperature is observed at 76.2 °C (± 0.02). A shoulder is visible (i.e. flatter slope followed by a steeper slope) in the denaturation peak, which is in line with what has been reported elsewhere [240]. The shoulder starting at 63 °C and the endotherm that is centred at around 75 °C can be assigned to denaturation of α-lactalbumin and β-lactoglobulin respectively [241]. PPIc does not show any endothermic peaks, suggesting complete denaturation. The fractionation conditions used to obtain PPIc are not known, but different studies reported that commercial pea protein isolate is generally denatured and display low solubilities [20, 61, 150]. Those observations are consistent with ours and is expected to be caused by harsh processing conditions (i.e. higher temperatures, pH changes, isoelectric precipitation). The lab-extracted PPIp and PPId still contain native protein, evidenced by clear denaturation peaks. The denaturation peaks shown for PPIp and PPId are rather similar. These single peaks comprise the thermal effects of both vicilin and legumin denaturation, based on literature in which it was reported that denaturation of those proteins occur at 71.8 °C and 87 °C respectively [40, 141]. The heat enthalpies for the protein denaturation in PPIp and PPId are quite similar, with 9.0 J / g (± 0.4) and 8.0 J / g (± 0.9), respectively.

It can be concluded that the precipitation and diafiltration processes yield proteins that are still native and show similar denaturation temperatures.

Table 7.3 Denaturation onset temperatures (T_{onset}), denaturation peak temperatures (T_d) and endothermic heat enthalpies (ΔH_d) of the protein isolates heated from 20 – 120 °C. The samples were measured in triplicate and standard deviations are shown in superscript.

Sample	T_{onset} (°C)	T_d (°C)	ΔH_d (J / g protein)
WPI	63.6 $^{\pm 0.37}$	76.2 $^{\pm 0.02}$	11.7 $^{\pm 0.6}$
PPId	70.5 $^{\pm 0.66}$	82.5 $^{\pm 0.13}$	8.0 $^{\pm 0.9}$
PPIp	73.0 $^{\pm 0.29}$	82.9 $^{\pm 0.11}$	9.0 $^{\pm 0.4}$
PPIc	None	None	None

7.3.2 Viscosity of the protein isolates

In this section we discuss the viscosities (at a shear rate of 54.2 s^{-1}) and particle size distributions of the protein isolates. The viscosity is a relevant functionality and can give an indication on the protein voluminosity or state of aggregation. Fig. 7.3A shows that PPIc has the highest viscosity per mass of protein, followed by PPIp, and the lowest viscosity is seen for PPId. Fractionation processes that include pH changes (i.e. solubilization at pH 8 and precipitation at pH 4.5) and higher temperature, expected to be applied to PPIc, enhance the viscosity. These higher viscosities for PPIc and PPIp are also consistent with the particle size distributions, shown in Fig. 7.3B. The aggregates observed in PPIc and PPIp comprise both soluble and insoluble aggregates, and are probably a result of isoelectric precipitation [60, 64]. Inherent to isoelectric precipitation is that protein-protein interactions are induced at a net charge of around zero. These interactions may be partially irreversible upon re-dispersion at neutral pH. Moreover, phytic acid present in pea could contribute to the formation of aggregates, as they can bind to proteins below pH 5 [27, 242]. Aggregates in PPIc and PPIp have a higher effective volume than single protein molecules. A higher volume leads to more friction and hence increases viscosity. Aggregates also explain the lower solubility of the isolates shown in Table 7.1. WPI and PPId contain fewer aggregates and are more soluble than PPIc and PPIp. In summary, fractionation processes in which pH and temperature are varied, yield protein isolates with lower solubilities, higher viscosities and larger protein aggregates. PPId that was obtained using diafiltration, shows a viscosity, solubility and particle size distribution most similar to WPI.

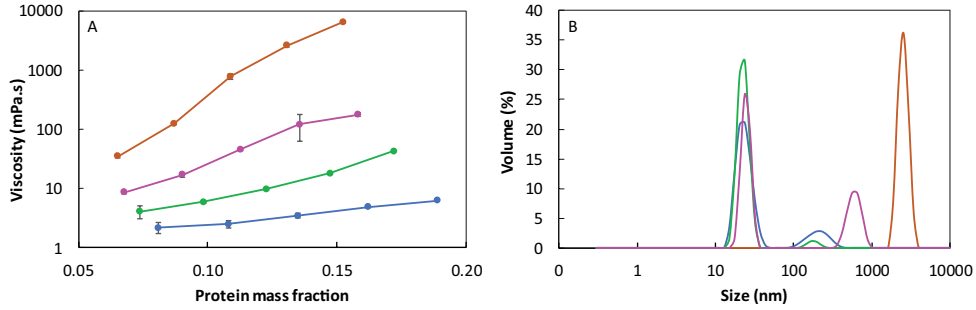

Figure 7.3 A. Viscosity as function of protein mass fraction and B. particle size distributions of WPI (—), PPIp (—), PPIc (—) and PPId (—) dispersions, measured at pH 7. Standard deviations are presented as error bars. The viscosity was measured at 52.4 s^{-1}; the minimum shear rate where all viscosities could be measured accurately.

7.3.3 Gelling behaviour of the protein isolates

Elastic moduli after heating

Fig. 7.4A shows that the elastic modulus (G') is higher for PPId than PPIp and PPIc in a protein concentration range of 7 to 17 wt.%. Even at protein concentrations of 11 wt. % PPIp, PPIc and PPId already behave as weak solid materials with loss factors (tan δ) of 0.325, 0.302 and 0.203 respectively. In Fig. 7.4A, WPI shows a strong increase in G' at a protein concentration of 11 wt. %, which identifies the gelling concentration at pH 7. Below this gelling concentration G' shows a steep increase with concentration. The concentration dependencies beyond the gelling concentration of WPI is rather similar to PPIp and PPIc, but the G' at the gelling concentration (13 wt. %) is much higher for WPI and is caused by an abrupt sol/gel transition (as shown later in Fig 7.6B). This is related to the type of network being formed. Gelling of WPI involves disulphide-mediated polymerization, which occurs when heating WPI above 85 °C at a pH between 3 and 7 [243]. For the pea protein isolate gels it is claimed that disulphide bonding does not play a major role [153]. We verified the role of disulphide bonding by using 20 mM of the thiol-blocking agent N-Ethylmaleimide (NEM). Fig. 7.4B shows the temperature sweeps with and without NEM for WPI and PPId. For WPI, preventing disulphide bonding results in a different viscoelastic behaviour during heating. During the first heating stage gelling is virtually absent and G' only starts to increase during the 10 minutes holding time at 95 °C and upon cooling. It appears that disulphide bonding affects the kinetics of gelation mostly, and to lesser extent the G' after heat treatment. PPId is less affected by the presence of a thiol blocking agent. The final G'-values are similar, although the gelation of PPId with

NEM starts slightly earlier compared to the PPId without NEM. PPIp with NEM showed the same trend as the one without (data not shown in Fig. 7.4B). The small difference between PPIp and PPId may be caused by the albumins present in the latter, as pea albumins are more abundant in sulphur groups than pea globulins [110]. In conclusion, disulphide bonding is a major contributor to the gelation of WPI at pH 7, whereas disulphide bonding does not play a major role for PPI gels, independent of the fractionation method applied.

The difference between the G' of PPId and PPIp was tested for significance at a concentration of 15 wt. %, by measuring the G' ($n \geq 4$) of PPI from multiple fractionation processes ($n \geq 2$). Process 1 and 2 yielded PPIp and PPId gels with significantly ($P < 0.05$) different G'. In Chapter 4 it was found that isoelectric precipitation reduces the capacity of pea protein to form firm gels, which is probably related to the formation of protein aggregates, as discussed before in section 7.3.1 and displayed in Fig. 7.3B. Protein aggregates are more abundantly present in PPIp and PPIc. Upon heating, these aggregates have less interaction sites per volume of protein compared to non-aggregated protein, which impairs the gelling capacity. PPId shows very limited aggregation and also forms gels with higher G' throughout the concentration range tested. How these differences are reflected in the microstructures is discussed in the next section.

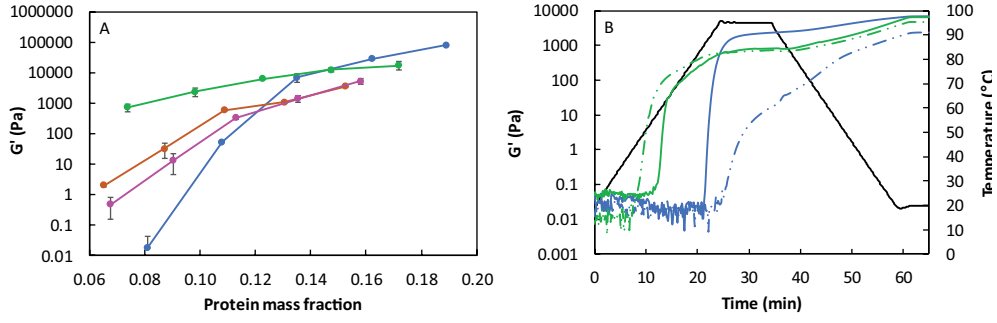

Figure 7.4 A. Elastic moduli (G') of the heat-set gels from WPI (—), PPIp (—), PPIc (—) and PPId (—), measured at 1% strain and 1 Hz, as function of protein mass fraction. B. Temperature sweeps of 15 wt. % WPI (—) and PPId (—) with (dashed line) and without (solid line) the thiol-blocking agent NEM. Samples were measured at least in duplicate and standard deviations are presented as error bars in 7.4A. Representative curves are shown in 7.4B.

Microstructure

The gels produced from 15 wt. % dry matter were further characterized by analysing their microstructures using confocal laser scanning microscopy (CLSM). Fig. 7.5 shows that the microstructure of the WPI gel is homogeneous, which is indicated by the lack of variation in contrast. It has been reported that whey protein, particularly β-lactoglobulin, forms gels after heating at pH > 6 and low salt content (~ 0.1%), due to the formation of long, fine strands [244]. Another study [245] showed that coarser gels are formed with increasing salt content. Fig. 7.5 shows a homogeneous WPI gel without any particles at microscale, which is related to the low salt content in the systems.

There are major differences in gel microstructures between the pea protein isolates. PPId form the most homogeneous gels at microscale. PPIp forms a more heterogenous gel with larger protein particles (5 – 10 μm) that contain higher quantities of protein than the surrounding, as indicated by the higher intensity of red. Even larger particles (10 - 100 μm) are seen for PPIc. These particles probably correspond to the largest PPIc particles of the size distribution shown in Fig. 7.3B. The heterogeneity and larger particles probably weaken the gelled systems of PPIp and PPIc, as the protein within these particles cannot actively contribute to a space-spanning network. This is consistent with their lower G' values, as discussed in section 7.3.3.

7.3.4 Gelling behaviour of pea and whey protein mixtures

Elastic moduli upon heating

WPI was combined with the three PPI's in ratios of 1:3, 2:2 and 3:1 and the gelation behaviour of those mixtures was studied. Fig. 7.6A-C show the temperature sweeps of mixtures with PPId, PPIp and PPIc (black dashed lines) as well as the single PPI and WPI systems (coloured lines). A few conclusions can be drawn with respect to the gelling behaviour of PPI-WPI mixtures. Firstly, Fig. 7.6A-C show that the final G' values of the 2:2 and 1:3 mixtures, represented by the black lines with longer intervals, are similar to the G' values of a pure WPI gel. For PPIc and PPId this is even true for the 3:1 ratio. This implies that at least half of the WPI can be replaced by any of the PPI's without compromising on the G' of the gel at the conditions studied (pH 7, 13 wt. % protein). This is also visualized in Fig. 7.6D, where the G' remains fairly constant for the combined systems with PPIc and PPId, where WPI is substituted up to 75%. It shows that pea protein isolate is a suitable substitute for whey protein isolate, as it can maintain the G' of WPI even when half or more is replaced.

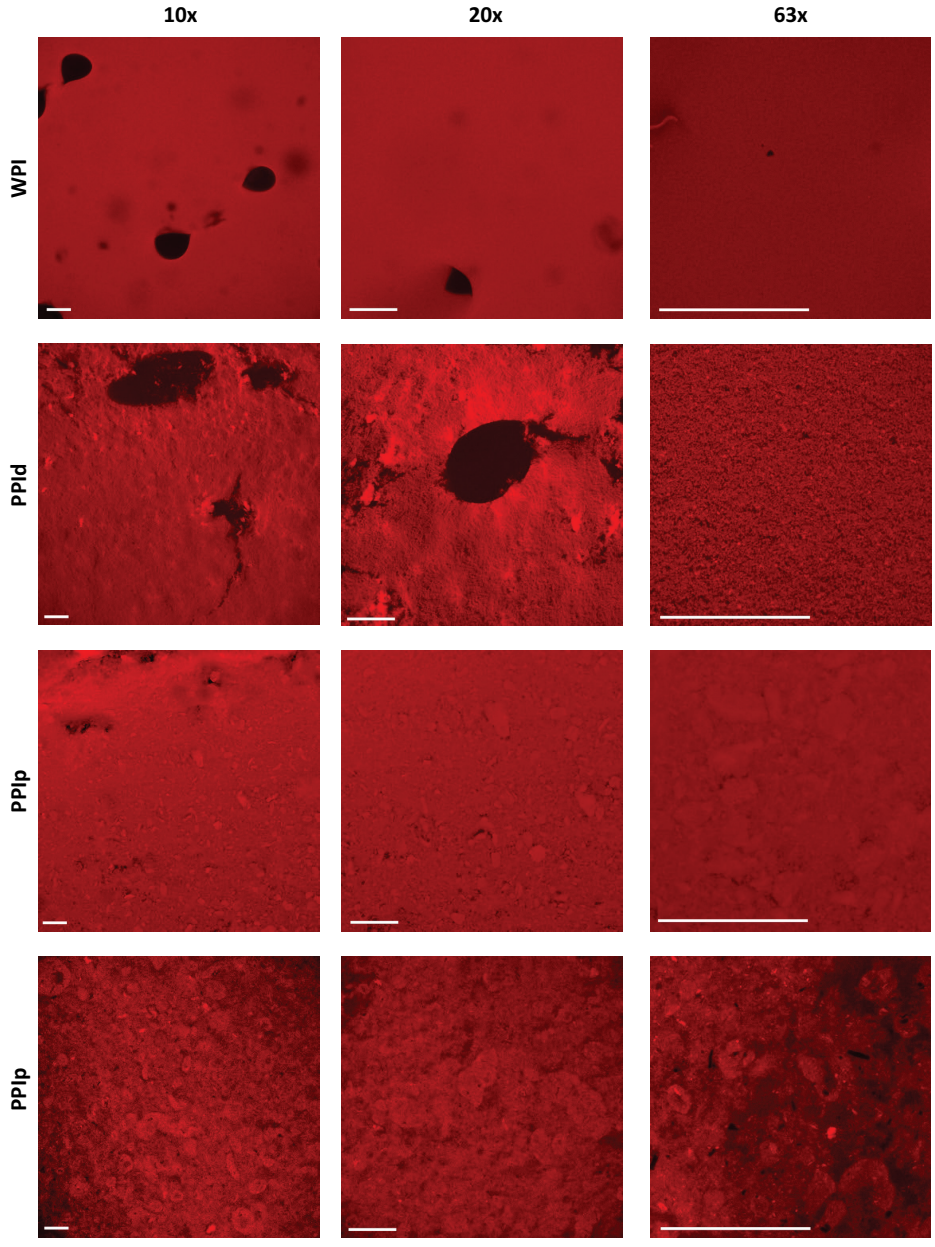

Figure 7.5 CLSM images visualizing the microstructures of heat-set gels from the protein isolates (15 wt. %, pH 7) at three magnifications, with protein shown in red. The white scale bar represents 100 μm.

Secondly, with increasing WPI concentrations the gelation onset moves from ~ 60 °C to 80 °C. As discussed in section 7.3.1, pea protein starts to denature around 72 °C with a peak at 83 °C, whereas WPI starts to denature at 64 °C and shows a peak at 76 °C. The gelation onset temperature is higher than the denaturation temperature. This indicates that denaturation of α-lactalbumin is not sufficient to induce gelation. Denaturation of β-lactoglobulin, starting at 75 °C [241], is required for WPI to form a gel. In case of PPI, reaching its denaturation onset temperature (~ 70 °C) is sufficient to increase the G'. The higher gelation onset temperature of WPI, relative to its lower denaturation temperature (Table 7.3), is also related to the neutral pH and low ionic strength [240]. The ionic strength is estimated to be around 60 mM, based on the mineral content shown in Table 7.2. This is likely to be an overestimation as not all minerals may be present as ions in solution (e.g. Ca^{2+} can be bound to α-lactalbumin). At 80 °C it is evident that disulphide bonding plays a major role in the sol/gel transition, as indicated by Fig. 7.4B. There the presence of a thiol-blocking agent inhibits this abrupt sol/gel transition. The observed gelation temperature for WPI is consistent with another study [243] where gelation of whey proteins was observed to start at 80 °C at pH 7. The authors claimed that this temperature was required to sufficiently unfold whey proteins and induce disulphide bonding and hydrophobic interactions, and ultimately form a gelled network. For the mixtures of PPI and WPI analysed in this study, it appears that the gelation onset of dispersions with WPI concentrations ≥ 50% is similar to that of 100% WPI. This implies that WPI aggregation, mediated by disulphide bonding and hydrophobic interactions, is essential for these combined proteins to form a gelled network. Thirdly, the initial G' before heating decreases with increasing WPI concentrations in the mixtures with PPIc and to lesser extent PPIp. For these protein isolates it was observed that the G' is higher than the G", even before heating (G" not shown here). This would indicate some kind of network already present. In mixtures with more WPI than PPI the pea protein aggregates are diluted to such extent that the G' before heating is as low as it is for pure WPI. When less than 50% of the protein is WPI, the pea proteins in PPIc and PPIp preserve the capacity to form some type of network that is able to store energy upon deformation.

Overall, the mixtures with different PPI's approach the rheological behaviour of pure WPI. This is true for any of the PPI's until 50% substitution and for PPId and PPIc even up to 75% substitution. Also the final gel strength (i.e. elastic modulus) of these mixtures is similar to that of a WPI gel. These findings make us conclude that PPI is a suitable substitute for WPI in heat-set gels.

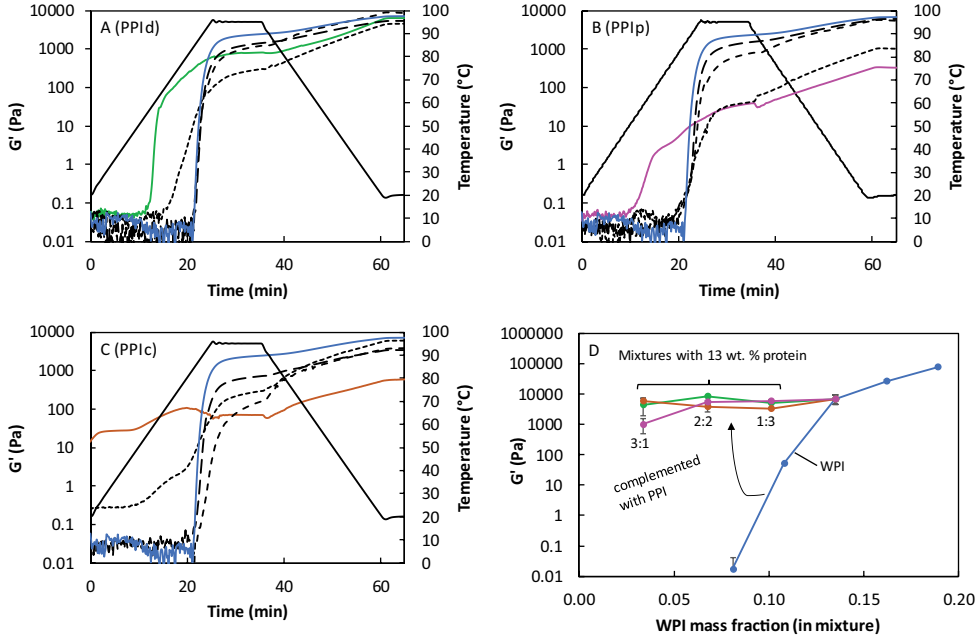

Figure 7.6 A-C. Temperature sweeps of 15 wt. % pea and whey protein mixtures at pH 7. The dashed line interval length is in incrementing order PPI : WPI (3:1, 2:2, 1:3) with WPI (—), PPIp (—), PPIc (—) and PPId (—). D. G′ of the gels as function of whey protein concentration in the mixtures with a total of 15 wt. % protein isolate, where the blue line represents the pure WPI gels. Samples were measured at least in duplicate and representative curves are shown (A-C) or standard deviations are shown with error bars (D).

Microstructure

Fig. 7.7 shows the microstructures of gels containing both PPI and WPI. The yellow to orange coloured regions represent PPI and the green regions represent WPI. Rhodamine B was used to label the pea protein, as it binds to hydrophobic patches of the protein [246, 247], and hence is expected to have higher affinity for pea than for whey protein due to its hydrophobic nature (Chapter 4). Colour intensities between pea and whey protein could vary between images and hence these images should not be used for any type of quantification. However, the images provide insight on the distribution of pea and whey proteins in the gel, where higher intensities of green correspond to regions with higher concentrations of WPI and higher intensities of red correspond with higher concentrations of PPI.

The mixtures of WPI with PPId form homogeneous gel structures at microscale,

which show great similarities with homogeneous structures obtained for gels containing only PPI or WPI. (Fig. 7.5). The mixtures with PPIp show micro-phase separation (Fig. 7.7), with clusters ranging from 5 μm (25% PPI) to 20 μm (75% PPI). These clusters have relatively high pea protein concentrations and are dispersed in a continuous matrix that is relatively low in pea protein. For PPIc-WPI mixtures, large clusters up to ~100 μm, high in pea protein concentration are seen. For these samples, it was noted that the gel was heterogeneous and that there were also regions with smaller clusters. The regions with smaller clusters looked similar to the case of PPIp and WPI mixtures with 75% WPI (Fig. 7.7).

Fig. 7.7 shows both proteins distributed on a micrometre scale. There are a few possibilities how these gels containing both PPI and WPI behave at nanoscale, explaining the gelation behaviour. In the mixtures with PPI, whey protein could form a continuous network with pea protein (aggregates) incorporated. A similar observation was made for mixed gels from soy and whey protein [196, 227] In those studies, it was concluded that whey protein formed the primary protein network with soy protein incorporated as particulate fillers. It is also possible that WPI interacts and co-aggregates with PPI. We hypothesize that this co-aggregation takes place when WPI is mixed with PPId, which contains mostly small protein molecules that are highly reactive at their gelation onset (Fig. 7.6A). For future research, it would be relevant to study the molecular interactions between whey and pea proteins to understand or even predict the gel network nano-structure of such plant-dairy protein gels. Furthermore, this research could be extended towards proteins from other pulses (e.g. chickpea, lupin, lentil), as there are resemblances between the proteins and their fractionation processes. Finally, our current research could inspire food producers to consider the history of fractionation processes that have led to a given protein fraction of plant based matter, in order to be able to tailor the replacement of animal protein ingredients by plant based protein ingredients, while at the same time ensuring minimal processing energy usage with a maximum of (multi-) functionality.

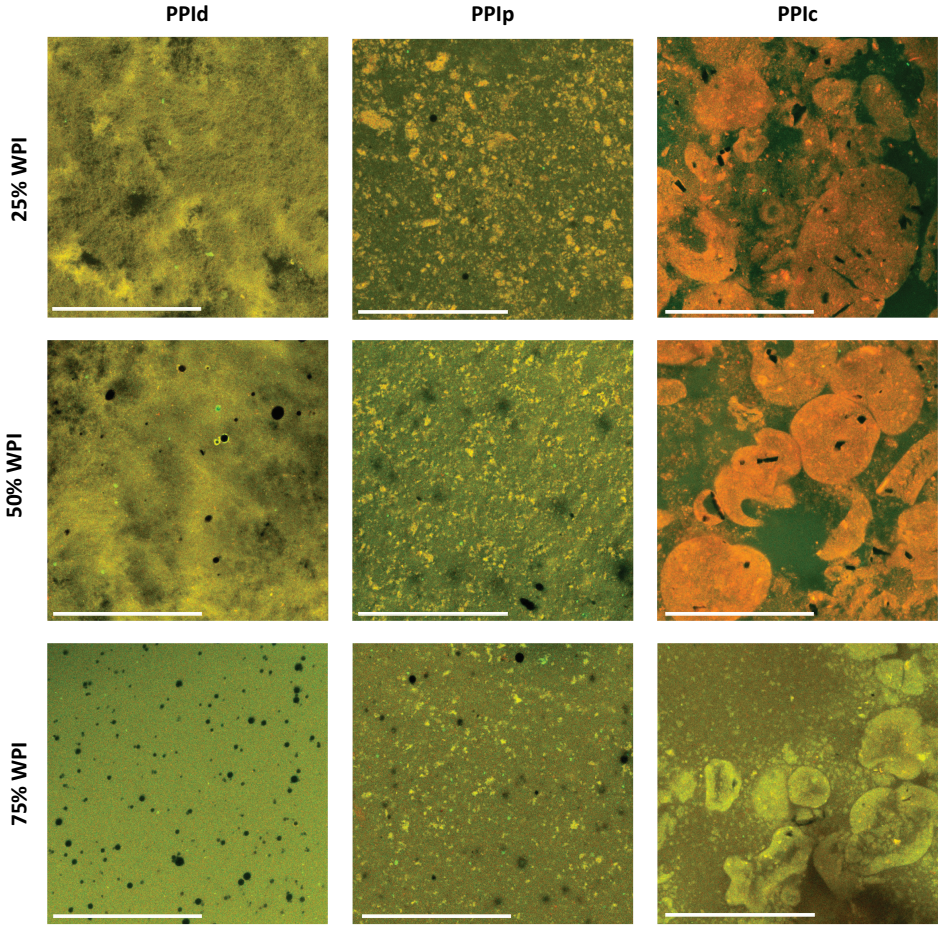

Figure 7.7 CLSM images visualizing the microstructures of the pea - whey protein mixtures at 63x magnification. PPI is visualized by higher intensities of red and WPI by higher intensities of green. The white scale bar represents 100 μm.

7.4 Conclusion

In this study we showed that pea protein fractionation processes have major impact on the functional bulk behaviour of pea proteins. Harsher processing (i.e. pH shifts, higher temperatures) yields protein isolates with lower solubility, higher viscosities and lower elastic moduli of the gels. In view of replacing whey (i.e. animal-based) proteins, one can optimize the protein fractionation process of plant based proteins by using diafiltration instead of precipitation. In the case of pea protein, this yields a plant protein isolate that approaches the functional behaviour of whey protein isolate. Diafiltrated pea protein isolate has comparable solubility and viscosity as whey protein isolate. In heat-set gels it actually can replace whey protein isolate in forming gels with similar strength. When it comes to partial replacement it is less crucial which type of fractionation process is used, as for different pea protein isolates WPI dominates the rheological behaviour at concentrations above 50% WPI.

Chapter 8

How pea fractions with different protein composition and purity can substitute WPI in heat-set gels

Abstract

In this study we explored the gelling behaviour of a pea protein concentrate (PPC), an albumin-fraction (ALB-F) and a globulin-rich fraction (GLB-RF), in comparison with and as substitute for whey protein isolate (WPI), by small oscillatory and large amplitude oscillatory shear (SAOS and LAOS) rheology. It was found that PPC formed the firmest gels (defined as highest elastic modulus), but this gel was not as firm as a pure WPI gel. ALB-F formed the softest gel due to its low protein purity. For a better view on the albumin gelling behaviour ALB-F was further diafiltrated and the albumin-enriched fraction was labelled ALB-RF. It turned out that albumins formed firmer gels per mass unit of protein than globulins. Also, the energy dissipation ratios – a measure for the plasticity of the gel – were determined as function of strain. The ALB-RF gel showed an increase in plastic response at larger strains compared to the GLB-RF gel (40% and 10% strain, respectively). ALB-F, PPC and GLB-RF were also examined on their ability to substitute WPI in heat-set gels. It was found that ALB-F / WPI mixtures formed firm gels and were least sensitive to changes in pH and ionic strength. It also appeared that disulphide bonding plays a more important role in the ALB-F / WPI mixtures upon heat-set gelation compared to the PPC / WPI and GLB-RF / WPI mixtures. The use of pea fractions as a substitute for WPI, particularly the ALB-F, could improve the resource efficiency of pea as an ingredient source.

This chapter is published as:

Kornet, R., Penris, S., Venema, P., van der Goot, A. J., Meinders, M. B., & van der Linden, E. (2021). How pea fractions with different protein composition and purity can substitute WPI in heat-set gels. Food Hydrocolloids, 120, 106891.

8.1 Introduction

Although dairy proteins are still widely applied in food products, plant proteins are becoming more prevalent in a variety of products, including milk-like beverages, yoghurts, cheeses, and meat analogues. The application of plant proteins in such products is facilitated by improved understanding of the differences in terms of functional behaviour (i.e. solubility, gel, emulsion, foam properties), particularly when aiming for substituting dairy proteins. In recent years numerous studies have been conducted on the physicochemical properties and functional behaviour of plant proteins, including pea protein [50, 53, 248-250]. Recently, the potential to replace whey proteins by pea protein fractions was studied. These studies revealed that whey proteins generally form firmer gels and more stable foams and emulsions compared with pea protein [50, 79]. The fact that full replacement of whey protein by pea protein leads to a different functional behaviour, explains the increased interested in partial substitution of whey protein isolate [190, 251, 252].

Pea proteins can be classified into globulins and albumins, with the former being more than 70% of the total protein content [73, 175]. The globulins can be classified into legumin, vicilin and convicilin, although the latter is sometimes considered part of the vicilin subgroup. At neutral pH, legumin is mostly present as a hexamer with a molecular weight of 320 – 380 kDa and vicilin and convicilin as trimers of 170 and 290 kDa, respectively [36, 108]. Compared with whey proteins, pea globulins are larger and more hydrophobic (Chapter 2 and 4). The other group of pea proteins are albumins. This is a collective name for a class of proteins, including PA1 and PA2 (two types of Pea Albumin), lectin and protease inhibitors [42]. Albumins are small and hydrophilic protein molecules, with molecular weights ranging between 4 and 26 kDa in their monomeric state [44, 174] and are rich in cysteine [253]. Studies on the gelling behaviour of pea albumins are scarce [32, 254] and studies on the heat-induced gelling behaviour of pea albumins are not available. Studies on pea globulins showed that they can form heat-induced and acid-induced gels, albeit that the resulting gels are weak [80, 255]. It was reported that heat-induced gelation is mainly driven by hydrophobic interactions and hydrogen bonding [153], and that disulphide bonding does not play a major role in pea protein gels [153].

The concept of enhancing functionality by (partially) substituting dairy proteins by plant proteins is not new. These studies cover a wide range of functionalities and mixtures, such as the flow behaviour of calcium caseinate and whey protein with wheat flour and soy protein isolate [225], gelling behaviour of whey protein with soy

protein [195, 196, 227] or less pure mixtures of soymilk and cow's milk [228]. However, most studies mentioned above make use of pea fractions with high protein purities (i.e. globulin protein isolates) as substitute for whey protein. The same was done in the previous chapter, where we showed that pea protein isolate could serve as a substitute for whey protein isolate by using specific fractionation routes . The advantage of such an approach is that the behaviour of the resulting mixtures is easier to understand and to predict. However, less pure fractions (that is, less processed) often have a lower environmental footprint [149, 171], and equal or even better functional properties [62, 90, 146].

In this study we therefore examined the ability of pea fractions – fractionated to different extents and with different purities – to substitute whey protein isolate in heat-set gels. The role of pH, ionic strength and disulphide bonding in these gelled mixtures was also studied. To better understand the contribution of pea proteins in these hybrid gels, we extensively characterized the rheological behaviour of individual pea albumin and globulin gels. The insights on the use of pure and less pure pea fractions as WPI substitutes could improve the resource efficiency of pea as an ingredient source.

8.2 Materials and methods

8.2.1 Materials

Yellow pea seeds (*Pisum Sativum* L.) were obtained from Alimex Europe BV (Sint Kruis, The Netherlands). BiPRO whey protein isolate was obtained from Davisco (Geneva, Switersland). All chemicals were obtained from Merck (Darmstadt, Germany) and were of analytical grade. N-Ethylmaleimide (NEM) had a purity of 98% or higher.

8.2.2 Pea fractionation process

An aqueous protein fractionation process was used to obtain a pea protein concentrate (PPC), an albumin fraction (ALB-F) and a globulin-rich fraction (GLB-RF). These labels are based on protein composition analysis originating from Chapter 2. Pea seeds were ground into flour with an average particle size of 80 μm. The flour was dispersed in deionized water (ratio 1:10) and the pH was adjusted to 8 with aliquots of a 1 M NaOH solution. After two hours of moderate stirring at room temperature the dispersion was centrifuged (10000g, 30 min, 20 °C) and the pellet was separated from the protein-enriched supernatant. Part of the supernatant was lyophilized and labelled as PPC (same as PPCa in other chapters). Further fractionation was conducted by precipitation of the pea globulins. The supernatant was brought to pH 4.5 with aliquots of a 1 M HCl solution and kept under moderate stirring at room temperature for two hours. The precipitated globulin fraction was separated from the albumins by centrifugation (10000g, 30 min, 20 °C). The supernatant was freeze dried and labelled as ALB-F. The pellet was redispersed at pH 7 for two hours, freeze dried and labelled as GLB-RF (same as PPIp in other chapters). A schematic overview of the full process is shown in Fig. 8.1.

An albumin-rich fraction (ALB-RF) was obtained by diafiltration, using the albumin-containing supernatant after isoelectric precipitation (ALB-F). The supernatant was diafiltrated at room temperature with a SartoJet Pump (Sartorius AG, Goettingen, Germany). A transmembrane pressure of around 1.7 bar was applied onto two 2 kDa Hydrosart membrane surfaces (Sartorius AG, Goettingen, Germany). The filtrate was discarded and the retentate was recirculated, while the decrease in filtrate conductivity was monitored. Filtration was stopped once the filtrate reached a conductivity of <50 μs / cm. Throughout the diafiltration process, water was added to the retentate, resulting in a diafiltration factor of 7.5. The collected retentate was freeze-dried and labelled ALB-RF.

The ash content was determined by weighing the remainder of the sample after overnight heating in a furnace at 550 °C. The protein content was calculated from the nitrogen content that was measured with a FLASH EA 1112 series Dumas (Interscience, Breda, The Netherlands), using a nitrogen conversion factor of 5.7. All protein contents were expressed on dry matter basis.

8.2.3 Mass balance

A mass balance was compiled from the protein content and protein recovery data multiple fractionation processes (n = 4). The total recovered mass was calculated for PPC, ALB-F and GLB-RF, using the mass balance equation (Eq. 8.1).

The mass balance reads:

$$x_{p,pf}\phi_{pf} = x_{p,p1}\phi_{p1} + x_{p,p2}\phi_{p2} + x_{p,s2}\phi_{s2} \tag{8.1}$$

Where x is the mass fraction (-) and ϕ the mass (g) with subscripts for protein (p), pea flour (pf), the pellet after first centrifugation (p1), the supernatant after first centrifugation (s1), the pellet after second centrifugation (p2) and the supernatant after the second centrifugation (s2).

The amount of total dry matter in the pea flour fraction is determined by:

$$m_{dm,pf} = \left(1 - x_{w,pf}\right)\phi_{pf} \tag{8.2}$$

The fraction (ζ) protein in the dry matter of the pea flour (purity) was obtained from:

$$\zeta_{p,pf} = \frac{m_{p,pf}}{m_{dm,pf}} = \frac{x_{p,pf}\phi_{pf}}{(1-x_{w,pf})\phi_{pf}} = \frac{x_{p,pf}}{(1-x_{w,pf})} \tag{8.3}$$

The recovered mass percentage of each fraction can be calculated using the equation below, where pea protein fraction (ppf) can be s1, p2 or s2.

$$dry\ matter\ recovery\ (\%) = \frac{\phi_{ppf}}{\phi_{pf}} * 100\% \tag{8.4}$$

The recovered mass of the first pellet (m_{p1}) was approximated by subtracting the mass of the first supernatant (m_{s1}) from the initial mass of pea flour (m_{pf}).

$$protein\ recovery\ (\%) = \frac{x_{p,ppf}\phi_{ppf}}{x_{p,pf}\phi_{pf}} * 100\% \quad (8.5)$$

The protein recovery in each fraction can be calculated using Eq. 8.5.

The total mass of each fraction was multiplied with the ash and carbohydrate content mass fractions to obtain the ash and carbohydrate content in the fraction. The protein content was measured for each batch (four times), the carbohydrate content was based on one batch, while ash content was determined of at least two batches. The results from carbohydrate analysis were reported in Chapter 2, and the method has been described there. Regardless of the number of batches, the compositional analyses themselves were always performed in duplicate or triplicate.

8.2.4 Conductivity measurements

The conductivity of the protein mixtures was measured with a CO 3000 L conductivity meter (VWR International, Leuven, Belgium) at 20 °C. The measured conductivities were used to calculate the ionic strengths – expressed as the equivalent of a NaCl molar concentration – using Eq. 8.6 [256].

$$Ionic\ strength\ (NaCl\ equiv\ M) = 1.02 \cdot 10^{-5} \cdot conductivity\ (\mu s.cm^{-1}) \quad (8.6)$$

8.2.5 Mineral composition

The samples were first heated in a microwave together with HNO_3 and concentrated HCl to destruct organic compounds. Subsequently, H_2O_2 was added and the samples were heated again to remove nitrous fumes. Calcium, copper, iron, potassium, magnesium, sodium, phosphor and zinc could now be detected and quantified by Inductively Coupled Plasa Atomic Emission Spectroscopy (ICP-AES) with a Thermo iCAP-6500 DV (Thermo Fischer Scientific, Cambridgeshire, United Kingdom). The chloride content was estimated by subtracting the total mineral mass from the ash content.

8.2.6 Sample preparation

The pea fractions were dispersed in deionized water in concentrations of 15 wt. % dry matter and the pH was adjusted to 3.8, 5.0 or 7.0 with aliquots of 1 M NaOH and 1 M HCl solutions. The initial ionic strength of the dispersions – calculated from the conductivities – was increased to 50 mM, 100 mM and 200 mM using NaCl. For determining the contribution of disulphide-bonding a 20 mM N-Ethylmaleimide

(NEM) solution was prepared as a solvent for the protein dispersion. After dispersing, the protein was solubilized under mild agitation at room temperature for two hours.

8.2.7 Small amplitude oscillatory shear (SAOS) rheology

The gelling behaviour of the dispersed pea fractions was studied by measuring their linear viscoelastic response upon heating and cooling with an MCR302 rheometer (Anton Paar, Graz, Austria). Such temperature sweeps can provide insight in the gelatinization behaviour of starch [257, 258] or the gelling behaviour of proteins [259, 260]. The rheometer was equipped with a sand-blasted CC-17 concentric cylinder geometry. To prevent solvent evaporation during heating, a solvent trap was placed on top of the cylinder. The dispersions were first heated to 95 °C, then kept at 95 °C for 10 min, and cooled with to 20 °C. Both the heating and cooling rate was 3 °C/min. The temperature was kept constant at 20 °C for another 5 min. The storage (G') and loss moduli (G") were recorded under constant oscillation at 1 Hz and 1% strain amplitude. After the temperature sweep, a frequency sweep was applied within the LVE (linear viscoelastic) regime at 1% strain deformation and a logarithmic increase from 0.01 – 10 Hz. Gel firmness was defined as the G' value after heat treatment.

8.2.8 Large amplitude oscillatory shear (LAOS) rheology

The non-linear rheological behaviour of the heat-set gels was studied by LAOS measurements, with oscillating strain at a frequency of 1 Hz and a temperature of 20 °C, and strain amplitude increasing logarithmically from 0.1% to 1000%. The end of the LVE regime was expressed as the critical strain, which was the strain amplitude at which the elastic modulus had decreased to 90% of its original plateau value.

The oscillating strain, stress and shear rate signals were recorded for each imposed sinusoidal strain amplitude. The resulting data was used to construct Lissajous plots. The elastic and viscous stress contributions were calculated using the Rheocompass Software (Anton Paar, Graz, Austria).

The area enclosed in a Lissajous curve is equivalent to the energy dissipated per unit volume during one oscillatory strain cycle. The ratio of dissipated energy over the energy dissipated by a perfect plastic material is termed the energy dissipation ratio [261]. This energy dissipation ratio (Φ) is calculated using Eq. 8.7 with the loss modulus (G") and the maximum stress (σ_{max}) at a given strain amplitude (γ_0) [209]. The energy dissipation ratio was plotted as a function of strain amplitude, to visualize the main information from the Lissajous curves in a compact manner.

$$\Phi = \frac{E_d}{(E_d)_{pp}} = \frac{\pi G_1^{"} \gamma_0}{4\sigma_{max}} \tag{8.7}$$

8.2.9 Statistical Analysis

All samples were prepared in duplicate and thereafter measured. The samples were prepared from one batch of pea fractions, and the mass balance was based on four batches. The mean values are shown and the standard deviations are given as a measure of error. In case of a range of datapoints with good reproducibility, a representative curve was selected. Claims regarding significant effects were supported by a Welch's unequal variances t-test performed in R, applied on independent samples. Significance was concluded when $P < 0.05$.

8.3 Results

8.3.1 Fractionation efficiency

Three pea fractions were produced by aqueous fractionation and exposed to different extents of fractionation (Fig. 8.1). The first fraction is a pea protein concentrate (PPC) as obtained via the supernatant after the first centrifugation step at pH 8. An additional centrifugation at pH 4.5 of PPC resulted in an albumin-fraction (ALB-F) in the supernatant and a globulin-rich fraction (GLB-RF) in the pellet. The efficiency of the fractionation processes is reflected in the protein recovery of the resulting fractions (Eq. 8.5). Limited fractionation yields PPC with a protein recovery of 74% (± 3.2%). The remaining 26% is lost in the pellet. Upon further fractionation – where albumins and globulins are separated – the combined protein recovery is 71% (19% for ALB-F and 52% for GLB-RF, with standard deviations of 1.5 and 7.3%, respectively). This shows that only 3% of the proteins are lost upon isoelectric precipitation. A schematic representation of the process is shown in Fig. 8.1. Also, a mass balance is included, which is based on the data from four batches.

The pea protein fractions used in this study were chosen because they could be obtained by applying (part of) a commonly reported aqueous fractionation process. Following this process to different extents yielded protein fractions with different purities. Fewer fractionation steps are beneficial in terms of environmental footprint and energy or water usage. First, more of the protein present in pea is used in less refined fractions. A better use means that a lower quantity of raw material needs to be cultivated and processed. This will give the biggest advantage as main resource use in primary production of crops. In addition, further processing requires more water, energy and in some cases chemicals. For example, the further fractionation towards GLB-RF requires around 25L water per kg of protein in addition. Less water use generally means less energy costs for drying [171].

8.3.2 Composition of the pea fractions

In Chapter 2, it was found that isoelectric precipitation induces a separation between albumins and globulins . This separation is based on the characteristic of globulins precipitating at pH 4.5 [31], and of the albumins remaining soluble [28, 44, 172].

Table 8.1 provides an overview of the composition of the pea fractions. The major constituent of PPC and GLB-RF is protein, more specifically pea globulin. Although the pea albumins end up in the ALB-F, the protein content of this particular pea

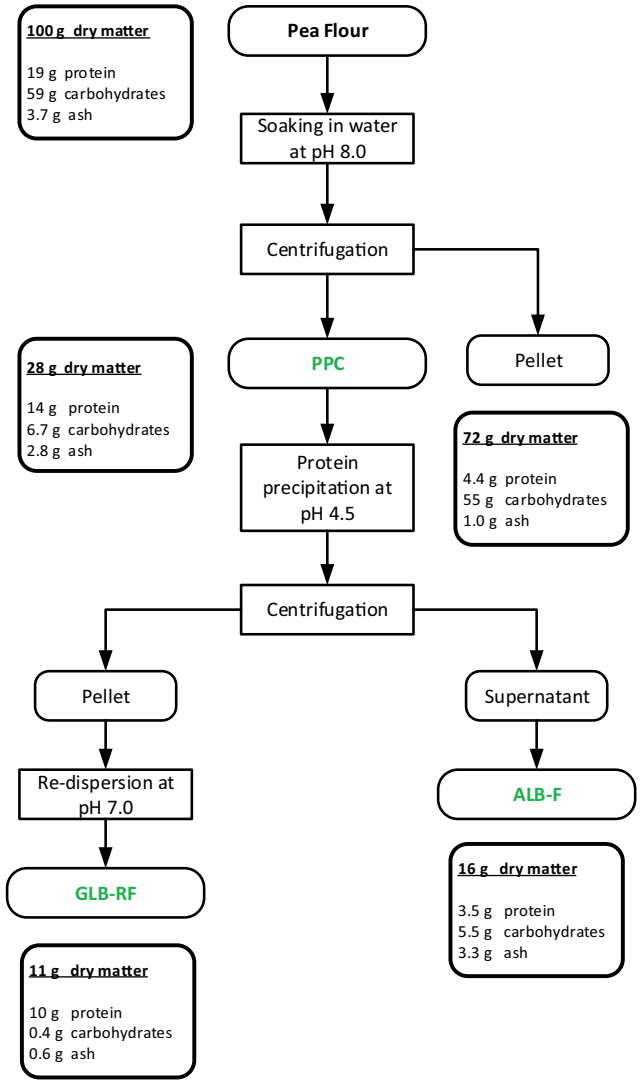

Figure 8.1 Schematic overview of the aqueous fractionation process used to obtain a pea protein concentrate (PPC), an albumin-fraction (ALB-F) and a globulin fraction (GLB-RF). A dry matter based mass balance is shown within the scheme, with the major fraction constituents shown (percentages are given in Table 8.1).

fraction is only 21 wt. %. This is a result of the low albumin content in pea seeds, which is less than 30% of the total protein content [73, 175] and the presence of soluble non-protein components in pea, which also end up in the supernatant in this process. Until now, the ALB-F is often considered a by-product from a globulin fractionation process, not suitable for use in food products. However, the economic potential of this fractionation process could be enhanced if ALB-F could serve as a functional ingredient, for example as whey proteins substitute.

Table 8.1 Composition of yellow pea, the pea fractions and of whey protein isolate. All quantities are expressed in grams per 100 gram of dry matter. All samples were measured at least in duplicate and the numbers in superscript represent the standard deviations.

Sample	Protein content (wt. %)	Total carbohydrate content (wt. %)	Starch or starch derivative content (wt. %)	Ash content (wt. %)
Pea	18.8 $^{\pm 0.2}$	59.0 $^{\pm 2.1}$	48.8 $^{\pm 1.7}$	3.6 $^{\pm 0.3}$
PPC	51.4 $^{\pm 0.8}$	23.6 $^{\pm 0.1}$	3.6 $^{\pm 0.2}$	11.7 $^{\pm 0.3}$
ALB-F	21.1 $^{\pm 0.2}$	34.9 $^{\pm 2.1}$	6.0 $^{\pm 0.0}$	20.8 $^{\pm 0.4}$
GLB-RF	87.3 $^{\pm 1.0}$	3.4 $^{\pm 0.6}$	0.3 $^{\pm 0.1}$	6.1 $^{\pm 0.0}$
WPI	100 $^{\pm 1.0}$	-	-	1.2 $^{\pm 0.2}$

The major pea fraction impurities are carbohydrates and ash (Table 8.1). In Chapter 2 was reported that over 90% of the carbohydrates in the pea fractions were present in the form of oligosaccharides – probably raffinose and stachyose – and the remainder as small polysaccharides of around 3 kDa. These soluble sugars were found to have minor influence on viscosity, and probably also on gelling behaviour. Minerals on the other hand – which quantity is reflected by the ash content – can affect functional properties. Therefore, the mineral content was analysed into more detail (Table 8.2). The pea fractions are relatively abundant in K^+ and P^{3+}, which probably originates from phytic acid and K-phytate. The former is commonly found in pea cotyledons where phosphate is stored [262]. Phytic acid is also considered to be an anti-nutrient, as it chelate minerals and consequently reduce their bioavailability [263]. Also Mg^{2+} and Ca^{2+} are quite abundantly present in the pea fractions, while Cu^+, Zn^{2+} and $Fe^{2+/3+}$ are only present in minor quantities. The relatively high Na^+ content of the pea fractions is a direct result from the pH adjustment using NaOH during the fractionation process. Except from Na^+, the GLB-RF contains significantly less minerals than PPC and ALB-F. Compared with the pea fractions, WPI shows even lower quantities of all minerals, except from Ca^{2+}.

Table 8.2 The mineral composition (g/kg) of yellow pea, the dried pea fractions and whey protein isolate. The results for pea, ALB-F and WPI were also previously reported in Chapter 7.

Sample	Ca^{2+}	Cu^{+}	$Fe^{2+/3+}$	K^{+}	Mg^{2+}	Mn^{2+}	Na^{+}	P^{3+}	Zn^{2+}
Pea	0.62	0.01	0.06	10.4	1.07	0.01	0.01	4.53	0.04
PPC	1.89	0.02	0.12	24.0	2.72	0.03	4.43	11.6	0.10
ALB-F	3.33	0.03	0.00	47.3	5.02	0.04	10.0	8.16	0.16
GLB-RF	0.44	0.01	0.22	2.2	0.41	0.02	16.4	14.9	0.04
WPI	0.88	0.00	0.00	0.4	0.06	0.00	6.31	0.61	0.00

8.3.3 Gelation of pea fractions and whey protein isolate

The rheological heat-induced gelling properties of WPI and the different pea fractions were characterised before measuring mixtures of those samples. Fig. 8.2 shows that WPI gels have the highest G', followed by PPC, GLB-RF and ALB-F. The gels were all standardized on 15 wt. %. The differences between these G' values – used as a measure for gel firmness – cannot be explained by the differences in protein content. For instance, PPC has a higher G' than GLB-RF, but the protein contents are 51% and 87%, respectively. Hence it is the type of protein that accounts for different gelling behaviour. Fig. 8.2 shows an abrupt sol/gel transition around 80 °C for WPI, which is close to the β-lactoglobulin denaturation temperature [241]. The pea fractions show a more gradual increase in G', which starts at lower temperatures. The gelling onset of GLB-RF begins at a temperature of around 60 °C. PPC starts to gel at around 65 °C, and ALB-F shows an increase in G' at around 70 °C. The order of the onset of gelation is consistent with previous protein denaturation measurements of Chapter 4, but the gelling onset temperatures are lower than the denaturation onset temperatures (77, 82 and 74 °C for PPC, ALB-F and GLB-RF, respectively). This could be related to differences in heating rate between the rheology and the differential scanning calorimetry (DSC) measurement. Furthermore, PPC and GLB-RF show a G' increase at both the heating and cooling stage, whereas the G' of ALB-F and WPI increases mostly upon heating.

The final average G' of the WPI gel is around 7 kPa (± 2 kPa). PPC shows a G' average value of around 2 kPa (± 0.6 kPa), which is higher compared to the other pea protein gels. GLB-RF forms a soft solid with a paste-like texture, which is also reflected in a lower G' value of 300 Pa (± 40 Pa). ALB-F shows the lowest G' of around 8 Pa (± 2 Pa). Although ALB-F behaves like a soft solid (where G' > G''), the appearance after heat treatment is that of a dispersion with large protein particles. The higher gel

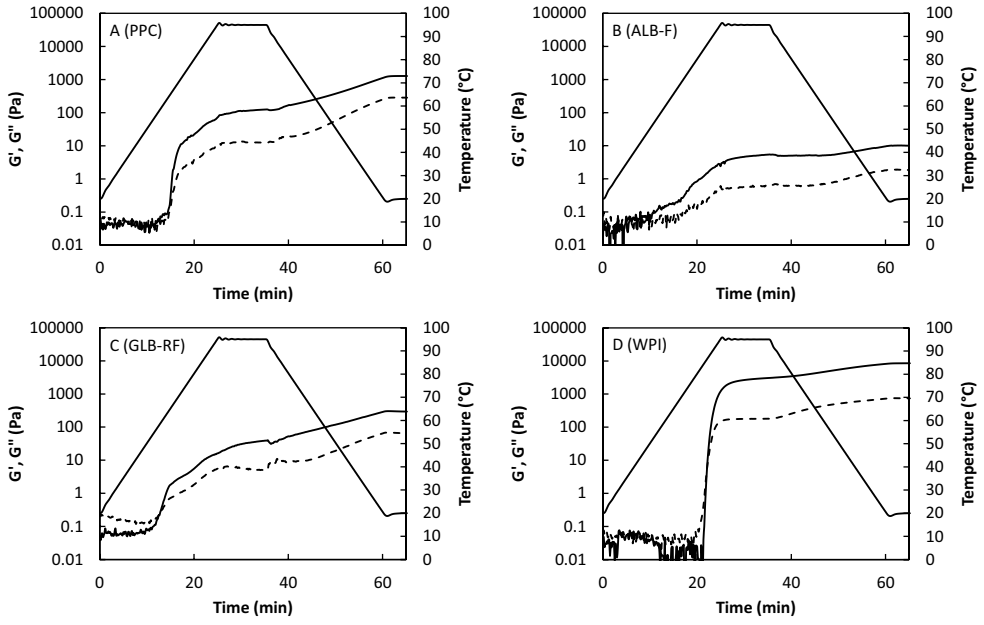

Figure 8.2 Temperature sweeps of A. PPC, B. ALB-F, C. GLB-RF and D. WPI. The samples were dispersed in concentrations of 15 wt. % dry matter and adjusted to pH 7. The G' (solid line) and G'' (dashed line) response was recorded over time. All samples were measured at least in duplicate and a representative curve was selected.

firmness of the PPC, compared with the purer GLB-RF, has studied in Chapter 4 and can be attributed to different factors, of which isoelectric precipitation is the most important one. In that particular study, it was also found that PPC was more ductile than GLB-RF, evidenced by a later transition from elastic to viscous behaviour upon large deformation. Since, the dry matter in dispersion was kept constant at 15 wt. %, the protein content varied between the samples. GLB-RF contains 87% protein (i.e. globulins), and it can be assumed that the gelling behaviour is dictated by the globulins. The gelling behaviour of albumins is not very clear, as the ALB-F shows a low G', probably as a result of the low protein content.

For a better comparison on the gelling behaviour of albumins with globulins – the ALB-F was further fractionated by diafiltration to increase the purity to 53.5 wt. % (dry matter basis). This new fraction was labelled albumin-rich fraction (ALB-RF). Also here, it is assumed that protein controls the gelling behaviour, as the impurities are mostly small polysaccharides (with molecular weights smaller than 2 kDa) and minerals.

The dry matter of the samples was kept constant at 15 wt. % (13 wt. % and 8 wt. % protein for GLB-RF and ALB-RF, respectively). Fig. 8.3 shows that the gelation of ALB-RF and GLB-RF both start around 50 °C, but the increase of ALB-RF is more gradual than GLB-RF. At the end of the temperature sweep, albumins form slightly firmer gels than globulins, with G' values of 545 Pa (± 46 Pa) and 324 Pa (± 43 Pa), respectively, despite of the difference in protein purity (53.5% versus 87.3%). This implies that albumins are better gelling agents per mass of protein than the globulins. The differences in non-linear rheological behaviour were also studied.

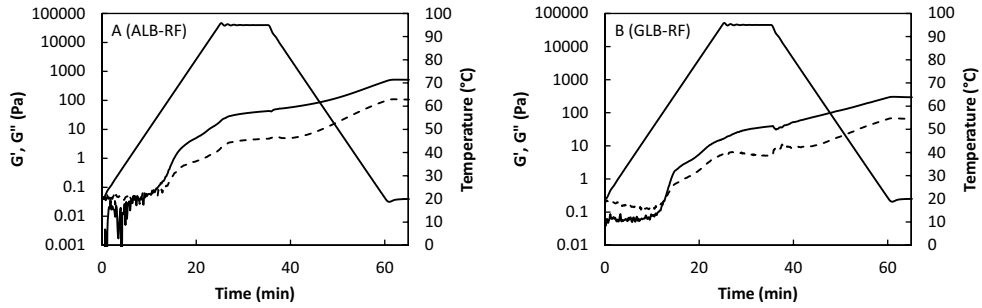

Figure 8.3 Temperature sweeps of an albumin-rich fraction (ALB-RF) (A) and a globulin-rich fraction (GLB-RF) (B). The samples were dispersed in concentrations of 15 wt. % dry matter and adjusted to pH 7. The G' (solid line) and G'' (dashed line) response was recorded over time. All samples were measured at least in duplicate and a representative curve was selected.

Fig. 8.4 shows Lissajous plots of ALB-RF and GLB-RF both within and beyond the linear viscoelastic (LVE) regime. The limit of the LVE regime was found by determining the critical strain γ_c (i.e. the strain amplitude at which the G' plateau value is reduced by 10%), which was 3.5% (± 0.4%) and 1.8% (± 0.1%), respectively, indicating that ALB-RF is more ductile than GLB-RF. Within the LVE regime, at a strain amplitude of 1%, the Lissajous plots had an elliptical shape, which indicates predominant linear viscoelastic behaviour. At 25% strain amplitude this elliptical shape showed deflections at maximum deformation in the case of ALB-RF, which indicates intracycle stiffening. At this strain amplitude, GLB-RF already showed plastic behaviour, with an initial rigid response (steep stress increase from left bottom corner) followed by flow (horizontal part where stress is quite constant), and recovery (top right corner). A similar response was seen for ALB-RF, but at a higher strain amplitude of 159%. At this strain amplitude GLB-RF already behaved almost fully viscous. Above 159%, ALB-RF showed self-intersections (i.e. lines from forward

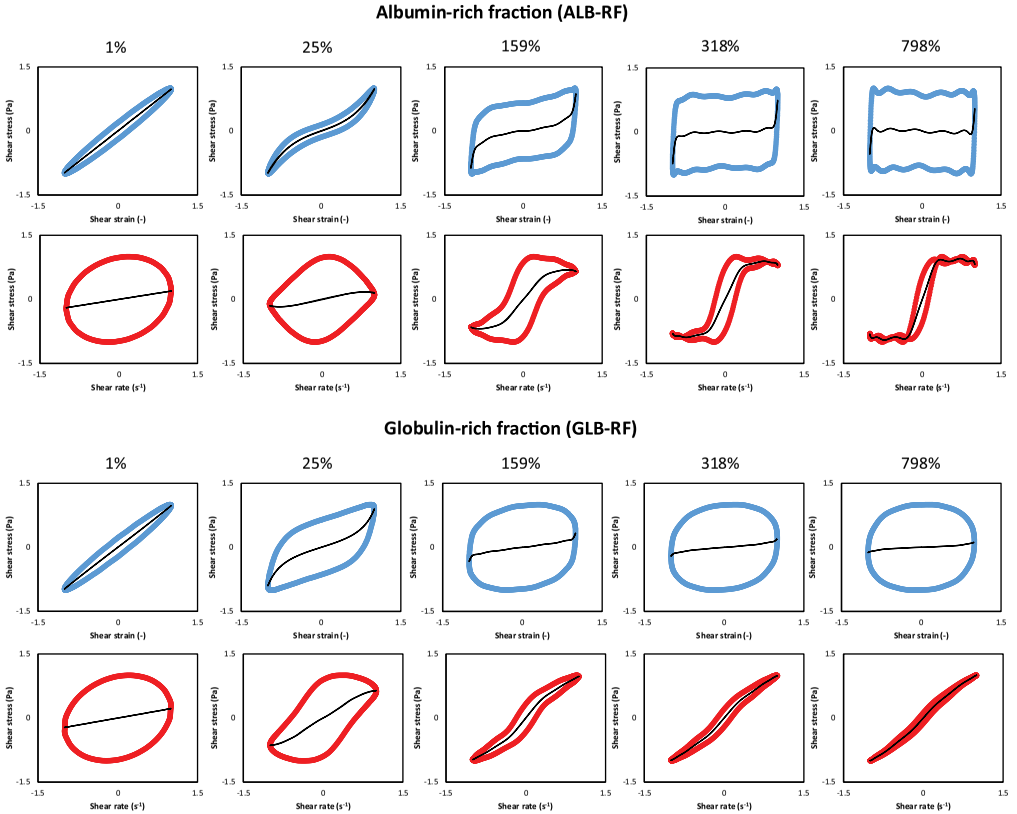

Figure 8.4 The response to deformation of ALB-RF and GLB-RF gels (15 wt. % dry matter, pH 7), visualized by elastic Lissajous plots of stress versus strain (—) and viscous Lissajous plots of stress versus strain rate (—). The normalized stress responses to oscillatory deformations at 1, 25, 159, 318, 798% are shown. The black line represents the elastic stress contribution. All samples were measured at least in duplicate and a representative curve was selected.

and backward oscillation cross-over at maximum strain) in the viscous Lissajous plot, which is a general indication of extreme nonlinearity being that existing stress is unloaded more quickly than new deformation is accumulated [264]. This implies reformation of crosslinks within the timescales of the oscillatory deformation [165]. GLB-RF showed almost purely viscous behaviour at strain amplitudes of 318% and 798%, indicated by the near-circular shape and the increased curve area. The integrated area inside the Lissajous plots reflects the energy dissipation, and thus the level of viscous response. The ratio of observed dissipation over perfect plasticity, termed the dissipation ratio, is a measure for the material's plasticity. To visualize the main information from the Lissajous plots in a compact way, the energy dissipation ratio was plotted as function of strain amplitude (Fig. 8.5). Also, far beyond the LVE regime ALB-RF behaved more elastic, as Fig. 8.5 shows a steep increase in dissipation ratio at around 10% strain amplitude for GLB-RF, whereas ALB-RF only started to increase around 40% strain amplitude. In conclusion, pea albumins form firmer gels and better resist deformation compared to pea globulins.

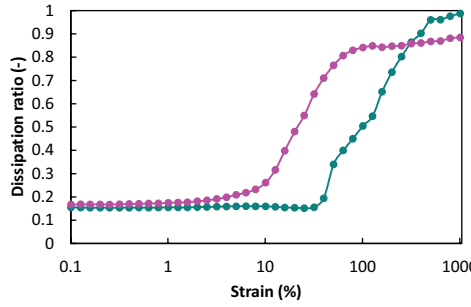

Figure 8.5 Energy dissipation ratio of ALB-RF (●) and GLB-RF (●) heat-set gels, prepared from a dispersion with 15 wt. % pea fractions, adjusted to pH 7. All samples were measured at least in duplicate and a representative curve was selected.

The gel properties are probably dictated by the proteins, because protein is the major component (53.5 wt. %) and the impurities are mostly oligosaccharides and salts. To get a better insight on the behaviour of the protein structure – and potentially detect the contribution of components based on relaxation times – the gels were exposed to a frequency sweep. Fig. 8.6 shows the G′ and G″ frequency dependency of ALB-RF and GLB-RF over a frequency range of 0.1 – 10 Hz. The G′ at frequencies below 0.1 Hz could not be studied due to low signal to noise ratios of the rheometer in these regions. From 0.1 – 10 Hz the G′ and G″ remain quite constant with increasing

frequency. This weak G′ dependency on frequency of both ALB-RF and GLB-RF gels indicate that either the system is highly elastic or that the whole frequency range is high enough to make important network cross-links seem permanent [265]. Such weak frequency dependency was also observed for commercial and salt-extracted pea protein isolate gels [150] and WPI heat-set gels [266].

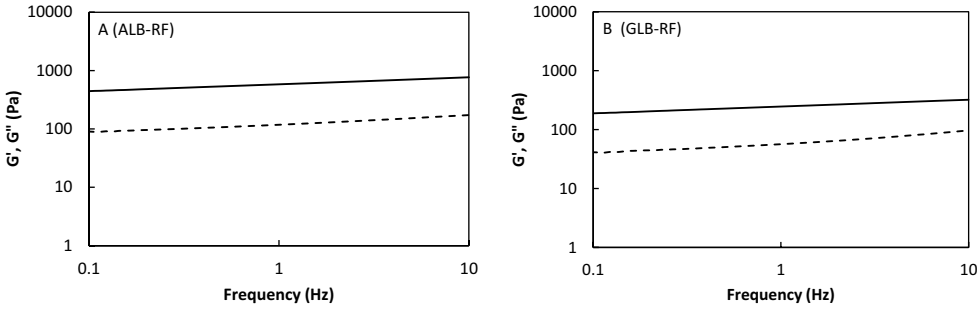

Figure 8.6 Frequency sweeps of A. ALB-RF and B. GLB-RF. The samples were dispersed in concentrations of 15 wt. % dry matter and adjusted to pH 7. The G′ (solid line) and G″ (dashed line) response was recorded over time. All samples were measured at least in duplicate and a representative curve was selected.

So far, pea albumins received less attention than pea globulins in scientific research. Although globulins may be able to form firmer gels if they were fractionated more mildly, it is remarkable that pea albumins – normally underutilized in a fractionation process – can compete with conventionally fractionated globulins in the context of heat-induced gelation. This also stresses the potential of using an ALB-F by-product as a functional ingredient or even as a WPI substitute.

8.3.4 Gelling behaviour and gel properties of pea fraction – WPI mixtures

Mixtures from pea fractions and WPI were prepared in ratios of 1:3, 2:2 and 3:1 with a total dispersed mass fraction of 15 wt. %. Fig. 8.7 shows the G′ of heat-set WPI gels in a concentration range of 9 – 21 wt. % (blue line). Note that to clearly demonstrate the effect of a decreasing WPI content in the pea fraction / WPI mixtures the horizontal axis in Fig. 8.7 was inverted. The dashed lines represent mixtures of WPI with the pea fractions in different ratios and a constant total mass of 15 wt. %. Gels made from the different pea fractions all showed lower G′ values than the gels containing only WPI. Even small amounts of WPI in the pea fractions (1:3) yielded higher G′ values than the pea fractions themselves. Fig. 8.7 shows that the G′ can reduce by a factor 10, with decreasing proportion of WPI in the GLB-RF / WPI mixtures. The inclusions

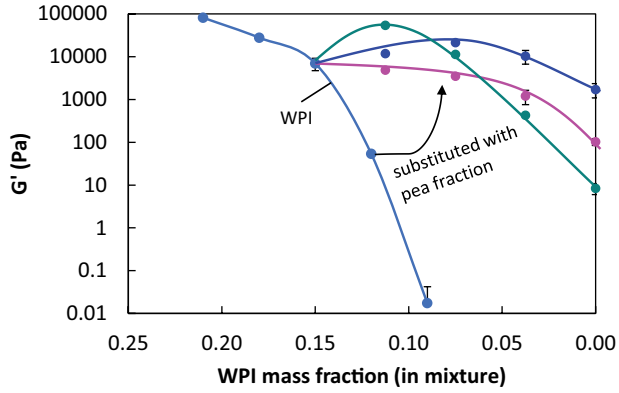

Figure 8.7 G' of heat-set gels produced from mixtures of PPC, ALB-F and GLB-RF with whey protein isolate (WPI). The dashed lines are a guide for the eye, and represent mixtures of PPC (—), ALB-F (—) and GLB-RF (—) with WPI in 1:3, 2:2 and 3:1. Also the G′ of pure pea fractions (0% WPI) and pure WPI (—) as function of WPI mass fraction are shown. All gels were produced from dispersions with a total of 15 wt. % dry matter, adjusted to pH 7. The samples were measured at least in duplicate and error bars represent the standard deviations. Note that the WPI mass fraction (on the horizontal axis) was inverted.

of PPC and ALB-F led to an increase in G′ at different ratios. Such a synergistic effect was not observed in Chapter 7, where WPI was replaced by pea protein isolates (PPIs). An overview on how the pea fractions in this study relate to the previously studied PPI in the context of WPI substitution (1:3 ratio) is shown in Table 8.3. Although the tan δ values – a measure for the solid-like behaviour of the gels – show small differences between pea fractions and protein isolates, larger variation in G′ is observed for the pea fractions compared with pea protein isolates. Also, higher G′ values can be reached with PPC and ALB-RF as substitute, compared with the different pea protein isolates. Although the pea protein isolates were versatile in their behaviour (i.e. viscosity, gelling, solubility), they behave more similar in substitution with WPI, compared with the differently processed pea fractions.

The high G′ of WPI / ALB-F mixtures suggest a synergistic effect, as the measured G′ is higher than the proportional sum of the G′ of the pea fractions and WPI gels. Such a synergistic effect could be caused by increased interactions (e.g. disulphide bonding), between the same type of proteins or between whey proteins and pea proteins. It could also be related to the minerals present in the pea fractions, as increased NaCl concentrations was found to have a positive effect on the G′ of WPI gels [267]. The effect of salt, as well as the role of disulphide bonding, will be discussed in the next sections.

Table 8.3 Comparison between the elastic moduli (G') and dissipation factors (tan δ (= G"/G')) of WPI combined with PPC, ALB-F and GLB-F and with the in Chapter 7 studied pea protein isolates PPIp (precipitated), PPId (diafiltrated) and PPIc (commercial) in a 3:1 ratio. Please note that GLB-RF and PPIp followed the same fractionation process, but that different pea fraction and WPI batches are compared.

	PPC	ALB-RF	GLB-RF	PPIp	PPId	PPIc
G' (kPa)	6.4 $^{\pm 0.0}$	54.4 $^{\pm 2.0}$	4.9 $^{\pm 0.3}$	6.1 $^{\pm 0.4}$	5.3 $^{\pm 0.5}$	3.5 $^{\pm 0.1}$
Tan δ	0.11 $^{\pm 0.00}$	0.13 $^{\pm 0.00}$	0.10 $^{\pm 0.00}$	0.11 $^{\pm 0.00}$	0.17 $^{\pm 0.01}$	0.12 $^{\pm 0.00}$

8.3.5 The pH and ionic strength sensitivity of substituted WPI gels

Gelling properties of proteins are influenced by pH and ionic strength. A pH close to the isoelectric point (pI) facilitates protein aggregation, due to reduced electrostatic repulsion. The pI of whey proteins is 5.2 [268] and the pI of pea globulins is between 4 and 5 [22, 68, 233]. Fig. 8.8 shows a G' increase for PPC and GLB-RF mixtures with WPI at pH 5.0 and 7.0 at low temperatures. Even at the very onset of the temperature sweep they display solid-like behaviour at the measured frequency (1 Hz), as G' > G" (or tan δ < 1). It is possible that at lower frequencies the G' would decrease, which would indicate a viscoelastic response, rather than the presence of an elastic network. These results may also suggest the presence of a weak network of aggregates formed around the pI of the proteins. Such behaviour (i.e. G' > G" with f = 1 Hz) was not observed for WPI [269], but was observed for the GLB-RF with an initial tan δ (= G"/G') of 0.59 (± 0.07), potentially indicating solid-like behaviour. However, the sudden drop in G' around 80 °C in Fig. 8.8 has not been seen in any of the pea fraction or WPI gels, which means that it is a property of the mixture. The temperature at which the decrease in G' occurs is similar to the gelling onset of WPI [223]. A similar sudden drop in G' was seen for heat-set gels from Bambara groundnut and WPI mixtures at pH 5. An initially formed gel network – facilitated by electrostatic attraction around the pI – was disrupted around the denaturation temperature of β-lactoglobulin [270]. This suggests that WPI denaturation causes breakdown of a network initially formed, and that denaturation has a temporary adverse effect on the gelation process.

At pH 7, the gelling onset starts at higher temperatures, around 70 °C for mixtures with PPC and around 80 °C for mixtures with GLB-RF. The mixtures of ALB-F with WPI (Fig. 8.8) show different behaviour. Except from a slightly earlier gelation onset, the curves at pH 3.7, 5.0 and 7.0 are quite similar, and so are the final G' values of the gels. ALB-F compares favourably with the other pea fractions as a WPI substitute. It does not only give firmer gels, but also appears quite insensitive to pH changes in the range of pH 3.8 to 7.0. This could be an advantage in food formulations with

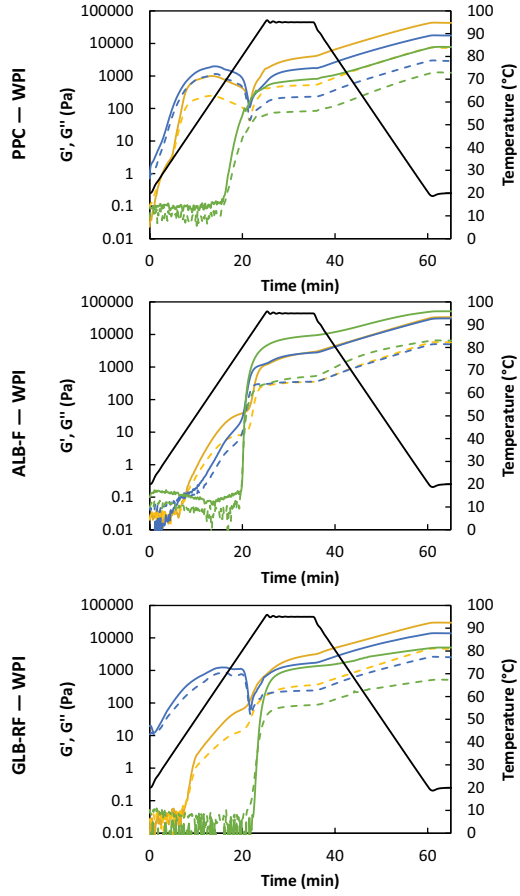

Figure 8.8 Mixtures of pea protein concentrate (PPC), albumin fraction (ALB-F) and globulin fraction (GLB-RF) with whey protein isolate (WPI) at pH 3.8 (—), 5.0 (—) and 7.0 (—). The pea and whey proteins were mixed in a ratio of 1:3. G' is represented by a solid line and G'' by a dashed line. All samples were measured in duplicate and a representative curve is shown.

an acidic pH, such as mayonnaise, cheese and yoghurt. The insensitivity of the ALB-F / WPI mixture, as well as its high G', could be a result of the high solubility of albumins at acidic pH. An additional explanation for the small pH-effect could be the high mineral (i.e. salt) content, present in ALB-F (Table 8.1). Like pH, salt screens the charges of protein, and greatly reduces the effect of electrostatic repulsion. To verify this, the influence of salt on the three mixtures was studied.

The effect of ionic strength on the heat-set gelation of WPI itself has been the subject of different studies. It has been reported that at pH's away from the isoelectric point,

the concentration at which gels can be formed (i.e. critical gel concentration) decreases with increasing ionic strength. At pH 7 the critical gel concentration decreases from around 55 g/L to 10 g/L when the ionic strength increased from 0.02 to 0.09 M NaCl, where after the critical gel concentration did not decrease further [271]. Also, the heat-set gel strength of WPI increases with increasing $CaCl_2$ or NaCl concentrations [266, 272-274]. Fig. 8.9 shows the G' of the pea fraction / WPI mixtures as function of ionic strength. The initial ionic strengths varied between the mixtures, with ALB-F / WPI mixtures already starting at 88 mM (NaCl equivalent). The PPC / WPI and GLB-RF / WPI mixtures had an initial ionic strength of 37 and 30 mM (NaCl equivalent), based on their conductivities. An increase of the ionic strength to 100 mM NaCl led to a G' increase for PPC / WPI and GLB-RF / WPI mixtures. This ionic strength range could not be measured for the GLB-RF / WPI mixtures, as the initial ionic strength was too high. From 100 mM NaCl onwards, the G' of all mixtures showed a small decrease with increasing ionic strength. This result suggests that the initial high salt content in ALB-F plays a major role in the gel firmness of the mixture, as for the mixtures with PPC and GLB-RF the G' mostly increases up to 100 mM NaCl. A similar effect was reported for WPI gels, where the critical concentration was affected by ionic strength till around 100 mM NaCl [271]. It is thus plausible that the effect of ionic strength on WPI has a large impact on the behaviour of the mixtures. This makes us conclude that after standardization on ionic strength, all three pea fractions could serve equally well as WPI substitute at pH 7 in terms of gel firmness, leading to G' values of around 50 kPa.

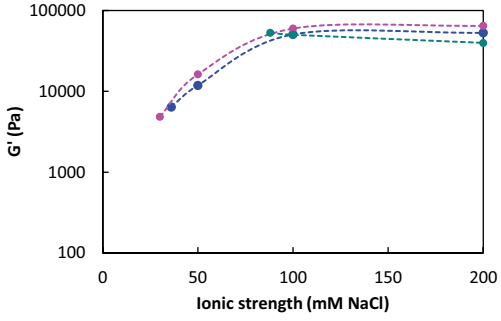

Figure 8.9 The G' of heat-set gels from mixtures of PPC (●), ALB-F (●) and GLB-RF (●) with whey protein isolate (WPI) in a 1:3 ratio as function of salt concentration (15 wt. % dry matter, pH 7). The initial ionic strength of the mixtures was calculated from the measured conductivities. NaCl was added to increase the ionic strengths to 50, 100 and 200 mM NaCl. All samples were measured in duplicate and average G' values are shown. The error bars, representing standard deviations, were smaller than the data points.

8.3.6 Covalent interactions in pea – whey proteins mixtures

In addition to weaker physical forces (i.e. electrostatic interactions, hydrophobic interactions and hydrogen bonding), covalent intermolecular disulphide bonding can also contribute to gelation, through formation of permanent chemical crosslinks within a gelled network [275]. For WPI it has been reported that disulphide bonding plays an important role in gelation, both heat-induced [276, 277] and acid-induced [278]. For pea globulins, disulphide bonding plays a limited role in the gel formation and hence has little to no effect on the elastic modulus after gelation [141, 153]. The role of disulphide bonding may however be affected by fractionation – more specifically by alkaline extraction – as the thiol pKa value of most cysteine residues range between 8 and 9 [279]. Above the pKa, deprotonated thiols can participate in sulfhydryl-disulfide exchange reactions. The pea fractions in this study were all exposed to alkaline extraction, but it is noted that a different fractionation route may influence the occurrence of disulphide bonding upon heat-set gelation.

The ability of pea albumins to form disulphide bonds has not been studied before, possibly because these proteins only comprise less than 30% of the total seed protein. However, PA1 and PA2 albumins collectively contain about 50% of the total sulphur amino acids in the pea seed [44]. Hence, we elaborate further on disulphide bonding in pea albumin in this study. Fig. 8.10 shows that the resulting gel firmness was significantly lower ($P < 0.05$), with a G′ value of 128 Pa (± 37 Pa) when disulphide bonding was inhibited, compared with 540 Pa (± 34 Pa) for the ALB-RF without NEM. The initial gelling behaviour upon heating was not affected, but upon cooling the G′ increase was less pronounced. This means that disulphide bonding affects heat-set gelation of pea albumins at the conditions studied. Also,

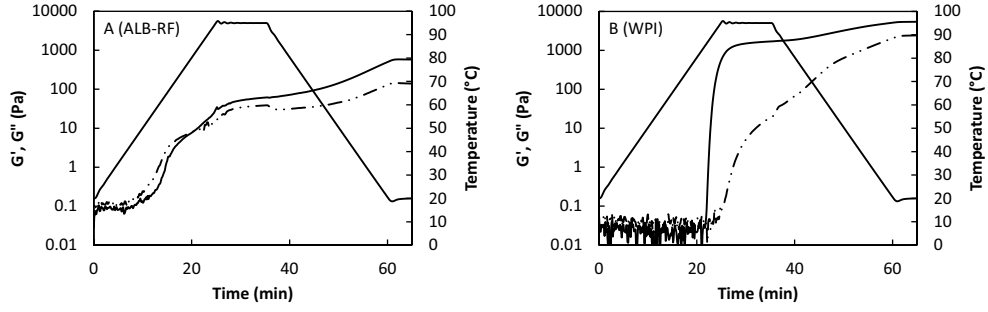

Figure 8.10 Heat-induced gelation of A. ALB-RF and B. WPI with disulphide bonding (solid line) and without (dashed line). Prior to gelation the dispersions were standardized on 15 wt. % dry matter and adjusted to pH 7. All samples were measured in triplicate and a representative curve was selected.

WPI showed reduced gelling in the presence of NEM. The abrupt sol/gel transition, typical for WPI, changed into a more gradual G' increase upon heating. However, a steeper increase was seen upon cooling, which eventually led to an average G' value of 2.4 kPa. This is lower compared to the situation without NEM, where the G' of WPI reached an average value of 7 kPa. The major difference between WPI and ALB-RF, with respect to the contribution of disulphide bonding, is the stage of the temperature cycle where G' increases. When disulphide bonding is inhibited, it is mostly upon heating that gelation is affected for WPI, whereas for ALB-RF it is mostly upon cooling. This difference in the stage at which disulphide bonding plays a role, is not necessarily temperature-dependent, but could also be time-dependent (i.e. disulphide bonding starts later in ALB-RF than in WPI).

For the mixtures, disulphide bonding plays a role in the gelation kinetics and gel firmness also, as shown in Fig. 8.11. The PPC / WPI mixtures showed a more gradual increase, upon NEM addition, in the heating stage. Also, the average G' value of the gel is lower (2 kPa) than without NEM (12 kPa). This indicates that disulphide bonding is an essential contributor to gelation of the PPC – WPI mixture. Disulphide bonding may occur both between whey proteins, and whey proteins and pea albumins. In the latter case, a larger difference would be expected in the ALB-F / WPI mixture. Here, the average G' values reduced from 50 kPa to 9 kPa in the presence of NEM. This large reduction in G' indicates that disulphide bonding plays a crucial role in these mixtures indeed, and makes it plausible that disulphide bonding occurs between WPI and ALB-F constituents, as the G' reduction in the WPI gel itself was much lower. For the GLB-RF – WPI mixtures a relatively small effect of NEM was seen. The average G' value reduced from 5 kPa to 3 kPa. This small reduction (36%) is probably a result of the inhibition of whey protein disulphide bonding, since NEM hardly affected globulin gelation.

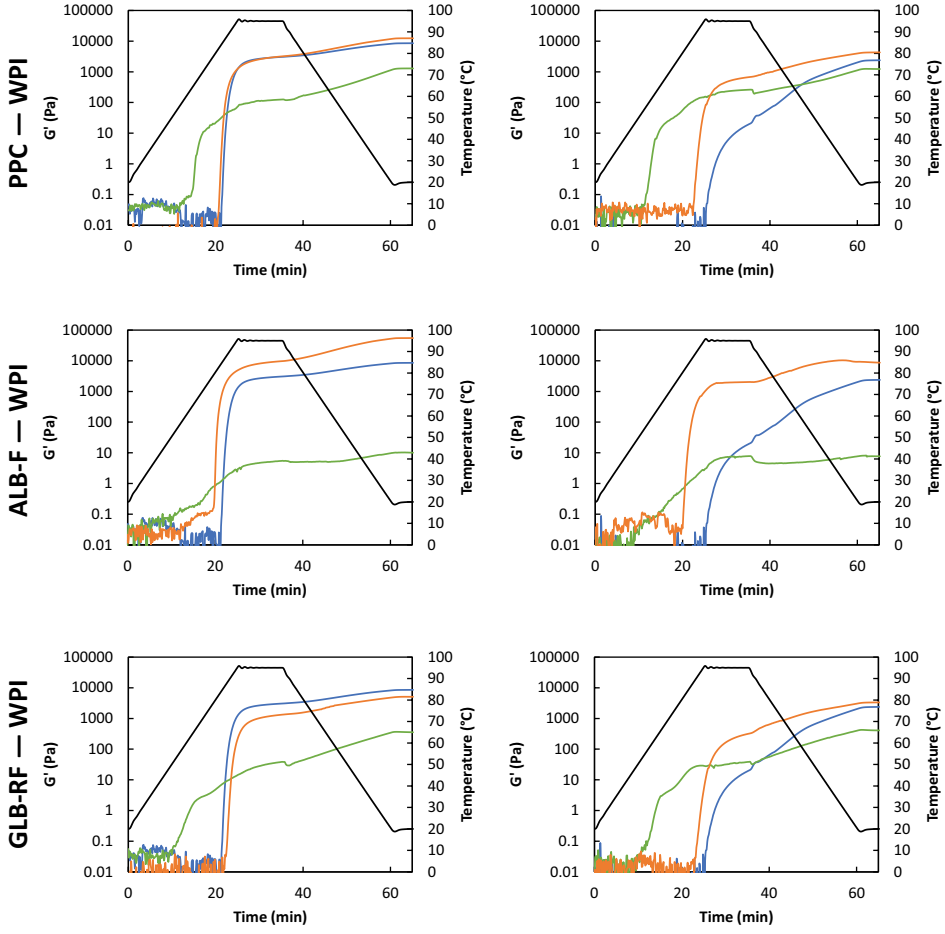

Figure 8.11 Temperature sweeps of the pea fractions (PPC, ALB-F and GLB-RF) (—), WPI (—) and mixtures of pea fraction and WPI in a 1:3 ratio (—), 15 wt. % dispersed at pH 7. In the left situation disulphide bonding was allowed to occur and in the right situation disulphide bonding was blocked by the thiol blocking agent N-Ethylmaleimide. All samples were measured in duplicate and a representative curve was selected.

8.4 Conclusion

In this study we evaluated the pea albumin and globulin gelling behaviour, both as individual gelling agents and in mixtures with whey protein isolate. By doing so, the ability of pea protein fractions to replace whey protein in heat set gels was quantified. It was found that the pea protein concentrate – a mixture of albumins and globulins – and the albumin-rich fraction formed firmer gels per mass of protein than the globulin-rich fraction, but none of the pea fractions studied were able to provide a similar gel firmness as whey proteins. When part of whey protein was substituted by the pea fractions, it turned out that mixtures of albumins with whey proteins showed the most stable gelling behaviour over a range of pH and ionic strengths. The other fractions also gave high gel firmness, but were more sensitive towards pH and ionic strength changes. The finding with albumins is especially interesting as this fraction is currently an underutilized by-product from the pea fractionation process. The use of this by-product as a WPI substitute will enhance the resource efficiency of peas. These results may guide both researchers and food manufacturers, to optimize plant protein fractionation processes and to bring most value to legumes such as pea, as a source for functional ingredients.

Chapter 9

General Discussion

9. General Discussion

Pea is a protein source that may play an important role in the protein transition, as pea can grow in moderate climates and has a high protein content with most of the essential amino acids present [18, 280, 281]. Before using pea as an ingredient source, the seeds are often milled and fractionated into protein and starch-enriched fractions. The most commonly reported protein fractionation process in literature is aqueous fractionation, which yields relatively pure protein ingredients, but also requires substantial amounts of energy and water, when compared to dry fractionation [49]. Furthermore, pea protein can denature and loose functionality because of harsh processing conditions [49, 149, 171]. Although some studies reported the use of alternative milder fractionation routes – such as dry fractionation – there is limited research available that explores the effect of less extensive fractionation on protein properties. Fewer fractionation steps require less water and energy compared to an extensive fractionation process, and is thus likely to be more sustainable [171]. However, limited fractionation also affects the protein purity, and potentially results in a different state of the protein. The **aim** of this thesis is to establish the effect of aqueous fractionation routes on the functionality of pea protein in terms of molecular and microstructural characteristics, for a variety of food model systems. The results of this thesis are categorized into three parts. The first part discusses pea protein dispersions and gels (**Chapters 2, 3 and 4)**. The second part covers pea protein model foods where oil and air are incorporated (**Chapters 5 and 6)**. The third part is about the incorporation of pea protein dairy protein dispersions and gels (**Chapters 7 and 8)**. A schematic overview of the thesis is presented in Fig. 9.1.

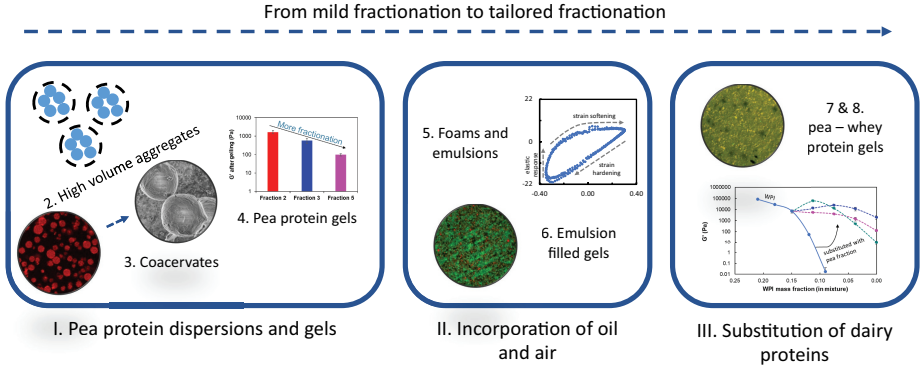

Figure 9.1 Graphical overview of the thesis content categorized in three parts. The numbers refer to the different chapters in the thesis.

9.1 Main findings: the relation between fractionation routes and protein functionality

In the first part of this thesis the impact of mild or limited fractionation on the molecular and microstructural characteristics of pea protein was studied to establish a relation between fractionation and functionality. In the second and third part we looked at how fractionation processes can be tailored to create fractions with specific functionality in food model systems. Fig. 9.2 provides a schematic overview of the different fractionation routes used in this thesis.

9.1.1 Main findings

I. Pea protein dispersions and gels

The first three chapters of this thesis cover the behaviour of pea proteins in dispersion at different pH, salt, temperature, and fractionation conditions. In **Chapter 2**, it was found that pea proteins occupied a large volume in dispersion at pH 7 and low salt concentrations, in the form of soluble aggregates. The fractionation process did not significantly influence the ability to form soluble aggregates, as a similar high viscosity and volume fraction were found for the globulin-rich fractions PPCn, PPCa and PPIp. However, fractionation did influence the formation of insoluble aggregates, which is illustrated by a lower solubility for PPIp, compared with the other two pea fractions. This resulted in a thickening capacity, specifically for PPIp (Fig. 9.2).

In **Chapter 3** the pH and salt concentration of the pea protein dispersion was changed, which induced liquid-liquid phase separation and the formation of coacervates (i.e. protein-rich spherical domains). The mildest fractionated PPCn formed most coacervates (Fig. 9.2). The coacervates from this pea fraction only contained globulins, not albumins, and had an internal protein content between 40 and 50 wt. %. More extensive fractionation (PPCa and PPIp) led to less coacervate formation, probably due to a decreased soluble protein concentration as a result of process-induced aggregation.

In **Chapter 4**, the pea fractions obtained by aqueous fractionation were heated to induce gelation. Also the gel properties were affected by the extent of fractionation. The limited fractionation PPCn and PPCa formed firmer and more ductile gels per mass of protein than the extensively fractionation PPIp (Fig. 9.2). PPCn and PPCa also had a more homogeneous microstructure than PPIp. The more heterogeneous microstructure of the latter could be attributed to aggregation that was induced by

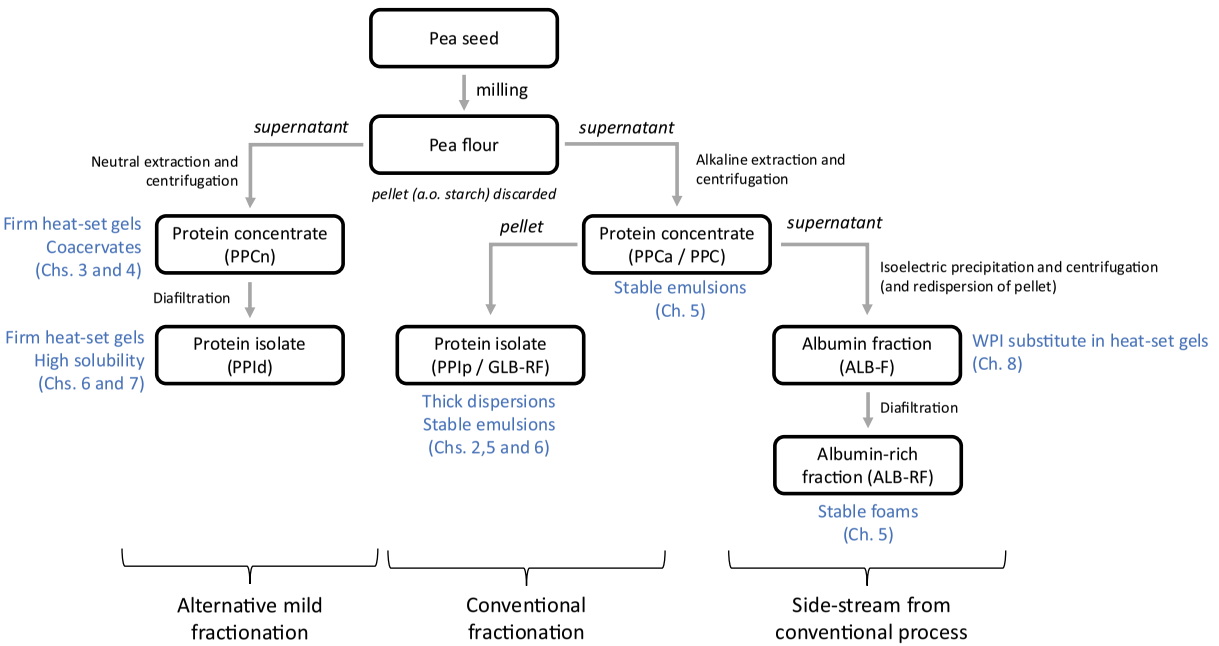

Figure 9.2 The fractionation processes used in this thesis with in blue the functional properties observed for the resulting pea fractions. All fractions were used as freeze-dried powders, except when stated otherwise. The relevant chapter numbers are given between brackets.

isoelectric precipitation. Also, the salt and sugar content of the pea fractions played a role. Limited processed pea fractions contained more salt and thus had a higher ionic strength in dispersion, which had a subtle positive effect on gel firmness. Also, sugars were expected to play a role by stabilizing the proteins upon freeze drying.

II. Incorporation of oil and air

The second part of this thesis covers the incorporation of oil and air in pea protein dispersions and gels, as well as the interfacial properties of oil-water and air-water interfaces. In **Chapter 5**, it was found that the type of protein in the pea fractions, rather than the extent of fractionation, had an important effect on the foam and emulsion properties. Three pea fractions were obtained: PPCa containing both globulins and albumins, ALB-RF containing albumins and PPIp containing globulins (in Chapter 4 referred to as GLB-RF). It turned out that the pea albumins could stabilize foams with a higher foam overrun – even comparable to whey protein isolate (Fig 9.2). The albumins formed a stiffer and more cohesive air-water interfacial layer than the globulins. Pea globulins on the other hand could form stabler emulsions than pea albumins, which was attributed to the larger size and higher net charge of the globulins, protecting the droplets against coalescence and flocculation. This research gave rise to the insight that (milder) fractionation could be tailored to specific functional properties.

In **Chapter 6** we built further on the insight that fractionation processes influence protein functionality. Here we explored an alternative fractionation route, where isoelectric precipitation was replaced by diafiltration to yield PPId. The behaviour of PPId was compared with PPIp in emulsions and emulsion filled gels. It was found that the emulsion properties of both pea protein isolates were quite similar. Both PPIs could stabilize emulsions with monomodal droplet sizes between 1-10 μm. After addition of 15 wt. % PPI to the aqueous phase of the emulsions, the emulsions were gelled through heating. It was found that PPId formed firmer gels than PPIp at both pH 5 and 7, but in the case of PPId the gel firmness decreased when the pH was decreased from 7 to 5, while the gel firmness of PPIp increased. The oil content had little effect on the gel firmness. The difference between PPId and PPIp was largest at pH 7, where PPId formed firmer and more cohesive gels (Fig. 9.2). This difference was attributed to the isoelectric precipitation process that induced aggregation in the case of PPIp, whereas the milder process used to obtain PPId did not induce such aggregation.

III. Incorporation of dairy proteins

The third part of this thesis focusses on hybrid plant-dairy protein dispersions and gels. Besides, it describes the ability of pea protein to replace dairy protein completely and how this ability is influenced by the fractionation method applied. In **Chapter 7**, three pea protein isolates were studied on their ability to substitute whey protein isolate (WPI) both partially and completely. These pea protein isolates were PPIp, PPId and a commercial PPIc. PPId was most suitable to replace WPI in dispersions and heat-set gels, because of similar solubility, viscosity and gel firmness. For partial substitution, it turned out that up to 50% of the WPI could be substituted by any of the PPIs, without affecting the gel firmness.

In **Chapter 8**, WPI is substituted by pea protein in heat-set gels, using pea fractions with different purities. These fractions were PPCa, ALB-F and PPIp. When the ALB-F was used as a substitute for WPI, a higher gel firmness was obtained compared to when PPIp or PPCa were used. This could be attributed to increased disulphide bonding in WPI – ALB-F mixtures. Moreover, the gel firmness of WPI with ALB-F was least affected by pH and salt changes. Also, the gelling behaviour of pea globulins and albumins were compared using PPIp and ALB-RF. It turned out that albumins could form firmer and more ductile gels than pea globulins.

Conclusion: towards tailored fractionation

The common denominator that links all the chapters is that fractionation influence protein functionality largely through controlling composition and state of all components in the protein fractions. From the first part of this thesis (Chapters 2 – 4) we conclude that mild fractionation impacts functionality of pea protein in dispersions and gels. We found that the protein state and protein composition were often the missing link between fractionation routes and resulting differences in functionality. Extensive fractionation increased the globulin content. These globulins formed soluble aggregates that could explain the high viscosity of pea protein isolate dispersions. Fractionation also changed the state of the protein (i.e. denaturation and aggregation). Denaturation and aggregation reduced the number of protein molecules available to induce coacervation. Aggregation also affected the heat-set gelling properties of pea protein; more aggregates resulted in a heterogeneous gel network that was softer and more brittle, compared with limited fractionation pea protein gels.

The insights from Chapter 2 – 4 led to the approach for the remaining chapters, which is tailored fractionation. We realized that functionality was influenced, and

could be thus controlled, by the fractionation method. Fractionation was used as a tool to either change the protein state (Chapters 6 and 7) or the composition of the proteinaceous ingredient (Chapter 5 and 8), so that the functional behaviour, such as foam capacity, solubility, or gel firmness, could be optimized. The overall conclusion was that pea protein can display a wide range of functional behaviours, and that this versatility is determined by different fractionation methods used. This concept is visualized in Fig. 9.2.

9.1.2 Boundaries of this research and directions for future research

The research described in this thesis shows that fractionation can tailor functionality. The boundaries of the research will be discussed in this section and related to suggestions for future research.

In **Chapter 2** the viscosity of pea protein dispersions was related to the presence of soluble aggregates with a rarefied structure. The claim that such aggregates were present was based on dynamic light scattering (DLS) measurements and on estimated volume fractions as function of the dispersed protein mass. Our research indicated the presence of soluble aggregates. It would however be interesting to get a deeper understanding of the physical properties of these aggregates. One way of doing this could be by sedimentation experiments using analytical ultracentrifugation (AUC). AUC could be used to determine Svedberg coefficients, and via those coefficients, the aggregate specific volumes could be determined.

The coacervation behaviour of pea protein solutions was discussed in **Chapter 3**. This study is phenomenological as it focusses on characterization of the coacervates and how fractionation influences the observed coacervation at different sample conditions. It would be valuable to find a mechanistic explanation for the coacervation itself, and how these coacervates are stabilized.

In **Chapter 5** it was concluded that pea albumin is a very good foam stabilizer, comparable to whey protein isolate. This conclusion was based on the behaviour of an albumin-enriched fraction with 52 wt. % protein. The approach to not use a highly purified fraction is in line with the concept of this thesis to use mild fractionation, but for future research it could be relevant to study the role of the impurities on foam properties, or to fractionate the albumin-enriched fraction even further.

Chapters 3, 6, 7 and 8 describe the gelling and gel properties of a variety of pea fractions, sometimes also in mixture with whey protein isolate. Gelling behaviour was studied with small amplitude oscillatory shear (SAOS) rheology and gel

properties were characterized using large amplitude oscillatory shear (LAOS) rheology. However, rheological parameters such as elastic modulus or energy dissipation ratio of such multi-component gels cannot always easily be linked to the behaviour on a molecular level, as found in single-component gels. It would be relevant to understand the interactions of the different components on a molecular level. This is not an easy task, but there are a few methods left undiscussed in this thesis. For instance, one could think of applying models to obtain more information about the fractal dimensions of the aggregates which make up the gelled matrix. In general, it would be relevant to study the mechanisms behind network transitions using a simpler approach with purer pea ingredients (e.g. legumin or vicilin protein isolates). Of course, the question remains how to obtain these pure proteins, without affecting their properties.

Throughout this thesis, a range of fractionation conditions were deployed, and also different sample conditions (i.e., pH, salt concentration, temperature) were tested. An extensive overview of the effect of sample conditions on functionality was out of scope, as this research primarily focussed on understanding the effect of fractionation on functionality. However, one can expect that the functionality of the pea fractions will change at different sample conditions. For instance, it was found recently that the state of globulins (aggregated or not) is largely dependent on the salt concentration [60]. When tailored fractionation is aimed for, one should probably also tailor fractionation to specific sample conditions. In practice, this means that the functionality of pea fractions – obtained via different fractionation routes – should be systematically studied over a wide range of sample conditions (e.g. pH 3 – 7, Ionic strength of ~0 – 1 M, etc.).

9.2 A broader perspective on fractionation methods and functionality

Protein purification of pea starts with grinding of the seed. A pea seed consists of storage cells with mainly starch granules (5 – 30 μm) and protein bodies (2 – 4 μm). A dried pea contains roughly 20 % protein and 50 % starch [282]. There are various fractionation routes that separate these components, such as aqueous and dry fractionation. The fractionation methods that are mostly reported in literature are discussed in the next section. In section 9.1.2 the effect on functionality is studied and related to the findings of this thesis.

9.2.1 Pea protein fractionation methods in literature

In recent years there has been an increasing interest in milder ways of fractionating plant proteins, both to reduce the energy and water consumption and to retain the native properties of the proteins [49, 57, 82, 90]. In addition to the commonly reported aqueous fractionation process, involving isoelectric precipitation, alternative fractionation routes have been proposed. These alternative fractionation routes include membrane filtration, salt extraction and dry fractionation. The different fractionation methods are described in this section, and a schematic overview is given in Fig. 9.3.

Aqueous fractionation

Isoelectric precipitation

Aqueous fractionation processes are mainstream for producing protein isolates from plant sources [49]. The first step is to produce pea flour by grinding – either hulled or de-hulled – pea seeds. In literature, sometimes the pea flour is defatted by hexane [283], but this is more common for other legumes that contain higher amounts of fat (> 5 %), such as chickpea, lupine or soy [21, 284, 285]. Pea fat content reported in literature ranges from 2 – 6 % fat [21, 286, 287]. Aqueous fractionation is based on the solubility properties of pea protein as function of pH. Typically, pea protein is first extracted from the flour at alkaline pH (7 – 9.5) and the isolated by centrifugation. This centrifugation step separates the soluble components including protein, from the insoluble components (i.e. starch, cell wall material). The protein-enriched supernatant is then brought to an acidic pH of 4.5, close to the point where most pea globulins are insoluble and centrifuged again [21, 53-55, 288]. The obtained pellet is rich in proteins and can be purified further by applying multiple washing steps [289]. To aid protein solubility and inhibit enzymatic and microbiological activity the

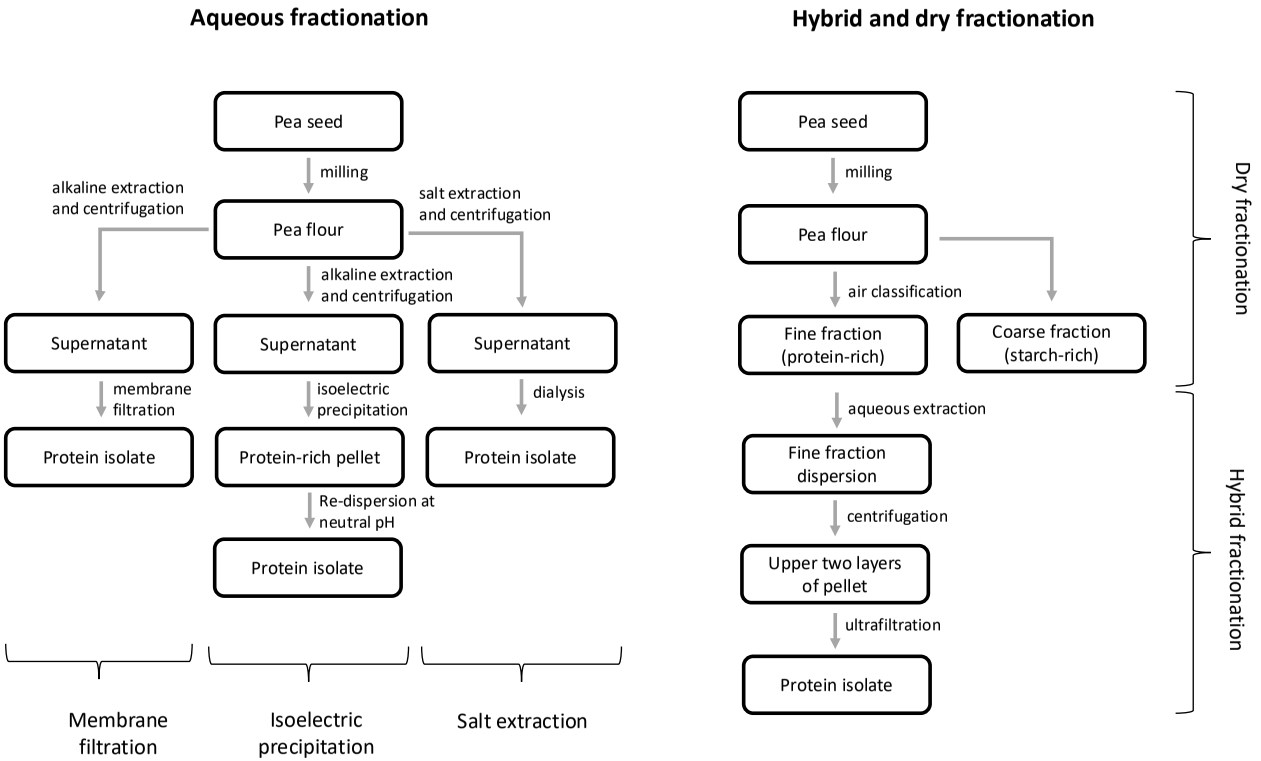

Figure 9.3 Schematic overview of the major fractionation routes applied in literature to obtain pea protein isolates.

extraction process may take place at higher temperatures (50 – 60 °C) [234]. A protein isolate is obtained after re-dispersion of the pellet at neutral pH and subsequent spray or freeze drying. The advantage of the isoelectric precipitation process is that it yields protein ingredients with high protein purities (80 – 90%). On the other hand it requires substantial amounts of energy and water and alters protein functionality as a result of pH changes and heating steps [49].

Salt extraction

Salt extraction is also an aqueous fractionation process commonly reported in literature, which is based on high protein solubility in a certain ionic strength range, also referred to as the salting-in phenomenon [22]. In the salt extraction process, proteins are extracted in salt solutions (e.g. using K_2SO_4, NaCl, KCl) at neutral pH. The extract is centrifuged to remove the solids (i.e., starch granules, cell wall material), where after the supernatant is dialysed to remove the salt [71, 150]. In contrast to isoelectric precipitation where mostly the globulins are recovered, salt extraction

Table. 9.1 Protein content and recovery (sometimes referred to as protein yield in literature) of pea fractions obtained using different fractionation routes. The nitrogen conversion factors used in literature ranges between 5.4 and 6.25 and thus were all protein content values recalculated using a nitrogen conversion factor of 5.7. Articles without information on the nitrogen conversion factor were excluded. All values in the table are expressed on dry powder basis and not dry matter basis. If moisture content data was lacking, the average moisture content from literature was used to convert from dry matter basis to dry powder basis. For the protein recovery, only the articles were included that expressed the recovery as the amount of protein recovered in a pea fraction divided over the initial amount of protein in the flour.

Fractionation routes	**Protein content (wt. % on dry powder basis)**		**Protein recovery (%)**	
Commercial	75.4 ± 5.1	n = 6 [55, 61, 62, 82, 90, 203]	-	
Isoelectric precipitation	75.7 ± 4.5	n = 11 [21, 50, 55, 60, 62-64, 71, 203, 295, 296]	52.7 ± 2.5	n = 3 [21, 60, 203]
Salt extraction	73.9 ± 4.4	n = 5 [50, 60, 71, 295, 296]	39.7	n = 1 [60]
Membrane filtration	79.0 ± 4.9	n = 5 [21, 61, 62, 203, 295]	60.0 ± 4.2	n = 2 [21, 203]
Dry fractionation (fine fraction)	45.5 ± 4.5	n = 6 [55, 56, 63, 82, 295, 297]	-	

results in a mixture of both globulins and albumins, due to the absence of a globulin precipitation step [50].

Membrane filtration

Membrane filtration is an alternative way of aqueous fractionation of legume proteins. The first fractionation steps are often similar to those applied in the isoelectric precipitation process. Pea proteins are extracted from the flour at alkaline conditions (pH 7 – 9) and the insoluble components are separated by centrifugation afterwards. Instead of isoelectric precipitation, the supernatant is further fractionated by membrane filtration [68, 202].

Dry fractionation

Dry fractionation is a fractionation technique that requires no water and less energy (e.g. no drying step is involved). First, the seeds are milled to produce flour with particles of different compositions. In starch-rich legumes such as pea, the storage cells (40 – 140 μm in size) consist of protein bodies (about 1-3 μm in size) and starch granules (5 – 30 μm in size) [57, 282]. The milling conditions are optimized to liberate the starch granules from the storage cells and to fragment the protein-rich regions into particles smaller than the starch granules. Subsequently, the pea flour can be fractionated using air classification, into a fine fraction and coarse fraction, enriched in protein and starch respectively [57, 82]. Electrostatic separation can be deployed as a post-treatment to further increase the purity of the fractions. This technique consists of a step in which the particles are charged by feeding them to a charging tube, followed by a second step in which the charged particles are separated in an electric field [290-292]. Electrostatic separation is based on tribo-electric charging behaviour, which is claimed to be species dependent. Protein bodies from different origins have different shapes, sizes and surface properties, resulting in different tribo-electric charging behaviour [293]

Hybrid fractionation

Aqueous fractionation results in a high protein purity (> 90 %), but also requires substantial amounts of water and energy. The water consumption was estimated to amount 15.2 m^3 to fractionate 1000 kg of pea, while the energy consumption for spray drying was reported to amount 4.8 MJ/kg water removed [171]. Dry fractionation requires less energy than aqueous fractionation – mostly because there is no drying step involved [171] – but results in lower purities, with potential impurities such as anti-nutritional factors and lipids that may oxidize [49, 82, 290]. Therefore, it was proposed to combine the two fractionation methods to synergize their individual

Table 9.2 Relative protein solubility indicating the effect of different fractionation processes on the solubility of pea protein. The relative solubility is defined as the ratio between the protein solubilities of fractionation method in the first column and those of the first row (only within studies and not between studies). The relative solubility values from different studies were averaged and reflect the relative solubility. A higher value reflects a higher protein solubility, with >1 meaning more soluble than the reference, and <1 less soluble than the reference. The numbers following ± are the standard deviations, the number following n represent the number of studies and the numbers between brackets refer to the corresponding literature. All solubility data was obtained from centrifugation experiments. Solubility is thus defined as the amount of protein that remains in the supernatant after solubilization and centrifugation, relative to the amount of dispersed protein prior to centrifugation. Only the solubilities around pH 7 and without added salt were included.

	Commercial		**Isoelectric precipitation**		**Salt extraction**		**Membrane filtration**	**Dry fractionation**
Commercial	1		-		-		-	-
Isoelectric precipitation	6.34 ± 5.46	n = 5 [50, 55, 60, 62, 203]	1		-		-	-
Salt extraction	15.6 ± 2.75	n = 2 [50, 60]	0.86 ± 0.21	n = 4 [60, 71, 295, 296]	1		-	-
Membrane filtration	3.93 ± 1.06	n = 3 [61, 62, 203]	1.23 ± 0.55	n = 4 [21, 62, 203, 295]	1.25	n = 1 [295]	1	-
Dry fractionation (fine fraction)	No data		1.71	n = 1 [63]	1.06	n = 1 [295]	No data	1

advantages. Such a hybrid fractionation process starts with milling followed by air classification. Then the coarse and fine fraction are further fractionated by mild aqueous fractionation through extraction and centrifugation. This hybrid method resulted in a protein purity of 62%, which is lower than extensive aqueous fractionation (80% on dry matter basis) [57, 82, 90, 171].

9.2.2 A broader perspective on the relation between fractionation and functionality

There are a variety of studies focusing on the effect of fractionation processes on pea protein functionality. Geerts et al. (2018) advocated that fractionation processes should not only be assessed in terms of their sustainability, but also in terms of resulting plant protein functionality [294]. In this section data from multiple studies is combined to investigate the effect of different fractionation processes on functionality. The type of functionalities discussed here include solubility, gel, foam and emulsion properties. Also, the effect of fractionation on protein content and protein recovery is included. Quantifying the protein content and solubility allowed us – after some recalculations and conversions – to bundle the results of a variety

Table 9.3 The average solubility of pea protein isolates obtained using different fractionation methods. Note that, in contrast to Table 9.2, this table provides an average of different studies, although results were obtained at different sample and centrifugation conditions. The numbers following ± are the standard deviations, the number following n represent the number of studies and the numbers between brackets refer to the corresponding literature.

Fractionation routes	Protein solubility (%)	
Commercial	18 ± 11	n = 6 [50, 55, 60-62, 203]
Isoelectric precipitation	66 ± 15	n = 11 [21, 50, 55, 60, 62-64, 71, 203, 295, 296]
Salt extraction	68 ± 24	n = 5 [50, 60, 71, 295, 296]
Membrane filtration	80 ± 17	n = 5 [21, 61, 62, 203, 295]
Dry fractionation (fine fraction)	72 ± 11	n = 3 [63, 295, 297]

Table 9.4 The influence of different fractionation routes of pea protein on their gelling properties. Only results obtained within the same study were compared.

Fractionation routes	Fractionation conditions	Results		Reference
Commercial Dry fractionation (DF)	Commercial: obtained from Roquette DF: The seeds were milled and air classified into a fine (protein-rich) fraction and a coarse fraction. The air flow was fixed at 52 m^3/h and the classifier wheel speed at 6000 rpm.	Gel firmness Commercial: 9 N DF: 2.5 N		Pelgrom et al. (2015) [82]
Commercial Isoelectric precipitation (IEP)	Commercial: obtained from ProPulse IEP: extraction at pH 8.5 and precipitation at pH 4.5.	Gel firmness Commercial: 12.5 kPa IEP: 11.05 kPa **Gel strength expressed as the strain at fracture. Higher indicates more ductile.*	Gel strength* Commercial: 0.62 IEP: 0.80	Shand et al. (2007) [55]
Isoelectric precipitation (IEP) Membrane filtration (MF)	IEP: Proteins were extracted at pH 9.5 and precipitated at pH 4.5. MF: The supernatant obtained after extraction at pH 9.5 and centrifugation was further fractionated by ultrafiltration using a 50 kDa cut off membrane.	Least gelling concentration IEP: 11.4 % (w/v) protein MF: 10.1 % (w/v) protein *LCG was recalculated here to protein concentration based on the protein content of the pea fractions.*		Boye et al. (2010) [21]
Isoelectric precipitation (IEP) Salt extraction (SE) Membrane filtration (MF) Dry fractionation (DF)	IEP: Extraction at pH 9 and precipitation at pH 4.5. MF: Extraction at pH 9 and ultrafiltration using a 5 kDa cut off membrane. SE: Extraction in a 0.1 M sodium phosphate buffer (pH 8). The extract was dialysed using a 0.5 – 1.0 kDa cut off membrane. DF: An air classified fine fraction was Obtained from the Alberta's Food Processing Development Centre.	Gel firmness (G') IEP: 0.67 kPa SE: 1.06 kPa MF: 3.83 kPa DF: -	Least gelling concentration IEP: 16% (w/v) protein SE: 12 % (w/v) protein MF: 12 % (w/v) protein DF: 18 % (w/v) protein	Yang et al. (2021) [295]

of studies. For gels, emulsions and foam properties, fewer studies were available that linked fractionation to a well-defined functionality. In these cases, results are primarily compared within the same study. The results gathered from a variety of literature sources are compared to the results in this thesis.

Protein content and recovery

Table 9.1 shows the effect of different fractionation routes on the protein content (wt. % protein on dry powder basis) and protein recovery / yield (defined as the recovery as the amount of protein recovered in a pea fraction divided over the initial amount of protein in the flour). Dry fractionation used to obtain a protein-enriched fine fraction results in the lowest protein content. Isoelectric precipitation and salt extracted pea protein isolate are comparable to commercial pea protein isolate in terms of protein content. When membrane filtration is used, the protein content is slightly higher, making it the most suitable fractionation route when a high protein purity is required. This can probably be attributed to the fact that with membrane filtration both globulins and albumins are recovered [152], while the other fractionation routes only yield globulins. Probably for the same reason, membrane filtration also results in the highest protein recovery. The lowest protein recovery is observed for salt extracted pea protein isolate. Fig. 9.4 shows the relation between protein content and protein recovery in a yield – purity curve, also showing that membrane filtration results in the highest protein content and recovery. The protein recovery using dry fractionation is highly dependent on the classifier wheel speed and the mill type

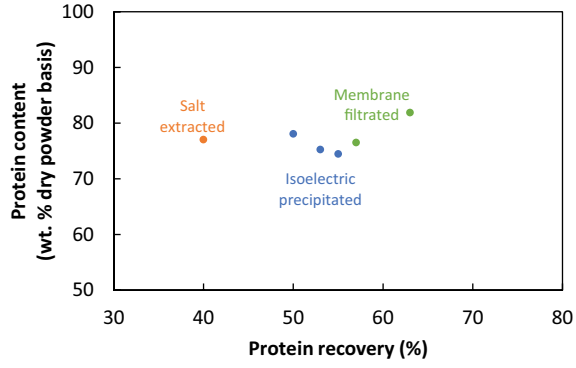

Figure 9.4 Relationship between protein content and protein recovery of different fractionation routes (sometimes referred to as yield-purity curve). Only the studies were included that expressed the recovery as the amount of protein recovered in a pea fraction divided over the initial amount of protein in the flour. Only a limited number of studies determined both the protein content and protein recovery, according to the definition in the previous sentence.

used. Pelgrom et al. (2013) showed that the protein content is inversely related to the protein yield. The highest protein yield (75%) was observed at the lowest classifier speed and the highest protein content (55%) was observed at the highest classifier speed [56].

Pea protein dispersions and gels

The literature was combined in a similar way to study the effect of fractionation routes on pea protein solubility. It has been reported that harsh processing, such as pH and temperature changes and the use of chemicals, leads to protein denaturation and a lower protein solubility (at neutral pH and room temperature) [60, 150]. Protein solubility can serve as an indicator for the extent fractionation has induced denaturation and aggregation. A lower solubility also influences other properties, such as emulsifying and gelling properties [55, 205, 213]. Solubility is sometimes also considered a practical indicator for the remaining protein functionality [125]. However, a low solubility may also be beneficial for specific applications, especially when semi-solid products such as meat analogues are aimed for [126, 127].

Table 9.2 shows relative solubilities to indicate the effect of different fractionation routes on the solubility of pea protein isolates. In this table, only solubilities within studies were compared, because different sample and measurements conditions were used in different studies. Table 9.3 was included to show the average solubility values of the pea protein isolates obtained using different fractionation routes. Tables 9.2 and 9.3 show that the commercial fractionation route consistently results in the lowest solubility (i.e., relative solubility < 1) compared with the other fractionation routes (n = 6). Salt extraction results in a better solubility than commercial pea protein isolate, but a lower solubility than the other fractionation routes. Isoelectric precipitation shows a higher solubility (> 1) than commercial and salt extraction, but lower than membrane filtration and dry fractionation. It thus shows membrane filtration is most suitable to obtain highly soluble pea proteins. This high solubility was also found in **Chapter 7**, where it was reported that diafiltration led to a higher pea protein solubility, even comparable with whey protein isolate. Also, dry fractionation seems to yield pea proteins with a high solubility, but the number of studies supporting this statement is limited.

Regarding the solubility of isoelectric precipitation pea protein isolate; it was found in **Chapter 2**, that part of the soluble protein is present as aggregates. In a more recent study, it was shown that the particle size distribution after isoelectric precipitation changed from multimodal at 0.1 M NaCl to monomodal at 2 M NaCl

Table 9.5 The influence of different fractionation routes of pea protein on their emulsifying properties. Emulsion droplet size depends on different process parameters and sample conditions, and thus is this table primarily suitable to compare results within studies

Fractionation routes	Fractionation conditions	Results	Reference
Commercial Limited fractionation (LF)	Commercial: obtained from Roquette LF: suspending the flour and centrifugation (2x) to separate solids and non-soluble proteins.	D [3,2] at 30% (w/v) oil Commercial: 1.2 μm LF: 1.0 μm *The heated emulsion from the LF pea protein showed a higher viscosity.*	Geerts et al. (2017) [90]
Isoelectric precipitation (IEP) Salt extraction (SE)	IEP: extraction at pH 9.5 and precipitation at pH 4.5. SE: Extraction in a 0.1 M phosphate buffer (pH 8) with 6.4% KCl	D [3,2] at 50 wt. % oil IEP: 1.85 μm SE: 8.90 μm ESI at 50 wt. % oil IEP: 12.4 min SE: 10.9 min	Karaca et al. (2011) [71]
Isoelectric precipitation (IEP) Membrane filtration (MF)	IEP: defatting with petroleum ether, extraction at pH 9.5 and precipitation at 4.5. MF: extraction at pH 9.5 and precipitation and ultrafiltration of the supernatant with a cut-off at 5 kDa.	D [3,2] at 50 wt. % oil IEP: 14.7 μm MF: 16.8 μm	Makri et al. (2005) [152]

[60]. This indicates that pea protein soluble aggregates, as discussed in **Chapter 2**, are only being formed at low salt concentrations. It is important to note that these results are thus not generic but depend on salt concentration. In **Chapter 3 and 4** it was also found that salt concentration had an important effect on the functionality. Coacervates were only formed at specific salt concentrations, and the gel strength was affected by the amount of salt present in the pea protein fractions. Not only fractionation, but also subtle effects, such as, the salt concentration are important factors to consider in the context of pea protein functionality.

Table 9.4 gives an overview on how fractionation affects gel properties of pea protein. In literature there are different methods of characterizing gel properties, including oscillatory shear rheology, compressional rheology and the least gelation concentration (LCG). Given the variety in sample conditions and measurement conditions, we compare results that were obtained within individual studies only. The study of Pelgrom et al. (2015) indicates that dry fractionated protein form softer gels than commercial pea protein [82]. Dry fractionation pea protein also had the highest LCG (i.e. the protein concentration required to form a self-supporting gel) [295]. The study of Shand et al. (2007) suggests that commercial and isoelectric precipitation pea protein yield almost similar gel firmness [55]. This is in line with what has been observed in **Chapter 7**, where commercial and isoelectric precipitated pea protein isolate had similar gel firmness over a range of concentrations. What is also consistent with the results of **Chapter 7** where it was found that membrane filtration results in the firmest pea protein gels and requires the least protein to form a self-supporting gel [21, 295].

Incorporation of oil and air

There are only few studies that compare the effect of different fractionation routes on the emulsification properties of pea protein. Some studies express the emulsification properties in terms of the emulsifying activity index (EAI) and emulsifying capacity (EC), while others use the average droplet size, also to determine droplet stability over time [21, 71, 90, 152]. However, the EC and EAI may not be the best parameters to quantify emulsion properties [298]. The EC is defined as the oil volume that can be emulsified per gram of protein. These EC values vary greatly throughout literature, and may sometimes reflect the amount of oil required to induce phase inversion, rather than the emulsifying capacity [299]. A disadvantage of comparing the EAI values reported in literature, is that they are often based on an older and incomplete definition from Pearce & Kinsella (1978) [300], even though the definition has been revised in more recent years [301]. Therefore, it was chosen to provide an overview

Table 9.6 The influence of different fractionation routes of pea protein on their foaming properties. The foam capacity was defined as the volume of the foam divided by the volume of the liquid. Because of different foaming conditions and sample conditions, results should be compared within the same study.

Fractionation routes	Relevant parameters	Results		Reference
Commercial Isoelectric precipitation (IEP) Salt extraction (SE)	Commercial: obtained from NutriPea IEP: protein from defatted flour was extracted at pH 9.5 and precipitated at 4.5. SE: protein from defatted flour was extracted in a 0.1 sodium phosphate buffer (pH 8) with 6.4% KCl. The supernatant was dialyzed with a cut-off at 6-8 kDa.	Foam capacity (FC) Commercial: 81% IEP: 167% SE: 229% *Foaming properties were also influenced by cultivar. The average of the different cultivar foam capacities was used here.*		Stone et al. (2015) [50]
Commercial Isoelectric precipitation (IEP) Membrane filtration (MF)	Commercial: obtained from Cosucra IEP: Extraction at unadjusted pH. The protein were precipitated at pH 3.4. MF: The same protein extract as in the IEP procedure was used. This extract was further fractionated by ultrafiltration with a cut off size of 5 kDa.	Foam capacity (FC) Commercial: 351% IEP: 351% MF: 377% **The foam stability was expressed relative to the commercial PPI*	Foam stability (FS)* Commercial: 100% IEP: 51% MF: 82%	Fuhrmeister & Meuser (2003) [62]
Isoelectric precipitation (IEP) Dry fractionation (DF)	IEP: Dehulled seeds were hydrated, grinded and sieved to remove cell wall material. Proteins were acid extracted (pH 2.5-3.0) and precipitated at their isoelectric point. DF: Dehulled seeds were pin milled to about 325-mesh and air classified at a cut off point of about 15 (800-mesh). The fine fraction was used as a protein-enriched fraction.	Foam capacity (FC) IEP: 153% DF: 274% *Foam stability was defined here as the time required for the volume to reduce by half.*	Foam stability (FS)* IEP: 60 min DF: >120 min	Sosulski & McCurdy (1987) [63]

Isoelectric precipitation (IEP) Membrane filtration (MF)	IEP: Proteins were extracted at pH 9.5 and precipitated at pH 4.5. MF: The supernatant obtained after extraction at pH 9.5 and centrifugation was further fractionated by ultrafiltration using a 50 kDa cut off membrane.	Foam capacity (FC) IEP: 580% MF: 590%	Boye et al. (2010) [21] Achouri et al. (2005) [302]
Isoelectric precipitation (IEP) Membrane filtration (MF)	IEP: Proteins were extracted at pH 9.5 and precipitated at pH 4.5. MF: The supernatant obtained after extraction at pH 9.5 and centrifugation was further fractionated by ultrafiltration using a 5 kDa cut off membrane.	Foam capacity (FC) IEP: 320% MF: 500%	Makri et al. (2005) [152]

of literature, where the droplet sizes were included. Because droplet size depends on different factors, such as emulsification method, only results within studies were compared. Table 9.5 shows that pea protein fractionated using isoelectric precipitation yields emulsions with smaller droplets, compared to salt extraction and membrane filtration. When commercially and limited fractionated pea proteins were compared the corresponding emulsion droplet sizes were similar. However, the number of studies is limited, and the processes used to obtain emulsions vary from each other. In **Chapter 6**, it was found that isoelectric precipitation and membrane filtration (i.e. diafiltration) resulted in very similar emulsion properties and droplet sizes, which is in line with the study of Makri et al. (2005). The result of **Chapter 5** also showed that the extent of fractionation did not significantly affect emulsion properties, consistent with the study of Geerts et al. (2017). However, the type of proteins used as stabilizer were important, as globulins appeared to be better emulsifiers than albumins (**Chapter 5)**. Based on the results of **Chapters 5 and 6** it can be concluded that if globulins are used as emulsifiers, the method of fractionation used is less relevant, at least at pH 7 and beyond the critical protein concentration. Table 9.5 is consistent with those results, but also shows that alternative fractionation routes, such as salt extraction, might impact the emulsifying properties of pea proteins .

Table 9.6 provides an overview of the relation between different fractionation routes and the foaming properties of the resulting fractions. To express the foam properties often the foam capacity and foam stability are used as parameters. Foam capacity is mostly standardized throughout literature, and typically defined as the ratio of the foam volume to the initial liquid volume (before foaming) expressed as a percentage. The definition of foam stability is less well-defined and is specified in Table 9.6 when applicable. It can be observed that commercial pea protein isolate has poorer foaming properties than the isolates obtained via isoelectric precipitation, salt extraction or membrane filtration [50, 62]. This might be related to the denatured and aggregated state of commercial pea protein. Also, protein fractions produced by isoelectric precipitation – known to induce protein aggregation – consistently show a lower foaming capacity. It appears that membrane filtration yields pea protein fractions with good foaming properties. One of the differences between membrane filtration and other fractionations techniques, such as, salt extraction and isoelectric precipitation, is that not only globulins but also albumins are recovered [152]. In **Chapter 5** it was concluded that particularly pea albumins had a high foaming capacity, which may explain why membrane filtration – also recovering albumins – consistently yield pea protein isolates with better foaming properties.

9.3 Towards the application of pea protein as a functional ingredient

This thesis offers new insights on pea protein fractionation and functionality but did not yet address the applicability of pea protein in food products. To apply plant protein – such as pea protein – in food products there are additional factors to consider besides functionality. These factors include sustainability, nutritional value, and organoleptic properties such as, colour and flavour.

9.3.1 Sustainability

The main driving force behind the protein transition is the urge for a more sustainable food production. It is the consensus that production of plant proteins is more sustainable than animal-derived proteins, and that food products with plant proteins are thus more sustainable than, for instance, meat and dairy products. While this may be generally conceived as true, it is important to remain critical on how sustainable the plant protein alternative really is. Production of plant proteins can be more sustainable. Extensive processes often used require chemicals to de-fat the flour or to aid the extraction process. Also, substantial amounts of water are used to extract the proteins, which subsequently leads to saline waste streams due to the use of caustic soda and hydrochloric acid. Finally, the protein extract needs to be dried, requiring substantial amounts of energy. The resulting plant protein isolate typically has a purity of around 90%, but the protein yield is often only 50 – 60%, which implies a loss of 40 – 50% protein [149]. Mild fractionation may not only yield specific functionalities, but has also been reported to be more sustainable [171].

9.3.2 Nutritional value

A healthy diet, needed to support human health and growth, contains a sufficient amount of nutrients. These nutrients include micro-nutrients (minerals and vitamins), and macro-nutrients (fats, carbohydrates and proteins). Most plant proteins lack one or more of the nine essential amino acids (i.e. the amino acids that cannot be synthesized by the human body and has to come from the diet) [303]. In the case of pea, the essential amino acid that is lacking is Tryptophan [281]. Table 9.7 shows that animal-based products have an essential amino acid composition closer to what an adult human being requires.

Foods of plant origin are often good sources of different vitamins, but less abundant in certain trace minerals (e.g., iron and zinc). Animal-based products on the other hand or often abundant in minerals, and sometimes these minerals are also better

Table. 9.7 Protein quality of plant and animal-based sources expressed in digestible indispensable amino acid score (DIAAS), with a higher value representing an essential amino acid composition closer to the requirement of an adult human being

Protein source	Essential amino acids score (DIAAS)
Beef	112
Milk	114
Egg	113
Soy	89
Green lentil	65
Chickpea	83
Wheat	45
Yellow pea	73
Pea protein concentrate	82

absorbed by the human small intestine when coming from an animal-based food (e.g. iron). From the plant protein sources, legumes are relatively high in different minerals, but not as complete as animal-based foods such as milk and meat [304].

The higher nutritional quality of animal-derived proteins is reached by ample nutrient supplementation to the feed. On the one hand, one could argue that part of our diet should still contain animal-derived proteins because it reduces the risk on nutrient deficiency. On the other hand, it could be more sustainable if the crops, now used for feed, would be used for human nutrition directly. This thesis provides insights on the functionality of plant protein in plant-based and hybrid plant-dairy based model foods. For the application of particularly pure plant-based foods, it could be important to involve nutritionists to ensure that plant-based alternatives are nutritionally as complete as possible.

Plant protein sources, such as legumes, also contain antinutritional factors. These include protease inhibitors, phytate and lectins. Protease inhibitors, which disrupt protein digestion [305], are mainly present in the pea cotyledon, and their trypsin inhibiting activity is about 13 times higher than in the hulls [306]. Protease inhibitors can be inactivated by heat, for instance by extrusion at 125 °C [307]. Also the phytate and tannin content of peas could be greatly reduced by heat treatment [308]. Also other methods, such as soaking, cooking and germination have been reported to remove some antinutritional factors, but often a combination of methods is required to reach sufficient removal [309]. Generally, processing treatments used to commercially produce legume proteins, improve digestibility thanks to the inactivation of antinutrients

(e.g. trypsin inhibitors) [305]. A challenge in plant protein manufacturing could be to design fractionation processes in such a way that antinutritional components are most optimally reduced, while the desired protein functionality remains unaffected.

9.3.3 Organoleptic properties

Also, the sensory perception of plant-based foods are important. Colour and flavour of plant protein ingredients may affect consumer acceptability of plant-based foods. Pea protein isolates often have a yellowish or brownish colour. However, limited studies have reported the colour of pea protein fractions, and how to reduce them. A recent study of Carmo et al. (2020) reported that de-hulling could make the colour of faba bean protein fractions light [310]. Off-flavours in pea have been more extensively studied. Volatiles that are associated to a beany flavour are naturally found in peas, but can also stem from fatty acid degradation, microbial spoilage or thermal degradation after harvesting [311]. Gao et al. (2020) quantified six volatiles that were associated with a beany flavour in foods, using SPME-GC-MS. They reported that an alkaline extraction pH of 9 resulted in significant lower amounts of these volatiles, compared with a pH of 8.5 and 9.5. In another study conducted by Wang and Arntfield (2015) the effect of salt and pH on flavour binding to pea proteins was examined. The authors found that higher salt concentrations (i.e. NaCl and $CaCl_2$) caused an increased binding of proteins to flavour molecules. The highest percentage of flavours bound as function of pH was reported to be at pH 5 [312]. This implies isoelectric precipitation (pH 4 – 5) not only reduces functional properties such as gelling capacity, but also induces the binding of flavour molecules to the proteins.

The pea fractions used in this thesis were also quantified on their volatiles, following the procedure of Gao et al. (2020). Six volatiles were selected that are generally associated with a beany or grassy flavour (Hexanal, 1-Pentanol, 1-Octen-3-ol, 3,5-Octadien-2-one), unpleasant or goat-like (Hexanoic acid) and pungent, rancid or tallow (Heptanoic acid) [313-315]. Fig. 9.5 shows the abundance of these volatiles relative to those in pea flour for PPCn, PPCa, ALB-F, PPIp, PPId and PPIc. It appears that particularly the mildly fractionated protein – such as PPIn and PPId – are high in off-flavours. These two fractions have in common that pH adjustments were avoided. These mild conditions may also have favoured the concentration of flavour components, or indirectly, components responsible for off-flavours (e.g. lipoxygenase). The most extensively fractionated PPIp and PPIc, were least abundant in the volatile components measured. This indicates that there may be a

trade-off between mildly fractionated pea protein with high functionality potential (e.g. high and low solubility can still be controlled by fractionation) and more off-flavours, and extensively fractionated pea protein with low functionality potential and fewer off-flavours. For the application of mildly processed pea fractions, it may thus be required to decrease the off-flavours in alternative ways. Tools to reduce off-flavours may include germination prior to fractionation, membrane filtration, enzymatic treatment, soaking and thermal treatment [311]. Alternatively, pea off-flavours could be masked using flavour masking substances. However, reducing colour and flavour in pea protein fractions upon fractionation would make them more easily and broadly applicable in food applications.

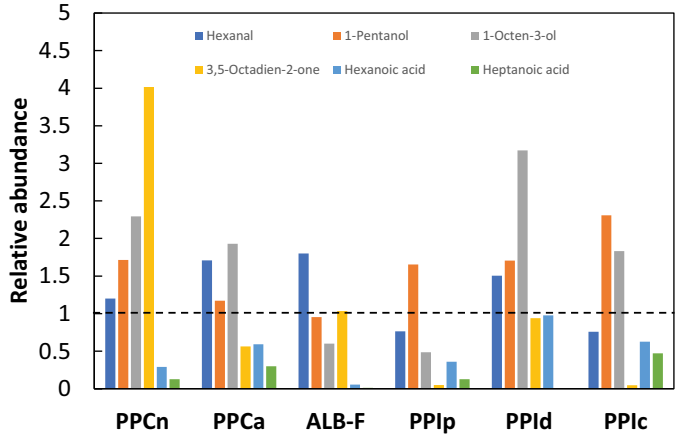

Figure 9.5 The abundance of six volatiles that were associated to off-flavours in the pea fractions from this thesis, all expressed relative to pea flour. The relative abundance was determined using HS-SPME-GC-MS following the protocol of Gao et al. (2020). The dashed line represents pea flour.

9.4 Conclusion and outlook

In this thesis we found that fractionation influences protein functionality. The highest functionality potential was observed when fewest processing steps were used. Each processing step reduces the functionality potential of pea protein (e.g., the variety of functionality pea protein can display). A careful design of the fractionation process can lead to a functionality that is tailored to specific product applications, while being more sustainable than conventional fractionation processes. In this concluding section, an outlook is provided with respect to the protein transition and the application of plant protein in foods.

9.4.1 Similarities and differences between legume proteins

With plant proteins becoming more important in the food industry, it is relevant to know the exchangeability of the ingredients and ingredient sources. This is relevant because when a certain ingredient is lacking, or becoming more expensive, it may need to be replaced by another with similar properties. Extensive research has been done on legumes, particularly soy, but is seems also essential to know to what extent the proteins in these legumes are similar. When looking at the extraction and precipitation conditions of legume proteins, they are all rather similar [22]. These conditions are based on the solubility of legume proteins, which is typically highest at alkaline pH and lowest at acidic pH values [316]. Their solubility is related to their charge and tendency to aggregate as a function of pH and similar charge dependencies on pH has been reported for different legumes, such as faba bean, lentil and yellow pea [317]. In terms of functionality, it was found that albumins from Bambara groundnut, mung bean and yellow pea consistently showed high foam ability and stability, while the globulins from these sources showed better emulsifying properties than albumins [318]. It was also reported that pea protein isolate and soy protein isolate show similar behaviour, at least qualitatively [319]. For both protein isolate gels the stiffness increased when electrostatic repulsion was decreased [320, 321]. Generality between legumes can thus also be found in their functional behaviour.

However, one cannot simply conclude that proteins from different legumes have the same functionality. Also differences in legume protein functionality have been reported. The main question is how the influence of legume type relates to the influence of other major factors. Examples of factors that also influence functionality are the legumin to vicilin ratio (which vary between legume varieties), batch-to-batch variation, composition of plant protein extracts, storage conditions and fractionation conditions [22, 255]. It would thus be valuable to identify the contributions of the main

factors influencing legume protein functionality, to know their exchangeability and possible improve their exchangeability.

9.4.2 Globulins and albumins are functionally distinct

The majority of studies on pea protein functionality do not distinguish between globulins and albumins, but primarily focus on globulins. The reason may be that pea protein fractionation often only recover globulins. However, Chapters 5 and 8 of this thesis illustrate that albumin can be highly functional in terms of foaming properties, and gelling properties when used as a partial substitute for WPI. It would be of great interest to study the functional properties of pea (and other legume) albumins in different food model systems. Pea globulins will probably remain the main protein stream, as around 70 – 80% of the pea proteins are globulins [73]. However, the resource efficiency of pea could increase when also the albumins are used as functional ingredients. In an ideal scenario this would lead to a situation where globulins and albumins are considered functionally distinct.

9.4.3 Hybrid plant-dairy protein foods

In recent years there has been some focus on interactions between pea protein and dairy proteins in functional model foods [79-81, 233, 322]. However, much more attention could be paid to such hybrid food products in the light of the protein transition. Analogous to the automotive industry, hybrid products can be a first and significant step towards the transition to more plant-based proteins. The advantage of a mixture of plant and dairy ingredients is that it is easier to maintain the texture and taste of dairy based products that it aims to replace. Moreover, as described earlier in this chapter, animal-derived proteins are often of better nutritional quality. Hybrid foods could contribute to a shift towards more plant-based proteins, while keeping it easier for consumers to have nutritionally complete diets. Therefore, it would be relevant if more research focuses on hybrid foods, thereby consider the current food textures that dairy and meat products deliver.

9.4.4 Functionality tailored fractionation

Functionality tailored fractionation is an optimization relative to the way pea proteins are fractionated now. Generally, pea protein is commercially available in the form of pea protein concentrates and isolates, which has the advantage that the plant protein portfolio is limited and clear. Moreover, pea protein isolates are high in protein and low in impurities, which reduces the amount of undesired component such as anti-nutrients or those causing off-

flavours. In case of tailored fractionation, more attention needs to be paid to the presence of undesired impurities. Also, shorter supply chains may be needed, as longer supply chains would require heat treatment of the ingredients to prevent enzymatic and microbial spoilage. Shorter supply chains may imply that a (major) food manufacturer fractionates raw ingredients on site and apply them in food products directly.

Tailored fractionation could bring us plant protein ingredients that are more functional, while requiring less water and energy to produce, compared with commercial plant protein isolates. This thesis provides a framework on the relation between fractionation, molecular and microstructural characteristics, and functionality, but it is not complete. Further research is needed to obtain a complete overview of how tailor-made mixtures can be obtained – ideally without generating any by-products – with a wide range of functional applications in food products. The first step towards that direction has been taken in this thesis, showing that tailored fractionation can be used to unlock a variety in functionality for pea protein.

References

1. Moschis, G.P., A. Mathur, and R. Shannon, Toward Achieving Sustainable Food Consumption: Insights from the Life Course Paradigm. Sustainability, 2020. **12**(13): p. 5359.

2. Aiking, H., Future protein supply. Trends in Food Science & Technology, 2011. **22**(2-3): p. 112-120.

3. Springmann, M., et al., Options for keeping the food system within environmental limits. Nature, 2018. **562**(7728): p. 519-525.

4. Lillford, P. and A.-M. Hermansson, Global missions and the critical needs of food science and technology. Trends in Food Science & Technology, 2021. **111**: p. 800-811.

5. Tziva, M., et al., Understanding the protein transition: The rise of plant-based meat substitutes. Environmental Innovation and Societal Transitions, 2020. **35**: p. 217-231.

6. Osen, R., et al., High moisture extrusion cooking of pea protein isolates: Raw material characteristics, extruder responses, and texture properties. Journal of Food Engineering, 2014. **127**: p. 67-74.

7. Smetana, S., et al., Meat alternatives: life cycle assessment of most known meat substitutes. The International Journal of Life Cycle Assessment, 2015. **20**(9): p. 1254-1267.

8. Bleakley, S. and M. Hayes, Algal proteins: extraction, application, and challenges concerning production. Foods, 2017. **6**(5): p. 33.

9. Loveday, S., Plant protein ingredients with food functionality potential. Nutrition Bulletin, 2020. **45**(3): p. 321-327.

10. Conlan, S., et al., Characterisation of the yam tuber storage protein dioscorin. Journal of plant physiology, 1998. **153**(1-2): p. 25-31.

11. Madar, Z. and A.H. Stark, New legume sources as therapeutic agents. British Journal of Nutrition, 2002. **88**(S3): p. 287-292.

12. Tenorio, A.T., et al., Understanding differences in protein fractionation from conventional crops, and herbaceous and aquatic biomass-Consequences for industrial use. Trends in Food Science & Technology, 2018. **71**: p. 235-245.

13. Brouwer, P., et al., Aquatic weeds as novel protein sources: Alkaline extraction of tannin-rich Azolla. Biotechnology Reports, 2019. **24**: p. e00368.

14. Delgado, M., F. Ligero, and C. Lluch, Effects of salt stress on growth and nitrogen fixation by pea, faba-bean, common bean and soybean plants. Soil Biology and Biochemistry, 1994. **26**(3): p. 371-376.

15. Giller, K.E. and G. Cadisch, Future benefits from biological nitrogen fixation: an ecological approach to agriculture, in Management of biological nitrogen fixation for the development of more productive and sustainable agricultural systems. 1995, Springer. p. 255-277.

16. Raza, A., et al., Nitrogen Fixation of Legumes: Biology and Physiology, in The Plant Family Fabaceae. 2020, Springer. p. 43-74.

17. Berghout, J., et al., TiFN project 16SS02. Safeguarding Product structure and mechanical properties while using new sustainable sources and processing steps: a multiscale and interdisciplinary approach. Crop / ingredient choice. 2017: Wageningen.

18. Boukid, F., C.M. Rosell, and M. Castellari, Pea protein ingredients: A mainstream ingredient to (re) formulate innovative foods and beverages. Trends in Food Science & Technology, 2021.

19. Eppendorfer, W.H. and B.O. Eggum, Sulphur amino acid content and nutritive value of pea and cauliflower crude protein as influenced by sulphur deficiency. Zeitschrift für Pflanzenernährung und Bodenkunde, 1995. **158**(1): p. 89-91.

20. Adebiyi, A.P. and R.E. Aluko, Functional properties of protein fractions obtained from commercial yellow field pea (Pisum sativum L.) seed protein isolate. Food Chemistry, 2011. **128**(4): p. 902-908.

21. Boye, J., et al., Comparison of the functional properties of pea, chickpea and lentil protein concentrates processed using ultrafiltration and isoelectric precipitation techniques. Food Research International, 2010. **43**(2): p. 537-546.

22. Boye, J., F. Zare, and A. Pletch, Pulse proteins: Processing, characterization, functional properties and applications in food and feed. Food Research International, 2010. **43**(2): p. 414-431.

23. Brummer, Y., M. Kaviani, and S.M. Tosh, Structural and functional characteristics of dietary fibre in beans, lentils, peas and chickpeas. Food Research International, 2015. **67**: p. 117-125.

24. Ratnayake, W.S., R. Hoover, and T. Warkentin, Pea starch: composition, structure and properties—a review. Starch-Stärke, 2002. **54**(6): p. 217-234.

25. Millar, K., et al., Proximate composition and anti-nutritional factors of fava-bean (Vicia faba), green-pea and yellow-pea (Pisum sativum) flour. Journal of Food Composition and Analysis, 2019. **82**: p. 103233.

26. Holl, F. and J. Vose, Carbohydrate and protein accumulation in the developing field pea seed. Canadian Journal of Plant Science, 1980. **60**(4): p. 1109-1114.

27. Carnovale, E., E. Lugaro, and G. Lombardi-Boccia, Phytic acid in faba bean and pea: effect on protein availability. Cereal Chemistry, 1988. **65**(2): p. 114-117.

28. Schroeder, H.E., Quantitative studies on the cotyledonary proteins in the genus Pisum. Journal of the Science of Food and Agriculture, 1982. **33**(7): p. 623-633.

29. Osborne, T.B., The vegetable proteins. 1924: Longmans, Green and Company.

30. Gatehouse, J.A., et al., The synthesis and structure of pea storage proteins. Critical Reviews in Plant Sciences, 1984. **1**(4): p. 287-314.

31. Barać, M.B., et al., Techno-functional properties of pea (Pisum sativum) protein isolates-a review. Acta Periodica Technologica, 2015. **46**: p. 1-18.

32. Djoullah, A., et al., Native-state pea albumin and globulin behavior upon transglutaminase treatment. Process Biochemistry, 2015. **50**(8): p. 1284-1292.

33. Gueguen, J., et al., Dissociation and aggregation of pea legumin induced by pH and ionic strength. Journal of the Science of Food and Agriculture, 1988. **44**(2): p. 167-182.

34. Mertens, C., et al., Agronomical factors influencing the legumin/vicilin ratio in pea (Pisum sativum L.) seeds. Journal of the Science of Food and Agriculture, 2012. **92**(8): p. 1591-1596.

35. Swanson, B.G., Pea and lentil protein extraction and functionality. Journal of the American Oil Chemists' Society, 1990. **67**(5): p. 276-280.

36. Barac, M., et al., Profile and functional properties of seed proteins from six pea (Pisum sativum) genotypes. International Journal of Molecular Sciences, 2010. **11**(12): p. 4973-4990.

37. Pedrosa, C., C. Trisciuzzi, and S.T. Ferreira, Effects of glycosylation on functional properties of vicilin, the 7S storage globulin from pea (Pisum sativum). Journal of Agricultural and Food Chemistry, 1997. **45**(6): p. 2025-2030.

38. Tzitzikas, E.N., et al., Genetic variation in pea seed globulin composition. Journal of Agricultural and Food Chemistry, 2006. **54**(2): p. 425-433.

39. Casey, R., Pea legumins and vicilins. Industrial Proteins in Perspective, 2003. **23**: p.

49-55.

40. O'Kane, F.E., et al., Characterization of pea vicilin. 1. Denoting convicilin as the α-subunit of the Pisum vicilin family. Journal of Agricultural and Food Chemistry, 2004. **52**(10): p. 3141-3148.

41. O'Kane, F.E., et al., Characterization of Pea Vicilin. 2. Consequences of Compositional Heterogeneity on Heat-Induced Gelation Behavior. Journal of Agricultural and Food Chemistry, 2004. **52**(10): p. 3149-3154.

42. Park, S.J., T.W. Kim, and B.K. Baik, Relationship between proportion and composition of albumins, and in vitro protein digestibility of raw and cooked pea seeds (Pisum sativum L.). Journal of the Science of Food and Agriculture, 2010. **90**(10): p. 1719-1725.

43. Vioque, J., et al., Comparative study of chickpea and pea PA2 albumins. Journal of agricultural and food chemistry, 1998. **46**(9): p. 3609-3613.

44. Higgins, T., et al., Gene structure, protein structure, and regulation of the synthesis of a sulfur-rich protein in pea seeds. Journal of Biological Chemistry, 1986. **261**(24): p. 11124-11130.

45. Gupta, R.K., S.S. Gangoliya, and N.K. Singh, Reduction of phytic acid and enhancement of bioavailable micronutrients in food grains. Journal of food science and technology, 2015. **52**(2): p. 676-684.

46. Le Guen, M.-P., Pea proteins for piglets: effects on digestive processes. 1993: Wageningen University and Research.

47. Vigeolas, H., et al., Combined metabolomic and genetic approaches reveal a link between the polyamine pathway and albumin 2 in developing pea seeds. Plant physiology, 2008. **146**(1): p. 74-82.

48. Clemente, A., et al., Eliminating anti-nutritional plant food proteins: the case of seed protease inhibitors in pea. PLoS One, 2015. **10**(8): p. e0134634.

49. Schutyser, M.A.I. and A.J. van der Goot, The potential of dry fractionation processes for sustainable plant protein production. Trends in Food Science & Technology, 2011. **22**(4): p. 154-164.

50. Stone, A.K., et al., Functional attributes of pea protein isolates prepared using different extraction methods and cultivars. Food Research International, 2015. **76**: p. 31-38.

51. Fredrikson, M., et al., Production process for high-quality pea-protein isolate with low content of oligosaccharides and phytate. Journal of agricultural and food chemistry, 2001. **49**(3): p. 1208-1212.

52. Barac, M., et al., Functional properties of pea (Pisum sativum, L.) protein isolates modified with chymosin. International Journal of Molecular Sciences, 2011. **12**(12): p. 8372-87.

53. Ladjal Ettoumi, Y., et al., Legume Protein Isolates for Stable Acidic Emulsions Prepared by Premix Membrane Emulsification. Food Biophysics, 2017. **12**(1): p. 119-128.

54. Rubio, L.A., et al., Characterization of pea (Pisum sativum) seed protein fractions. Journal of the Science of Food and Agriculture, 2014. **94**(2): p. 280-287.

55. Shand, P.J., et al., Physicochemical and textural properties of heat-induced pea protein isolate gels. Food Chemistry, 2007. **102**(4): p. 1119-1130.

56. Pelgrom, P.J.M., et al., Dry fractionation for production of functional pea protein concentrates. Food Research International, 2013. **53**(1): p. 232-239.

57. Schutyser, M.A.I., et al., Dry fractionation for sustainable production of functional legume protein concentrates. Trends in Food Science & Technology, 2015. **45**(2): p. 327-335.

58. Ruiz, G.A., et al., A hybrid dry and aqueous fractionation method to obtain protein-

rich fractions from quinoa (Chenopodium quinoa Willd). Food and Bioprocess Technology, 2016. **9**(9): p. 1502-1510.

59. Geerts, M.E., Functionality-driven fractionation the need for mild food processing. 2018, Wageningen University.

60. Tanger, C., J. Engel, and U. Kulozik, Influence of extraction conditions on the conformational alteration of pea protein extracted from pea flour. Food Hydrocolloids, 2020. **107**: p. 105949.

61. Taherian, A.R., et al., Comparative study of functional properties of commercial and membrane processed yellow pea protein isolates. Food Research International, 2011. **44**(8): p. 2505-2514.

62. Fuhrmeister, H. and F. Meuser, Impact of processing on functional properties of protein products from wrinkled peas. Journal of Food Engineering, 2003. **56**(2-3): p. 119-129.

63. Sosulski, F. and A. McCurdy, Functionality of flours, protein fractions and isolates from field peas and faba bean. Journal of Food Science, 1987. **52**(4): p. 1010-1014.

64. Cui, L., et al., Functionality and structure of yellow pea protein isolate as affected by cultivars and extraction pH. Food Hydrocolloids, 2020. **108**: p. 106008.

65. Einstein, A., Eine neue bestimmung der moleküldimensionen. 1905, ETH Zurich.

66. Willenbacher, N. and K. Georgieva, Rheology of disperse systems. Product Design and Engineering, 2013: p. 7-49.

67. Kiosseoglou, V. and A. Paraskevopoulou, Functional and physicochemical properties of pulse proteins. Pulse Food: Processing, Quality and Nutraceutical Applications, Elsevier Inc., London, 2011: p. 57-90.

68. Lam, A.C.Y., et al., Pea protein isolates: Structure, extraction, and functionality. Food Reviews International, 2016. **34**(2): p. 1-22.

69. O'Kane, F.E., Molecular characterisation and heat-induced gelation of pea vicilin and legumin, in Product Design and Quality Management Group; Food Chemistry. 2004: Wageningen.

70. Sun, X.D. and S.D. Arntfield, Gelation properties of salt-extracted pea protein isolate induced by heat treatment: Effect of heating and cooling rate. Food Chemistry, 2011. **124**(3): p. 1011-1016.

71. Karaca, A.C., N. Low, and M. Nickerson, Emulsifying properties of chickpea, faba bean, lentil and pea proteins produced by isoelectric precipitation and salt extraction. Food Research International, 2011. **44**(9): p. 2742-2750.

72. Ladjal-Ettoumi, Y., et al., Pea, chickpea and lentil protein isolates: Physicochemical characterization and emulsifying properties. Food Biophysics, 2016. **11**(1): p. 43-51.

73. Kimura, A., et al., Comparison of Physicochemical Properties of 7S and 11S Globulins from Pea, Fava Bean, Cowpea, and French Bean with Those of Soybea -- French Bean 7S Globulin Exhibits Excellent Properties. Journal of Agricultural and Food Chemistry, 2008. **56**(21): p. 10273-10279.

74. Farjami, T. and A. Madadlou, An overview on preparation of emulsion-filled gels and emulsion particulate gels. Trends in Food Science & Technology, 2019. **86**: p. 85-94.

75. Li, F., et al., Gelation behaviour and rheological properties of acid-induced soy protein-stabilized emulsion gels. Food Hydrocolloids, 2012. **29**(2): p. 347-355.

76. de Souza Paglarini, C., S. Martini, and M.A.R. Pollonio, Using emulsion gels made with sonicated soy protein isolate dispersions to replace fat in frankfurters. LWT, 2019. **99**: p. 453-459.

77. Yang, M., F. Liu, and C.-H. Tang, Properties and microstructure of transglutaminase-set soy protein-stabilized emulsion gels. Food Research International, 2013. **52**(1): p. 409-418.

78. Iqbal, A., et al., Nutritional quality of important food legumes. Food chemistry, 2006. **97**(2): p. 331-335.

79. Wong, D., T. Vasanthan, and L. Ozimek, Synergistic enhancement in the co-gelation of salt-soluble pea proteins and whey proteins. Food Chemistry, 2013. **141**(4): p. 3913-9.

80. Chihi, M.L., N. Sok, and R. Saurel, Acid gelation of mixed thermal aggregates of pea globulins and β-lactoglobulin. Food Hydrocolloids, 2018. **85**: p. 120-128.

81. Mession, J.-L., S. Roustel, and R. Saurel, Interactions in casein micelle – Pea protein system (part I): Heat-induced denaturation and aggregation. Food Hydrocolloids, 2017. **67**: p. 229-242.

82. Pelgrom, P.J.M., R.M. Boom, and M.A.I. Schutyser, Functional analysis of mildly refined fractions from yellow pea. Food Hydrocolloids, 2015. **44**: p. 12-22.

83. Schwenke, K.D., et al., Functional properties of plant proteins. Part 2. Selected physicochemical properties of native and denatured protein isolates from faba beans, soybeans, and sunflower seed'. Die Nahrung, 1981. **25**(1): p. 59 - 69.

84. Rhee, K.C., Functionality of soy proteins. Protein Functionality in Food Systems, 1994: p. 311-324.

85. Batista, A.P., et al., Accessing gelling ability of vegetable proteins using rheological and fluorescence techniques. International Journal of Biological Macromolecules, 2005. **36**(3): p. 135-143.

86. Berghout, J.A.M., R.M. Boom, and A.J. van der Goot, Understanding the differences in gelling properties between lupin protein isolate and soy protein isolate. Food Hydrocolloids, 2015. **43**: p. 465-472.

87. Linnemann, A.R. and D.S. Dijkstra, Toward sustainable production of protein-rich foods: appraisal of eight crops for Western Europe. Part I. Analysis of the primary links of the production chain. Critical Reviews in Food Science and Nutrition, 2002. **42**(4): p. 377-401.

88. Warnakulasuriya, S.N. and M.T. Nickerson, Review on plant protein–polysaccharide complex coacervation, and the functionality and applicability of formed complexes. Journal of the Science of Food and Agriculture, 2018. **98**(15): p. 5559-5571.

89. Gharsallaoui, A., et al., Effect of high methoxyl pectin on pea protein in aqueous solution and at oil/water interface. Carbohydrate Polymers, 2010. **80**(3): p. 817-827.

90. Geerts, M.E.J., et al., Mildly refined fractions of yellow peas show rich behaviour in thickened oil-in-water emulsions. Innovative Food Science & Emerging Technologies, 2017. **41**: p. 251-258.

91. Boisen, S., S. Bech-Andersen, and B.r.O. Eggum, A critical view on the conversion factor 6.25 from total nitrogen to protein. Acta Agriculturae Scandinavica, 1987. **37**(3): p. 299-304.

92. de Almeida Costa, G.E., et al., Chemical composition, dietary fibre and resistant starch contents of raw and cooked pea, common bean, chickpea and lentil legumes. Food Chemistry, 2006. **94**(3): p. 327-330.

93. Nijsse, J. and A.C. van Aelst, Cryo-planing for cryo-scanning electron microscopy. Scanning, 1999. **21**(6): p. 372-378.

94. Goldstein, J.I., et al., Scanning electron microscopy and X-ray microanalysis. 2017: Springer.

95. Englyst, H.N. and J.H. Cummings, Simplified method for the measurement of total non-starch polysaccharides by gas-liquid chromatography of constituent sugars as alditol

acetates. Analyst, 1984. **109**(7): p. 937-942.

96. Ahmed, A.E.R. and J.M. Labavitch, A simplified method for accurate determination of cell wall uronide content. Journal of Food Biochemistry, 1978. **1**(4): p. 361-365.

97. Thibault, J., Automatisation du dosage des substances pectiques par la méthode au métahydroxydiphényle. Lebensmittel Wiss. Technol., 1979. **12**: p. 247-251.

98. Soesanto, T. and M.C. Williams, Volumetric interpretation of viscosity for concentrated and dilute sugar solutions. The Journal of Physical Chemistry, 1981. **85**(22): p. 3338-3341.

99. Ma, Z., et al., Thermal processing effects on the functional properties and microstructure of lentil, chickpea, and pea flours. Food Research International, 2011. **44**(8): p. 2534-2544.

100. Pernollet, J.-C., Protein bodies of seeds: ultrastructure, biochemistry, biosynthesis and degradation. Phytochemistry, 1978. **17**(9): p. 1473-1480.

101. Simsek, S., et al., Starch characteristics of dry peas (Pisum sativum L.) grown in the USA. Food Chemistry, 2009. **115**(3): p. 832-838.

102. Tulbek, M., et al., Pea: a sustainable vegetable protein crop, in Sustainable Protein Sources. 2017, Elsevier. p. 145-164.

103. Peterbauer, T., et al., Chain Elongation of Raffinose in Pea Seeds isolation, characterization, and molecular cloning of a multifunctional enzyme catalyzing the synthesis of stachyose and verbascose. Journal of Biological Chemistry, 2002. **277**(1): p. 194-200.

104. Tiwari, B.K. and N. Singh, Pulse chemistry and technology. 2012: Royal Society of Chemistry.

105. Tosh, S., et al., Nutritional profile and carbohydrate characterization of spray-dried lentil, pea and chickpea ingredients. Foods, 2013. **2**(3): p. 338-349.

106. Lee, J.C. and S.N. Timasheff, The stabilization of proteins by sucrose. Journal of Biological Chemistry, 1981. **256**(14): p. 7193-7201.

107. Wijayanti, H.B., N. Bansal, and H.C. Deeth, Stability of whey proteins during thermal processing: A review. Comprehensive Reviews in Food Science and Food Safety, 2014. **13**(6): p. 1235-1251.

108. Croy, R., et al., The purification and characterization of a third storage protein (convicilin) from the seeds of pea (Pisum sativum L.). Biochemical Journal, 1980. **191**(2): p. 509-516.

109. Shewry, P.R., J.A. Napier, and A.S. Tatham, Seed storage proteins: structures and biosynthesis. The Plant Cell, 1995. **7**(7): p. 945.

110. Schroeder, H.E., Major albumins of Pisum cotyledons. Journal of the Science of Food and Agriculture, 1984. **35**(2): p. 191-198.

111. Arakawa, T. and S.N. Timasheff, [3] Theory of protein solubility, in Methods in enzymology. 1985, Elsevier. p. 49-77.

112. Cohn, E.J. and J.T. Edsall, Proteins, amino acids and peptides as ions and dipolar ions. 1943: Reinhold Publishing Corporation; New York.

113. Ries-Kautt, M. and A. Ducruix, Inferences drawn from physicochemical studies of crystallogenesis and precrystalline state, in Methods in enzymology. 1997, Elsevier. p. 23-59.

114. Rai, R., Advances in Food Biotechnology. 2015: Wiley.

115. Jiang, J., J. Chen, and Y.L. Xiong, Structural and emulsifying properties of soy protein isolate subjected to acid and alkaline pH-shifting processes. Journal of Agricultural and Food Chemistry, 2009. **57**(16): p. 7576-7583.

116. Morison, K.R. and F.M. Mackay, Viscosity of lactose and whey protein solutions. International Journal of Food Properties, 2001. **4**(3): p. 441-454.

117. Dengate, H., D. Baruch, and P. Meredith, The density of wheat starch granules: a tracer dilution procedure for determining the density of an immiscible dispersed phase. Starch-Stärke, 1978. **30**(3): p. 80-84.

118. Rahman, M.S., Food properties handbook. 2009: CRC press.

119. Alting, A.C., et al., Number of thiol groups rather than the size of the aggregates determines the hardness of cold set whey protein gels. Food Hydrocolloids, 2003. **17**(4): p. 469-479.

120. Boutin, C., et al., Characterization and acid-induced gelation of butter oil emulsions produced from heated whey protein dispersions. International Dairy Journal, 2007. **17**(6): p. 696-703.

121. Vreeker, R., et al., Fractal aggregation of whey proteins. Food Hydrocolloids, 1992. **6**(5): p. 423-435.

122. Tung, M.A., Rheology of protein dispersions. Journal of Texture Studies, 1978. **9**(1-2): p. 3-31.

123. Chao, D. and R.E. Aluko, Modification of the structural, emulsifying, and foaming properties of an isolated pea protein by thermal pretreatment. CyTA-Journal of Food, 2018. **16**(1): p. 357-366.

124. McCarthy, N.A., et al., Emulsification properties of pea protein isolate using homogenization, microfluidization and ultrasonication. Food Research International, 2016. **89**: p. 415-421.

125. Jambrak, A.R., et al., Effect of ultrasound treatment on solubility and foaming properties of whey protein suspensions. Journal of Food Engineering, 2008. **86**(2): p. 281-287.

126. Samard, S. and G.H. Ryu, A comparison of physicochemical characteristics, texture, and structure of meat analogue and meats. Journal of the Science of Food and Agriculture, 2019. **99**(6): p. 2708-2715.

127. Ryu, G.-H., Extrusion cooking of high-moisture meat analogues. Extrusion Cooking: Cereal Grains Processing, 2020: p. 205.

128. Berghout, J.A., Functionality-driven fractionation of lupin seeds. 2015, Wageningen University.

129. Chen, N., et al., pH and ionic strength responsive core-shell protein microgels fabricated via simple coacervation of soy globulins. Food Hydrocolloids, 2020. **105**: p. 105853.

130. Cochereau, R., et al., Mechanism of the spontaneous formation of plant protein microcapsules in aqueous solution. Colloids and Surfaces A: Physicochemical and Engineering Aspects, 2019. **562**: p. 213-219.

131. Mohanty, B. and H. Bohidar, Systematic of alcohol-induced simple coacervation in aqueous gelatin solutions. Biomacromolecules, 2003. **4**(4): p. 1080-1086.

132. Chen, N., et al., Resolving the Mechanisms of Soy Glycinin Self-Coacervation and Hollow-Condensate Formation. ACS Macro Letters, 2020. **9**: p. 1844-1852.

133. Moschakis, T. and C.G. Biliaderis, Biopolymer-based coacervates: Structures, functionality and applications in food products. Current Opinion in Colloid & Interface Science, 2017. **28**: p. 96-109.

134. Wang, J.C., S.H. Chen, and Z.C. Xu, Synthesis and properties research on the nanocapsulated capsaicin by simple coacervation method. Journal of Dispersion Science and Technology, 2008. **29**(5): p. 687-695.

135. Chen, N., et al., Exploiting salt induced microphase separation to form soy protein microcapsules or microgels in aqueous solution. Biomacromolecules, 2017. **18**(7): p. 2064-2072.

136. Li, X., et al., Encapsulation using plant proteins: Thermodynamics and kinetics of wetting for simple zein coacervates. ACS Applied Materials & Interfaces, 2020. **12**(13): p. 15802-15809.

137. Lui, D., J. Litster, and E. White, Precipitation of soy proteins: particle formation and protein separation. AIChE Journal, 2007. **53**(2): p. 514-522.

138. Nahar, M., et al., Effect of pH and salt concentration on protein solubility of slaughtered and non-slaughtered broiler chicken meat. Sains Malaysiana, 2017. **46**(5): p. 719-724.

139. Tibaduiza, D.M., Electrostatic Force Between Two Colloidal Spheres. arXiv preprint arXiv:1602.09074, 2016.

140. Sağlam, D., et al., The influence of pH and ionic strength on the swelling of dense protein particles. Soft Matter, 2013. **9**(18): p. 4598-4606.

141. O'Kane, F.E., et al., Heat-induced gelation of pea legumin: Comparison with soybean glycinin. Journal of Agricultural and Food Chemistry, 2004. **52**(16): p. 5071-5078.

142. Berghout, J., et al., Comparing functional properties of concentrated protein isolates with freeze-dried protein isolates from lupin seeds. Food Hydrocolloids, 2015. **51**: p. 346-354.

143. Izutsu, K., et al., Stabilization of protein structure in freeze-dried amorphous organic acid buffer salts. Chemical and Pharmaceutical Bulletin, 2009. **57**(11): p. 1231-1236.

144. Imamura, K., et al., Characteristics of Sugar Surfactants in Stabilizing Proteins During Freeze–Thawing and Freeze–Drying. Journal of Pharmaceutical Sciences, 2014. **103**(6): p. 1628-1637.

145. Fedorov, M.V., et al., Self-assembly of trehalose molecules on a lysozyme surface: the broken glass hypothesis. Physical Chemistry Chemical Physics, 2011. **13**(6): p. 2294-2299.

146. Papalamprou, E., et al., Influence of preparation methods on physicochemical and gelation properties of chickpea protein isolates. Food Hydrocolloids, 2009. **23**(2): p. 337-343.

147. Sridharan, S., et al., Pea flour as stabilizer of oil-in-water emulsions: Protein purification unnecessary. Food Hydrocolloids, 2020. **101**: p. 105533.

148. Ntone, E., J.H. Bitter, and C.V. Nikiforidis, Not sequentially but simultaneously: Facile extraction of proteins and oleosomes from oilseeds. Food Hydrocolloids, 2020. **102**: p. 105598.

149. van der Goot, A.J., et al., Concepts for further sustainable production of foods. Journal of Food Engineering, 2016. **168**: p. 42-51.

150. Sun, X.D. and S.D. Arntfield, Gelation properties of salt-extracted pea protein induced by heat treatment. Food Research International, 2010. **43**(2): p. 509-515.

151. Puppo, M., et al., β-Conglycinin and glycinin soybean protein emulsions treated by combined temperature–high-pressure treatment. Food Hydrocolloids, 2011. **25**(3): p. 389-397.

152. Makri, E., E. Papalamprou, and G. Doxastakis, Study of functional properties of seed storage proteins from indigenous European legume crops (lupin, pea, broad bean) in admixture with polysaccharides. Food Hydrocolloids, 2005. **19**(3): p. 583-594.

153. Sun, X.D. and S.D. Arntfield, Molecular forces involved in heat-induced pea protein gelation: effects of various reagents on the rheological properties of salt-extracted pea protein gels. Food Hydrocolloids, 2012. **28**(2): p. 325-332.

154. Kato, A. and S. Nakai, Hydrophobicity determined by a fluorescence probe method

and its correlation with surface properties of proteins. Biochimica et biophysica acta (BBA)-Protein structure, 1980. **624**(1): p. 13-20.

155. Creighton, T.E., Protein Structure: A Practical Approach. 1997: IRL Press at Oxford University Press.

156. Wierenga, P.A., et al., Importance of physical vs. chemical interactions in surface shear rheology. Advances in Colloid and Interface Science, 2006. **119**(2-3): p. 131-139.

157. Ellman, G.L., Tissue sulfhydryl groups. Archives of biochemistry and biophysics, 1959. **82**(1): p. 70-77.

158. Cho, K.S., et al., A geometrical interpretation of large amplitude oscillatory shear response. Journal of Rheology, 2005. **49**(3): p. 747-758.

159. Ewoldt, R.H., A. Hosoi, and G.H. McKinley, New measures for characterizing nonlinear viscoelasticity in large amplitude oscillatory shear. Journal of Rheology, 2008. **52**(6): p. 1427-1458.

160. Mession, J.-L., et al., Thermal Denaturation of Pea Globulins (Pisum sativum L.). Molecular Interactions Leading to Heat-Induced Protein Aggregation. Journal of Agricultural and Food Chemistry, 2013. **61**(6): p. 1196-1204.

161. Biliaderis, C., T. Maurice, and J. Vose, Starch gelatinization phenomena studied by differential scanning calorimetry. Journal of Food Science, 1980. **45**(6): p. 1669-1674.

162. Bandyopadhyay, R., et al., Slow dynamics, aging, and glassy rheology in soft and living matter. Solid state communications, 2006. **139**(11-12): p. 589-598.

163. Precha-Atsawanan, S., D. Uttapap, and L.M. Sagis, Linear and nonlinear rheological behavior of native and debranched waxy rice starch gels. Food Hydrocolloids, 2018. **85**: p. 1-9.

164. Birbaum, F.C., et al., Shear localisation in interfacial particle layers and its influence on Lissajous-plots. Rheologica Acta, 2016. **55**(4): p. 267-278.

165. Duvarci, O.C., G. Yazar, and J.L. Kokini, The comparison of LAOS behavior of structured food materials (suspensions, emulsions and elastic networks). Trends in Food Science & Technology, 2017. **60**: p. 2-11.

166. Yazar, G., et al., Non-linear rheological behavior of gluten-free flour doughs and correlations of LAOS parameters with gluten-free bread properties. Journal of Cereal Science, 2017. **74**: p. 28-36.

167. Fuongfuchat, A., et al., Linear and non-linear viscoelastic behaviors of crosslinked tapioca starch/polysaccharide systems. Journal of Food Engineering, 2012. **109**(3): p. 571-578.

168. Burger, T.G. and Y. Zhang, Recent progress in the utilization of pea protein as an emulsifier for food applications. Trends in Food Science & Technology, 2019. **86**: p. 25-33.

169. Möller, A.C., A. van der Padt, and A.J. van der Goot, From raw material to mildly refined ingredient–Linking structure to composition to understand fractionation processes. Journal of Food Engineering, 2020: p. 110321.

170. Assatory, A., et al., Dry fractionation methods for plant protein, starch and fiber enrichment: A review. Trends in Food Science & Technology, 2019. **86**: p. 340-351.

171. Lie-Piang, A., et al., Less refined ingredients have lower environmental impact–A life cycle assessment of protein-rich ingredients from oil-and starch-bearing crops. Journal of Cleaner Production, 2021: p. 126046.

172. Yang, S., et al., Selective Complex Coacervation of Pea Whey Proteins with Chitosan To Purify Main 2S Albumins. Journal of Agricultural and Food Chemistry, 2020. **68**(6): p. 1698-1706.

173. Ghumman, A., A. Kaur, and N. Singh, Functionality and digestibility of albumins and

globulins from lentil and horse gram and their effect on starch rheology. Food Hydrocolloids, 2016. **61**: p. 843-850.

174. Lu, B.Y., L. Quillien, and Y. Popineau, Foaming and emulsifying properties of pea albumin fractions and partial characterisation of surface-active components. Journal of the Science of Food and Agriculture, 2000. **80**(13): p. 1964-1972.

175. Casey, R., et al., Quantitative variability in Pisum seed globulins: its assessment and significance. Plant Foods for Human Nutrition, 1982. **31**(4): p. 333-346.

176. Berton-carabin, C.C., L. Sagis, and K. Schroën, Formation , Structure , and Functionality of Interfacial Layers in Food Emulsions. Annual Review of Food Science and Technology, 2018. **9**: p. 551-87.

177. Lucassen, J. and M. Van Den Tempel, Dynamic measurements of dilational properties of a liquid interface. Chemical Engineering Science, 1972. **27**(6): p. 1283-1291.

178. Sagis, L.M.C., et al., Dynamic heterogeneity in complex interfaces of soft interface-dominated materials. Scientific Reports, 2019. **9**(1): p. 1-12.

179. Ewoldt, R.H., A.E. Hosoi, and G.H. McKinley, New measures for characterizing nonlinear viscolasticity in large amplitude oscillatory shear (LAOS). Journal of Rheology, 2008. **52**(6): p. 2008.

180. Yang, J., et al., Nonlinear interfacial rheology and atomic force microscopy of air-water interfaces stabilized by whey protein beads and their constituents. Food Hydrocolloids, 2020. **101**: p. 105466.

181. Ntone, E., et al., Adsorption of rapeseed proteins at oil/water interfaces. Janus-like napins dominate the interface. Journal of Colloid and Interface Science, 2020. **583**: p. 459-469.

182. Souza, P.F.N., The forgotten 2S albumin proteins: Importance, structure, and biotechnological application in agriculture and human health. International Journal of Biological Macromolecules, 2020. **164**: p. 4638-4649.

183. Yang, J., et al., Foams and air-water interfaces stabilised by mildly purified rapeseed proteins after defatting. Food Hydrocolloids, 2021. **112**.

184. Rühs, P.A., et al., Shear and dilatational linear and nonlinear subphase controlled interfacial rheology of β-lactoglobulin fibrils and their derivatives. Journal of Rheology, 2013. **57**(3): p. 1003-1022.

185. Gunning, A.P., et al., Atomic Force Microscopy of Interfacial Protein Films. Journal of Colloid and Interface Science, 1996. **183**(2): p. 600-602.

186. Hinderink, E.B.A., et al., Behavior of plant-dairy protein blends at air-water and oil-water interfaces. Colloids and Surfaces B: Biointerfaces, 2020. **192**: p. 111015.

187. Williams, G. and D.C. Watts, Non-Symmetrical Dielectric Relaxation Behaviour Arising from a Simple Empirical Decay Function. Transactions of the Faraday Society, 1969. **66**(1): p. 80-85.

188. Phillips, J.C., Stretched exponential relaxation in molecular and electronic glasses. Reports on Progress in Physics, 1996. **59**: p. 1133-1207.

189. Klafter, J. and M.F. Shlesinger, On the Relationship among Three Theories of Relaxation in Disordered. Proceedings of the National Academy of Sciences of the United States of America, 1986. **83**(4): p. 848-851.

190. Hinderink, E.B., et al., Synergistic stabilisation of emulsions by blends of dairy and soluble pea proteins: contribution of the interfacial composition. Food Hydrocolloids, 2019. **97**: p. 105206.

191. Geremias-Andrade, I.M., et al., Rheology of emulsion-filled gels applied to the development of food materials. Gels, 2016. **2**(3): p. 22.

192. Schmitt, C., et al., Heat-induced and acid-induced gelation of dairy/plant protein dispersions and emulsions. Current Opinion in Food Science, 2019. **27**: p. 43-48.

193. Panyam, D. and A. Kilara, Enhancing the functionality of food proteins by enzymatic modification. Trends in Food Science & Technology, 1996. **7**(4): p. 120-125.

194. Zeeb, B., D.J. McClements, and J. Weiss, Enzyme-based strategies for structuring foods for improved functionality. Annual Review of Food Science and Technology, 2017. **8**: p. 21-34.

195. Jose, J., L. Pouvreau, and A.H. Martin, Mixing whey and soy proteins: Consequences for the gel mechanical response and water holding. Food Hydrocolloids, 2016. **60**: p. 216-224.

196. McCann, T.H., et al., Rheological properties and microstructure of soy-whey protein. Food Hydrocolloids, 2018. **82**: p. 434-441.

197. Vestergaard, M., S.H.J. Chan, and P.R. Jensen, Can microbes compete with cows for sustainable protein production-A feasibility study on high quality protein. Scientific reports, 2016. **6**(1): p. 1-8.

198. Jung, S., et al., Functionality of soy protein produced by enzyme-assisted extraction. Journal of the American Oil Chemists' Society, 2006. **83**(1): p. 71-78.

199. Kornet, R., et al., Less is more: Limited fractionation yields stronger gels for pea proteins. Food Hydrocolloids, 2021. **112**: p. 106285.

200. Adenekan, M.K., et al., Effect of isolation techniques on the characteristics of pigeon pea (Cajanus cajan) protein isolates. Food Science & Nutrition, 2018. **6**(1): p. 146-152.

201. Peng, Y., et al., Functional properties of mildly fractionated soy protein as influenced by the processing pH. Journal of Food Engineering, 2020. **275**: p. 109875.

202. Alonso-Miravalles, L., et al., Membrane filtration and isoelectric precipitation technological approaches for the preparation of novel, functional and sustainable protein isolate from lentils. European Food Research and Technology, 2019. **245**(9): p. 1855-1869.

203. Kornet, R., et al., Substitution of whey protein by pea protein is facilitated by specific fractionation routes. Food Hydrocolloids, 2021: p. 106691.

204. Kiosseoglou, A., et al., Physical characterization of thermally induced networks of lupin protein isolates prepared by isoelectric precipitation and dialysis. International Journal of Food Science & Technology, 1999. **34**(3): p. 253-263.

205. Sikorski, Z.E., Functional properties of proteins in food systems. Chemical and Functional Properties of Food Proteins, 2001: p. 113-135.

206. Kim, K., J. Renkema, and T. Van Vliet, Rheological properties of soybean protein isolate gels containing emulsion droplets. Food hydrocolloids, 2001. **15**(3): p. 295-302.

207. Tang, C.-H., L. Chen, and E.A. Foegeding, Mechanical and water-holding properties and microstructures of soy protein isolate emulsion gels induced by CaCl2, glucono-δ-lactone (GDL), and transglutaminase: Influence of thermal treatments before and/or after emulsification. Journal of Agricultural and Food Chemistry, 2011. **59**(8): p. 4071-4077.

208. Tangsuphoom, N. and J.N. Coupland, Effect of surface-active stabilizers on the microstructure and stability of coconut milk emulsions. Food Hydrocolloids, 2008. **22**(7): p. 1233-1242.

209. Ewoldt, R.H., et al., Large amplitude oscillatory shear of pseudoplastic and elastoviscoplastic materials. Rheologica Acta, 2010. **49**(2): p. 191-212.

210. Larson, A.M., Multiphoton microscopy. Nature Photonics, 2011. **5**(1): p. 1-1.

211. Sala, G., et al., Effect of droplet–matrix interactions on large deformation properties of emulsion-filled gels. Journal of Texture Studies, 2007. **38**(4): p. 511-535.

212. Van Vliet, T., Rheological properties of filled gels. Influence of filler matrix interaction. Colloid and Polymer Science, 1988. **266**(6): p. 518-524.

213. Beverung, C., C.J. Radke, and H.W. Blanch, Protein adsorption at the oil/water interface: characterization of adsorption kinetics by dynamic interfacial tension measurements. Biophysical Chemistry, 1999. **81**(1): p. 59-80.

214. Sagis, L.M. and E. Scholten, Complex interfaces in food: Structure and mechanical properties. Trends in Food Science & Technology, 2014. **37**(1): p. 59-71.

215. Wolz, M. and U. Kulozik, Thermal denaturation kinetics of whey proteins at high protein concentrations. International Dairy Journal, 2015. **49**: p. 95-101.

216. Vermeer, A.W. and W. Norde, The thermal stability of immunoglobulin: unfolding and aggregation of a multi-domain protein. Biophysical Journal, 2000. **78**(1): p. 394-404.

217. Doan, C.D. and S. Ghosh, Formation and stability of pea proteins nanoparticles using ethanol-induced desolvation. Nanomaterials, 2019. **9**(7): p. 949.

218. Sala, G., Food gels filled with emulsion droplets: linking large deformation properties to sensory perception. 2007.

219. Manski, J., et al., Influence of dispersed particles on small and large deformation properties of concentrated caseinate composites. Food hydrocolloids, 2007. **21**(1): p. 73-84.

220. Mooney, M., The viscosity of a concentrated suspension of spherical particles. Journal of colloid science, 1951. **6**(2): p. 162-170.

221. Pal, R., Complex shear modulus of concentrated suspensions of solid spherical particles. Journal of colloid and interface science, 2002. **245**(1): p. 171-177.

222. Ptaszek, P., Large amplitudes oscillatory shear (LAOS) behavior of egg white foams with apple pectins and xanthan gum. Food Research International, 2014. **62**: p. 299-307.

223. Ainis, W.N., C. Ersch, and R. Ipsen, Partial replacement of whey proteins by rapeseed proteins in heat-induced gelled systems: Effect of pH. Food Hydrocolloids, 2018. **77**: p. 397-406.

224. Alves, A.C. and G.M. Tavares, Mixing animal and plant proteins: Is this a way to improve protein techno-functionalities? Food Hydrocolloids, 2019. **97**: p. 105171.

225. Onwulata, C., M. Tunick, and S. Mukhopadhyay, Flow behavior of mixed-protein incipient gels. International Journal of Food Properties, 2014. **17**(6): p. 1283-1302.

226. Beliciu, C.M. and C.I. Moraru, The effect of protein concentration and heat treatment temperature on micellar casein–soy protein mixtures. Food Hydrocolloids, 2011. **25**(6): p. 1448-1460.

227. Comfort, S. and N.K. Howell, Gelation properties of soya and whey protein isolate mixtures. Food Hydrocolloids, 2002. **16**(6): p. 661-672.

228. Grygorczyk, A., et al., Gelation of recombined soymilk and cow's milk gels: Effect of homogenization order and mode of gelation on microstructure and texture of the final matrix. Food Hydrocolloids, 2014. **35**: p. 69-77.

229. Ersch, C., et al., Modulating fracture properties of mixed protein systems. Food Hydrocolloids, 2015. **44**: p. 59-65.

230. Roesch, R.R. and M. Corredig, Study of the effect of soy proteins on the acid-induced gelation of casein micelles. Journal of Agricultural and Food Chemistry, 2006. **54**(21): p. 8236-8243.

231. Martin, A.H., L. Marta, and L. Pouvreau, Modulating the aggregation behaviour to restore the mechanical response of acid induced mixed gels of sodium caseinate and soy proteins. Food Hydrocolloids, 2016. **58**: p. 215-223.

232. Roesch, R.R. and M. Corredig, Heat-induced soy− whey proteins interactions: Formation of soluble and insoluble protein complexes. Journal of Agricultural and Food Chemistry, 2005. **53**(9): p. 3476-3482.

233. Chihi, M.L., et al., Heat-induced soluble protein aggregates from mixed pea globulins and β-lactoglobulin. Journal of Agricultural and Food Chemistry, 2016. **64**(13): p. 2780-2791.

234. Lam, A., et al., Pea protein isolates: Structure, extraction, and functionality. Food Reviews International, 2018. **34**(2): p. 126-147.

235. Gatehouse, J.A., R.R. Croy, and D. Boulter, Isoelectric-focusing properties and carbohydrate content of pea (Pisum sativum) legumin. Biochemical Journal, 1980. **185**(2): p. 497-503.

236. Brown, E., M. Heit, and D. Ryan, Phytic acid: an analytical investigation. Canadian Journal of Chemistry, 1961. **39**(6): p. 1290-1297.

237. Crean, D. and D. Haisman, The interaction between phytic acid and divalent cations during the cooking of dried peas. Journal of the Science of Food and Agriculture, 1963. **14**(11): p. 824-833.

238. Samotus, B., Role of phytic acid in potato tuber. Nature, 1965. **206**(4991): p. 1372-1373.

239. Cornacchia, L., C.c. Forquenot de la Fortelle, and P. Venema, Heat-induced aggregation of whey proteins in aqueous solutions below their isoelectric point. Journal of Agricultural and Food Chemistry, 2014. **62**(3): p. 733-741.

240. Fitzsimons, S.M., D.M. Mulvihill, and E.R. Morris, Denaturation and aggregation processes in thermal gelation of whey proteins resolved by differential scanning calorimetry. Food Hydrocolloids, 2007. **21**(4): p. 638-644.

241. Boye, J. and I. Alli, Thermal denaturation of mixtures of α-lactalbumin and β-lactoglobulin: a differential scanning calorimetric study. Food Research International, 2000. **33**(8): p. 673-682.

242. Maga, J.A., Phytate: its chemistry, occurrence, food interactions, nutritional significance, and methods of analysis. Journal of Agricultural and Food Chemistry, 1982. **30**(1): p. 1-9.

243. Monahan, F.J., J.B. German, and J.E. Kinsella, Effect of pH and temperature on protein unfolding and thiol/disulfide interchange reactions during heat-induced gelation of whey proteins. Journal of Agricultural and Food Chemistry, 1995. **43**(1): p. 46-52.

244. Langton, M. and A.-M. Hermansson, Fine-stranded and particulate gels of β-lactoglobulin and whey protein at varying pH. Food Hydrocolloids, 1992. **5**(6): p. 523-539.

245. Mulvihill, D., D. Rector, and J. Kinsella, Effects of structuring and destructuring anionic ions on the rheological properties of thermally induced β-lactoglobulin gels. Food Hydrocolloids, 1990. **4**(4): p. 267-276.

246. Ersch, C., et al., Microstructure and rheology of globular protein gels in the presence of gelatin. Food Hydrocolloids, 2016. **55**: p. 34-46.

247. Bartasun, P., et al., A study on the interaction of rhodamine B with methylthioadenosine phosphorylase protein sourced from an Antarctic soil metagenomic library. PLoS One, 2013. **8**(1): p. e55697.

248. Zhao, H., et al., Comparison of wheat, soybean, rice, and pea protein properties for effective applications in food products. Journal of Food Biochemistry, 2020. **44**(4): p. e13157.

249. Lam, A.C.Y., et al., Physicochemical and functional properties of protein isolates obtained from several pea cultivars. Cereal Chemistry, 2017. **94**(1): p. 89-97.

250. Ge, J., et al., The health benefits, functional properties, modifications, and

applications of pea (Pisum sativum L.) protein: Current status, challenges, and perspectives. Comprehensive Reviews in Food Science and Food Safety, 2020. **19**(4): p. 1835-1876.

251. Ji, J., et al., Preparation and stabilization of emulsions stabilized by mixed sodium caseinate and soy protein isolate. Food Hydrocolloids, 2015. **51**: p. 156-165.

252. Yerramilli, M., N. Longmore, and S. Ghosh, Improved stabilization of nanoemulsions by partial replacement of sodium caseinate with pea protein isolate. Food Hydrocolloids, 2017. **64**: p. 99-111.

253. Mariotti, F.o., et al., The influence of the albumin fraction on the bioavailability and postprandial utilization of pea protein given selectively to humans. The Journal of Nutrition, 2001. **131**(6): p. 1706-1713.

254. Djoullah, A., F. Husson, and R. Saurel, Gelation behaviors of denaturated pea albumin and globulin fractions during transglutaminase treatment. Food Hydrocolloids, 2018. **77**: p. 636-645.

255. Mession, J., et al., Effect of globular pea proteins fractionation on their heat-induced aggregation and acid cold-set gelation. Food Hydrocolloids, 2015. **46**: p. 233-243.

256. Butré, C.I., P.A. Wierenga, and H. Gruppen, Effects of ionic strength on the enzymatic hydrolysis of diluted and concentrated whey protein isolate. Journal of Agricultural and Food Chemistry, 2012. **60**(22): p. 5644-5651.

257. Singh, N. and L. Kaur, Morphological, thermal, rheological and retrogradation properties of potato starch fractions varying in granule size. Journal of the Science of Food and Agriculture, 2004. **84**(10): p. 1241-1252.

258. Vallons, K.J. and E.K. Arendt, Effects of high pressure and temperature on the structural and rheological properties of sorghum starch. Innovative Food Science & Emerging Technologies, 2009. **10**(4): p. 449-456.

259. Monteiro, S.R. and J.A. Lopes-da-Silva, Critical evaluation of the functionality of soy protein isolates obtained from different raw materials. European Food Research and Technology, 2019. **245**(1): p. 199-212.

260. Tang, Q., Rheology of whey protein solutions and gels: thesis submitted for the degree of Doctor of Philosophy in Food Technology at Massey University, New Zealand. 1993, Massey University.

261. Schreuders, F., et al., Small and large oscillatory shear properties of concentrated proteins. Food Hydrocolloids, 2021. **110**: p. 106172.

262. Lott, J., D. Goodchild, and S. Craig, Studies of mineral reserves in pea (Pisum sativum) cotyledons using low-water-content procedures. Functional Plant Biology, 1984. **11**(6): p. 459-469.

263. Zhou, J.R. and J.W. Erdman Jr, Phytic acid in health and disease. Critical Reviews in Food Science & Nutrition, 1995. **35**(6): p. 495-508.

264. Ewoldt, R.H. and G.H. McKinley, On secondary loops in LAOS via self-intersection of Lissajous–Bowditch curves. Rheologica Acta, 2010. **49**(2): p. 213-219.

265. Clark, A.H., Structural and mechanical properties of biopolymer gels. Food Polymers, Gels and Colloids, 1991: p. 322-338.

266. Lorenzen, P.C. and K. Schrader, A comparative study of the gelation properties of whey protein concentrate and whey protein isolate. Le Lait, 2006. **86**(4): p. 259-271.

267. Hussain, R., et al., Combined effect of heat treatment and ionic strength on the functionality of whey proteins. Journal of Dairy Science, 2012. **95**(11): p. 6260-6273.

268. Ju, Z.Y. and A. Kilara, Gelation of pH-aggregated whey protein isolate solution induced by heat, protease, calcium salt, and acidulant. Journal of Agricultural and Food

Chemistry, 1998. **46**(5): p. 1830-1835.

269. Shiroodi, S.G. and Y.M. Lo, The effect of pH on the rheology of mixed gels containing whey protein isolate and xanthan-curdlan hydrogel. Journal of Dairy Research, 2015. **82**(4): p. 506-512.

270. Diedericks, C.F., et al., Effect of pH and mixing ratios on the synergistic enhancement of Bambara groundnut-whey proteins gels. Food Hydrocolloids, 2021: p. 106702.

271. Renard, D. and J. Lefebvre, Gelation of globular proteins: effect of pH and ionic strength on the critical concentration for gel formation. A simple model and its application to β-lactoglobulin heat-induced gelation. International Journal of Biological Macromolecules, 1992. **14**(5): p. 287-291.

272. Schmidt, R., et al., The effect of dialysis on heat-induced gelation of whey protein concentrate 1. Journal of Food Processing and Preservation, 1978. **2**(2): p. 111-120.

273. Schmidt, R.H., et al., Multiple regression and response surface analysis of the effects of calcium chloride and cysteine on heat-induced whey protein gelation. Journal of Agricultural and Food Chemistry, 1979. **27**(3): p. 529-532.

274. Hermansson, A.-M., Functional properties of proteins for foods-swelling. Lebensmittel-Wissenschaft und Technologie, 1972.

275. Dickinson, E. and J. Chen, Heat-set whey protein emulsion gels: role of active and inactive filler particles. Journal of Dispersion Science and Technology, 1999. **20**(1-2): p. 197-213.

276. Shimada, K. and J.C. Cheftel, Sulfhydryl group/disulfide bond interchange reactions during heat-induced gelation of whey protein isolate. Journal of Agricultural and Food Chemistry, 1989. **37**(1): p. 161-168.

277. Visschers, R.W. and H.H. de Jongh, Disulphide bond formation in food protein aggregation and gelation. Biotechnology Advances, 2005. **23**(1): p. 75-80.

278. Alting, A.C., et al., Formation of disulfide bonds in acid-induced gels of preheated whey protein isolate. Journal of Agricultural and Food Chemistry, 2000. **48**(10): p. 5001-5007.

279. Jensen, K.S., R.E. Hansen, and J.R. Winther, Kinetic and thermodynamic aspects of cellular thiol–disulfide redox regulation. Antioxidants & Redox Signaling, 2009. **11**(5): p. 1047-1058.

280. Helms, M., Food sustainability, food security and the environment. British Food Journal, 2004.

281. Sá, A.G.A., Y.M.F. Moreno, and B.A.M. Carciofi, Plant proteins as high-quality nutritional source for human diet. Trends in Food Science & Technology, 2020. **97**: p. 170-184.

282. Kornet, C., et al., Yellow pea aqueous fractionation increases the specific volume fraction and viscosity of its dispersions. Food Hydrocolloids, 2020. **99**: p. 105332.

283. Tömösközi, S., et al., Isolation and study of the functional properties of pea proteins. Food/Nahrung, 2001. **45**(6): p. 399-401.

284. King, J., C. Aguirre, and S. De Pablo, Functional properties of lupin protein isolates (Lupinus albus cv Multolupa). Journal of Food Science, 1985. **50**(1): p. 82-87.

285. L'hocine, L., J.I. Boye, and Y. Arcand, Composition and functional properties of soy protein isolates prepared using alternative defatting and extraction procedures. Journal of Food Science, 2006. **71**(3): p. C137-C145.

286. Barać, M.B., et al., Techno-functional properties of pea (Pisum sativum) protein isolates-a review. Acta Period. Techn, 2015. **46**: p. 1-18.

287. Sumner, A., M. Nielsen, and C. Youngs, Production and evaluation of pea protein

isolate. Journal of Food Science, 1981. **46**(2): p. 364-366.

288. Barac, M., et al., Functional properties of pea (Pisum sativum, L.) protein isolates modified with chymosin. Int J Mol Sci, 2011. **12**(12): p. 8372-87.

289. Toews, R. and N. Wang, Physicochemical and functional properties of protein concentrates from pulses. Food Research International, 2013. **52**(2): p. 445-451.

290. Pelgrom, P.J.M., et al., Pre- and post-treatment enhance the protein enrichment from milling and air classification of legumes. Journal of Food Engineering, 2015. **155**: p. 53-61.

291. Hemery, Y., et al., Potential of dry fractionation of wheat bran for the development of food ingredients, part II: Electrostatic separation of particles. Journal of Cereal Science, 2011. **53**(1): p. 9-18.

292. Wang, J., et al., Lupine protein enrichment by milling and electrostatic separation. Innovative Food Science & Emerging Technologies, 2016. **33**: p. 596-602.

293. Wang, J., et al., Analysis of electrostatic powder charging for fractionation of foods. Innovative Food Science & Emerging Technologies, 2014. **26**: p. 360-365.

294. Geerts, M., et al., Exergetic comparison of three different processing routes for yellow pea (Pisum sativum): Functionality as a driver in sustainable process design. Journal of Cleaner Production, 2018. **183**: p. 979-987.

295. Yang, J., et al., Extraction methods significantly impact pea protein composition, structure and gelling properties. Food Hydrocolloids, 2021. **117**: p. 106678.

296. Tian, S., W.S. Kyle, and D.M. Small, Pilot scale isolation of proteins from field peas (Pisum sativum L.) for use as food ingredients. International journal of food science & technology, 1999. **34**(1): p. 33-39.

297. Wang, Y., et al., Impact of alcohol washing on the flavour profiles, functionality and protein quality of air classified pea protein enriched flour. Food Research International, 2020. **132**: p. 109085.

298. Maud Meijers, P.W., Predictive estimation of emulsion properties of pea legumin and vicilin blends, R. Kornet, Editor. 2019: Wageningen.

299. Teuling, E., Unicellular protein: isolation, techno-functionality and digestibility. 2018, Wageningen University.

300. Pearce, K.N. and J.E. Kinsella, Emulsifying properties of proteins: evaluation of a turbidimetric technique. Journal of Agricultural and Food Chemistry, 1978. **26**(3): p. 716-723.

301. Tcholakova, S., et al., Interrelation between drop size and protein adsorption at various emulsification conditions. Langmuir, 2003. **19**(14): p. 5640-5649.

302. Achouri, A., et al., Functional properties of glycated soy 11S glycinin. Journal of Food Science, 2005. **70**(4): p. C269-C274.

303. Wu, G., Amino acids: biochemistry and nutrition. 2013: CRC Press.

304. Wu, G., et al., Production and supply of high-quality food protein for human consumption: sustainability, challenges, and innovations. Annals of the New York Academy of Sciences, 2014. **1321**(1): p. 1-19.

305. Berrazaga, I., et al., The role of the anabolic properties of plant-versus animal-based protein sources in supporting muscle mass maintenance: a critical review. Nutrients, 2019. **11**(8): p. 1825.

306. Gatel, F., Protein quality of legume seeds for non-ruminant animals: a literature review. Animal Feed Science and Technology, 1994. **45**(3-4): p. 317-348.

307. Van der Poel, A., et al., Effect of infrared irradiation or extrusion processing of maize on its digestibility in piglets. Animal feed science and technology, 1989. **26**(1-2): p. 29-43.

308. Adamidou, S., et al., Chemical composition and antinutritional factors of field peas (Pisum sativum), chickpeas (Cicer arietinum), and faba beans (Vicia faba) as affected by extrusion preconditioning and drying temperatures. Cereal chemistry, 2011. **88**(1): p. 80-86.

309. Vidal-Valverde, C., et al., Effect of processing on some antinutritional factors of lentils. Journal of Agricultural and Food Chemistry, 1994. **42**(10): p. 2291-2295.

310. do Carmo, C.S., et al., Is dehulling of peas and faba beans necessary prior to dry fractionation for the production of protein-and starch-rich fractions? Impact on physical properties, chemical composition and techno-functional properties. Journal of food engineering, 2020. **278**: p. 109937.

311. Roland, W.S., et al., Flavor aspects of pulse ingredients. Cereal Chemistry, 2017. **94**(1): p. 58-65.

312. Wang, K. and S.D. Arntfield, Effect of salts and pH on selected ketone flavours binding to salt-extracted pea proteins: The role of non-covalent forces. Food Research International, 2015. **77**: p. 1-9.

313. Gao, Z., et al., Effect of alkaline extraction pH on structure properties, solubility, and beany flavor of yellow pea protein isolate. Food Research International, 2020. **131**: p. 109045.

314. PubChem. [cited 2021 12 January]; Available from: https://pubchem.ncbi.nlm.nih.gov.

315. Acree, T. and H. Arn. Flavornet and human odor space. [cited 2021 12 January]; Available from: http://flavornet.org/.

316. Torki, M., et al., Protein fractionation and characterization of some legumenous seeds. Annals of Agricultural Science, Moshtohor (Egypt), 1987.

317. Guldiken, B., J. Stobbs, and M. Nickerson, Heat induced gelation of pulse protein networks. Food Chemistry, 2021. **350**: p. 129158.

318. Yang, J., Rethinking Plant Protein Extraction - Interfacial and Foaming Properties of Mildly Derived Plant Protein Extracts, in Physics and Physical Chemistry of Foods. 2021, Wageningen University: Wageningen.

319. Nicolai, T. and C. Chassenieux, Heat-induced gelation of plant globulins. Current Opinion in Food Science, 2019. **27**: p. 18-22.

320. Renkema, J.M., H. Gruppen, and T. Van Vliet, Influence of pH and ionic strength on heat-induced formation and rheological properties of soy protein gels in relation to denaturation and their protein compositions. Journal of Agricultural and Food Chemistry, 2002. **50**(21): p. 6064-6071.

321. Sun, X.D. and S.D. Arntfield, Dynamic oscillatory rheological measurement and thermal properties of pea protein extracted by salt method: Effect of pH and NaCl. Journal of Food Engineering, 2011. **105**(3): p. 577-582.

322. Mession, J.-L., S. Roustel, and R. Saurel, Interactions in casein micelle - Pea protein system (Part II): Mixture acid gelation with glucono-δ-lactone. Food Hydrocolloids, 2017. **73**: p. 344-357.

Summary

For sustainability reasons there is an ongoing shift from animal- to plant-based proteins, which is often referred to as the protein transition. The research in this thesis was in the context of that protein transition, where the focus was on mild fractionation routes (i.e., using fewer or alternative processing steps) to produce different pea protein fractions. The functional behaviour of these protein fractions was studied. In Chapters 2 – 4 the behaviour of different pea protein fractions in dispersions and gels is described. Chapters 5 and 6 describe the functional behaviour of different pea fractions in model foods when oil or air are incorporated. Chapters 7 and 8 describe dairy protein gels and dispersions where the dairy proteins are partially replaced by pea protein fractions. While the first part of this thesis (Chapters 2 – 4) primarily focused on milder fractionation, the second and third part (Chapters 5 – 8) focus on tailored fractionation, where the fractionation is tailored to obtain specific protein functionalities.

I. Pea protein dispersions and gels

A commonly used aqueous fractionation process was used to produce pea protein fractions. This process is used to produce pea protein isolates, but here we also used pea protein fractions that were obtained during the initial stages of the fractionation process. In total five fractions were produced and compared. The first fraction used was pea flour. The second and third fractions were obtained after extraction of pea protein from the flour at either neutral pH or alkaline pH, followed by centrifugation. The supernatants recovered after centrifugation were labelled PPCn (pea protein concentrate neutral extracted) and PPCa (alkaline extracted). The fourth and fifth fraction were obtained after isoelectric precipitation of the PPCa supernatant and were thus most extensively fractionated. This supernatant, with precipitated proteins, was centrifuged. The supernatant after this second centrifugation step was rich in albumins and referred to as ALB-F (albumin-fraction). The pellet was redispersed at pH 7 and labelled PPIp (pea protein isolate precipitated).

In **Chapter 2** the pea seeds were visualized using electron microscopy. The images revealed that protein bodies and starch granules were concentrated in storage cells in the pea cotyledon. The composition of the different pea protein fractions was also studied. PPCn and PPCa contained around 50 wt. % protein, ALB-F around 20 wt. % and PPIp around 85 wt. %. The major impurities were oligosaccharides and salts. Finally, the viscosity of the pea protein fraction dispersions at pH 7 was measured, and it was found that pea protein has substantial thickening capacity. After estimation of the protein volume fractions, it was hypothesized that pea

protein forms soluble aggregates with a high specific volume, which largely explains the rheological behaviour. **Chapter 3** also describes the behaviour of pea protein fractions in dispersions, but here the effect of pH and different salt concentrations were explored to study coacervation behaviour. It was found that coacervation, or liquid-liquid phase separation, occurred between pH 6.0 and 6.5. The coacervates (i.e., spherical liquid domains that are rich in protein) from PPCn formed at pH 6.25 were further characterized. We found that coacervation induced separation of globulins and albumins, with globulins (mostly legumin) in the coacervates, and albumins in the continuous phase. Also, the internal protein content of the coacervates at pH 6.25 was found to be 23 – 30 wt. % protein, depending on the salt concentration. The phenomenon of coacervation was most pronounced for the mildest fractionated PPCn, as in the more extensively processed fractions also protein aggregates were formed. **Chapter 4** reports the gelling behaviour of pea protein fractions upon heating. The effect of aqueous fractionation steps on the heat-set gelling capacity and firmness is discussed and it is shown that mild fractionation results in a better gelling capacity of pea protein. The gels were further characterized using large amplitude oscillatory shear (LAOS) rheology, and it was found that mildly processed pea fractions formed not only firmer, but also more ductile gels in terms of protein mass. Isoelectric precipitation, lower ionic strength of the pea fraction dispersions, and the lack of sugars upon freeze-drying were identified as factors responsible for a reduced gelling capacity after extensive fractionation.

II. Incorporation of oil and air

In the second part of this thesis pea protein fractions are studied on their ability to stabilize model food systems in which oil or air are incorporated. In **Chapter 5** the emulsification and foaming properties of PPCa, ALB-RF (obtained after diafiltration of the ALB-F) and PPIp (here labelled globulin-rich fraction, or GLB-RF) were studied. At the air-water interface, the ALB-RF displayed strong in-plane interactions, thereby forming a stiff interfacial layer. These interfacial properties also translated into a high foam overrun and foam stability. PPC and GLB-RF, both abundant in globulins, formed weaker air-water interfacial layers, and displayed lower foam overruns and foam stabilities. It was concluded that albumins had better foaming properties than globulins. On the other hand, PPC and GLB-RF were better able to stabilize emulsions. The results of this chapter clearly illustrate that fractionation can be tailored to specific functionalities. In **Chapter 6,** the effect of two different fractionation routes on the ability of PPI to form emulsion filled gels was studied. One of the routes was the aqueous fractionation route yielding PPIp, which was also

described in Chapter 2. In the other route, pea proteins were extracted at neutral pH and were further fractionated using diafiltration, instead of isoelectric precipitation. The resulting pea protein isolate was labelled PPId. Interfacial and bulk rheology were used to investigate the emulsion-filled gelling behaviour and gel properties of PPIp and PPId. It was found that both PPIs formed emulsion oil droplets of similar sizes, and that the interfacial protein networks were relatively weak. Both PPIs were able to form emulsion-filled gels, with oil concentrations up to 30 wt. %, but PPId formed firmer gels at pH 7. At pH 5 PPIp and PPId formed equally firm gels and emulsion-filled gels. This effect was attributed to the pre-aggregated state of PPIp, caused by isoelectric precipitation. The aggregates in PPIp led to a softer and more heterogeneous gelled network compared to PPId. Also, no oil reinforcement was observed in any of the emulsion-filled gels. Based on the weak protein interactions at the interface, we hypothesized that the proteins at the interface only weakly interacted with the protein matrix.

III. Substitution of dairy proteins

In the third part of this thesis the partial and full substitution of dairy protein by pea protein in dispersions and gels is studied. **Chapter 7** compares the viscosity, solubility and gel firmness of PPIp, PPId and PPIc (commercial) with WPI (whey protein isolate). It was found that PPId most closely resembled the viscosity, solubility and gelling capacity of WPI, which was related to its unaggregated state. Diafiltration, used to obtain PPId, did not induce protein aggregation, which resulting in a high solubility, low viscosity, and high gelling capacity. WPI was also partially substituted by the PPIs in ratios of 1:3, 2:2 and 3:1. It was found that half of the WPI could be replaced by any of the PPIs, without affecting gelling behaviour and gel firmness significantly. The gel microstructures were also visualized using confocal microscopy. Also in **Chapter 8** WPI was substituted, but now by the pea protein fractions PPCa, ALB-F and PPIp, of which some were less pure compared to the pea protein isolates. First the gelling behaviour of ALB-RF (obtained after diafiltration of ALB-F) and PPIp were characterized by small and large amplitude oscillatory shear (SAOS and LAOS) rheology, to establish the differences in gelling behaviour between pea albumins and globulins. It was found that albumins could form firmer gels than globulins, which is particularly relevant when considering that albumins are just a by-product from the aqueous fractionation process. The pea fractions were also used to substitute WPI in heat-set gels. It turned out that in the mixtures of WPI with pea protein fractions, higher gel firmness was seen with low purity pea protein fractions. Particularly, substitution by ALB-F resulted in high gel

firmness. This effect was attributed to the formation of additional disulphide bonds between whey proteins and pea albumins. Moreover, the ALB-F / WPI gel firmness was least affected by changes in pH and salt concentrations.

The common denominator of this thesis is that a clear relation exists between the fractionation method and the resulting functional properties of pea protein fractions. Actually, a broad range of functional properties could be achieved with only one raw material, showing the versatility of pea as a protein source. The work described in this thesis revealed that changes due to fractionation could be related to changes in the composition and state of pea proteins in the various fractions. This also led to the realization that pea protein functionality can be controlled by applying tailored fractionation methods. Other insights from this thesis were that pea globulins and albumins are functionally distinct proteins, and that they can easily be separated upon fractionation. The thesis ends with highlighting the fact that potential application of tailor-made pea protein fractions, also require more insights into other factors such as sustainability, nutritional value, and organoleptic properties of the pea protein fractions. The knowledge generated in this research and described in this thesis may facilitate further research on these factors, and may contribute to the development of highly functional pea protein ingredients.

Samenvatting

Om duurzaamheidsredenen is er een verschuiving gaande van het gebruik van dierlijke naar plantaardige eiwitten. Deze verschuiving staat ook wel bekend als de eiwit transitie. Het onderzoek in dit proefschrift is uitgevoerd in de context van die transitie, waarbij de focus lag op het verkennen van milde fractioneringsroutes (dat wil zeggen, minder of alternatieve zuiveringsstappen) om verschillende eiwitrijke erwtenfracties te maken. Het functionele gedrag van deze eiwitfracties is onderzocht. In hoofdstukken 2 – 4 staan het gedrag van eiwitfracties in dispersies en gelen beschreven. Hoofdstukken 5 en 6 beschrijven het functionele gedrag van verschillende eiwitfracties in model voedingsmiddelen na incorporatie van olie of lucht. Hoofdstukken 7 en 8 beschrijven gelen en dispersies waarin zuiveleiwitten gedeeltelijk zijn vervangen door eiwitfracties van erwt. Waar het eerste gedeelte van dit proefschrift (hoofdstukken 2 – 4) zich vooral richt op milde fractionering, richtten het tweede en derde gedeelte (hoofdstukken 5 – 8) zich met name op fractionering dat is toegespitst op specifiek functioneel gedrag van de eiwitfracties.

I. Dispersies en gelen van erwteneiwit fracties

Een veelgebruikt nat fractioneringsproces is hier gebruikt om eiwitfracties te maken vanuit erwt. Dit proces wordt normaal gesproken gebruikt om eiwit isolaten te produceren, maar hier gebruikten we ook erwten eiwitfracties die werden verkregen na beperkte fractionering. In totaal zijn er vijf fracties geproduceerd en onderzocht. De eerste fractie was erwtenmeel. De tweede en derde fractie werden verkregen na extractie van erwteneiwit uit dit erwtenmeel bij ofwel neutrale, ofwel alkalische pH, gevolgd door een centrifugestap. De supernatanten werden PPCn (neutraal geëxtraheerde erwten eiwitisolaat) en PPCa (alkalisch geëxtraheerde erwten eiwitisolaat) genoemd. The vierde en vijfde fractie werden verkregen na iso-elektrische precipitatie van PPCa (supernatant) en waren dus het meest intensief gefractioneerd. Dit supernatant, met geprecipiteerde eiwitten, werd gecentrifugeerd. Het supernatant na deze tweede centrifugeerstap was rijk aan albumine en werd dus ook ALB-F (albumine fractie) genoemd. Het pellet werd opnieuw gedispergeerd bij pH 7 en werd PPIp (geprecipiteerd erwten eiwitisolaat) genoemd.

In **Hoofdstuk 2** werden de erwtenzaden gevisualiseerd met behulp van elektronenmicroscopie. De afbeeldingen lieten zien dat eiwitlichamen en zetmeelkorrels waren geconcentreerd in opslagcellen in de zaadlob van de erwt. De samenstelling van de verschillende eiwitfracties is ook onderzocht. PPCn en PPCa bevatten ongeveer 50 % massa eiwit, ALB-F ongeveer 20 % massa eiwit en PPIp ongeveer 85 % massa eiwit. De belangrijkste niet-eiwit componenten waren oligosachariden

en zouten. Met behulp van viscositeitsmetingen van de erwten eiwitfracties bij pH 7 werd vastgesteld dat erwteneiwit dispersies sterk kan verdikken. Na een afschatting van de eiwit volume fracties, werd de hypothese voorgesteld dat erwteneiwit oplosbare aggregaten vormt met een hoog specifiek volume, als verklaring voor het reologisch gedrag van de dispersies. **Hoofdstuk 3** beschrijft eveneens het gedrag van erwten eiwit in dispersies, maar in dit hoofdstuk werd het effect van pH en zoutconcentraties op het vormen van eiwit coacervaten (druppelvormige colloïdale deeltjes) onderzocht. Het bleek dat coacervatie, of vloeistof-vloeistof fasescheiding, plaatsvond tussen een pH van 6.0 en 6.5. De coacervaten van PPCn die vormden bij pH 6.25 werden uitvoeriger gekarakteriseerd. We stelden vast dat coacervatie leidde tot een scheiding van globulinen en albuminen, waarbij globulinen (met name legumine) aanwezig waren in de coacervaten, en de albuminen in de continue fase. Verder bleek dat het interne eiwitgehalte van de coacervaten bij pH 6.25 tussen de 23 en 30 % massa lag, afhankelijk van de zoutconcentratie. Het fenomeen coacervatie was het meest duidelijk te zien in de mild gefractioneerde PPCn, aangezien in de intensiever bewerkte fracties ook eiwitaggregaten werden gevormd. **Hoofdstuk 4** beschrijft het geleergedrag van erwten eiwitfracties tijdens verhitten. Het effect van natte fractioneringsstappen op de hitte-geïnduceerde geleercapaciteit en gel stevigheid wordt besproken en het bleek dat milde fractionering resulteert in een betere geleercapaciteit van erwteneiwit. De gelen zijn uitvoeriger gekarakteriseerd met behulp van grote amplitude oscillerende afschuiving (GAOS) reologie en dit leidde tot het inzicht dat mild bewerkte erwten eiwitfracties niet alleen stevigere, maar ook ductielere gelen vormen, per massa eiwit. Iso-elektrische precipitatie, lagere ionische sterkte van de erwten eiwitdispersies en het gebrek aan suikers tijdens vriesdrogen werden geïdentificeerd als factoren verantwoordelijk voor een verminderde geleercapaciteit na intensieve fractionering.

II. Incorporatie van olie en lucht

Het tweede gedeelte van dit proefschrift beschrijft in hoeverre erwten eiwitfracties, model voedingsmiddelen met daarin olie of lucht geïncorporeerd, kunnen stabiliseren. In **Hoofdstuk 5** werd het emulgeer- en schuimgedrag van PPCa, ALB-RF (verkregen na diafiltratie van ALB-F) en PPIp (in het betreffende hoofdstuk globuline-rijke fractie, of GLB-RF, genoemd) onderzocht. Aan het lucht-water grensvlak liet de ALB-RF sterkte interacties zien, wat een indicatie is voor een stevige eiwitlaag aan het grensvlak. Deze grensvlakeigenschappen konden worden vertaald naar een hoog schuimvermogen en -stabiliteit. PPCa en GLB-RF, beiden rijk in globuline eiwit, vormden zwakker geïnteracteerde lagen aan

het lucht-water grensvlak en lieten ook een lagere schuimcapaciteit en -stabiliteit zien. De conclusie was dan ook dat albumine betere schuimeigenschappen heeft dan globuline. Aan de andere kant bleken PPCa en GLB-RF beter in staat om emulsies te stabiliseren. De resultaten van dit hoofdstuk laten duidelijk zien dat fractionering toegespitst kan worden op functionaliteit. In **Hoofdstuk 6** werd het effect van twee verschillende fractioneringsroutes op het vermogen van PPI (erwten eiwitisolaat) om emulsie gevulde gelen te vormen onderzocht. Een van de routes was het natte fractioneringsproces dat leidde tot de PPIp fractie, wat ook beschreven staat in hoofdstuk 2. Bij de andere route werden erwten eiwitten geëxtraheerd bij neutrale pH en verder gefractioneerd met behulp van diafiltratie, in plaats van iso-elektrische precipitatie. Het resulterende erwteneiwit isolaat werd PPId genoemd. Grensvlak- en bulkreologie werden gebruikt om de emulsie gevulde geleergedrag en geleigenschappen te onderzoeken. Het bleek dat de emulsie druppels gevormd met behulp van de PPI's van vergelijkbare grootte waren en dat de eiwitnetwerken aan het grensvlak relatief zwak waren. Beide PPI's waren in staat om emulsie gevulde gelen te vormen met olie concentraties tot 30 % massa, maar PPId vormde stevigere gelen bij pH 7. Bij pH 5 vormden PPIp en PPId gelen en emulsie gevulde gelen van vergelijkbare stevigheid. Dit effect werd geweten aan de vooraf geaggregeerde staat van PPIp, wat veroorzaakt was door iso-elektrische precipitatie tijdens de fractionering. De aggregaten in PPIp veroorzaakten een zachtere en meer heterogeen gegeleerd netwerk in vergelijking met PPId. Verder werd er geen versteviging door de olie waargenomen in de emulsie gevulde gelen. Op basis van de zwakke eiwit interacties aan het grensvlak werd de hypothese voorgesteld dat de eiwitten aan het grensvlak ook slechts zwakke interacties vormden met de eiwit matrix, als verklaring voor de observatie dat olie de gelen niet verstevigde.

III. Substitutie van zuivel eiwitten

In het derde gedeelte van dit proefschrift is de gedeeltelijke en volledige substitutie van zuiveleiwitten door erwten eiwitten in dispersies en gelen onderzocht. **Hoofdstuk 7** vergelijkt de viscositeit, oplosbaarheid en gel stevigheid van PPIp, PPId en PPIc (commercieel erwten eiwitisolaat) met WPI (wei eiwitisolaat). Het bleek dat PPId het dichtst in de buurt kwam van WPI wat betreft viscositeit, oplosbaarheid en geleercapaciteit, wat te maken had met de niet-geaggregeerde staat van PPId. De fractioneringsmethode van PPId veroorzaakte namelijk geen aggregatie en leidde dan ook tot een hoge oplosbaarheid, lage viscositeit en hoge geleercapaciteit. WPI werd ook gedeeltelijk gesubstitueerd door de PPI's in ratio's van 1:3, 2:2 en 3:1. Het bleek dat de helft van het WPI kon worden vervangen door een willekeurige

PPI zonder dat het geleergedrag en gel stevigheid significant verminderden. De microstructuur van de gelen werd tot slot nog gevisualiseerd met behulp van confocale microscopie. Ook in **Hoofdstuk 8** werd WPI gesubstitueerd, maar nu door de erwten eiwitfracties PPCa, ALB-F en PPIp, waarvan sommigen minder zuiver waren in vergelijking met de erwteneiwit isolaten uit hoofdstuk 7. Eerst werd het geleergedrag van ALB-RF (verkregen na diafiltratie van ALB-F) en PPIp gekarakteriseerd met kleine en grote amplitude oscillerende afschuiving (KAOS en GAOS) reologie, om de verschillen in geleergedrag en geleigenschappen tussen erwt albumine en globuline vast te stellen. Het bleek dat albumine stevigere gelen kon vormen dan globuline, wat in het bijzonder relevant is omdat albumine slechts een bijproduct is in het natte fractioneringsproces. De erwten eiwitfracties werden ook gebruikt om WPI te substitueren in hitte-geïnduceerde gelen. Het bleek dat in de mengsels van WPI met erwten eiwitfracties, stevigere gelen werden gevormd bij fracties met een lagere eiwitzuiverheid. De gelen waren het stevigst als WPI gedeeltelijk werd vervangen door ALB-F. Dit effect kon worden verklaard door de vorming van additionele zwavelbruggen tussen wei eiwitten en albuminen. Daarbij was de stevigheid van ALB-F / WPI gelen het minst gevoelig voor veranderingen in pH en zoutconcentraties.

De rode lijn in dit proefschrift is dat er een duidelijke relatie bestaat tussen fractioneringsmethode en resulterende functionele eigenschappen van erwtenfracties. Een wijd scala aan functionele eigenschappen kan worden verkregen vanuit slechts één grondstof, ofwel: erwt is een veelzijdige bron van functioneel eiwit. Het onderzoek liet verder zien dat veranderingen in fractionering leidt tot veranderingen in samenstelling en staat van het eiwit in de verschillende fracties. Dit leidde ook tot de realisatie dat eiwit functionaliteit kan worden beheerst door middel van toegespitste fractioneringsmethoden. Een ander inzicht uit dit proefschrift is dat erwt globulinen en albuminen functioneel verschillend zijn, en dat ze bovendien gemakkelijk gescheiden kunnen worden door fractionering. In het laatste hoofdstuk van dit proefschrift wordt de nadruk gelegd op het feit dat er voor de implementatie van toegespitste fractionering eerst meer inzichten nodig zijn omtrent de duurzaamheid, voedingswaarde en organoleptische eigenschappen van de eiwitfracties. De resultaten uit dit proefschrift kunnen nader onderzoek naar dergelijke onderwerpen faciliteren, en ook op die manier bijdragen aan de ontwikkeling van hoogwaardige functionele ingrediënten uit erwt.

Acknowledgements

Before starting my PhD, I could not have imagined what a journey it would be. The past four years I witnessed, and contributed to, an exciting transition in food science. I also grew personally. The experience and development – of which part is documented in this thesis – are not simply my achievement however, but rather a result of large and small contributions from supervisors, colleagues, and friends.

The biggest contributors to the PhD project were my supervisors Paul Venema, Marcel Meinders, Atze Jan van der Goot and Erik van der Linden. They turned out to be among the smartest people I know. I want to thank them for giving me the opportunity to do a PhD in Food Physics; I will always be grateful for that. Paul, thank you for your supervision. From the beginning you helped me to get on track with my PhD, you made time to answer my questions and involved me with student supervision from the very beginning. You taught me a great deal about physics and the application of physics in food science. You also encouraged me to not only use techniques to measure samples, but also to get an understanding of the principles behind the techniques. The freedom you gave me is also something I very much appreciated, as it helped me to become an independent researcher. I would also like to thank Marcel, who was not only my supervisor, but also the project leader of the overall TiFN project. The project was set up and managed very well, and it helped us the PhD candidates to learn from other projects and to broaden our view. Marcel, already quite early in the project it became clear to me that the PhD candidate's development had a high priority for you, and this is something I really appreciated. You also taught me to critically reflect on my results and to make sure that claims could be substantiated by results and reasoning. This helped me to become a more meticulous researcher. I am also very happy to have been supervised by Atze Jan. The project, and me personally, really benefited from his expertise in plant protein extraction and food structuring. Atze Jan, thank you for always being swift and constructive in reviewing my work and answering my e-mails. It was always really appreciated to hear your perspective on new findings. Your supervision helped me to become a better writer and more nuanced researcher. Last but not least, I would like to thank Erik for his supervision. I was always very impressed how you could connect and structure results that were discussed during meetings. Towards the end of my PhD, I sometimes also consulted you for non-research related questions, such as career advice. You really gave me some valuable insights on science and other aspects of life. Your supervision became an example for me and helped me to become a better supervisor myself. Erik, Atze Jan, Marcel and Paul, I really enjoyed working with you all, and I hope we can stay in touch in the future.

Part of the PhD trajectory was to supervise students during their BSc and MSc thesis projects. Thank you, Mark, Jody, Danni, Justus, Jolien, Katja, Maria, Carol, Simone, Dirk and Sarah! I really enjoyed being your supervisor, which was also because of your motivation, interests, and hardworking attitudes. It was a privilege to work with you. In fact, this thesis is a shared accomplishment, and you were all major contributors.

I would also like to thank all my Food Physics colleagues, particularly those from the Hot Office. I really enjoyed the first two years, in which I shared the office with Xilong, Naomi and Wenjie; there are countless memories that still make me smile. Also, the people from Hot Office 2.0, Lei, Naomi, Ahmed and Xudong; thank you for all the nice talks. Furthermore, I would like to thank Els, Floris, Harry, Miranda and Roy, you were always accessible and willing to help, even though I could see you were very busy at times. Furthermore, I would like to thank Elke, Guido, Jasper and Leonard. I was always very impressed with your hard-work and expertise; I am happy I got to know you. Thanks as well to all my other PhD colleagues: Annika, Aref, Arianne, Belinda, Bo, cool Cai and Cai the king of osmometry, Claudine, Evelen, Gerard, Jack, Joon, Luka, Manolo, Marco, Monica, Ninna, Ornicha, Parisa, Pauline, PDF, Penghui, Philipp, Raisa, Robert, Suraj, Umer, Xiangyu, Xiao and Zhihong. You certainly made my time at FPH memorable, not the least during our FPH trip to Singapore and Indonesia. Tere Makasi! Although I appreciated all my FPH colleagues, I would particularly like to thank Xilong, Wenjie, Philipp, Naomi, Marco (& Elisa), Melika, Lei, Jack, Claudine, Belinda and Annika for all the nice chats during borrels and other activities.

My PhD project was embedded within a larger project organized by the Top Institute Food and Nutrition (TiFN). I would like to thank all people involved for their contribution and discussions: Dana, Eleni, Emma, Helene, Irene, Jack, Jacqueline, Jan, Marcel, Marius, Martha, Maud, Mira and Simha. Particularly Simha, Jack and Eleni for the fruitful collaborations, it was great working with you! Eleni, Simha and Costas, I also really enjoyed the Hydrocolloids conference and subsequent trip in Australia, thank you for this memorable trip! Maud, thank you for all the help with SEC and answering protein related questions; you are very knowledgeable about the chemistry behind pea proteins. Mira, Irene and Helene, thank you for extracting such large quantities of protein, my work would not have been possible without you! Finally, I would like to thank the experts from Danone Nutricia, Le Groupe Bel, PepsiCo and Unilever for their useful suggestions and for giving us some ideas about their challenges with the application of plant proteins.

Ook wil ik mijn familie en vrienden bedanken voor alle steun! Vooral mijn ouders; bedankt voor jullie liefde, steun en hulp tijdens het studeren en tijdens mijn promotieonderzoek! Het meeste heb ik echter te danken aan mijn lieve vrouw Marleen. Een PhD onderzoek is niet altijd makkelijk, maar jij hielp me door de moeilijkere fases. Tegelijkertijd kan wetenschap bedrijven ook erg leuk en soms zelfs bijna verslavend zijn. Zo nu en dan haalde je me uit de 'Food Science' bubbel en liet me de andere mooie en belangrijke dingen in het leven zien. Het mooiste onderdeel daarvan was onze dochter Rhodé. Niets maakt me vrolijker dan haar te horen schateren als ik spelletjes met haar speel. Marleen en Rhodé, jullie geven mijn leven echt kleur, en ik kijk uit naar onze toekomstige avonturen samen!

About the author

List of publications

Overview of completed training activities

About the author

Remco Kornet was born in Werkendam in the Netherlands on 30 June 1994. In 2011, after finishing secondary school, he went to the HAS University of Applied Sciences to study Food Technology. During his BSc programme he got the chance to do internships at multiple companies, which amongst others took place at a UHT manufacturing site of Fonterra in New Zealand and an R&D facility of Danone Nutricia in the Netherlands. In the fourth year of his BSc program, he specialized in dairy science and product development. He completed his Bachelor programme with an internship at the NIZO research institute. During this time Remco became acquainted with plant proteins and some of the science behind it. After he obtained a BSc degree in 2015, Remco continued with the MSc programme Food Technology at Wageningen University, during which he specialized in Ingredient Functionality. He did his MSc thesis project at the chair group of Physics and Physical Chemistry of Foods on the design of a micro delivery system with pH sensitive shell for controlled release at acidic pH. To conclude his MSc programme, he did an internship at FrieslandCampina where he contributed to the development of a new spreadable product and the development of cheese from protein concentrates. After obtaining his MSc degree in 2017, Remco was hired as a PhD candidate at the chair group of Physics and Physical Chemistry of Foods. This PhD project was initiated by the Top Institute Food and Nutrition (TiFN) as part of a larger project called *Sustainable Ingredients.* His PhD project focused on the relation between pea protein fractionation and functionality and on the functionality of hybrid plant-dairy protein blends.

Email: remcokornet@gmail.com

Scan to view my LinkedIn profile

List of publications

This thesis

- **Cornelis Kornet (Remco)**, Paul Venema, Jaap Nijsse, Erik van der Linden, Atze Jan van der Goot, Marcel Meinders (2020). Yellow pea aqueous fractionation increases the specific volume fraction and viscosity of its dispersions. *Food Hydrocolloids*, *99*, 105332.
- **Remco Kornet**, Justus Veenemans, Paul Venema, Atze Jan van der Goot, Marcel Meinders, Leonard Sagis, Erik van der Linden (2021). Less is more: Limited fractionation yields stronger gels for pea proteins. *Food Hydrocolloids*, *112*, 106285.
- **Remco Kornet**, Carol Shek, Paul Venema, Atze Jan van der Goot, Marcel Meinders & Erik van der Linden (2021). Substitution of whey protein by pea protein is facilitated by specific fractionation routes. *Food Hydrocolloids, 117, 106691*.
- **Remco Kornet**, Simone Penris, Paul Venema, Atze Jan van der Goot, Marcel Meinders & Erik van der Linden (2021). How pea fractions with different protein composition and purity can substitute WPI in heat-set gels. *Food Hydrocolloids, 120, 106891*
- **Remco Kornet**, Sarah Lamochi Roozalipour, Paul Venema, Atze Jan van der Goot, Marcel Meinders & Erik van der Linden. Coacervation in pea protein solutions: the effect of pH, salt and fractionation processing steps. ***Submitted***
- **Remco Kornet***, Jack Yang*, Paul Venema, Erik van der Linden & Leonard M.C. Sagis. Pea fractionation can be optimized to yield protein-enriched fractions with a high foaming and emulsifying capacity. ***Submitted***
- **Remco Kornet***, Simha Sridharan*, Paul Venema, Leonard M.C. Sagis, Constantinos V. Nikiforidis, Atze Jan van der Goot, Marcel Meinders & Erik van der Linden. Fractionation methods affect the gelling properties of pea protein in emulsion-filled gels. ***In preparation***

Other research

- Eleni Ntone*, **Remco Kornet***, Paul Venema, Marcel Meinders, Erik van der Linden, Johannes H. Bitter, Leonard M.C. Sagis, Constantinos V. Nikiforidis. Napins and cruciferins in rapeseed protein extracts have complementary roles in structuring emulsion-filled gels. ***Submitted***
- Jack Yang, **Remco Kornet**, Claudine Diedericks, Quihuizi Yang, Claire C. Berton-Carabin, Constantinos V. Nikiforidis, Paul Venema, Erik van der Linden, Leonard M.C. Sagis. Rethinking plant protein extraction: albumin – from waste stream to an excellent foaming ingredient. ***Submitted***

* shared first authorship

Overview of completed training activities

Discipline specific courses

Rheology course	Wageningen, the Netherlands	2018
Masterclass dairy protein biochemistry	Wageningen, the Netherlands	2018
Summer course glycosciences [2]	Wageningen, the Netherlands	2018
Summer course food proteins: functionality, modification and analysis	Wageningen, the Netherlands	2018

Conferences and symposia

Thermodynamics and phase transitions in food processing	Wageningen, the Netherlands	2018
NRV rheology seminar	Wageningen, the Netherlands	2019
ISFRS conference [1]	Zürich, Switzerland	2019
DoF conference [1]	Porto, Portugal	2019
Food Valley summit: the protein planet	Wageningen, the Netherlands	2019
Hydrocolloids conference [1]	Melbourne, Australia	2020
NIZO plant protein conference	Online	2020
2nd emerging meat alternative conference	Online	2020
Conference S&T for meat analogues	Online	2021
35th EFFoST conference [1]	Lausanne, Switzerland	2021

General courses

VLAG PhD week	the Netherlands	2018
Introduction to R	Wageningen, the Netherlands	2018
PhD workshop carousel	Wageningen, the Netherlands	2018
Scientific publishing	Wageningen, the Netherlands	2018
Supervising BSc and MSc students	Wageningen, the Netherlands	2018
Scientific writing	Wageningen, the Netherlands	2018
Big data analysis in the life sciences	Wageningen, the Netherlands	2019
Applied statistics in R	Online	2020
Adobe InDesign	Online	2021
Popular science writing	Online	2021

Other activities

Preparation of research proposal	Wageningen, the Netherlands	2017
PhD study trip [1, 2]	Singapore and Indonesia	2018
Weekly science meetings within chair group [1]	Wageningen, the Netherlands	2017 - 2021
Quarterly project TiFN / partner meetings [1]	Wageningen, the Netherlands	2017 - 2021

[1] oral presentation, [2] poster presentation

Colophon

This research formed part of a project that was organised by TiFN, a public-private partnership on precompetitive research in food and nutrition, and executed under its auspices. The public partners were responsible for the study design, data collection and analysis, decision to publish, and preparation of the manuscript. The private partners Danone, Fromageries Bel, Pepsico, Unilever have contributed to the project through regular discussions. Co-funding for the project was obtained from and Top-Consortium for Knowledge and Innovation Agri&Food (TKI).

Financial support from Wageningen University and TiFN for performing this research as well as for printing this thesis is gratefully acknowledged.

Layout and cover design: Remco Kornet
Printed by Proefschriftenmaken

This PhD thesis describes the effect of mild aqueous fractionation processes on the functionality of pea protein, in terms of molecular and micro-structural characteristics. The thesis is structured according to the type of model foods studied. The first part focusses on pea protein dispersions and gels. The second part reports on the stabilization of oil and air after incorporation in foams, emulsions and emulsion-filled gels. The third part addresses hybrid plant-dairy protein dispersions and gels. The results from this research led to the realization that fractionation can be tailored to specific pea protein functionality.